NASA CR-121090

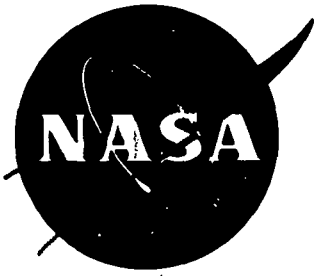

DEVELOPMENT OF GAS-PRESSURE BONDING PROCESS FOR AIR-COOLED TURBINE BLADES

by

K. E. Meiners, Program Director

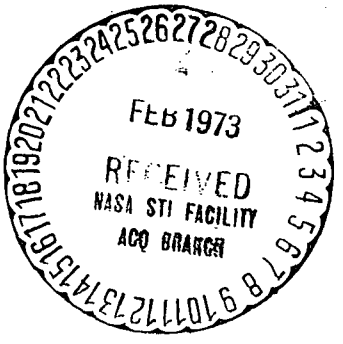

BATTELLE
Columbus Laboratories

prepared for

NATIONAL AERONAUTICS AND SPACE ADMINISTRATION

NASA Lewis Research Center
Cleveland, Ohio
Contract NAS 3-10491
Edward L. Warren, Project Manager

Requests for copies of this report should be referred to

National Aeronautics and Space Administration
Scientific and Technical Information Facility
P.O. Box 33
College Park, Md. 20740

NASA CR-121090

FINAL REPORT

DEVELOPMENT OF GAS-PRESSURE BONDING PROCESS FOR AIR-COOLED TURBINE BLADES

by

K. E. Meiners, Program Director

BATTELLE
Columbus Laboratories
505 King Avenue
Columbus, Ohio 43201

prepared for

NATIONAL AERONAUTICS AND SPACE ADMINISTRATION

February 15, 1972

CONTRACT NAS 3-10491

NASA Lewis Research Center
Cleveland, Ohio
Edward L. Warren, Project Manager

Page Intentionally Left Blank

TABLE OF CONTENTS

TABLE OF CONTENTS
(Continued)

LIST OF TABLES

LIST OF TABLES
(Continued)

LIST OF FIGURES

LIST OF FIGURES
(Continued)

LIST OF FIGURES
(Continued)

LIST OF FIGURES
(Continued)

LIST OF FIGURES
(Continued)

FINAL REPORT

on

DEVELOPMENT OF GAS-PRESSURE BONDING PROCESS FOR AIR-COOLED TURBINE BLADES

(Contract NAS 3-10491)

to

NATIONAL AERONAUTICS AND SPACE ADMINISTRATION
Lewis Research Center
Cleveland, Ohio

from

BATTELLE
Columbus Laboratories

by

K. E. Meiners, Program Director

ABSTRACT

An investigation was conducted on the application of gas-pressure bonding to the joining of components for convectively cooled turbine blades and vanes. A processing procedure was established for joining the fins of Udimet 700 and TD NiCr sheet metal airfoil shells to cast B1900 struts without the use of internal support tooling. Alternative methods employing support tooling were investigated. Testing procedures were developed and employed to determine shear strengths and internal burst pressures of flat and cylindrical bonded finned shell configurations at room temperature and 1750 F. Strength values were determined parallel and transverse to the cooling fin direction. The effect of thermal cycles from 1750 F to room temperature on strength was also investigated.

SUMMARY

To avoid materials limitations which would hold turbine-inlet temperatures to around 1700 F, cooling designs have been devised to maintain hot section components, primarily vanes and blades, at their allowable working temperature while

the surrounding gas temperature exceeds that temperature by several hundred degrees. However, with the steady increase in the differential between metal working temperature and gas temperature, the complexity in cooling design has increased to the point that the most efficient and thus attractive designs can no longer be fabricated by the traditional methods of casting and forging. The most obvious fabrication method for these designs is to produce them as two or more components and subsequently join these with a process such as diffusion bonding in which joint properties can equal or exceed those of the parent material. The objective of this program was to demonstrate the feasibility of this approach using the gas-pressure bonding process on simulated blade components.

Process development studies were conducted to establish procedures for machining; forming; bond surface preparation; support tooling; bonding cycle conditions (temperature, pressure, and time); and inspection. Electrical discharge machining was successfully employed to prepare simulated cooling shrouds with various fin and channel configurations from TD NiCr and Udimet 700 0.060-in. sheet. It was found that configurations were such that high-efficiency joints between cooling fins and cast B1900 substrates could be achieved without supporting the channels against collapse. Bonding parameters of 2000 F/10,000 psi/1 hr and 1900 F/10,000 psi/1 hr yield excellent joints in the TD NiCr/B1900 and Udimet 700/B1900 systems, respectively. The corresponding gas pressures required to achieve those interface pressures do not alter the dimensions of the cooling configuration. A nickel diffusion activator was found to be beneficial in the Udimet 700/B1900 system. Both bond systems were sensitive to surface preparation. None of the several nondestructive inspection techniques evaluated (ultrasonics, neutron radiography, and liquid crystals) were apparently capable of reliably detecting small flaws in the cooling structure bond.

Flat specimens were evaluated by a compression shear test with the force applied either parallel to or transverse to the cooling fins. Shear strengths in the range of 70 to 100 percent of fin material tensile yield strength were achieved. At 1750 F, shear strength values ranged from 10 to 100 percent of normal fin material strength, depending on test conditions and prior thermal history. Thermal cycling adversely affected strength in TD NiCr/B1900 samples. In the Udimet 700/B1900 system, thermal cycles appeared to affect only transverse strength. In all tests, transverse strength was significantly lower than parallel strength. Cylindrical specimens, simulating airfoil sections, were evaluated by internal gas-pressure bursting and yielded results similar to the shear test.

Very promising results were achieved during the investigation. Satisfactory bonds, as measured by metallographic examination, were obtained in both materials systems with finned shell/strut assemblies simulating a typical blade airfoil geometry. A complete feasibility demonstration on actual turbine blade hardware, however, was beyond the scope of this program. The pronounced strength degradation observed in TD NiCr/B1900 joints after thermal cycling cannot be explained by literature values of thermal expansion which indicate near perfect compatibility. Either the degradation mechanism is not completely understood or the expansion values are in possible error.

INTRODUCTION

Background

Turbine engine performance improvements currently hinge on increasing turbine inlet temperature. Current metallic blade materials, however, pose a severe limit to that temperature if operated uncooled. Hence, the turbine designer devised cooling techniques to maintain such hot section components as blades and vanes at their allowable working temperature while the gas temperature is several hundred degrees higher. The differential between metal temperature and gas temperature has increased steadily because the materials limit has not increased markedly. Moreover, the large temperature differential requires that the heat exchanger in the cooled blade, vane, or stator be highly efficient. Efficient heat exchangers have large surface areas and high-velocity coolant flows. Consequently, many of the attractive cooled blade designs, such as the model illustrated in Figure 1, have a multiplicity of small cross-section coolant passages separated by thin conduction fins. Many of these designs cannot be feasibly fabricated by investment casting, the normal method of producing high-temperature blades and vanes. In other cases, the design can be cast but at an unacceptably high cost and rejection rate. To gain full utilization of current material and design technology, the cooled structure must be broken down into components that can be economically fabricated. These, then, must be joined in such a manner that the whole has a satisfactory reliability in the turbine operating environment over a lifetime that does not penalize operations by increased overhaul requirements. Diffusion bonding, as a result of ability to achieve joint properties equivalent to base metal, is an obvious candidate for this joining operation. The gas-pressure bonding process, with its fluid medium of pressure application and insensitivity to external configuration, appeared ideally suited for this joining problem.

Objective

The principal objective of the program was to develop gas-pressure bonding procedures applicable to the fabrication of a multicomponent (finned shell/cast strut) turbine blade.

Scope

The program was conducted in four experimental tasks:

1. Process Development of TD NiCr/B1900 and Udimet 700/B1900 Systems and Evaluation of Nondestructive Inspection Methods

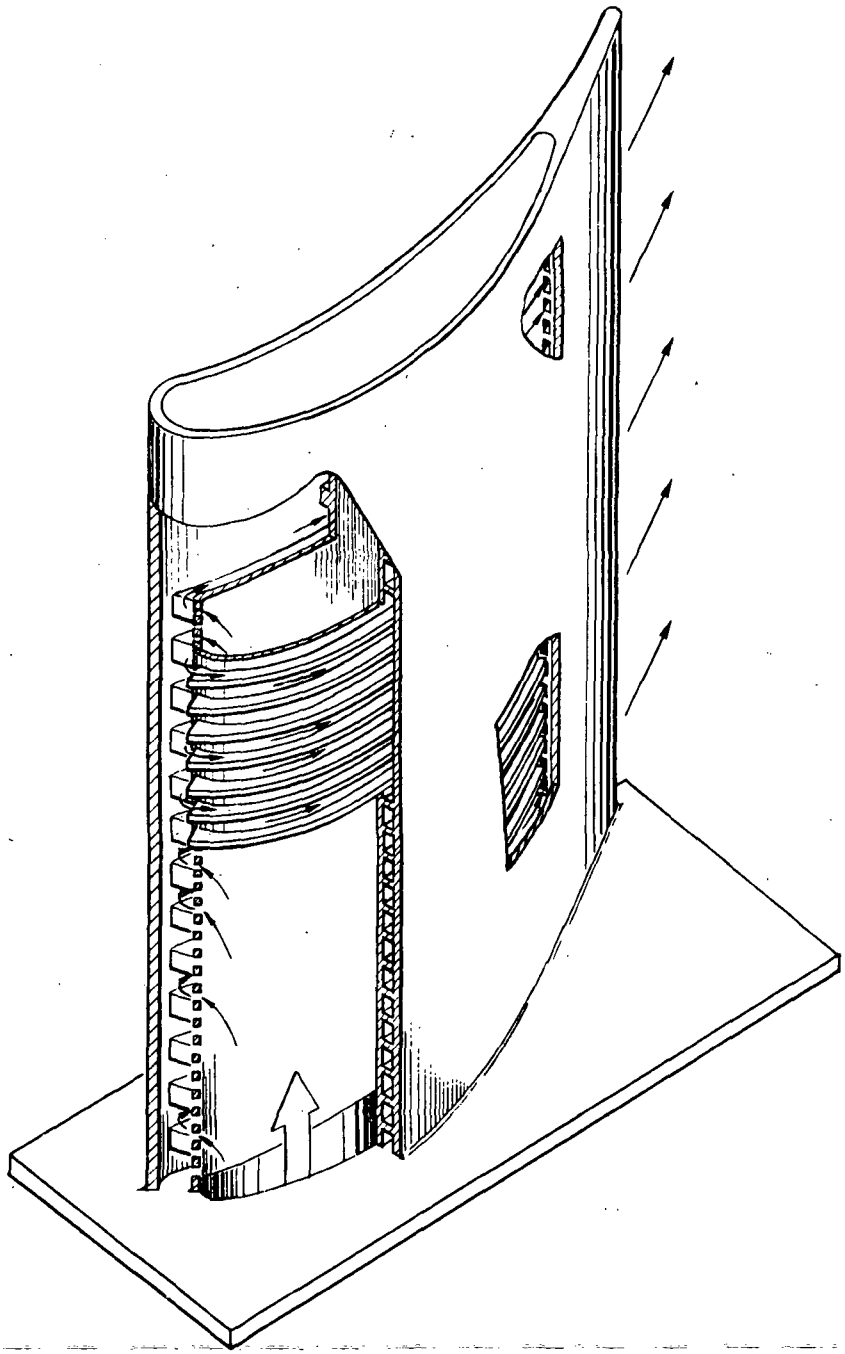

FIGURE 1. CORDWISE FIN BLADE COOLING CONFIGURATION

2. Evaluation of TD NiCr/B1900 Cylindrical Specimens

3. Refinement of Udimet 700/B1900 Joining Process

4. Evaluation of Udimet 700/B1900 Cylindrical Specimens.

In Task 1 materials were procured for the entire program. These consisted of TD NiCr sheet, Udimet 700 sheet, B1900 cast plates, and B1900 cast cylinders. Machining procedures were established for preparing the sheet metal finned shell which consists of 0.012- and 0.036-in.-wide fins. Gas-pressure bonding parameters were investigated and evaluated by metallographic and mechanical test techniques against the following criteria:

(1) Ninety percent of more of the contacting area shall be bonded. The length of the maximum acceptable defect (nonbond) shall not be greater than 0.05 in. (1.3 mm), and in each fin, any two adjacent defects shall be separated by their total combined lengths. Defects separated by less than this distance and agglomerations of defects measuring less than 0.050 in. (1.3 mm) shall be considered single defects.

(2) Air passages shall not be clogged or otherwise obstructed.

(3) Deformation of fins of either size shall not reduce the cross section of air passages by more than 15 percent.

(4) The bonding process shall not lower the high-temperature tensile properties of the strut material below those meeting aircraft engine manufacturers' specifications.

Various NDT methods such as ultrasonic inspection and neutron radiography were evaluated in an attempt to verify bond quality.

The parameters studied were surface preparation, temperature, pressure, and time. Also, the need for internal mandrels between fins and external reinforcement bridges was evaluated. Mechanical testing was conducted at room temperature and 1750 F (1228 K) in such a manner that the test fin-to-strut bond resistance to shearing forces was evaluated both parallel and perpendicular to the fin direction. Optimum parameters are those that yield the highest resultant strength properties while meeting the other bonding criteria. Process recommendations were established on the basis of the results of the evaluation.

In the second task, TD NiCr/B1900 cylindrical finned shell specimens were prepared by the process recommended in Task 1. The finned shells were formed such that the fins ran in the axial and circumferential directions in an equal number of specimens. These specimens were then burst tested at room temperature and 1750 F in the as-bonded condition and after 10 thermal cycles between 1750 F and room temperature.

The third task involved the reevaluation of Udimet 700/B1900 bonding procedures necessary to refine the Task 1 process recommendations for that system. Three duplicate process cycles were performed and evaluated by 1750 F shear tests to establish process reproducibility.

The fourth task entailed bonding four Udimet 700 finned shells to a single B1900 cylinder employing the refined process established in Task 3. The specimens were to be shear tested at 1750 F.

Gas-Pressure Bonding Process

Gas-pressure bonding is an idealized solid-state bonding process performed in a high-pressure autoclave in which the bonding force is applied with inert gas at elevated temperatures. The isostatic nature of this process allows large-diameter components of various sizes and shapes to be bonded into a single unit without recourse to large dies and heavy punches and equipment.

A cold-wall autoclave containing a resistance heater attains the high gas pressures and temperatures required for bonding. Insulating material is placed between the wire-wound furnace and the inside wall and heads of the autoclave to prevent overheating of the vessel walls. A sectional view of a large-diameter autoclave typical of the gas-pressure bonding autoclaves used in the program is shown in Figure 2.

To prepare assemblies for processing, the components to be bonded are cleaned and assembled into containers which are then welded, evacuated, and sealed. A gas-pressure bonding assembly and container similar to those used in this program are illustrated schematically in Figure 3. The sealed containers are placed in the heater inside the autoclave, and the temperature and pressure required for bonding are applied. The high gas pressure is transmitted by plastic flow of the containers to the components, which locally deform at contact points to achieve metallurgical bonding. Subsequently; the bonding container is removed by machining away the container welds and a portion of the container; the remainder is mechanically stripped from the external surfaces of the bonded assembly.

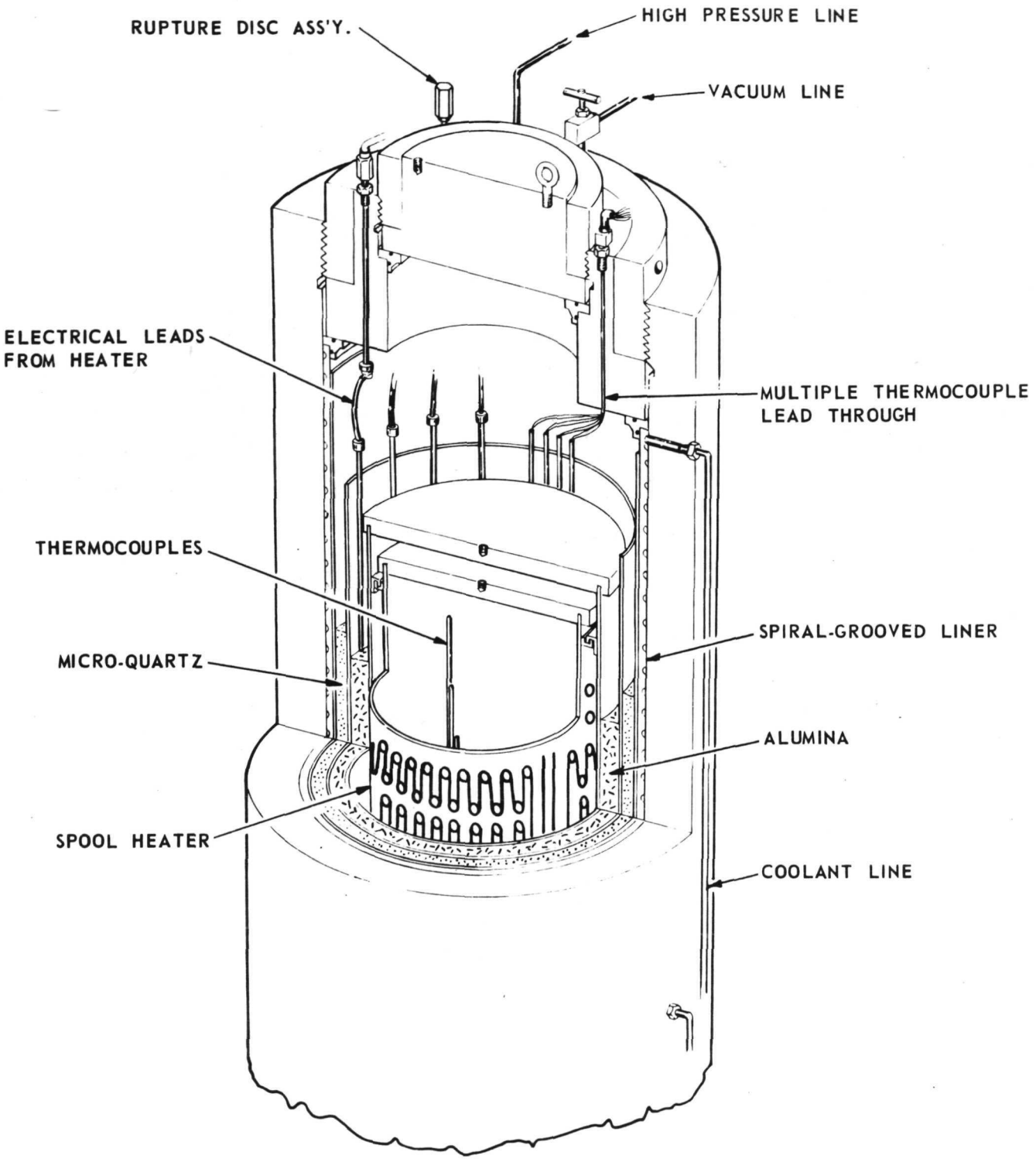

FIGURE 2. HIGH-TEMPERATURE COLD-WALL AUTOCLAVE

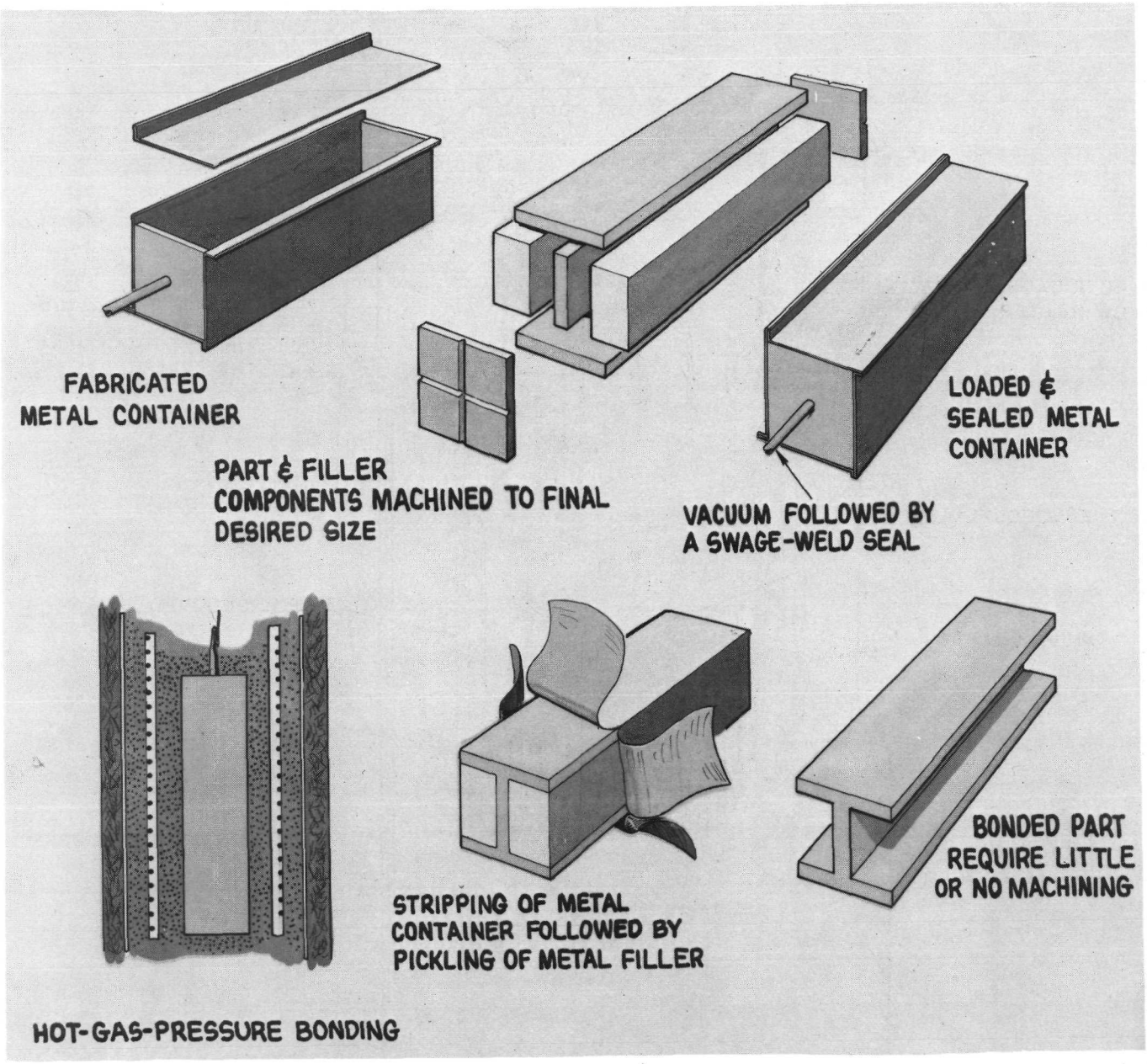

FIGURE 3. GAS-PRESSURE BONDING PROCESS SCHEMATIC

PROCESS DEVELOPMENT STUDIES

Procurement and Characterization of Materials

B1900 Castings

A quantity of cast B1900 plates, 2 by 10 by 0.125 in., and cylinders, 2.5-OD by 0.125-wall by 2 in. high, were procured.* These investment castings were prepared by the vendor in accordance with Specification PWA-663E from a vacuum-melted master heat consisting of 100 percent virgin materials. The heat employed for the cylindrical castings procured for this program was also used by the vendor to cast production turbine vanes.

The vendor certification and subsequent evaluation performed at Battelle were compared against Specification PWA-663. The data obtained during this characterization are summarized in Table 1. The material was found to meet the specification. All plate castings were radiographed and found to be essentially free of defects. An occasional microvoid was detected in several plates; however, the size and location of these voids were such as to be of no significant concern. Radiography also pointed up local thickness variations in and among the various castings of the order of ±10 percent.

Sample castings were examined metallographically both in the as-received (as cast) condition and after the PWA-663 heat treatment.** Representative microstructures of the two conditions are presented in Figures 4 and 5, respectively. The structures appeared quite normal. Hardness was determined prior and subsequent to heat treatment; the response appeared normal. The as-cast hardness was R_C 36; the heat-treated hardness was R_C 41.

Udimet 700 Sheet

A quantity of developmental Udimet 700 sheet was procured*** and characterized. The sheets were nominally 6 by 18 by 0.060 in., and were supplied by the vendor in a solution-annealed condition (2000 F ± 25 F/water quench) and with a sand-blasted surface. No commercial specification for Udimet 700 in sheet form existed. Hence, a forged blade specification, General Electric C50T6457, was employed as a guide to compositional limits. The vendor in-house specification and typical bar properties were used to gage mechanical properties. Table 2 summarizes the data obtained. Difficulty was encountered in arriving at a satisfactory balance between a need to protect the sheet from air at temperatures above 1800 F (a precaution not generally of concern in bar stock) and a sufficiently rapid quench

*B1900 castings supplied by Austenal Company under license to Pratt & Whitney Aircraft.

**2000 F for 20 min in air/air cool; repeated treatment; 1975 F for 4 hr/air cool; 1650 F for 10 hr/air cool; all temperatures ±25 F.

***Supplied by ALLVAC-Teledyne.

TABLE 1. B1900 ALLOY CASTING CHARACTERIZATION SUMMARY

	Heat Identification		
	54V3979 (Plates)	54V3630 (Cylinders)	PWA-663 Specification
Composition, w/o			
Carbon	0.10	0.11	0.08 - 0.013
Manganese	0.01	0.01	0.20 max
Sulfur	0.001	0.001	0.015 max
Silicon	0.12	<0.10	0.25 max
Chromium	7.73	7.98	7.50 - 8.50
Cobalt	9.75	10.10	9.50 - 10.50
Molybdenum	6.03	6.03	5.75 - 6.25
Aluminum	6.00	6.00	5.75 - 6.25
Tantalum	4.38	4.27	4.00 - 4.50
Titanium	1.02	1.00	0.80 - 1.20
Boron	0.013	0.012	0.010 - 0.020
Zirconium	0.07	0.08	0.05 - 0.10
Iron	0.16	0.16	0.35 max
Tungsten	<0.10	<0.10	0.10 max
Niobium	0.10	<0.10	0.10 max
Nickel	Balance	Balance	Balance
Room-Temperature Mechanical Properties[a]			
Ultimate Tensile Strength[b], ksi	133 (131)	135	125 min
Yield Strength at 0.2% Offset[b], ksi	111 (123.5)	114	111 min
Tensile Elongation[b, c], percent in 1 in.	6.0 (4.5)	6.0	5.0 min
R_C Hardness[b]	37 (41)	35	34 - 44
Stress Rupture at 1400 F			
Stress, ksi	94	94	94
Life, hr	35.3	43.8	>23
Elongation, percent in 1 in.	1.8	2.3	>1.5
Stress Rupture at 1800 F			
Stress, ksi	29	29	29
Life, hr	39.9	43.7	>30
Elongation, percent in 1 in.	6.0	6.0	>3.0

(a) All properties obtained from material heat treated in accordance with PWA-663.
(b) Values in parentheses represent average of three or more determinations at Battelle.
(c) Elongation in Battelle tests was based on 2-in. gage length, which is responsible for low apparent elongation value.

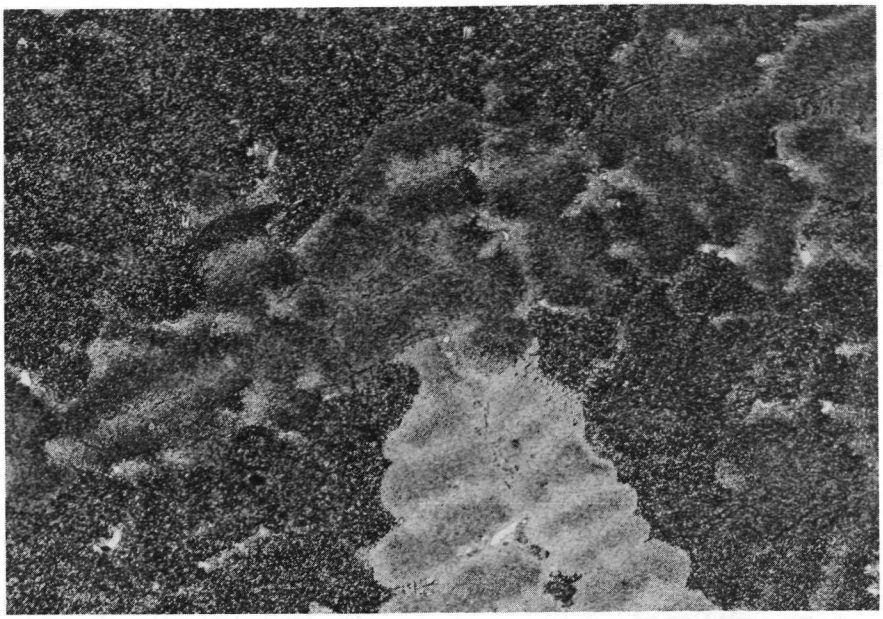

100X 50 H_2O:50 NCl:25 HNO_3 3C869

a. Etched

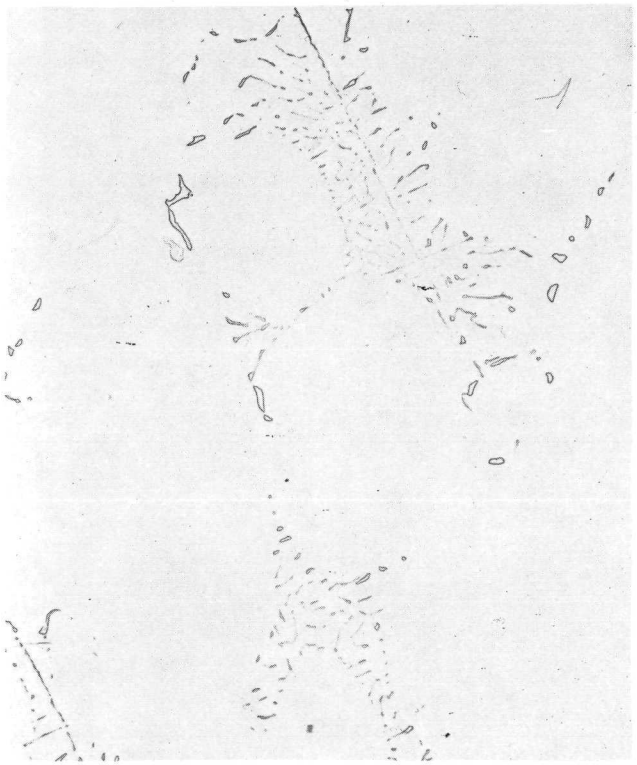

250X 3C868

b. As Polished

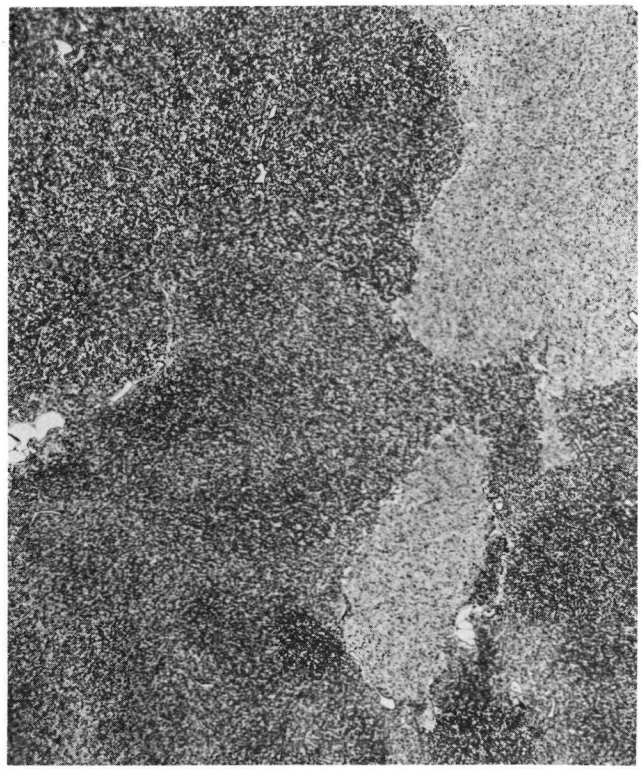

250X 50 H_2O:50 HCl:25 HNO_3 3C870

c. Etched View at Higher Magnification

FIGURE 4. MICROSTRUCTURE OF TYPICAL B1900 CASTING IN AS-RECEIVED (AS CAST) CONDITION

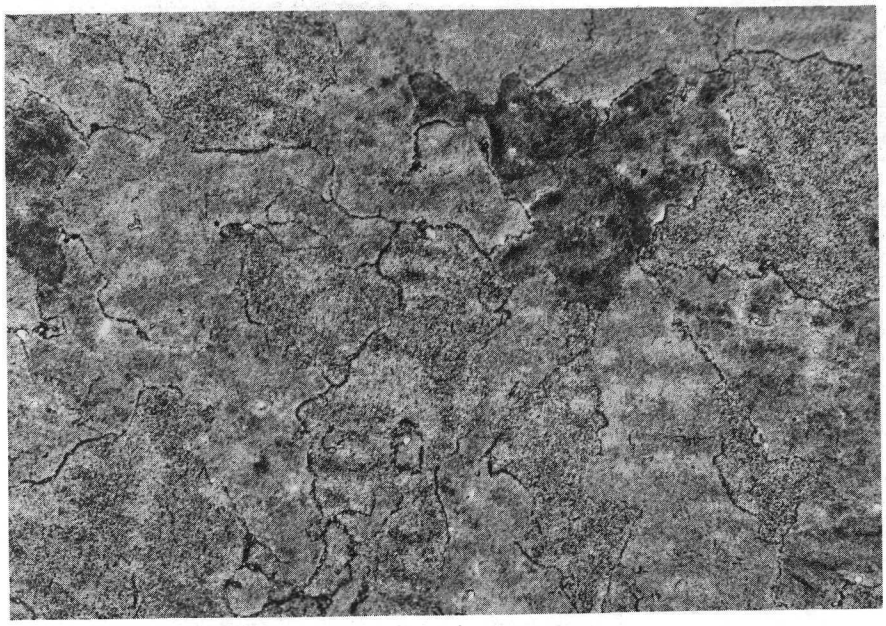

100X 50 H_2O:50 HCl:25 HNO_3 3C872

a. Etched

250X 3C871

b. As Polished

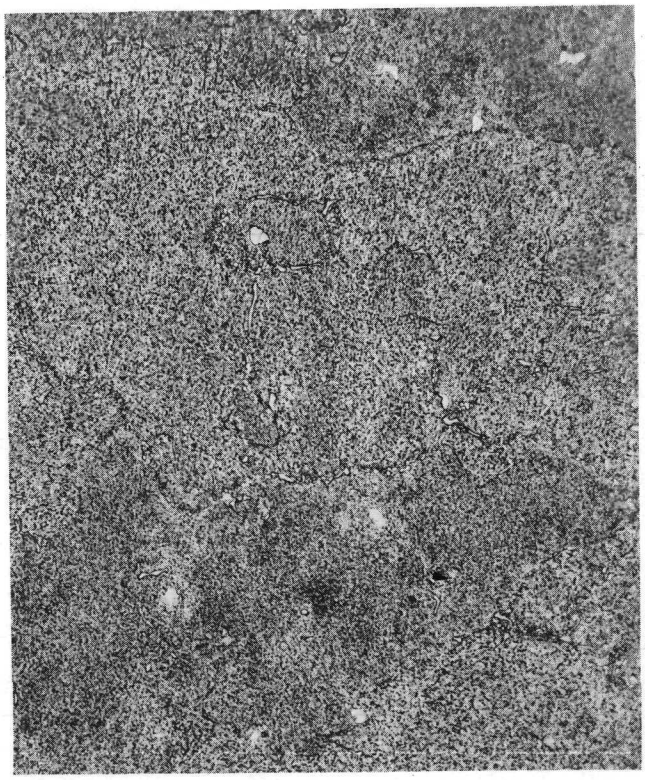

250X 50 H_2O:50 HCl:25 HNO_3 3C873

c. Etched View at Higher Magnification

FIGURE 5. MICROSTRUCTURE OF TYPICAL B1900 CASTING AFTER HEAT TREATMENT SPECIFIED IN PWA-663

TABLE 2. UDIMET 700 ALLOY SHEET CHARACTERIZATION SUMMARY

	Heat 6541	GE Specification C50T64S7
Composition, w/o		
Carbon	0.113	0.15 max
Manganese	0.01	0.15 max
Silicon	0.02	0.20 max
Sulfur	0.004	0.015 max
Chromium	14.85	13.00 - 17.00
Titanium	3.45	2.75 - 3.75
Boron	0.013	0.010 - 0.018
Aluminum	4.55	3.75 - 4.75
Cobalt	17.50	14.00 - 20.00
Molybdenum	5.10	4.50 - 5.50
Iron	0.85	4.00 max
Copper	0.01	0.10 max
Zirconium	<0.02	0.06 max
Nickel	Balance	Balance

	Solution Annealed[a] (Air Cool)	Aged[b] (Furnace Cool)	Typical Values[c]
Room-Temperature Mechanical Properties[d]			
Ultimate Tensile Strength, ksi	175	185	204
Yield Strength at 0.2% Offset, ksi	131	115	140
Tensile Elongation, percent in 2 in.	16	17	16 - 22
R_C Hardness	46	--	38 - 42

(a) Heat treated in air through first step of C50T64S7 sequence only (2135 ± 15 F/4 hr/air cool) due to severe oxidation.

(b) Heat treated through full C50T64S7 sequence in vacuum followed by argon quench. Quench rate was not equivalent to air cool. Sequence consists of 2135 ± 15 F/4 hr/air cool; 1975 ± 25 F/4 hr/air cool; 1550 ± 25 F/24 hr/air cool; 1400 ± 25 F/16 hr/air cool.

(c) No values for room-temperature strength are specified in C50T64S7; typical values are for bar stock taken from "High Temperature High Strength Nickel Base Alloys", International Nickel Company, Inc. (1964).

(d) Mechanical properties measured at Battelle are an average of three determinations.

time for an effective solutionizing treatment. A proper balance was not achieved. Consequently, mechanical properties were about 10 percent below typical bar values.

Samples were examined metallographically in the as-received condition and after solution annealing in air. The as-received condition represents a slightly lower annealing temperature, 2000 ± 25 F, and a small amount of postanneal working from the rapid quench, sand blast, and roller leveling.* This condition is illustrated in Figure 6. The higher solution-anneal temperature, 2135 ± 15 F, as illustrated in Figure 7, results in a significantly larger grain size. Figure 7c illustrates the surface corrosion and alloy depletion encountered during air atmosphere annealing.

TD NiCr Sheet

Two sheets of nominally 0.060-in.-thick TD NiCr sheet were procured. Vendor and Battelle characterization data for both sheets were compared against commercial specifications for this developmental material. The results of this comparison are summarized in Table 3. Both sheets met specifications for room-temperature properties and composition. Sheet No. 1 (Heat 2697-1) did not meet the specification for 2000 F properties; the vendor did not wish to release this sheet for that reason. The properties were within 10 percent of minimum, however, and the material was accepted as satisfactory for the purpose of joining development. A representative microstructure of this material is shown in Figure 8.

Generation of Process Evaluation Specimen Components

During the course of the process development effort, several specimen geometries were evolved and employed to evaluate various facets of the cooled turbine blade fabrication problem. Unmachined coupons were used initially; later, more complex specimens of the design shown in Figure 9 were evolved to obtain torsion-induced shear strength data. Lastly, specimens of the design shown in Figure 10 were fabricated for compression-induced shear strength information and to simulate the problems posed in the bonding of a finned sheet metal shell to a cast blade strut. This shell specimen consists of two zones of 0.012-in. fins (L and N) on either side of a zone of 0.036-in. fins (Zone M). Central to specimen component generation was an evaluation of machining methods applicable to the TD NiCr and Udimet 700 components. Conventional milling, photoetching, electrochemical machining (ECM), and electrical discharge machining (EDM) were considered. In all specimen configurations, the B1900 component consisted of an unmachined 2 by 2-in. square prepared by edge grinding. Pursuant to the objectives of the program, the bonding surface of the B1900 component plate was never ground or otherwise treated to remove existing, as-received surface irregularities.

*The as-quenched condition left the sheet in an unacceptable warped condition. The vendor subsequently straightened the sheet by roller leveling.

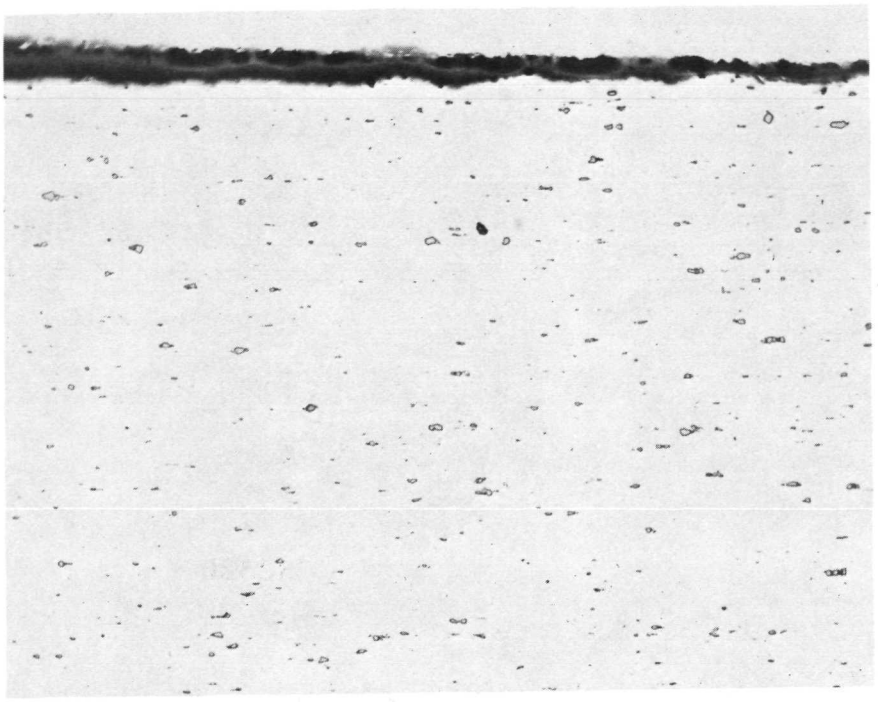

100X 4C128

a. As-Polished View

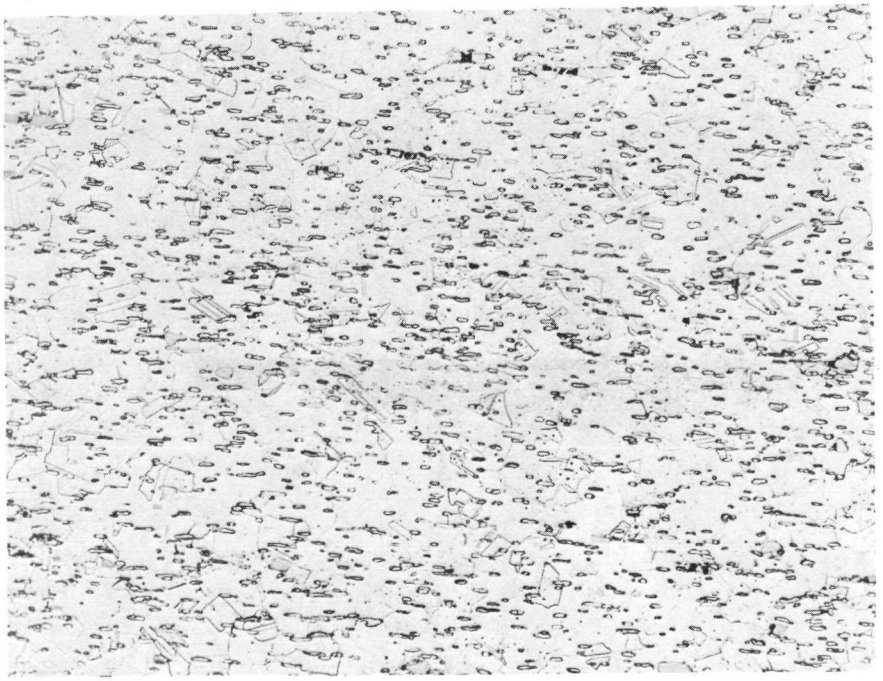

250X Marble's Etch 4C131

b. Etched View

FIGURE 6. MICROSTRUCTURE OF AS-RECEIVED UDIMET 700 SHEET

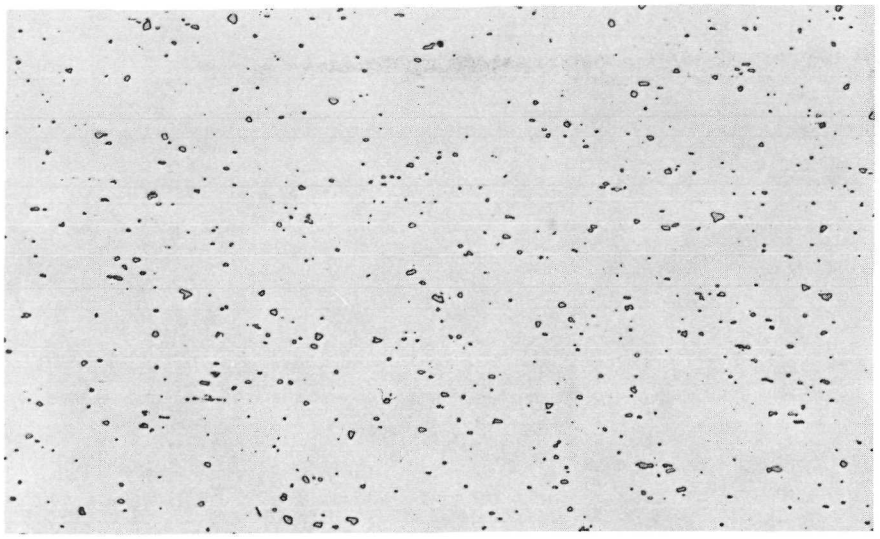

a. Sheet Center As Polished

100X 5C320

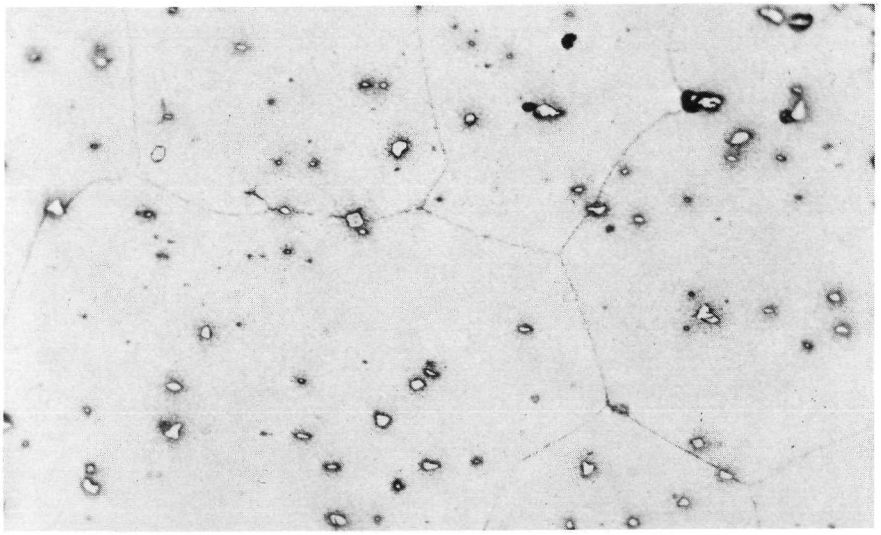

b. Sheet Center Etched

250X Marble's Etch 5C322

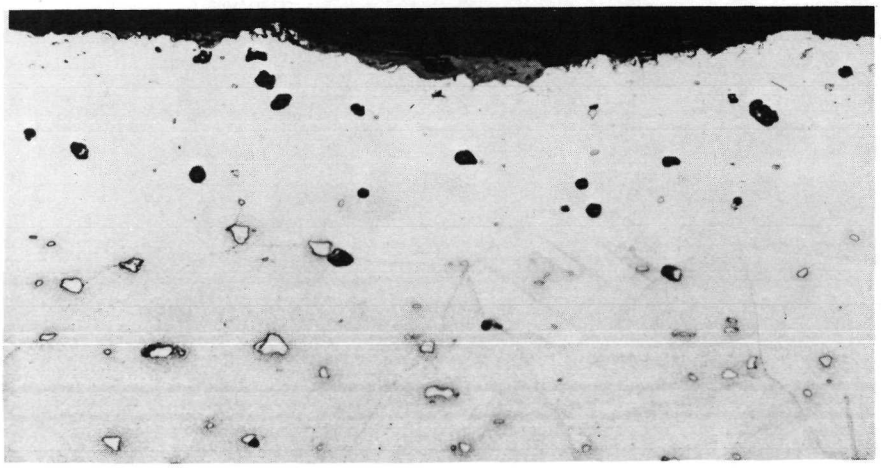

c. Sheet Surface Etched

250X Marble's Etch 5C325

FIGURE 7. MICROSTRUCTURE OF UDIMET 700 SHEET AFTER A SOLUTION ANNEAL IN AIR AT 2135 F FOR 4 HR FOLLOWED BY AIR COOLING

TABLE 3. TD NiCr ALLOY SHEET CHARACTERIZATION SUMMARY

	Heat Identification		Specification B50TF46S1 (GE) and MMS-1503 (MDAC)
	2697-1	2789-1	
Composition, w/o			
Chromium	19.38	19.31	19.00 - 23.00
ThO_2	1.9	1.9	1.80 - 3.00
Nitrogen	0.004	0.006	Not specified
Carbon	0.0241	0.0195	0.10 max
Sulfur	0.0061	0.0054	0.05 max
Cobalt	Not determined	Not determined	0.30 max
Copper	Not determined	Not determined	0.20 max
Nickel	Balance	Balance	Balance
Room-Temperature Mechanical Properties[a]			
Ultimate Tensile Strength[b], ksi	126.6 (131)	126.8	115 min
Yield Strength at 0.2% Offset[b], ksi	89.6 (93)	84.7	75 min
Tensile Elongation[b], percent in 1 in.	18.0 (16)	21.3	10 min
105-Deg Bend, T	3	1.5	4 min
R_C Hardness[c]	30	--	30 typical
2000 F Mechanical Properties[a]			
Ultimate Tensile Strength, ksi	13.6	17.1	15 min
Yield Strength at 2% Offset, ksi	13.4	16.6	Not specified
Tensile Elongation, percent in 1 in.	2.0	4.4	2.0 min
Stress Rupture			
Stress, ksi	4.0	5.5	6.0
Life, hr	>20	>20	>20
Elongation, percent	7.4	7.8	Not specified

(a) Material tested in stress-relieved condition.

(b) Values in parentheses are an average of three Battelle determinations.

(c) Battelle hardness data; average of six determinations; room-temperature hardness is not specified in either commercial specification.

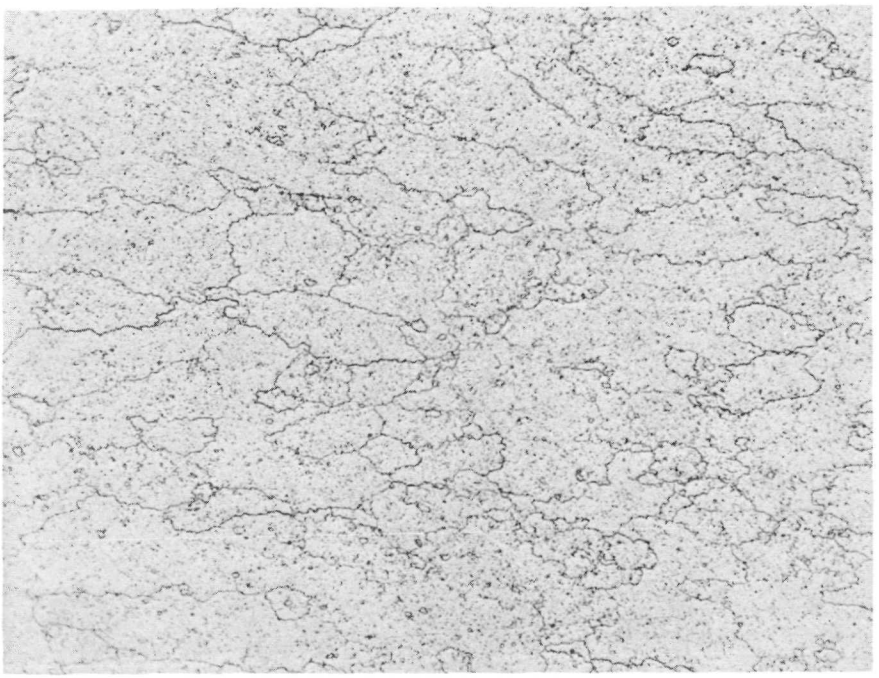

250X Electroetch in 10% Oxalic Acid at 4 V 4C133

FIGURE 8. TYPICAL MICROSTRUCTURE OF AS-RECEIVED TD NiCr SHEET

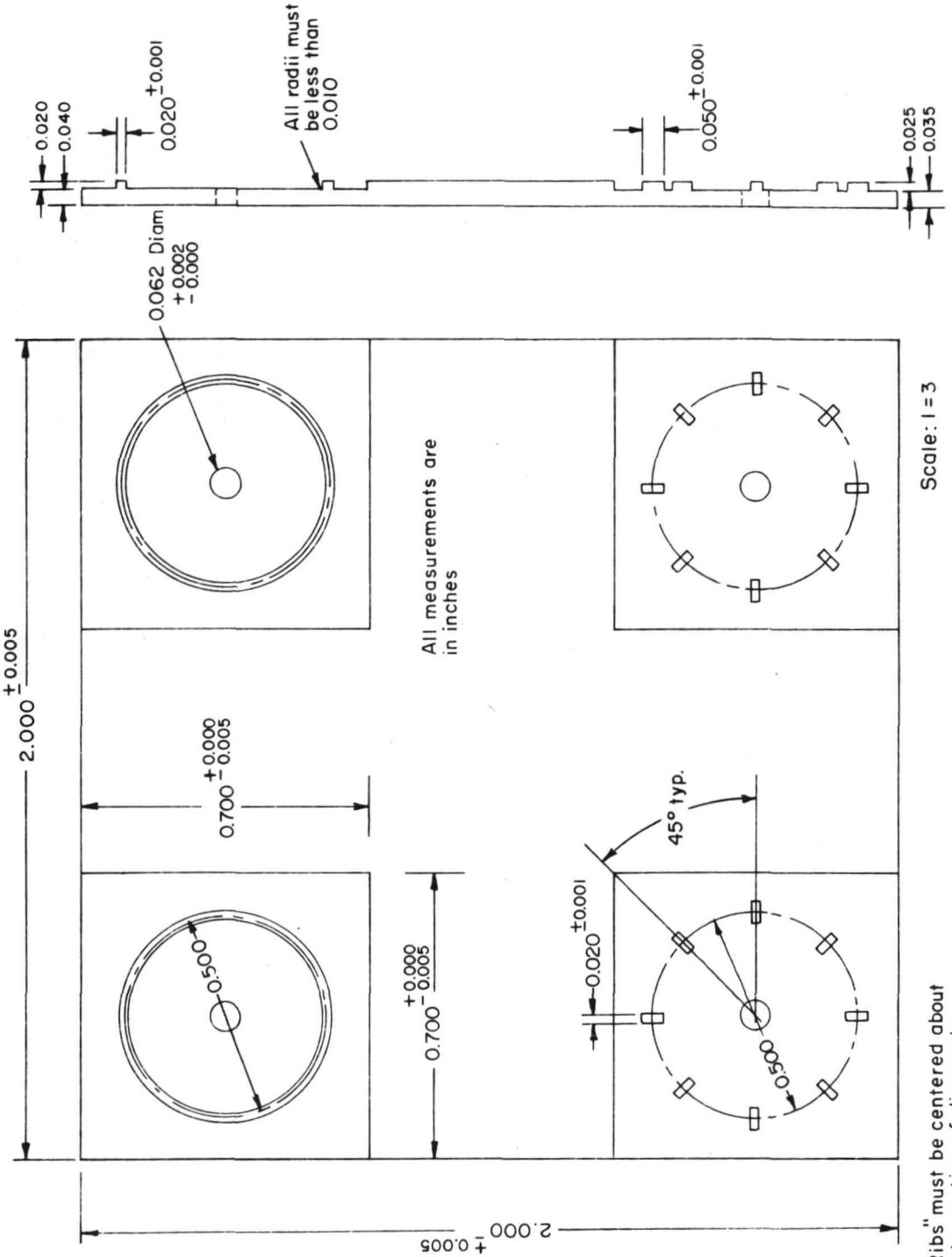

FIGURE 9. SKETCH OF TD NiCr OR UDIMET 700 COMPONENT OF BONDING COUPON DESIGNED TO YIELD TORSIONAL SHEAR SPECIMENS

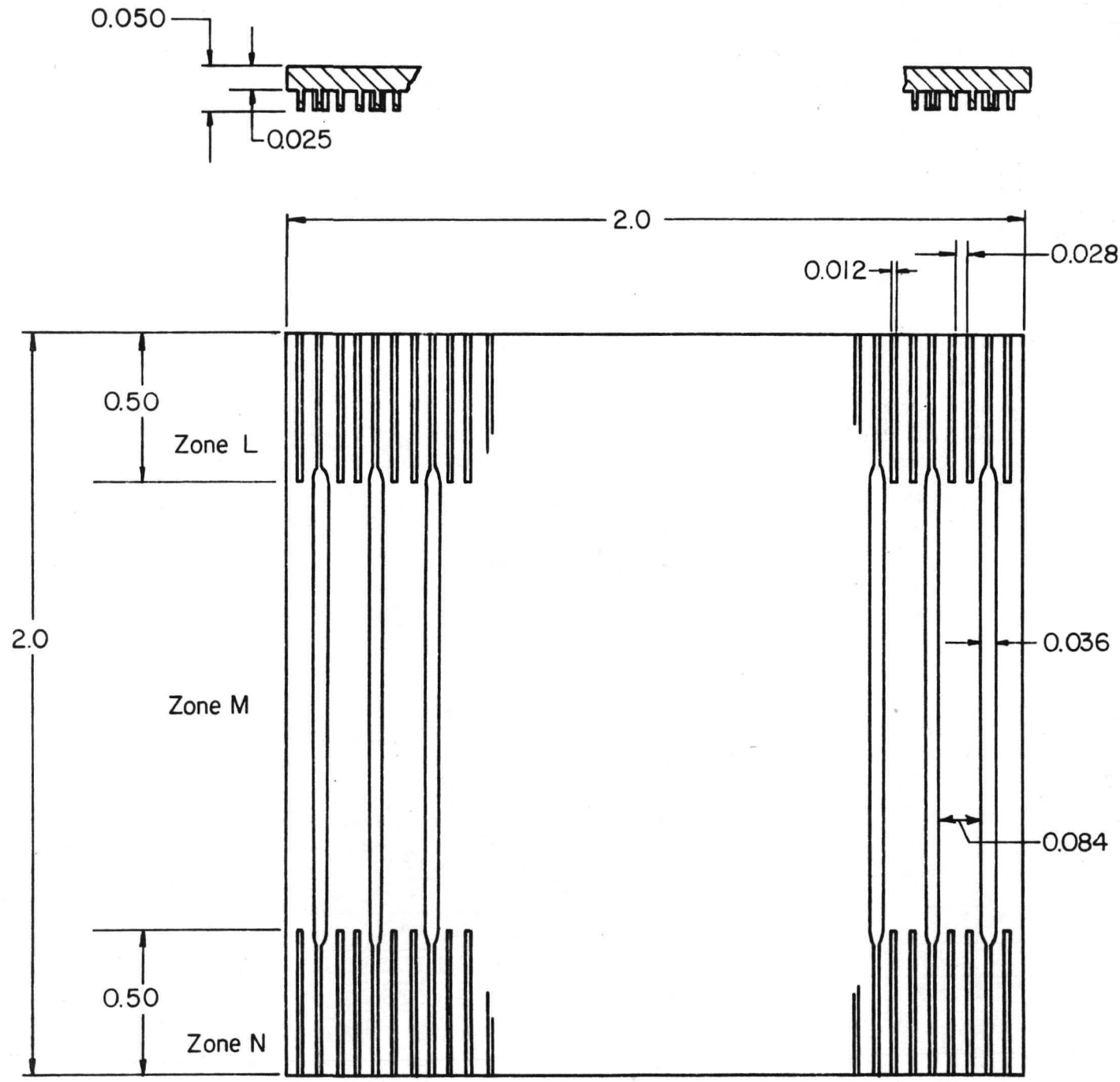

FIGURE 10. SKETCH OF FINNED SHELL COMPONENTS PREPARED FROM UDIMET 700 OR TD NiCr SHEET

Compression shear specimens were derived from this component after bonding to a B1900 plate.

Variations in bond surface profile across a typical as-cast 2 by 2-in. square B1900 plate component commonly were of the order of 0.010 in.

Unmachined Coupons

Initial parametric experiments in each of the two joint systems of concern, B1900/TD NiCr and B1900/Udimet 700, utilized unmachined 2 by 2-in. coupons. The sheet metal components were prepared by shearing blanks at room temperature, which were than ganged and edge ground. The B1900 was rough cut using a thin SiC wheel, ganged, and edge ground to final size. The specimens produced from these coupons were employed for metallographic evaluation of general bond quality as a function of bonding temperature, pressure, and time, and of various surface conditioning treatments such as cleaning, etching, electropolishing, abrasion, and plating. In certain instances, the bonded plain coupons were machined for evaluation by torsional shear and tensile shear.

Evaluation and Selection of Candidate Machining Techniques

Conventional milling techniques were quickly rejected on the basis of cost. Preparation of either the torsional shear or finned shell configurations, shown previously in Figures 9 and 10, with either a rotary cutter or end mill would require relatively expensive, nonstandard tools. Tool life would be short, and labor cost high. Electrochemical machining (ECM) was judged to be probably the optimum method for preparing production quantities of finned shells. The method appeared to require more effort in the area of tooling and process parameter definition than could be justified by the small number of specimens needed in the present effort. Consequently, the evaluation was quickly narrowed to two alternatives, photoetching and electrical discharge machining (EDM). A brief experimental evaluation was conducted on each.

Test panels of TD NiCr and Udimet 700 were coated with KMER* photoresist. The resist was exposed through a mask simulating the finned shell pattern. Subsequently, the resist was developed, and the panels etched. Previous experiments had shown that an etch composed of equal parts of concentrated HCl, HNO_3, and 42-deg Bé $FeCl_3$ performed well on Udimet 700; a solution of 20 percent HCL, 20 percent HNO_3, and 60 percent 42-deg Bé $FeCl_3$ similarly performed well on TD NiCr. The panels were etched in a splash-type system. It was found that etching depth could be controlled with satisfactory precision. The etching rate was approximately 0.00035 in. per min. As long as etching was terminated at a shallow depth, less than 0.005 in. typically, a satisfactorily sharp channel sidewall configuration could be maintained, and patterns such as shown earlier in Figures 9 and 10 could be produced with a precision level of the order of ±0.001 in. As the etched depth was increased to the required 0.025 in., however, the sidewall profile became very unsatisfactory as a consequence of side cutting, i.e.,

*Eastman Kodak Company.

undercutting of the photoresist. At the original surface plane, TD NiCr was cut 0.001 in. laterally at each side for every 0.003 in. of depth cut. In a similar fashion, Udimet 700 was etched 0.001 in. laterally per side for every 0.002 in. of depth cut. Figure 11 demonstrates the effect of lateral cutting. Both the Udimet 700 and TD NiCr samples illustrated were etched to a depth of 0.025 in. The resulting channel sidewall profiles are shown and compared by means of the line overlay to an ideal machined profile.

To prepare a Udimet 700 finned shell pattern in Zones L and N where the fins are 0.012 in. and the channels 0.028 in., for example, the unexposed resist in the pattern could only be 0.004 in. wide to account for the 0.024 in. of total anticipated lateral cutting that would occur in etching to a 0.025-in. depth. The resulting channel cross section would be nearly semicircular according to the results shown by the samples illustrated in Figure 11. The flow area available for blade cooling air would be considerably less than that afforded by the nearly rectangular cross section shown in Figure 10.

With some reluctance, photoetching was abandoned in favor of EDM which could yield the preferred channel configuration within the state of the art. For the limited number of samples required, EDM was judged to be both more economical and expeditious. For the sake of uniformity, it was concluded that the torsional shear specimens as well as the finned shell components should be prepared by EDM. It did appear probable, however, that the former could have been satisfactorily prepared by the photoetch method. Advances made in photoetching technology, notably spray etching systems and special techniques for minimizing side etching, since the time of these experiments would possibly lead to a different conclusion in regard to the preferred finned shell machining method.

Application of EDM to Torsional Shear and Finned Shell Components

Methods were devised during this portion of the program to ensure a high degree of dimensional control in the machined Udimet 700 and TD NiCr sheet components. As-received sheet stock was found to be far from flat and not readily responsive to flat annealing. Consequently, it was necessary to use an oversize blank which was then brought to within 0.001 in. of flat by firmly fixturing it to the bed of the EDM machine. Lack of such a step to flatten the blank during machining gave rise to cutting depth variations of the order of 0.010 to 0.015 in. over a 2 by 2-in. blank. EDM electrode design and fabrication were found to be critical to achieving and maintaining dimensional tolerances. In the case of the finned shell, the most satisfactory electrode design consisted of three precision machined components which were mechanically joined and subsequently low-temperature brazed to a steel backing plate. An example is shown in Figure 12. The electrode fins, which produce the channels of the finned shell workpiece, were 0.250 in. deep. Deeper fins had a tendency to warp laterally with respect to the fin direction, causing errors of the order of 0.010 in. in fin position. Joints in the electrode made parallel to the fin direction and not firmly joined by a method such as described above had a tendency to open up during EDM, leaving unacceptably high ridges in the machined workpiece at the position of the open

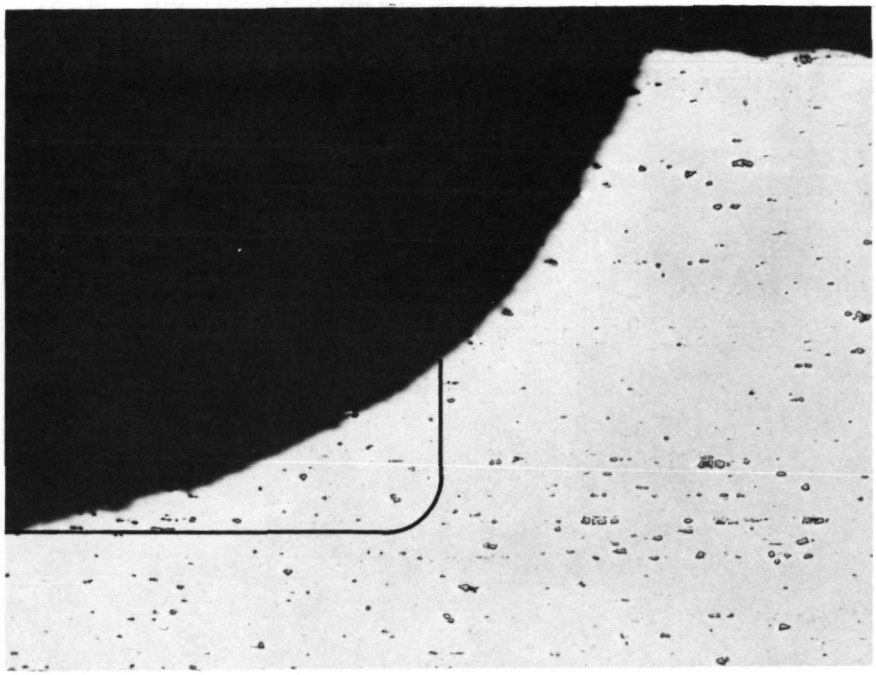

100X As Polished 4C127

a. Udimet 700 Sample

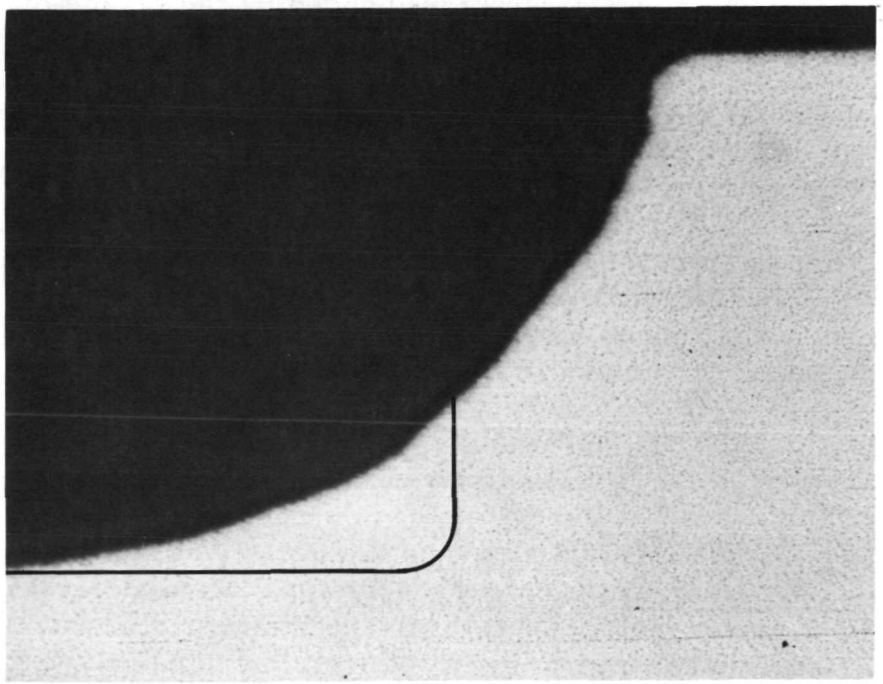

100X As Polished 4C129

b. TD NiCr Sample

FIGURE 11. CROSS SECTION OF 0.024-IN.-DEEP CHANNEL PRODUCED BY PHOTOETCHING

joint. Employing the mechanical fixturing of the blank and the above approach to electrode fabrication, tolerances of ±0.001 in. were held on fin and channel width and height. Position of the fin centerline was held to within ±0.003 in. of design nominal.

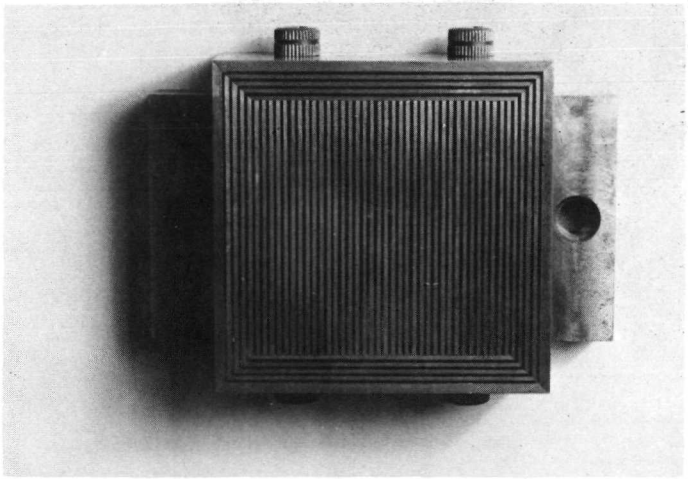

FIGURE 12. TELLURIUM-COPPER EDM ELECTRODE EMPLOYED TO MACHINE BURST-TEST FINNED SHELLS

Channel surface finish was directly influenced by the choice of EDM electrode material. The roughest finish resulted from the use of graphite; brass yielded a slightly smoother finish; and tungsten-copper produced a finish of 45 to 60 μin. rms. A finish in this range appeared desirable for the turbine cooling application, having enough roughness to cause some breakup of the boundary layer air but not irregular to the point where rapid oxidation could effect a change in air flow characteristics. Tungsten-copper exhibited a very favorable wear ratio during EDM and, hence, required less redressing and replacement than brass, for example. However, tungsten-copper is difficult to machine. Through experiment, it was found that tellurium-copper offered a more cost-effective choice. Tellurium-copper was much easier to machine than tungsten-copper and a less costly raw material as well. Moreover, its wear ratio is only slightly inferior to tungsten-copper. Graphite and several copper-base alloys, including tellurium-copper, were evaluated. All of these left a relatively heavy black residue on the machined channel surface. The deposition of this residue is initiated by decomposition of the hydrocarbon electrolyte under the heat released during capacitor discharge in the EDM cycle, and for the present application at least was considered to be a patently undesirable feature of this machining process. The deposit, basically carbon, could have deleterious effects on the properties of Udimet 700 and TD NiCr if not removed, and its successful removal proved to be a rather difficult task. Specialized chemical etching procedures were developed to remove all traces of the deposit.

Figures 13 and 14 illustrate, respectively, representative EDM-prepared torsional shear specimen and finned shell specimen components for bonding development studies. In the case of the torsional shear specimen, Figure 13, carbon steel support tooling was also fabricated by EDM to occupy the empty volume

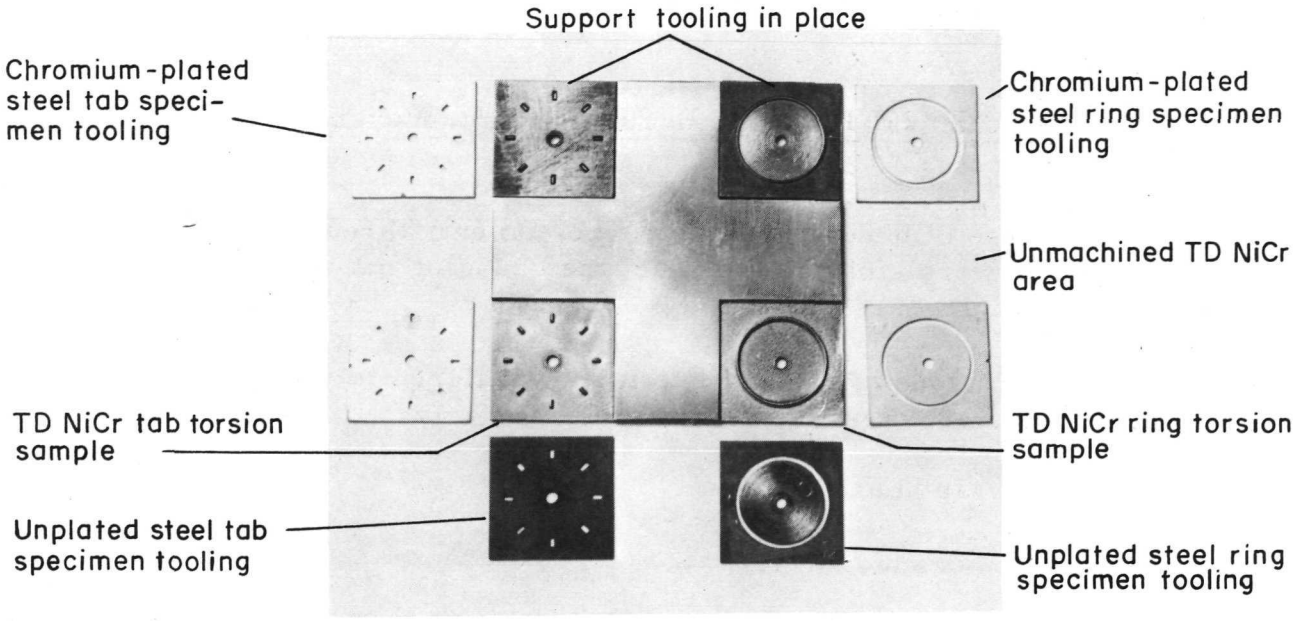

FIGURE 13. TD NiCr TORSION SPECIMEN BONDING COUPON COMPONENT PREPARED BY EDM

The steel support tooling shown was also prepared by EDM.

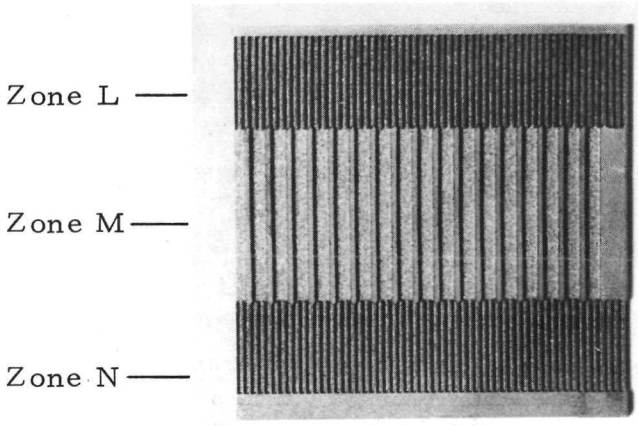

FIGURE 14. UDIMET 700 FINNED SHELL COMPONENT PREPARED BY EDM

about the "rings" and "tabs" of the shear specimen portions of the sample. The support tooling is also shown in Figure 13.

Mechanical Property Evaluation Procedures

During the course of bonding process development, three shear strength evaluation techniques were employed to meet the changing needs of the development effort. These techniques are listed below:

(1) Ring and tab types of torsion specimens designed to yield longitudinal and transverse shear data, respectively

(2) Tensile overlap shear

(3) Compression-loaded shear.

By far the greatest volume of test data was obtained with the compression-loaded technique. This method was most suitable for evaluating the finned shell specimens produced by the bonding process selected during the study. Shear strength data obtained by the torsion method and the compression-loaded method from samples experiencing similar process conditions were found to be in good agreement. Further, tensile overlap shear data, which were obtained from the unmachined area of the bonding coupon shown previously in Figures 9 and 13, also exhibited reasonable agreement. A more detailed discussion of the three evaluation methods follows.

Torsion Shear Test Method

Method Description and Specimen Design. Many shear test methods have a deficiency in that a state of pure shear is not achieved. Consequently, the maximum shear stresses are accompanied by normal stresses which can affect the test results. For the purpose of evaluating bond quality for process development and selection, it was desirable that the shear strength evaluation technique be one in which normal stresses were eliminated. Shear strength data were required in both the longitudinal and transverse directions with respect to the direction of the cooling fins and channels in the bonded structure. In the longitudinal case, a state of pure shear can be developed by fabricating the fin in the form of a closed circle or ring such as shown in Figure 15. A torque applied to the component containing the ring such that the torque axis coincides with the center of the ring will generate pure shear in the bond between the ring and a stationary face plate. The shear stress at the ring/face plate interface, which simulates the finned shell/strut bond interface in an air-cooled turbine blade, is readily calculated.

The component containing the ring was driven at a constant rate by the movable head of a torsion machine. The other component, representing a cast blade

strut, was fixed by the stationary head which was in turn attached to a torsion load cell. This load cell was also instrumented to measure lateral and vertical deflection as well as axial tension and compression forces. A measurement of these undesired forces during machine and grip checkout and in subsequent ring specimen tests showed all forces except torque to be insignificant, as expected.

A similar test method was used to study bond shear strength transverse to the fin direction. The torsion specimen employed to accomplish this test is shown in Figure 16. Here, the torque applied to the sheet metal component is transferred through radial fin elements ("tabs") and the bond to the stationary cast B1900 component by circumferential shear stresses. It was recognized that, in this case, the desired state of pure shear was not achieved because of the tendency of the tabs to bend and thus develop stresses normal to the face plates of the specimen. However, it was concluded that the normal stress magnitude generated was no more severe than that generated in any other transverse direction test. Further, it was desirable to have a similar test specimen geometry and evaluation method for both force application directions required in the study.

The specimens shown in Figures 15 and 16 were designed on the basis of the following considerations:

(1) The possibility of buckling the square face plates (through which the torque is applied) should be minimized. Buckling is discouraged by a high ratio of fin diameter to face-plate edge length.

(2) The distance between the fin and the loaded edges of the face plate should be sufficient to allow local stress effects to damp out. This makes desirable a small ratio of fin diameter to face-plate edge length.

(3) The magnitude of contact pressures on the corners of the face plates should be minimized (the torque is actually applied by pressure at the corners). This makes a small-diameter fin and small fin width desirable.

(4) Shearing of the face plate rather than the fin must be avoided. This requires, as a minimum, that the fin width be less than the face-plate thickness.

(5) The introduction of extraneous stresses ("diagonal tension") in the fin by a tendency to buckle as a tube must be avoided. This makes desirable a small ratio of fin height to fin width.

(6) The radial gradient of shear stresses within the fin should be minimized. This requires a small ratio of fin width to fin diameter.

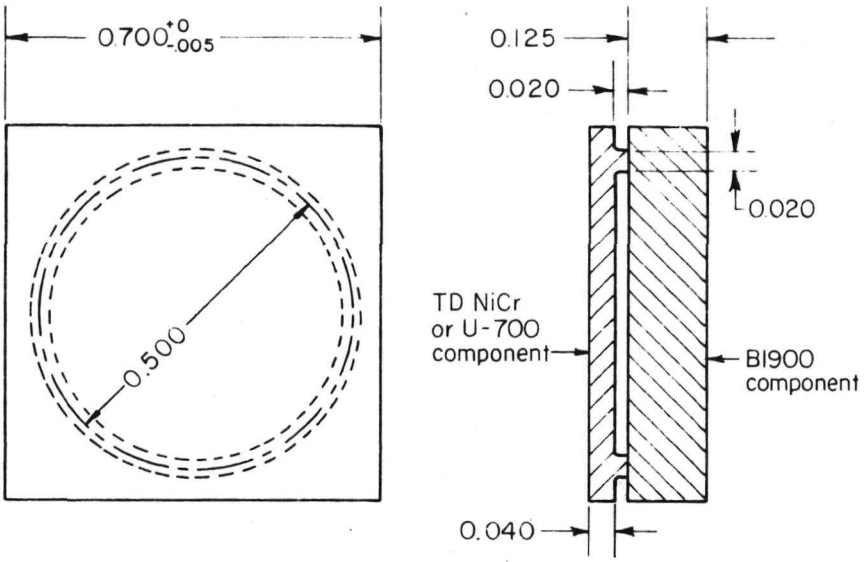

FIGURE 15. CIRCUMFERENTIAL STRESS SHEAR TEST SPECIMEN DESIGN (TORSION RING SPECIMEN)

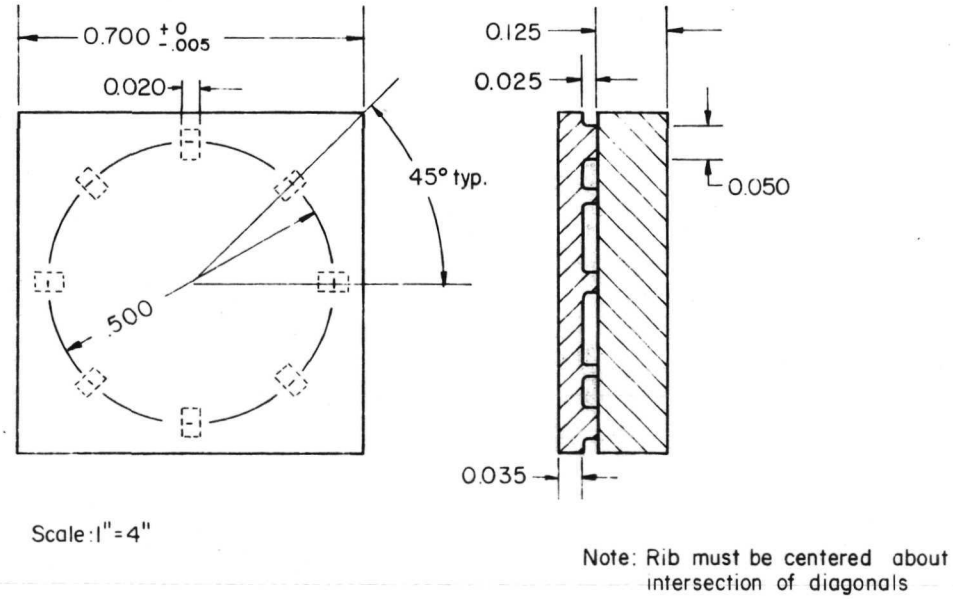

FIGURE 16. TRANSVERSE STRESS SHEAR TEST SPECIMEN DESIGN (TORSION TAB SPECIMEN)

Specimen Fabrication. Three methods of fabrication were employed to produce the specimens shown previously in Figure 15. Initially, both the ring specimen (Figure 15) and tab specimen (Figure 16) were prepared by EDM of the TD NiCr or Udimet 700 sheet component illustrated earlier in Figure 13. The 2 by 2-in. parent coupon was joined to an unmachined B1900 component. Later, the respective ring and tab specimens were cut from the parent coupon before joining to an appropriately smaller B1900 plate.

Alternative methods were employed subsequently to prepare ring-type specimens. Several specimens were fabricated from bonded unmachined 2 by 2-in. coupons. This coupon was sectioned to yield 0.700-in.-square specimens from the corners. A 0.480-in.-diameter hole was then bored in the specimens by EDM to establish the inside diameter of the ring section. Next, the specimen was mounted on a rotating spindle; a 0.062-in.-wide slot was ground from the edge to establish the 0.520-in. outside diameter of the ring. These samples were unsatisfactory in general as a result of the increased slot width, which caused a corresponding decrease in sheet thickness. This led to buckling instability during torsion testing. Figure 17 illustrates a group of TD NiCr/B1900 specimens fabricated by the above approach in which the buckling problem is very evident. It should be pointed out that thinning of the sheet metal component was often in excess of the 0.031 in. anticipated. Grinding wheel wobble contributed up to 0.015 in. additional removal. Hence, the resultant face-plate thickness could be as thin as 0.016 in. as compared to the 0.040 in. called out in the design.

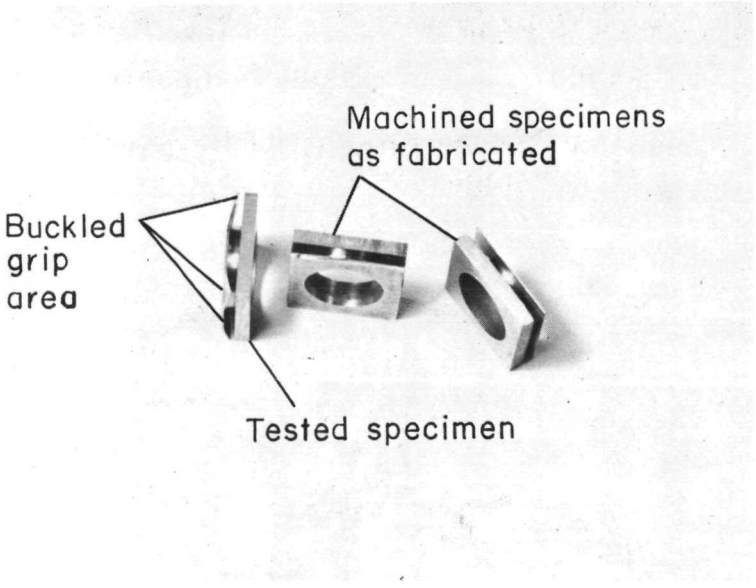

FIGURE 17. TORSION SHEAR SPECIMENS PREPARED FROM BONDED UNMACHINED COUPONS

The specimen at the left buckled during testing.

To eliminate buckling, the sheet metal components in subsequent ring specimens were premachined. Specimens of this type are illustrated in various states of fabrication and after testing in Figure 18. The ring detail, consisting of a

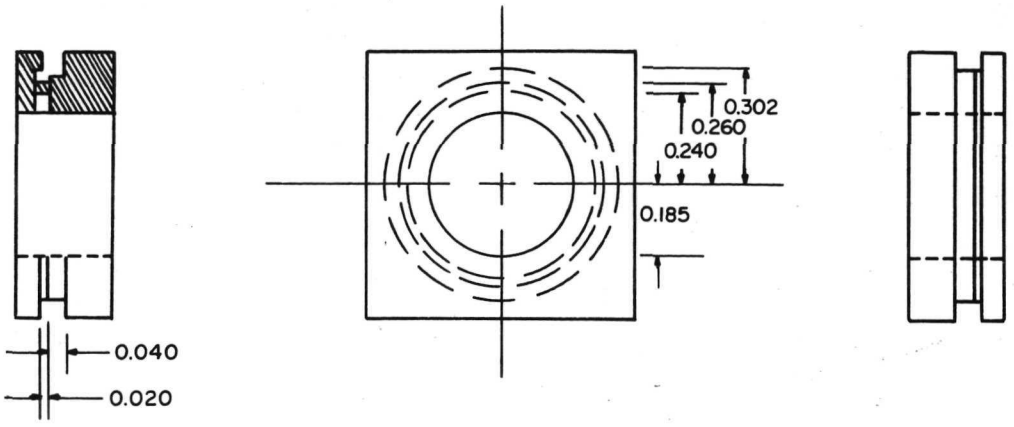

a. Sketch of Specimen Design

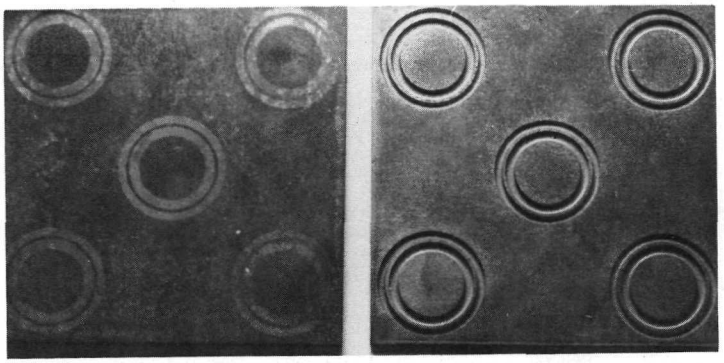

B1900 Shell Component

b. Bonding Coupon After EDM Preparation of Shell Component

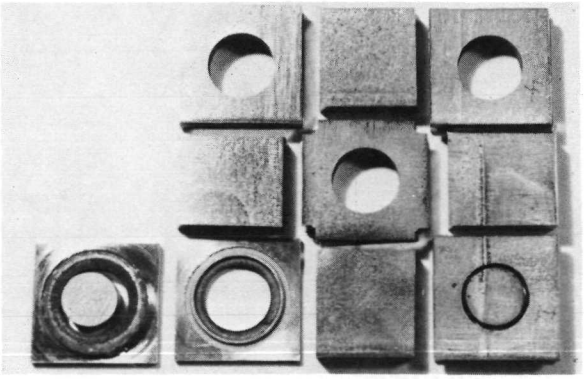

c. Coupon After Bonding and Evaluation

FIGURE 18. TORSION CIRCIMFERENTIAL SHEAR SPECIMEN DESIGNED FOR MAXIMUM BUCKLING RESISTANCE

0.020-in. ring flanked by a 0.042-in. outside and 0.055-in. inside groove 0.020 in. deep, was established by EDM of the sheet component prior to bonding. After bonding, the individual specimens were cut from the parent coupons. A central hole, 0.375 in. in diameter, was pierced by EDM to expose the inside groove. Access to the outside groove was achieved by grinding an edge slot in a fashion similar to the immediately previous approach. In this case, however, the slot was biased toward the B1900 component, leaving the sheet component at least 0.040 in. thick. This yielded an extremely stable specimen configuration which easily transmitted high-torque loads to the ring section without buckling.

While the torsion shear test method proved to be a valuable and easily interpreted tool for evaluating bond strength, the torsion specimen configuration became much less representative of cooled blade hardware as a result of a shift in bonding approach away from the use of support tooling. Further, the process conditions required for finned shell simulations of blade hardware became incompatible with the existing torsion specimen design. Consequently, the torsion method was abandoned in favor of the compression-induced shear test method described later.

Tensile Overlap Shear Test Method

Early in the process development effort a few specimens were evaluated by tensile overlap shear. The specimen configuration is shown in Figure 19. This simple specimen was prepared from bonded, unmachined coupons. The test method appeared to yield reasonably reliable data. However, stresses generated normal to the bond plane in this test were known to be very significant. Because of the nature of the specimen, the bond plane fell between two noncoincident loading planes during the test. This is apparent in Figure 19. As a result, a strong counterclockwise moment was generated about the test section. The test section rotated to relieve the moment. At failure, the degree of rotation was quite significant, as evidenced by the specimens shown in Figure 19b. The specimens were loaded through pin grips by an Instron testing machine using a crosshead rate of 0.02 in. per min.

While tensile overlap shear specimens could have been obtained from finned shell specimens (Figure 14) selected as the medium for process development, very inefficient use of the specimen results. Only four test samples may be cut from a 2 by 2-in. evaluation coupon. Further, to ensure that the fin/strut joint is stressed to failure, assuming near 100 percent joint efficiency, the bond area under test may not exceed the smallest cross section of the finned shell. In practice, only one 0.036-in. (Zone M) or three 0.012-in. (Zones L or N) fins may be evaluated per mechanical test sample. This deficiency could be overcome by bonding or brazing a stiffener to the sheet metal component to increase its tensile-load-bearing capability. However, this was considered a questionable practice since it introduces a processing scheme to which blade hardware would not be subject.

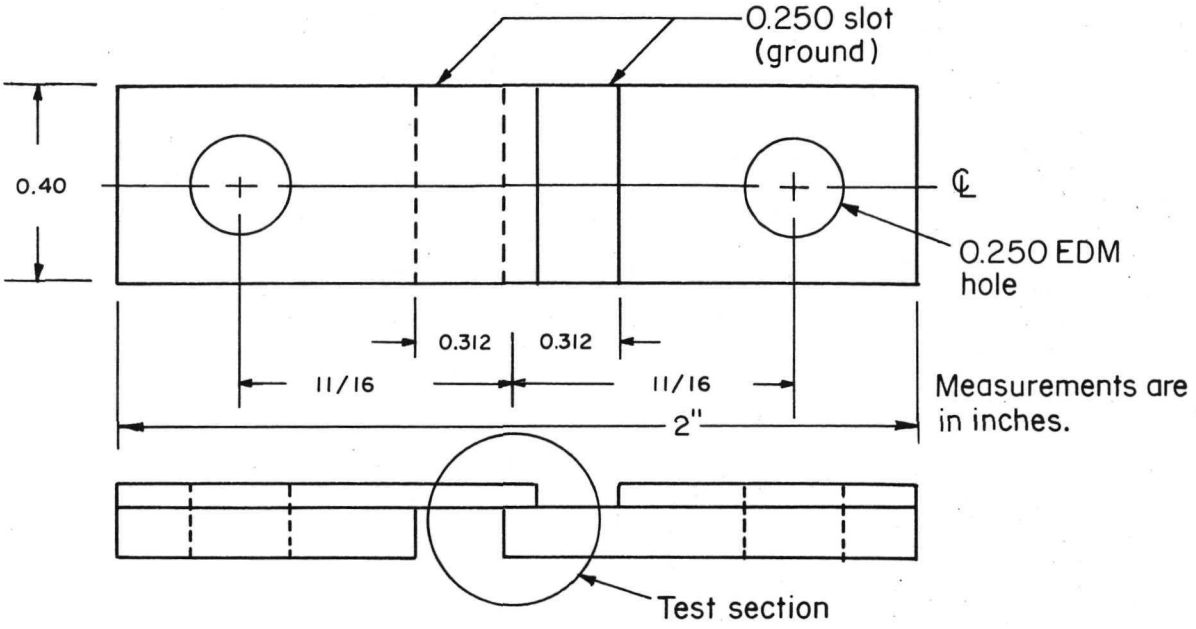

a. Sketch of Specimen Design

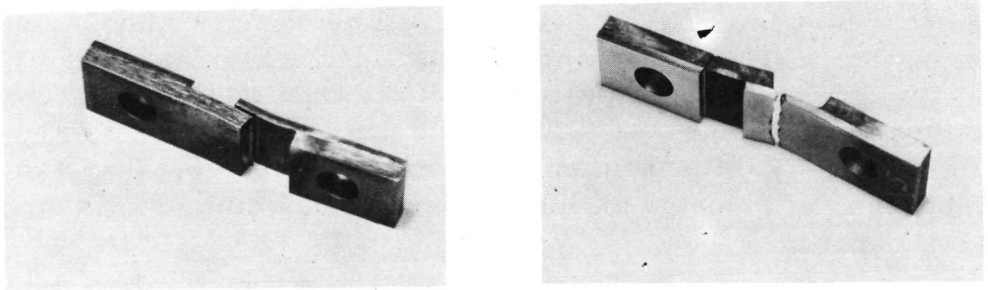

Shear Failure Tensile Failure

b. Specimens After Test; Note Rotation of Test Section

FIGURE 19. TENSILE LAP-SHEAR SPECIMEN PREPARED FROM UNMACHINED COUPONS

Compression-Loaded Shear Test Method

The compression technique was devised as a result of the shift in bonding approach away from support tooling and the decision to employ the finned shell specimen shown earlier in Figures 10 and 14 for bonding process development. Figures 20 and 21 illustrate the shear specimen designs selected for the different fin and channel width zones in the finned shell. Some of the features of the design are enumerated below:

(1) The design yields almost 100 percent efficient utilization of the joining coupon and is inexpensive to prepare.

(2) The sample evaluates over three times more joint area than does the tensile shear specimen which is limited by the tensile load on the shell component.

(3) The same sample may be tested either longitudinally or transversely or may be cut on a nonorthogonal plane.

(4) The samples may be identified with respect to location within the parent joining coupon to evaluate the uniformity of the joint.

(5) The sample is small enough to be mounted for microscopy, removed from the mount, and tested to failure, permitting a high degree of correlation between microstructure and mechanical behavior.

(6) The sample is amenable to testing both at room temperature and 1750 F.

(7) The specimen and test method are amenable to both curved and flat surfaces.

Figure 22 illustrates the loading fixture employed during room-temperature tests; two actual fixtures, flat and curved specimen models, are illustrated in this figure along with a flat specimen. The loading fixtures are essentially compression cages in which the load-transmitting members are fully supported by an external member to minimize unwanted tensile and flexural forces on the test specimen. The fixture is loaded in tension using an Instron or other universal testing machine; the test generates a load-time or load-displacement diagram, depending on test setup. Shear stress at failure was calculated by dividing the failure load by the actual fin area under test as determined by postfailure measurement. The measurement procedure was standardized. Each fin was measured at three points (both ends and center) along its length using a 10X-magnification optical micrometer. The specimen area was then computed as the sum of the products of average fin width multiplied by fin length. This measurement and area determination procedure was used for all room- and elevated-temperature compression shear tests performed in this program. All tests were performed at a standard crosshead displacement rate of 0.02 in. per min.

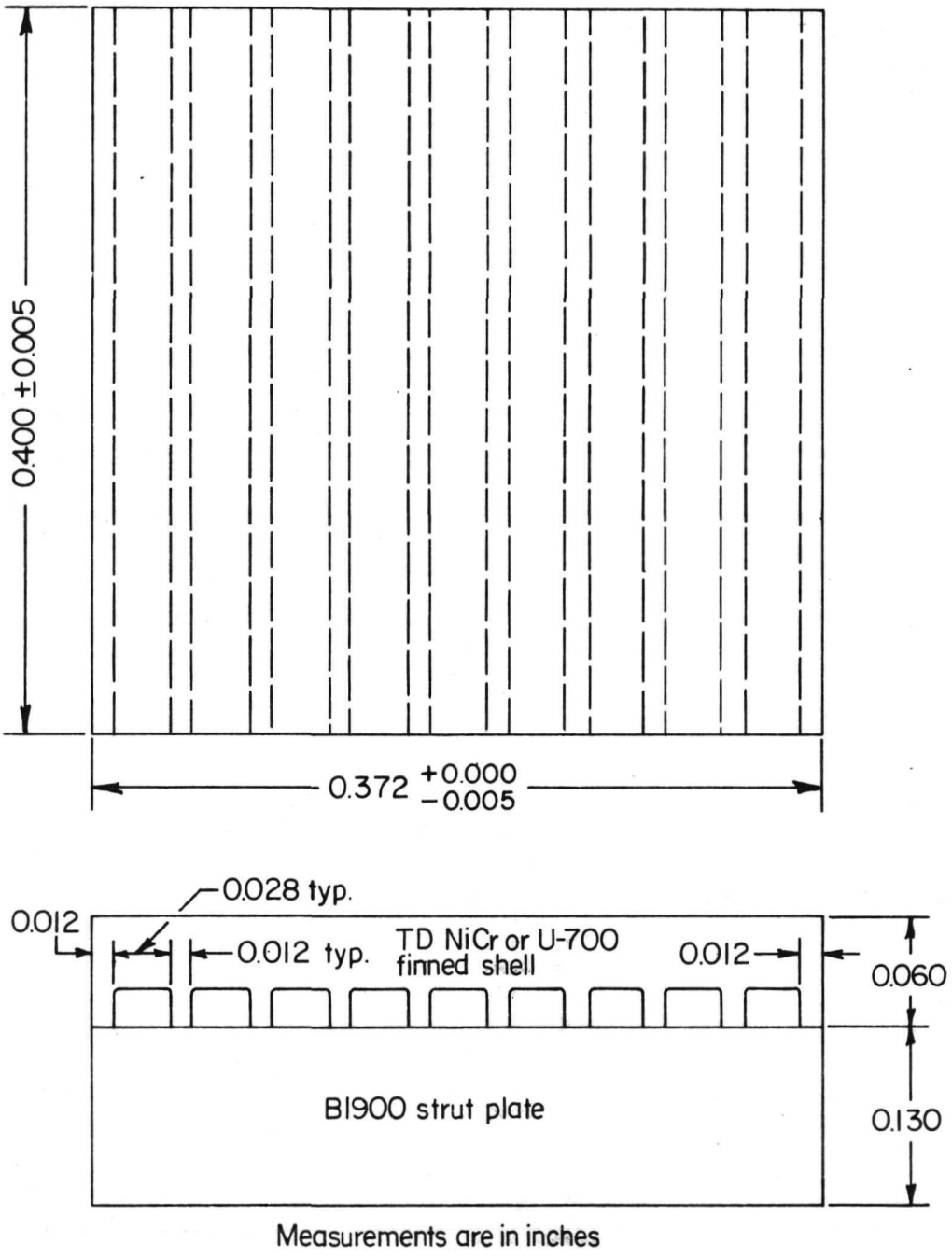

FIGURE 20. SKETCH OF ZONE L SPECIMEN FOR TESTING IN COMPRESSION-INDUCED SHEAR

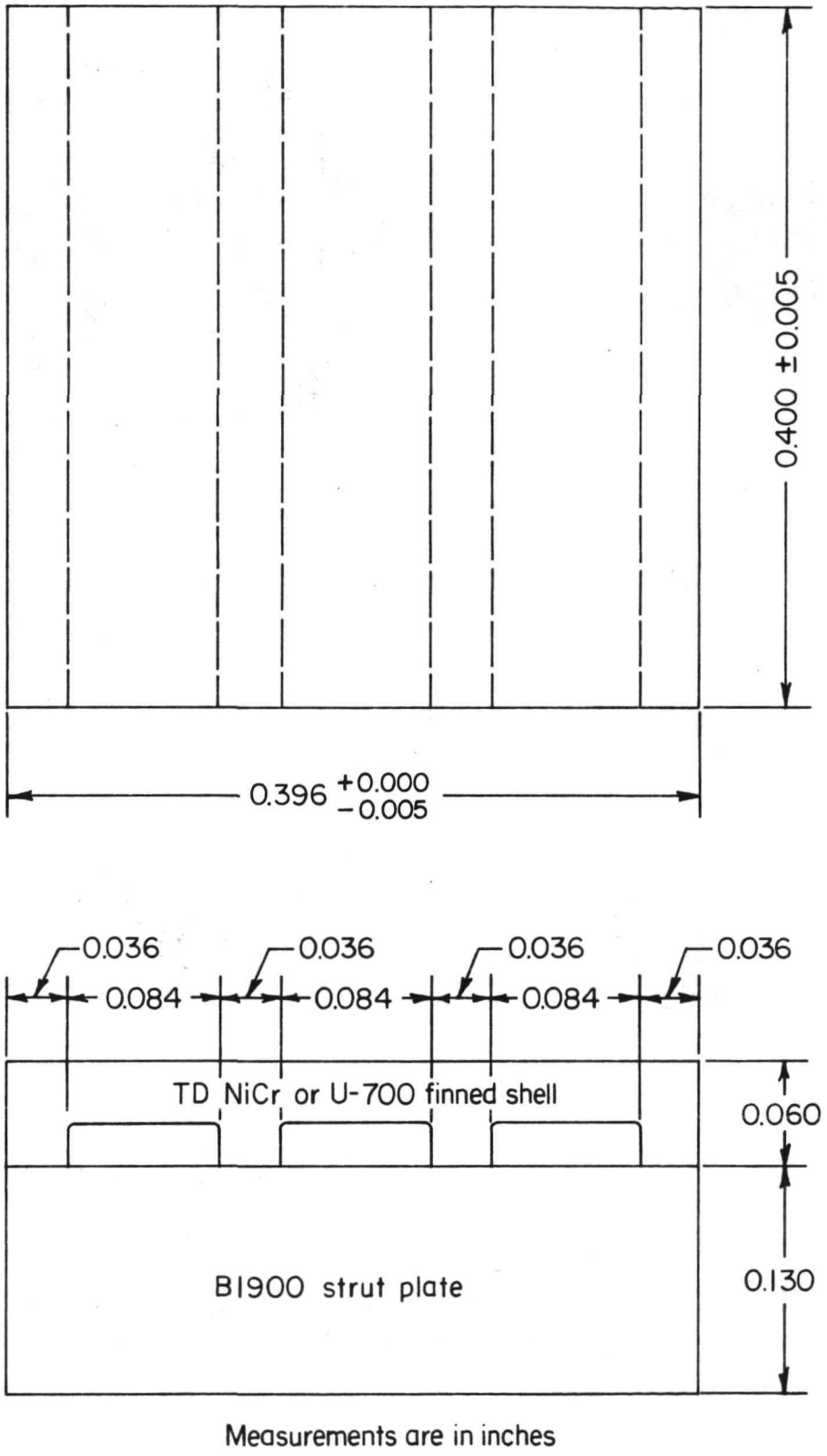

FIGURE 21. SKETCH OF ZONE M SPECIMEN FOR TESTING IN COMPRESSION-INDUCED SHEAR

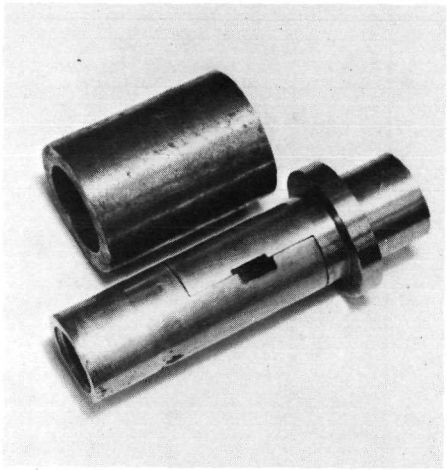

a. Flat Specimen Fixture

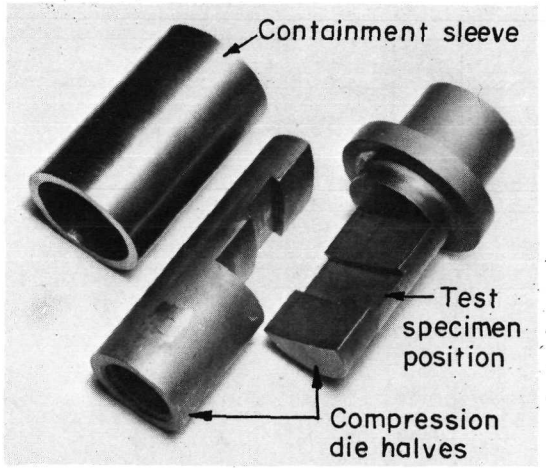

b. Curved Specimen Fixture

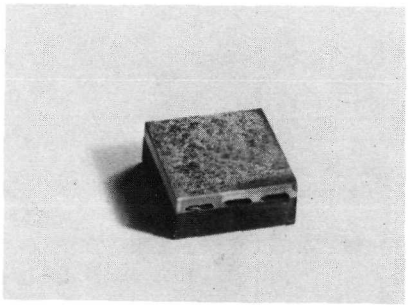

c. Flat Specimen Before Test

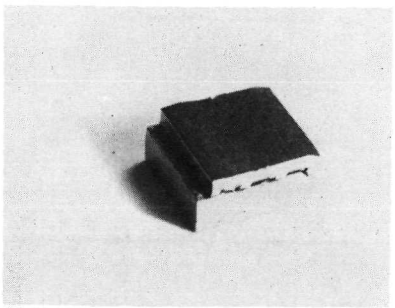

d. Flat Specimen After Test

FIGURE 22. ROOM-TEMPERATURE COMPRESSION SHEAR TEST FIXTURES AND SPECIMEN

A few elevated-temperature (1750 F in air) shear tests were performed in a test fixture quite similar to that employed at room temperature and illustrated previously in Figure 22. At high temperatures in an environment where refractory metals are not permissible, the selection of a satisfactory fixture material became a severe problem. In brief, the main fixture components were machined from TD nickel; B1900 inserts were used to transmit the load from the fixture to the specimen. The fixture was necessarily quite massive in order to handle the loads required to fracture the specimen. This bulk proved to be an inconvenient and time-consuming factor in the heatup cycle and in loading and unloading the fixture. When, after a few tests, the containment sleeve began to distort from a combination of inadequate elevated-temperature strength and a tendency to seize on the moving die component, the direct compression fixture illustrated in Figures 23 and 24 was substituted. The new fixture had no effect on specimen configuration since the loading method at the specimen was unchanged.

The direct compression fixture performed very satisfactorily and decreased significantly the time required to perform each test. As may be seen in the test setup shown in Figure 25, the compression rams that load the fixture may remain in the furnace at temperature at all times during the testing routine. This permits a more rapid heatup, since only the relatively small mass of the fixture itself has to be brought to temperature. Moreover, the bulk of the fixture is nickel which, because of its thermal conductivity, heats rapidly and uniformly. At room temperature a gap was permitted between the B1900 containment sleeve and nickel die. At 1750 F this gap was closed by the differential thermal expansion between these two materials.

The test procedure was quite simple. The specimen and various B1900 punches and guides were assembled in their proper position in the die groove, as shown in Figure 24. A longitudinal specimen is shown in place in Figure 25. Transverse specimens were machined such that the fins were 90 deg from the force application. Subsequently, the remaining die half was placed over the specimen, and the die halves enclosed by the B1900 sleeve. This assembly and B1900 plates were placed between the preheated stainless steel compression rams, and the furnace shell was closed. It was established by blank runs with a thermocouple in the specimen position and a thermocouple at the fixture exterior that 30 min was sufficient to bring the fixture to a uniform temperature of 1750 F. The fixture and specimen were heated under no load. All other aspects of the test were the same as for any normal compression test. After completion, the fixture was removed from the furnace and quenched in water to room temperature before the specimen was removed.

The test was limited in one respect. The active B1900 punch was permitted a displacement of only 0.080 in. The objective was to limit punch projection below the 0.100-in. width of the punch to ensure no buckling. It was assumed that strains of the order 30 percent, such as produced by full 0.080-in. travel of the punch, would not be permissible in blade hardware even if failure did not occur. Most specimens did fail within the strain limit imposed.

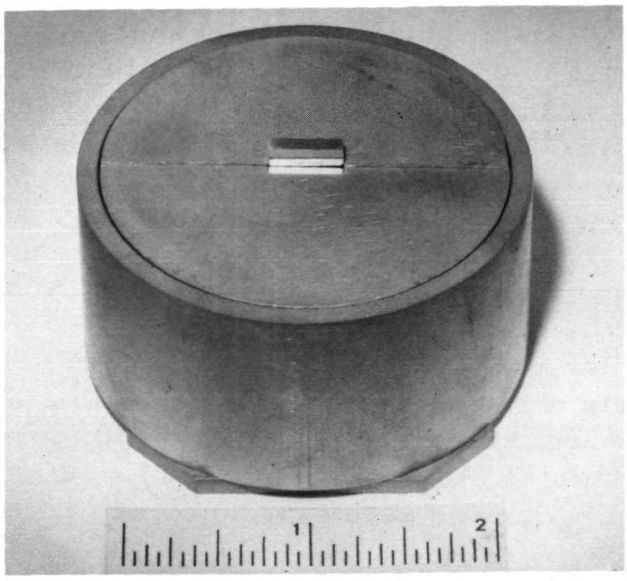

45180

a. Assembled Fixture

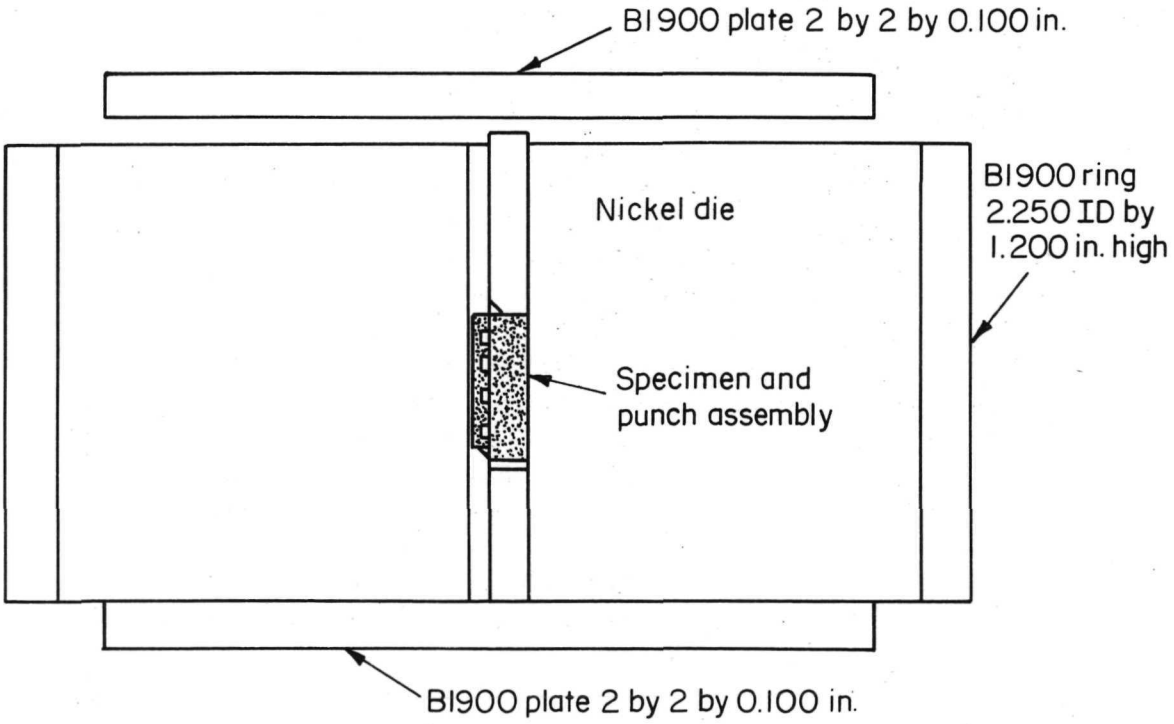

b. Cross-Section Sketch

FIGURE 23. ELEVATED-TEMPERATURE COMPRESSION SHEAR TEST FIXTURE

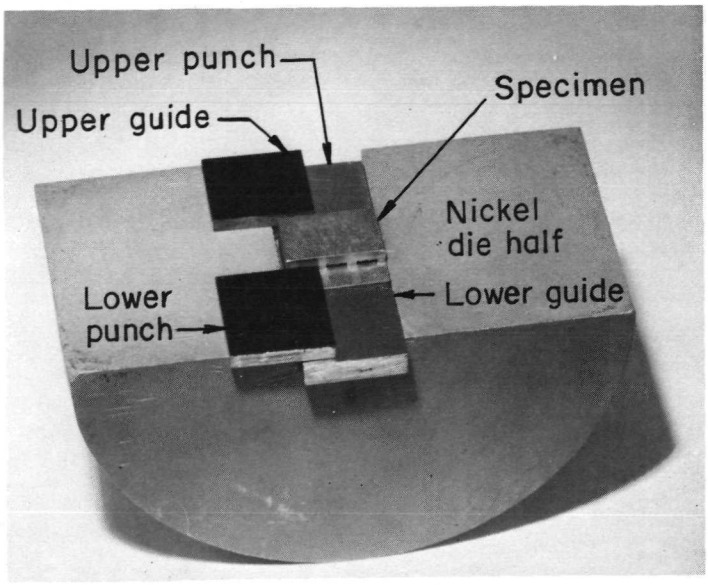

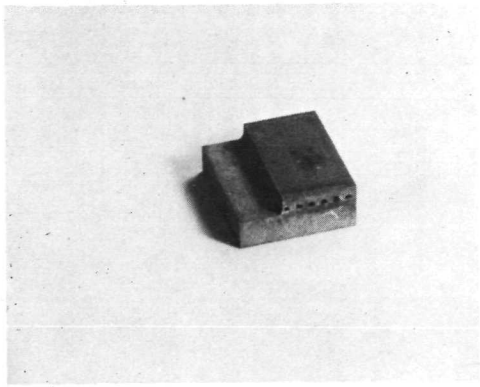

45181

a. Punches and Specimen Assembled in Die Half

b. Transverse Zone L Specimen

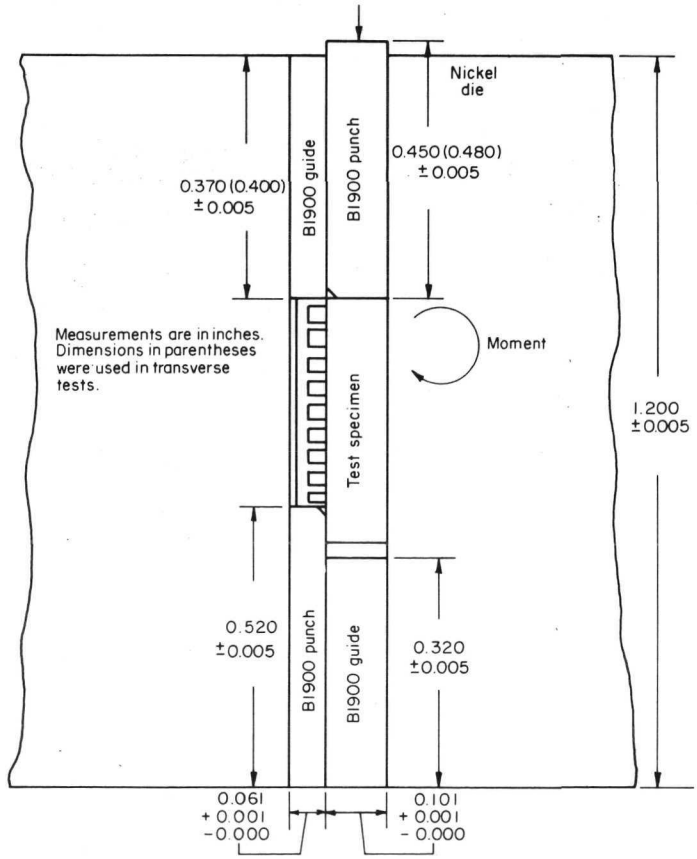

c. Punch and Specimen Arrangement During Testing

FIGURE 24. DETAIL OF PUNCH AND SPECIMEN ARRANGEMENT IN ELEVATED-TEMPERATURE COMPRESSION SHEAR TEST FIXTURE

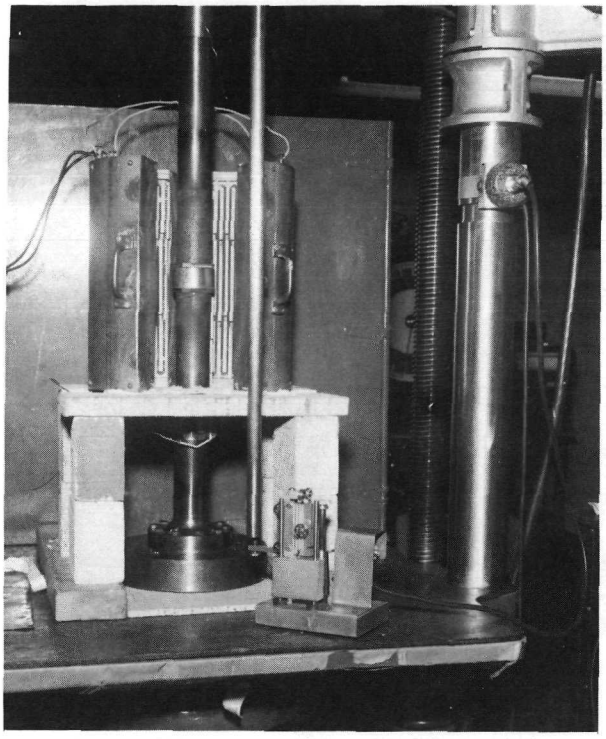

a. General View

45196

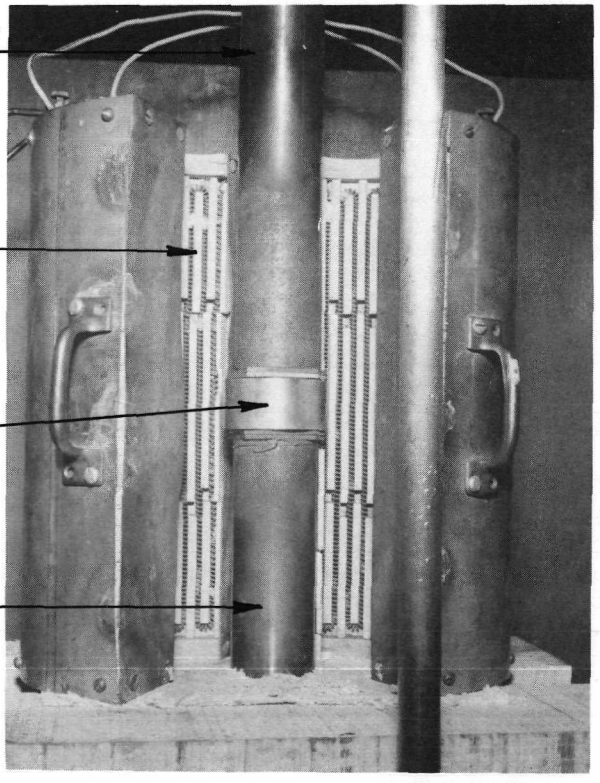

b. Details of Setup

45197

FIGURE 25. TEST SETUP FOR ELEVATED-TEMPERATURE SHEAR TESTING OF FINNED SHELL SAMPLES

One improvement to the fixture design was found necessary during the course of testing. As viewed in Figure 24, it may be seen that the nickel die must resist a clockwise moment. The local stress from this moment tended to deform the base of the guide slot in the specimen area. To prevent deformation, the guide slot in both halves of the nickel die was milled 0.100 in. deeper and lined with 0.100-in.-thick B1900.

Development of Bonding Process Procedures

Preliminary Investigation of Process Requirements

During this segment of the process development effort several process elements such as surface treatment requirements; process temperature, pressure, time, and atmosphere; structural support needs and effects; and bonding container design and fabrication were considered, investigated, and established to a point where a bonding approach could be selected for refinement.

Consideration of Support Tooling Requirements. The finned shell configuration, which is illustrated schematically in Figure 26, was analyzed to determine the relationship between applied gas pressure during diffusion bonding and the resultant stresses in the shell structure. The essential results of that analysis are contained in Figure 26. It was determined that fin buckling could be safely ignored. Similarly, the B1900 component may be ignored because of its thickness and strength properties. The compressive stress generated in each fin element was found to be 3.33 times the applied gas pressure. This relationship holds for both fin width cases, Zone L and Zone M, because the ratio of fin width to channel width is constant in the two cases. The fin compressive stress is of interest from two aspects. First, this stress represents, in an unsupported condition, the pressure experienced at the bond interface assuming no losses. Secondly, this stress must be less than the compressive yield strength of the fin material at the bonding temperature, if unsupported.

The second critical region in the structure is the span over the cooling channel. The stress in this span is a function of applied gas pressure, span thickness, and span width. Hence, the relationship between applied pressure and resultant stress is different in the two channel width zones, Zones L or N and Zone M, in Figure 26. Zone M is the more critical as a result of the 0.084-in. channel width. A range in the value of the function coefficient is given in both cases. The range represents the limits established between taking the span distance as the centerline distance between fins or merely the edge to edge fin separation. The higher value was considered to be very conservative, but with a lack of experimental data and directly applicable material property information an exact value could not be defined. In Zones L and N, however, channel collapse is not the limiting factor since the conservative collapse coefficient is smaller than the fin compressive stress coefficient. The structure is, therefore, not

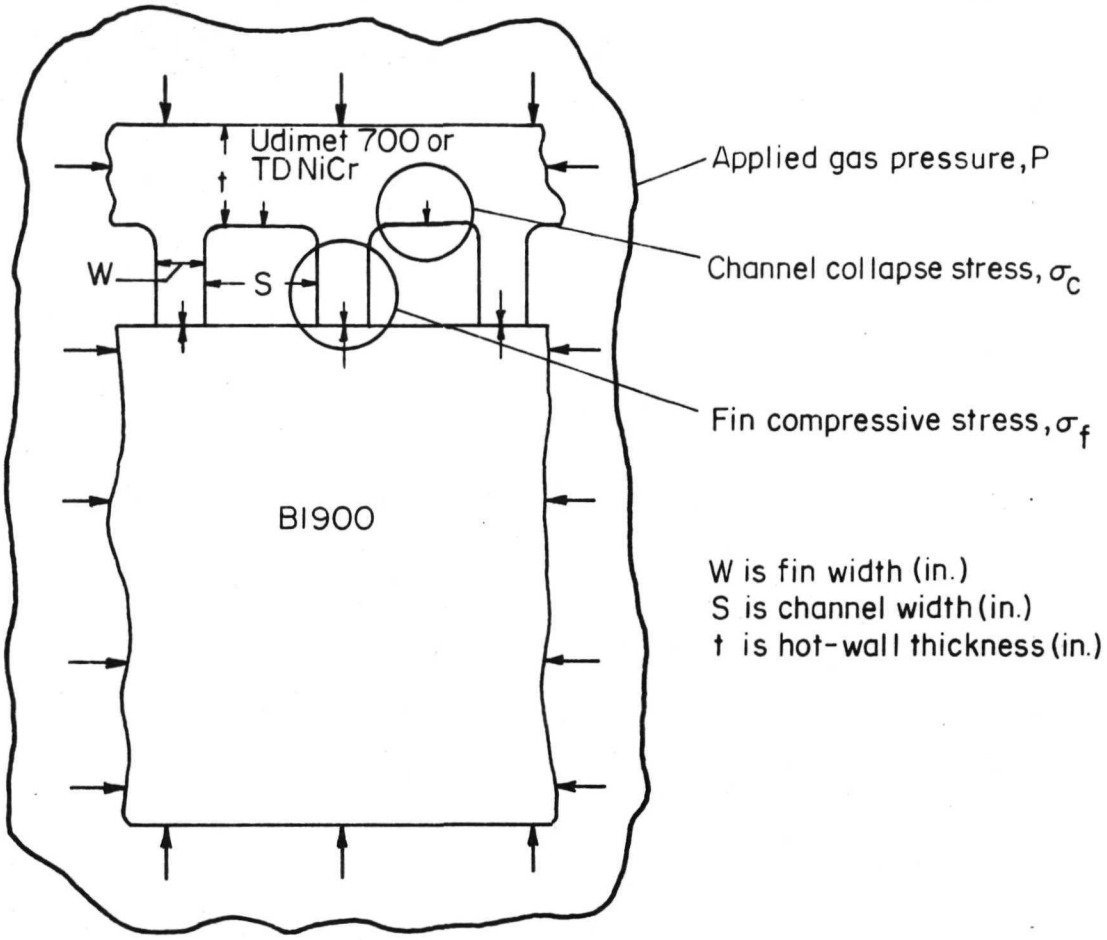

$$\sigma_f = \left(\frac{S + W}{W}\right)P \quad \sigma_c \cong 1/2 \left(\frac{S^2}{t^2}\right) P \rightarrow 1/2 \left(\frac{(S + W)^2}{t^2}\right)P \ .$$

ZONES L OR N

W = 0.012
S = 0.028
t = 0.025
th

then $\sigma_f = 3.33\ P$

$\sigma_c = 0.63\ P \rightarrow 1.28\ P$

ZONE M

W = 0.036
S = 0.084
t = 0.025

then $\sigma_f = 3.33\ P$

$\sigma_c = 5.64\ P \rightarrow 11.52\ P$

FIGURE 26. MODEL OF STRESSES IMPOSED ON FINNED SHELL DURING GAS-PRESSURE BONDING

limited in a bonding sense. Interface pressures up to the compressive yield of the finned shell material can be applied without distorting the structure. It was, therefore, concluded that Zones L and N of the finned shell could be processed without internal support. Conversely, it appeared that Zone M would require support of at least a limited nature to prevent collapse. Referring again to Figure 26, it is noted that the collapse coefficient at its smallest value for Zone M is larger than the compressive stress or bonding pressure coefficient. Consequently, the structure is pressure limited from the diffusion bonding viewpoint.

Table 4 summarizes pertinent mechanical property and thermal expansion data obtained from several sources; the data cover room temperature and the 1800 to 2200 F temperature range projected for satisfactory diffusion bonding. It was predicted that a fin bearing stress, σ_f, on the order of 10,000 psi would be required to achieve bonds approaching 100 percent efficiency. Accordingly, the applied pressure would be of the order of 3,000 psi, which in turn yields a channel collapse stress of 16,920 to 34,560 psi in the case of Zone M (Figure 26). The conservative value limits bonding temperature to less than 1800 F for TD NiCr and slightly more than 1800 F for Udimet 700. The less conservative analysis indicates allowable bonding temperature limits of 1900 F and 2000 F, respectively, for Udimet 700 and TD NiCr. Since even the temperatures predicted from the "risky" analysis were considered, in the absence of proof to the contrary, to be on the low side for satisfactory bonding, it was concluded that support tooling would be necessary.

A flat coupon sample of Udimet 700 and TD NiCr, 1 in. wide by 2 in. long, was processed at 2200 F and 10,000 psi in an attempt to experimentally refine the channel collapse function coefficient. The 2200 F temperature was selected on the basis of prior satisfactory bonding results involving similar alloys. Channels 0.020, 0.040, 0.060, 0.080, and 0.120 in. wide by 0.005 in. deep were machined in the plates by photoetching. Collapse stresses were computed using the less conservative coefficient and compared to the 2200 F yield strengths of TD NiCr and Udimet 700. It was concluded that all but the 0.020-in.-wide channel would collapse in the case of Udimet 700. However, in the case of TD NiCr only the 0.120-in.-wide channel should collapse. Metallographic and radiographic examination after the 2200 F/10,000 psi/1 hr gas-pressure bonding cycle revealed that all channels in the TD NiCr sample, except the 0.120-in. channel, were undeformed. The 0.120-in.-wide channel was approximately 50 percent collapsed. Hence, the predictions for TD NiCr were fully realized experimentally. The Udimet 700 results were not as satisfactory. Both radiography and metallographic examination indicated collapse of all five channels while, by calculation, the 0.020-in.-wide channel should have survived. Since the computation appeared to perform well for TD NiCr, it was concluded that either the specimen experienced an overtemperature condition or that the strength of Udimet 700 at 2200 F may be less than that indicated in Table 4. At 2200 F Udimet is approaching or at an incipient melting condition and its strength would be very sensitive to temperature. Although not conclusively established, the less conservative collapse coefficient presented earlier in Figure 26 appeared to be valid for TD NiCr and probably results in a more accurate prediction than the conservative value.

TABLE 4. MECHANICAL STRENGTH AND THERMAL EXPANSION PROPERTIES OF B1900, UDIMET 700, AND TD NiCr

Base Material	Temperature, F	Property				
		Ultimate Tensile Strength, ksi	0.2% Offset Yield Strength, ksi	Elongation, percent	Modulus, 10^6 psi	Expansion, 10^{-6}/F
B1900	RT	141	120	8	31	6.5
	1800	80	60	7	22.4	8.84
	2000	39	28	11	--	9.01
	2200	5	3	--	--	--
Udimet 700	RT	204	140	17	32.4	7.50
	1800	52	44	28	22.1	9.65
	2000	15	12	35	--	10.30
	2200	3	2	100	--	--
TD NiCr	RT	135	90	20	35	--
	1800	20	18	4	23.6	8.8
	2000	18	16	4	--	8.95
	2200	12.5	12.5	1	--	--

Preliminary Gas-Pressure Bonding Experiments. The bonding experiments summarized in Tables 5 and 6 were performed to identify appropriate surface treatment procedures and bonding conditions for the TD NiCr/B1900 and Udimet 700/B1900 systems. Experiments 2 through 4 in each system were complicated by support tooling problems, which are discussed in the next section. As a consequence, no torsion shear data were obtained from this initial study. Strength information was obtained from tensile overlap shear tests, however.

The initial bonding experiment was performed at 2200 F and 10,000 psi held for 3 hr. Three 1.0-in.-square trilaminate specimens (Udimet 700/B1900/TD NiCr) were prepared, surface treated, and assembled into a stainless steel bonding container. The bonding container was evacuated, sealed, and subjected to the gas-pressure bonding cycle. The surface treatment procedure employed on the various materials is presented in Table 7. After bonding, the stainless steel container was removed, and the three specimens separated. Specimen A was sectioned and examined metallographically; the bond microstructure is illustrated in Figures 27 (B1900/Udimet 700) and 28 (B1900/TD NiCr). The bond between Udimet 700 and B1900 (Figure 27) appeared to be of good quality; no voids were observed along the length of the bond, and the Udimet 700 deformed to mate completely with the surface topography of the B1900. This was anticipated since the applied pressure was approximately five times the yield strength of Udimet 700 at the bonding temperature. The yield strength of B1900 was exceeded as well, but Udimet 700 is the weaker and thinner of the two, and it was assumed that all the deformation occurred in the Udimet 700. It was noted that the bond interface was very clean except for discrete precipitate particles, probably carbides. The microstructure of the TD NiCr/B1900 bond (Figure 28) also appeared to be quite clean. Again, discrete particles at the bond interface were noted. In this case the particles were probably predominantly Cr_2O_3 from the TD NiCr with some carbide precipitation from the B1900. The presence of discrete, well dispersed particulate matter at a bond interface does not necessarily degrade bond quality. If the precipitate is present as a continuous or semicontinuous film, however, bond quality is seriously degraded. Although the B1900/TD NiCr bond was nearly 100 percent continuous, several small voids of the order of 0.001 to 0.002 in. long by 0.0005 in. high were noted, and are shown in Figure 28. These were remnants of the original B1900 surface topography. Small surface depressions of the type shown in Figure 28 had to be closed from the B1900 side since the bonding pressure was less than the bulk yield strength of TD NiCr. However, the B1900 also did not flow to fill these small voids. B1900 apparently has a higher resistance to plastic flow under isostatic compression conditions than would be expected from the 2200 F tensile yield.

Specimen B of the trilaminates was evaluated in a room-temperature impact test. The specimen was placed in a steel die and struck twice with 6900 ft-lb forging hammer. Both bond planes were parallel with the impact force direction. The specimen was shortened by approximately 20 percent. The Udimet 700 grew 20 percent and the B1900 15 percent in thickness; the TD NiCr did not thicken. It appeared, on the basis of this test, that the bonds created under conditions of 2200 F and 10,000 psi held for 3 hr possessed excellent room-temperature mechanical strength. The impacted specimen was examined metallographically.

TABLE 5. SUMMARY OF PRELIMINARY TD NiCr/B1900 GAS-PRESSURE BONDING EXPERIMENTS[a]

Experiment	Bonding Conditions: Temperature, F	Bonding Conditions: Pressure, psi	Bonding Conditions: Time, hr	Surface Preparation (TD NiCr/B1900)	Specimen/ Type	Evaluation Results: Metallography	Evaluation Results: Strength/Test	Evaluation Results: General
1	2200	10,000	3	EP/EP	T-A/TL	Excellent	--	Bond interface appears very clean; microscopic surface irregularities not closed
					B/TL	Excellent	Excellent/Impact	
					C/TL	--	--	
2	2200	10,000	1	EP/EP	5/T	Good	39.1 ksi/OT	Bond interface not as clean as above; torsion samples not bonded; no discernible effect of surface preparation
					6/T	Good	>35.4 ksi/OT[b]	
					7/T	Good	>41.8 ksi/OT[c]	
				EP/GBF	8/T	Good	41.5 ksi/OT	
				EP/GBC	9/T	Good	37.4 ksi/OT	
3	2000	10,000	3	EP/EP	10/T	Good	--	Al_2O_3 contamination and general tooling incompatibility
					11/T	--	--	
4	2000	10,000	1	EP/EP	14A/TT	--	--	Specimens failed when tooling dissolved
					14B/TT	--	--	
					14C/TR	--	--	
					14D/TR	--	--	

(a) Explanation of symbols:
- EP - electropolish
- GBF - 100-μin. rms, grit blasted
- GBC - 150-μin. rms, grit blasted
- TL - trilaminate
- T - 2-in. -square torsion coupon
- TT - 0.7-in. -square torsion tab specimen
- TR - 0.7-in. -square torsion ring specimen

(b) TD NiCr parent material failed in tension at 133,500 psi without shearing bond.

(c) TD NiCr parent material failed in tension at 131,000 psi without shearing bond.

TABLE 6. SUMMARY OF PRELIMINARY UDIMET 700/B1900 GAS-PRESSURE BONDING EXPERIMENTS(a)

Experiment	Bonding Conditions: Temperature, F	Bonding Conditions: Pressure, psi	Bonding Conditions: Time, hr	Surface Preparation (U-700/B1900)	Specimen/ Type	Evaluation Results: Metallography	Evaluation Results: Strength/Test	Evaluation Results: General
1	2200	10,000	3	EP/EP	U-A/TL	Excellent	--	Very clean bond interface; bond ductile at RT
					B/TL	Excellent	Excellent/Impact	
					C/TL	--	--	
2	2200	10,000	1	EP/EP	8/T	Very good	43.1 ksi/OT	Bond interface not quite as clean as above; no discernible difference in surface preparation effect; tooling problems
					9/T	--	41.0 ksi/OT	
				EP/GBF	10/T	--	38.8 ksi/OT	
				EP/GBC	11/T	--	--	
				EP/EP	12/T	--	--	
3	2000	10,000	3	EP/EP	6/T	Good	--	Tooling problems; Al_2O_3 contamination
4	2000	10,000	1	EP/EP	14A/TT	--	--	Specimens failed when tooling dissolved
					14B/TT	--	--	
					14C/TR	--	--	
					14D/TR	--	--	
					15A/TT	--	--	
					15B/TT	No bond	--	
					15C/TR	--	--	
					15D/TR	--	--	

(a) Explanation of symbols:

EP - electropolish
GBF - 100-μin. rms, grit blasted
GBC - 150-μin. rms, grit blasted
TL - trilaminate
T - 2-in. -square torsion coupon
TT - 0.7-in. -square torsion tab specimen
TR - 0.7-in. -square torsion ring specimen
OT - overlap tensile shear.

TABLE 7. SURFACE TREATMENT PROCEDURE FOR B1900, UDIMET 700, AND TD NiCr USED IN PRELIMINARY GAS-PRESSURE BONDING STUDY

B1900 Procedures

(1) Degrease in methyl ethyl ketone
(2) Rinse in alcohol (methyl or ethyl)
(3) Scrub in detergent solution (Shipley Scrub Cleaner II)
(4) Rinse in hot water
(5) Soak in alkaline cleaner for 2 to 3 min at 140 to 160 F

Na_2CO_3	20 g/l
Na_2PO_4	20 g/l
NaOH	15 g/l
SNAP	0.5 g/l (wetting agent)

(6) Rinse in water
(7) Anodic etch at 2 amp per in.^{2} for 3 min in HNO_3-methanol (one part HNO_3 to two parts methanol by volume)(a)
(8) Rinse in water
(9) Hand scrub in warm Alconox detergent solution
(10) Rinse in warm water
(11) Ultrasonic clean in hot (180 F minimum) Alconox detergent solution
(12) Rinse very thoroughly in hot water
(13) Rinse in hot distilled water (180 F minimum)
(14) Rinse and store in ethyl alcohol (200 proof).

Udimet 700 Procedures

(1) Perform Steps (1) through (6) of B1900 procedures
(2) Anodic etch at 6 amp per in.^{2} for 30 sec in HNO_3-methanol solution (one part HNO_3 to two parts methanol by volume); maintain solution below 80 F(a)
(3) Perform Steps (8) through (14) of B1900 procedures but substitute Shipley Scrub Cleaner II for Alconox.

TD NiCr Procedures

(1) Perform Steps (1) through (6) of B1900 procedures
(2) Anodic etch at 5 amp per in.^{2} for 30 sec; maintain solution temperature below 80 F; use same etch bath as used for B1900(a)
(3) Perform Steps (8) through (14) of B1900 procedures.

(a) In evaluating other treatments, the anodic etch was replaced by grit blasting, SiC grit paper abrasion, or chemical etching in HNO_3-HF or HNO_3-HCl-$FeCl_3$.

The bond microstructures are shown in Figure 29. No disruption of the Udimet 700/B1900 bond could be detected; the only change from the as-bonded microstructure presented earlier in Figure 27 was the evidence of twinning in the B1900 and Udimet 700 grains from cold working. This test was rather conclusive proof that no brittle phases are produced in the Udimet 700/B1900 system during diffusion bonding. The TD NiCr/B1900 bond interface was also intact after testing; the TD NiCr itself failed, however. While failure of the TD NiCr/B1900 couple appeared to initiate at or near the interface, within an extremely short distance the fracture was entirely contained within the TD NiCr. It appeared from this test that the TD NiCr/B1900 system could develop high joint efficiency. However, the Cr_2O_3 phase in the TD NiCr may tend to impose a ductility limitation of the bond system.

Figures 30 and 31 illustrate the bond microstructures of Udimet 700/B1900 and TD NiCr/B1900 resulting from a torsion coupon experiment performed at 2200 F and 10,000 psi held for 1 hr. Three different B1900 surface preparations were evaluated. In two of the Udimet 700/B1900 coupons and a like number of TD NiCr/B1900 samples, the B1900 was grit blasted rather than anodically etched. Neither the resulting bond microstructure nor overlap tensile shear strength results indicated any discrimination between preparation methods. In general, the bond microstructures in this experiment were moderately inferior to those of the trilaminate specimens. All torsion coupon samples exhibited a small to moderate quantity of precipitate at the bond interface. However, the quantity appeared larger than that observed in trilaminate specimens. Consequently, the joint efficiency of the torsion coupons may have been somewhat adversely affected.

The tensile shear results were very consistent between samples; Udimet 700/B1900 samples yielded an average room temperature tensile shear strength of 41,000 psi; TD NiCr/B1900 exhibited an average room temperature value of 39,000 psi. A Knoop indenter hardness traverse was performed on Specimen T-9 (Figure 31); a 50-g indenter load was employed. Zones near the bond interface were found to have a slightly higher hardness than those of the respective bulk materials. The fine-grained chill zone of the B1900 casting was slightly harder than the columnar-grained base alloy. Similarly, a TD NiCr zone adjacent to the bond interface was detectably harder than the bulk material, while a second zone approximately 0.0005 in. from the interface was softer than the base alloy. Chromium diffusion from the TD NiCr toward the B1900 member was suspected.

Two experiments were conducted at 2000 F and 10,000 psi, one held 3 hr and the other 1 hr. The bond microstructures resulting from the 3-hr cycle were of the same quality and appearance as those presented in Figures 30 and 31 from the 2200 F experiment. No bond microstructures were obtained from the 1-hr experiment.

Supplemental Bonding Experiments. In order that bonding studies could continue during a parallel effort directed toward analyzing and solving difficulties experienced with bonding support tooling, the platen press and dead weight, vacuum furnace bonding experiments (summarized in Table 8) were performed. The platen

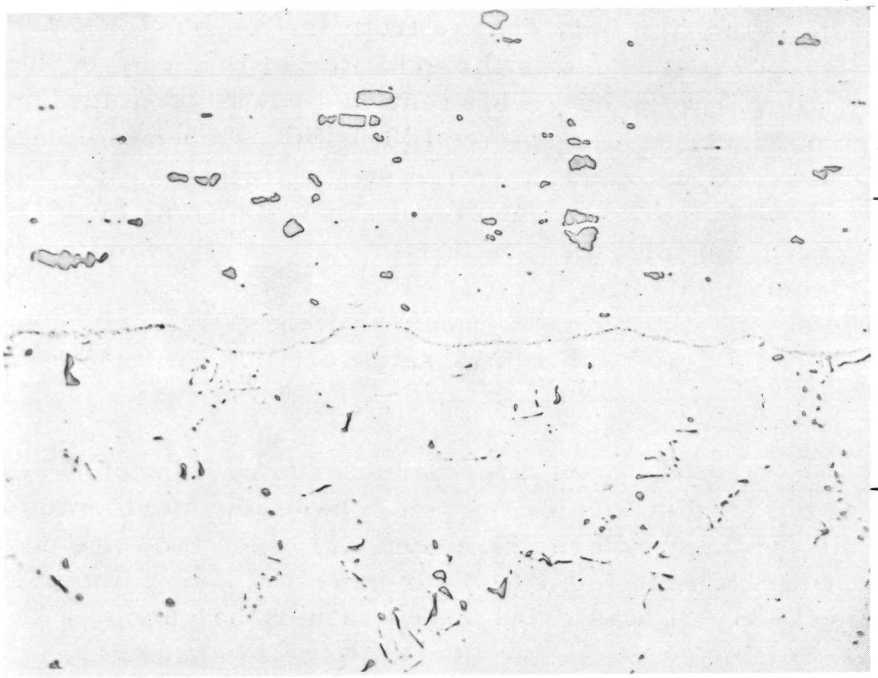

250X 4C395

a. As Polished

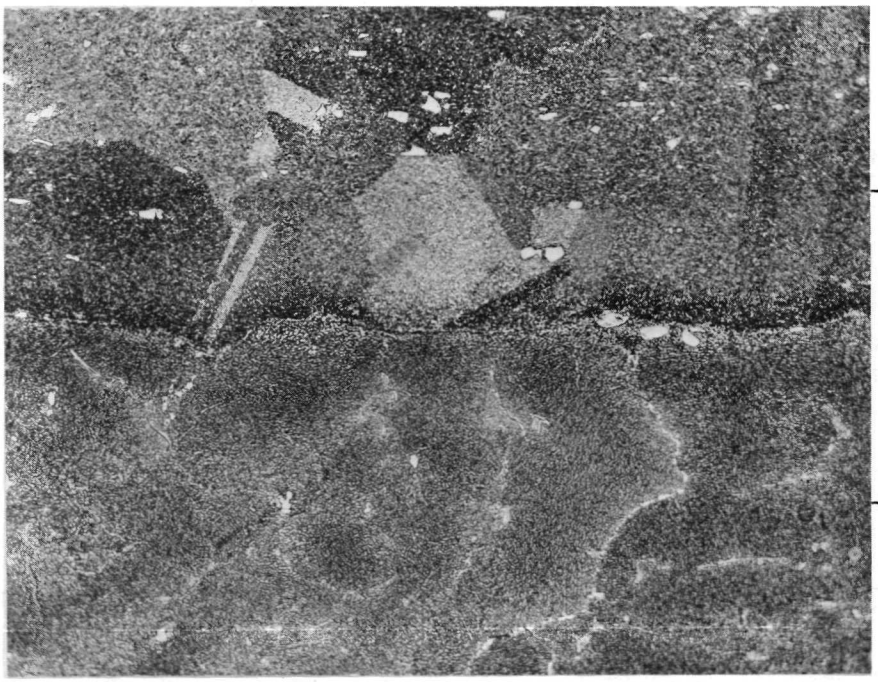

250X 4C396

b. Marble's Etch

FIGURE 27. B1900/UDIMET 700 DIFFUSION BOND PRODUCED AT CONDITIONS OF 2200 F/10,000 PSI/3 HR

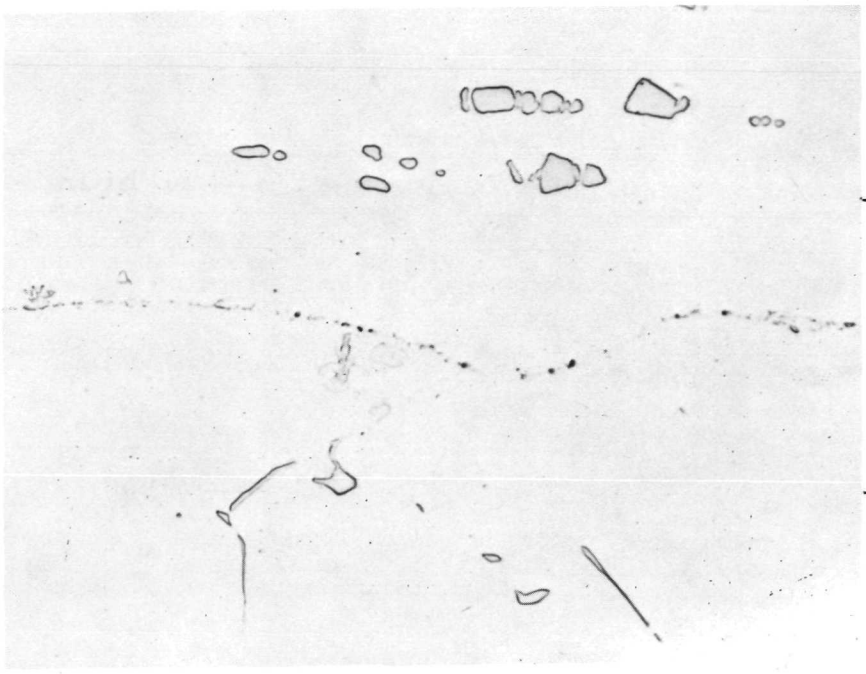

750X 4C399

c. As-Polished View at Higher Magnification

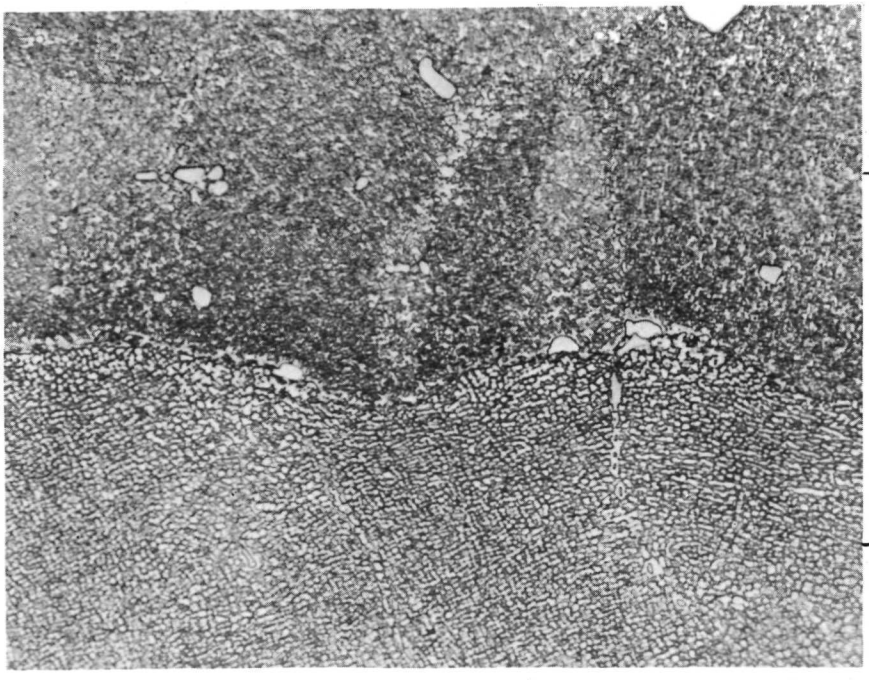

750X Marble's Etch 4C400

d. Etched View at Higher Magnification

FIGURE 27. (CONTINUED)

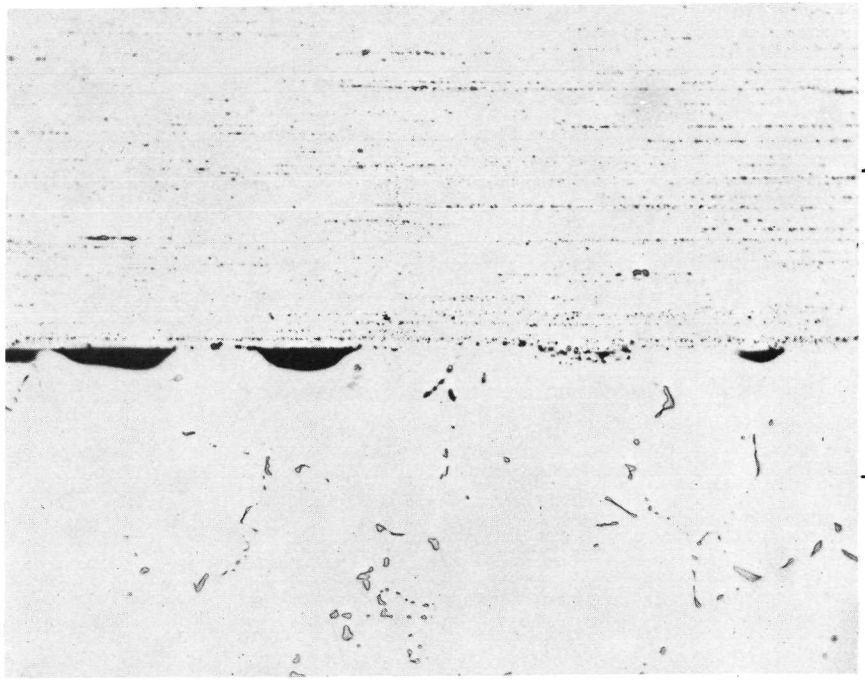

250X 4C403

a. As Polished

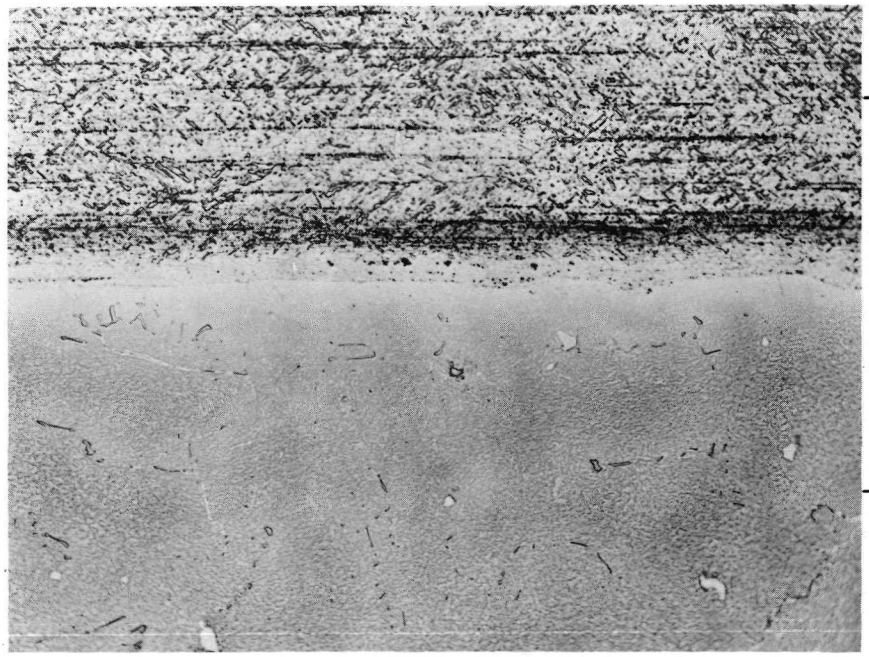

250X 4C406

b. Marble's Etch

FIGURE 28. B1900/TD NiCr DIFFUSION BOND PRODUCED AT CONDITIONS OF 2200 F/10,000 PSI/3 HR

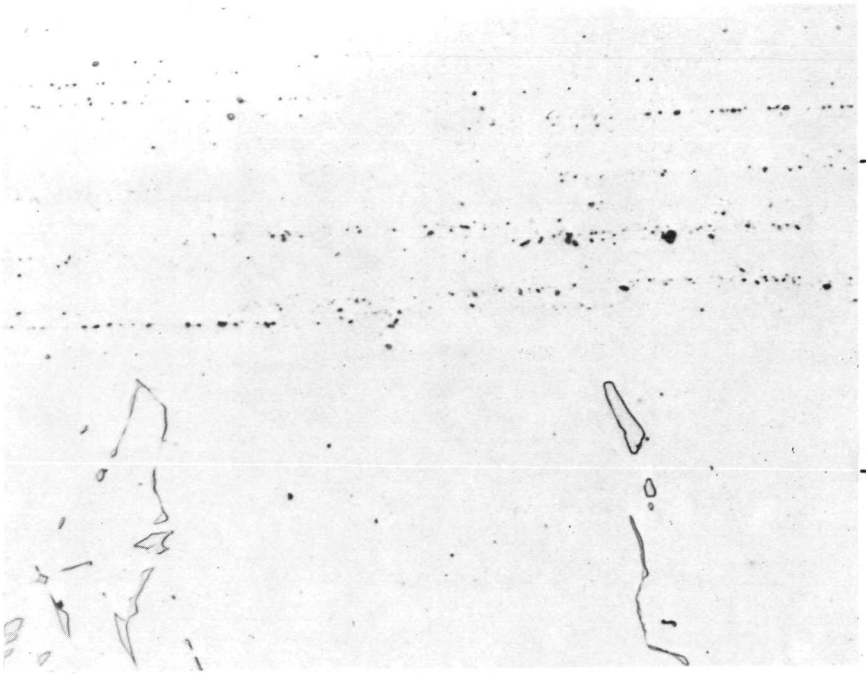

750X 4C407

c. As-Polished View at Higher Magnification

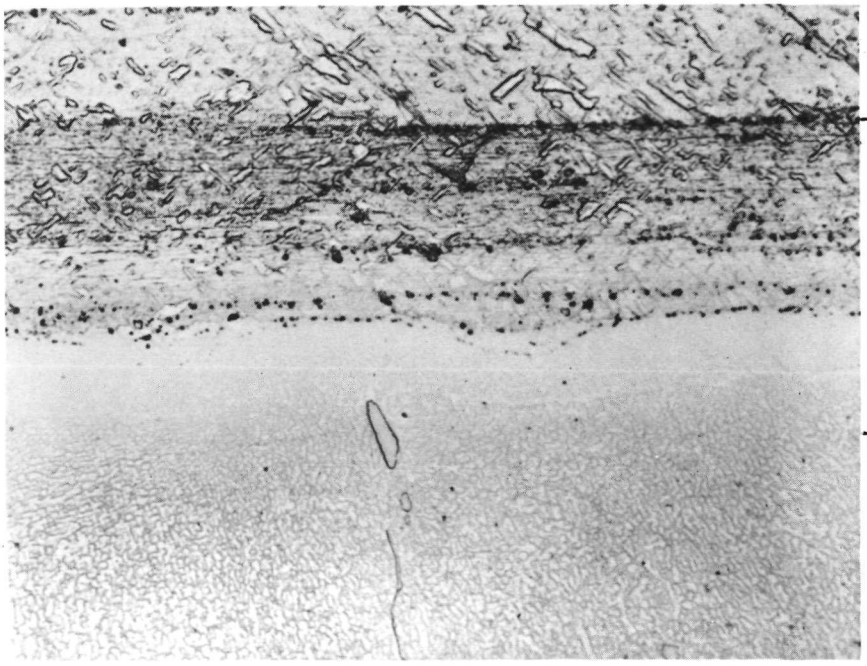

750X Marble's Etch 4C408

d. Etched View at Higher Magnification

FIGURE 28. (CONTINUED)

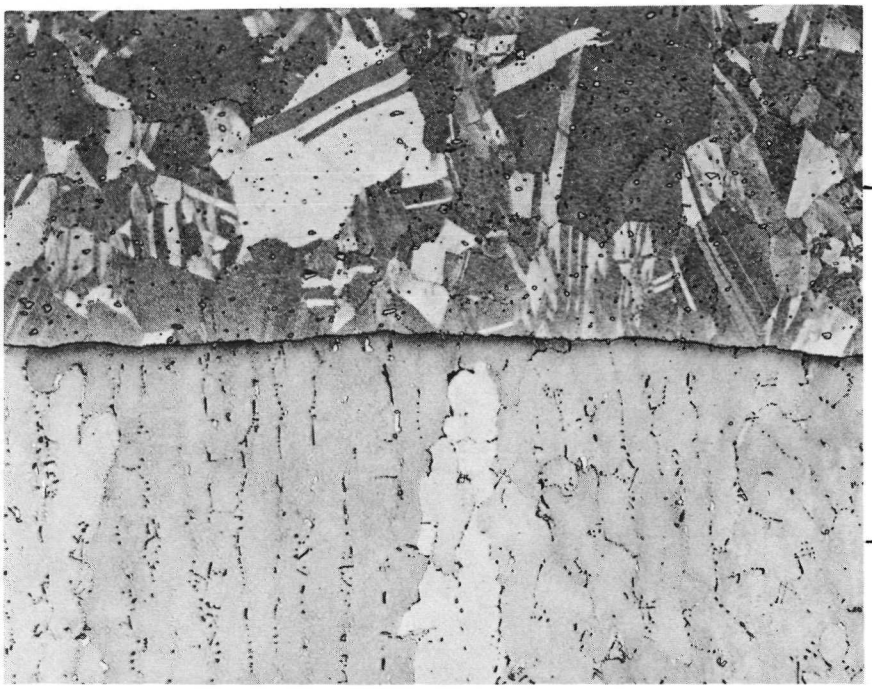

100X 50 H_2O:50 HCl:25 HNO_3 5C355

a. Udimet 700/B1900 Bond

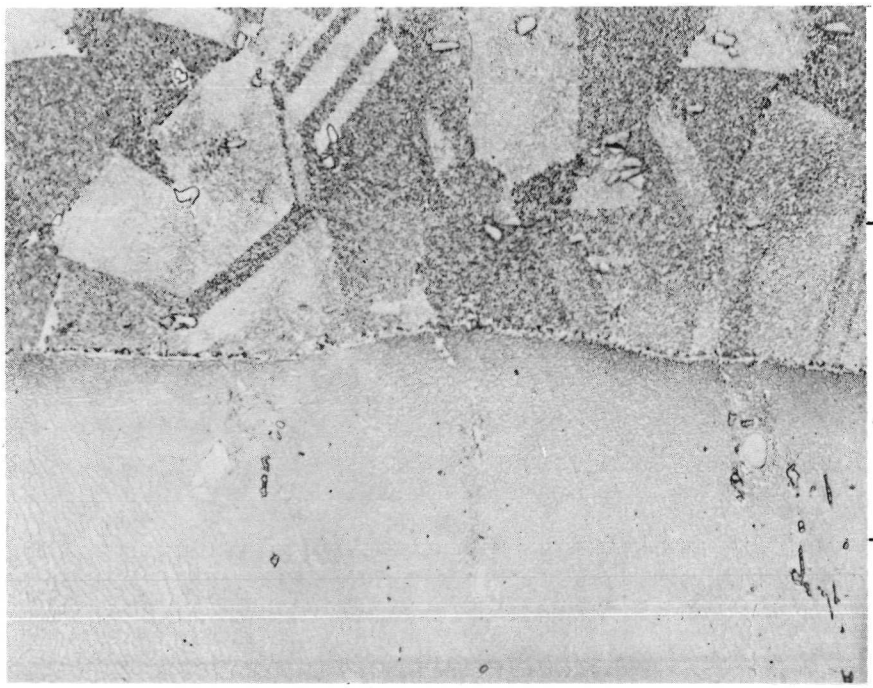

750X 50 H_2O:50 HCl:25 HNO_3 5C359

b. Udimet 700/B1900 Bond at Higher Magnification

FIGURE 29. TRILAMINATE DIFFUSION BOND SPECIMENS AFTER ROOM-TEMPERATURE IMPACT

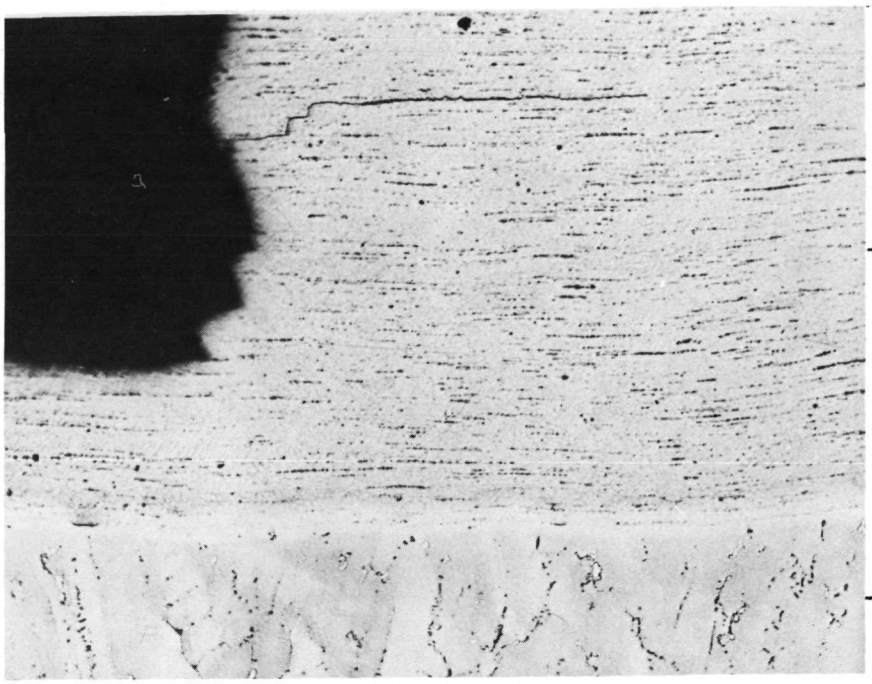

100X 50 H_2O:50 HCl:25 HNO_3 5C354

c. TD NiCr/B1900 Bond

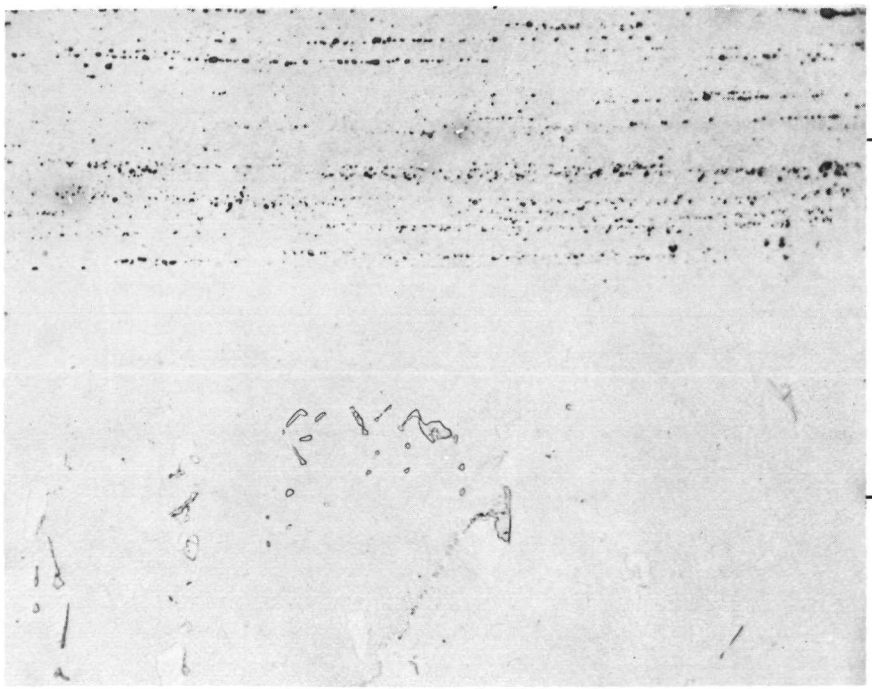

750X 50 H_2O:50 HCl:25 HNO_3 5C360

d. TD NiCr/B1900 Bond at Higher Magnification

FIGURE 29. (CONTINUED)

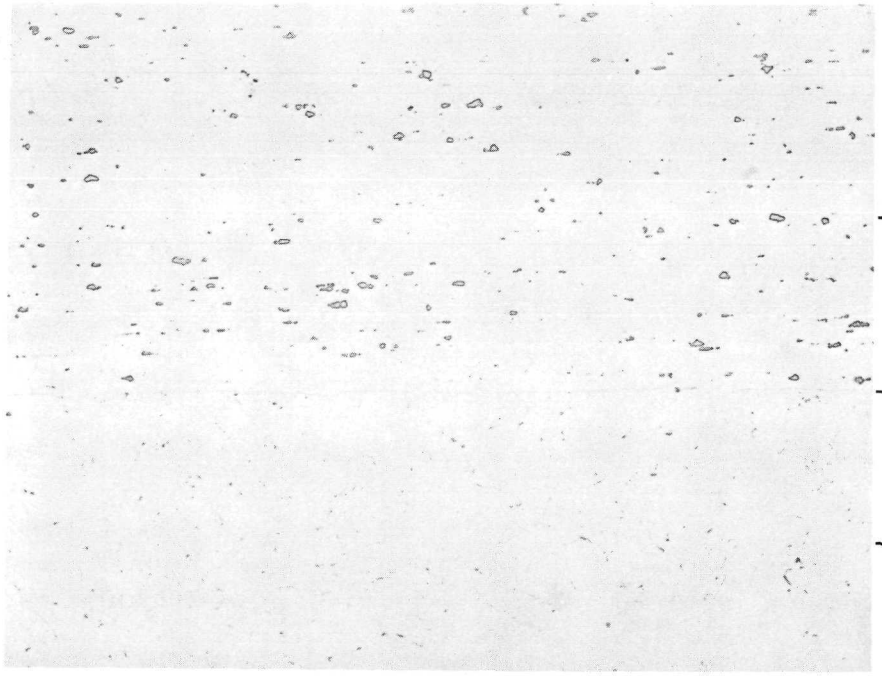

100X As Polished 5C992

a. Both Surfaces Electroetched

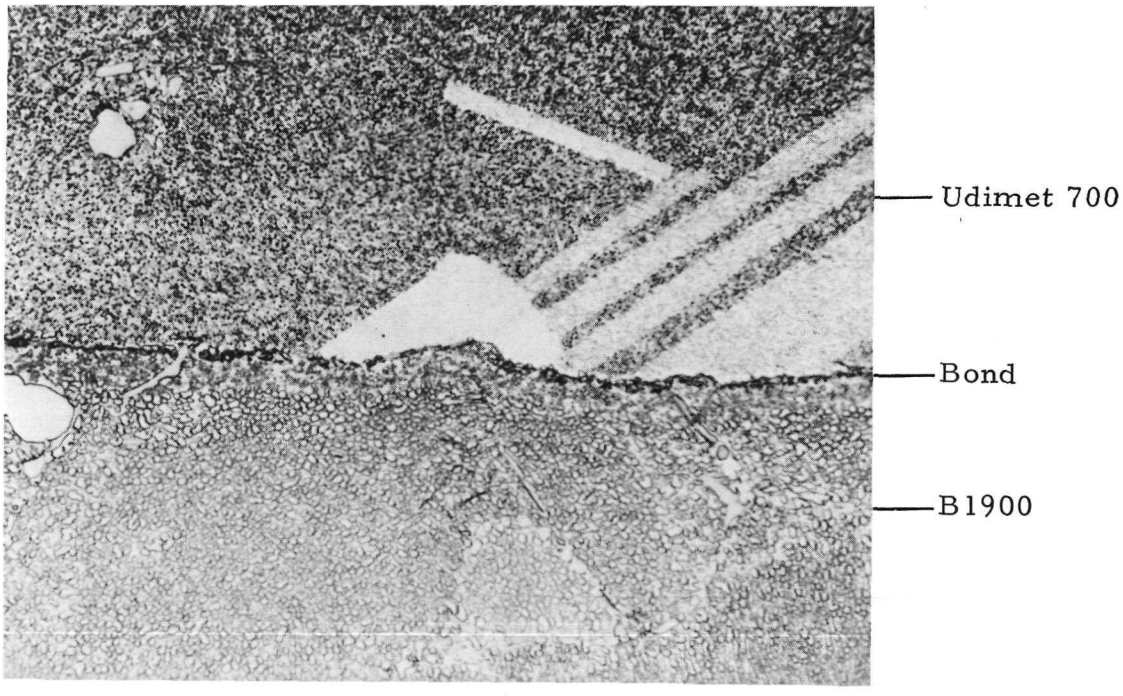

750X Marble's Etch 6C009

b. Higher Magnification View of Electroetched Surfaces

FIGURE 30. UDIMET 700/B1900 DIFFUSION BONDS PRODUCED UNDER CONDITIONS OF 2200 F/10,000 PSI/1 HR

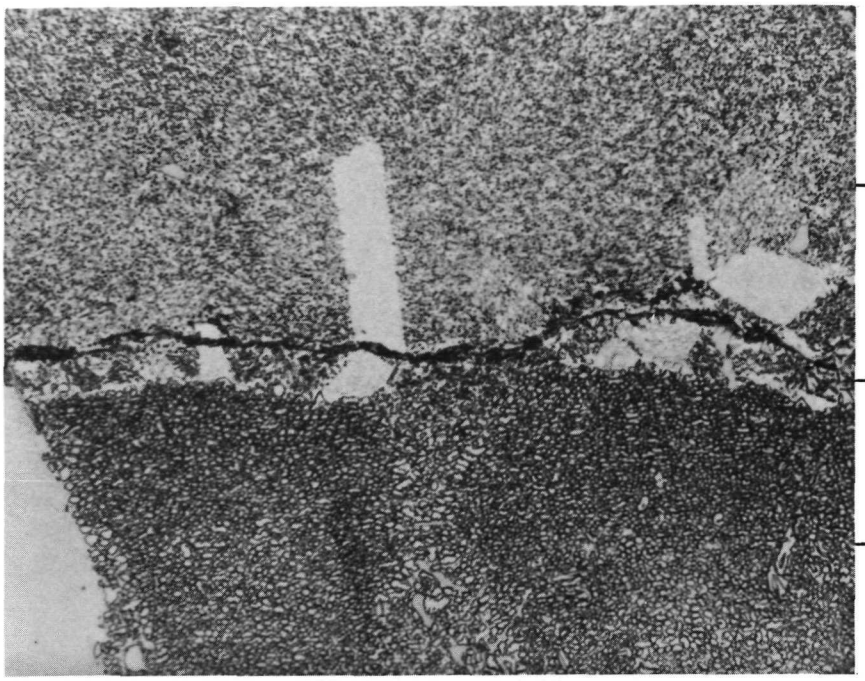

750X Marble's Etch 5C964

c. B1900 Surface Grit Blasted (100 μin. rms)

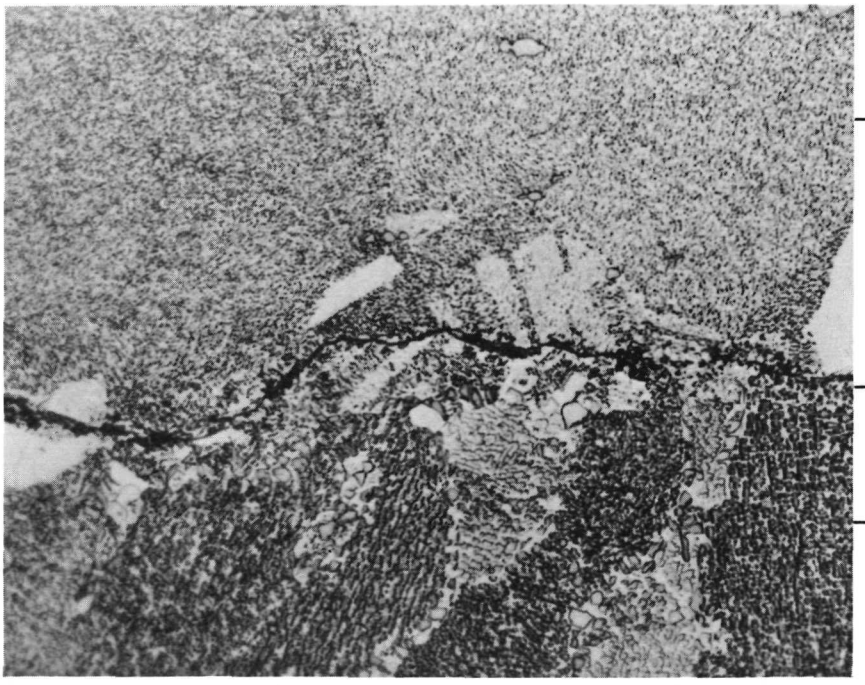

750X Marble's Etch 5C966

d. B1900 Surface Grit Blasted (150 μin. rms)

FIGURE 30. (CONTINUED)

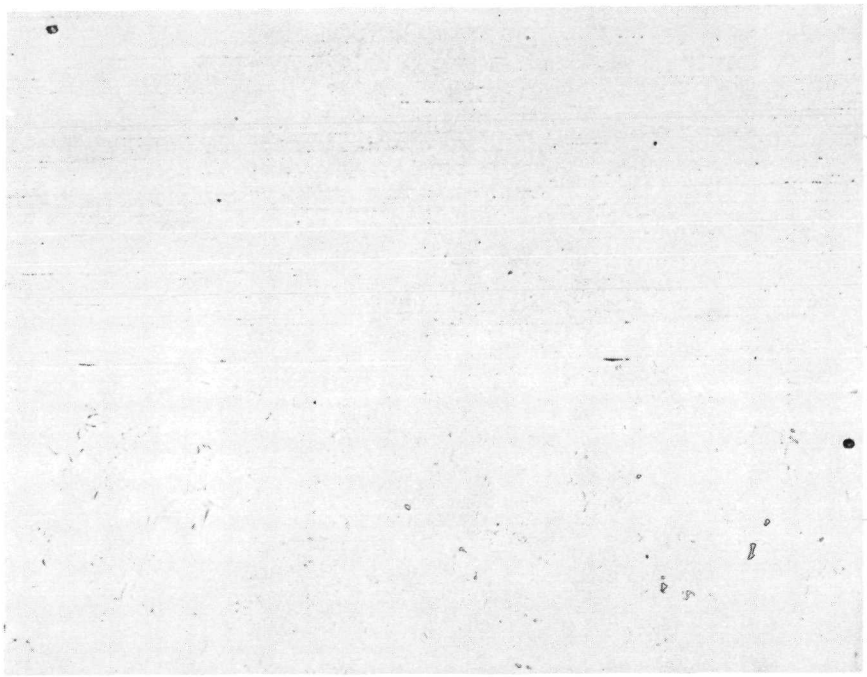

100X As Polished 5C991

a. Both Surfaces Electroetched

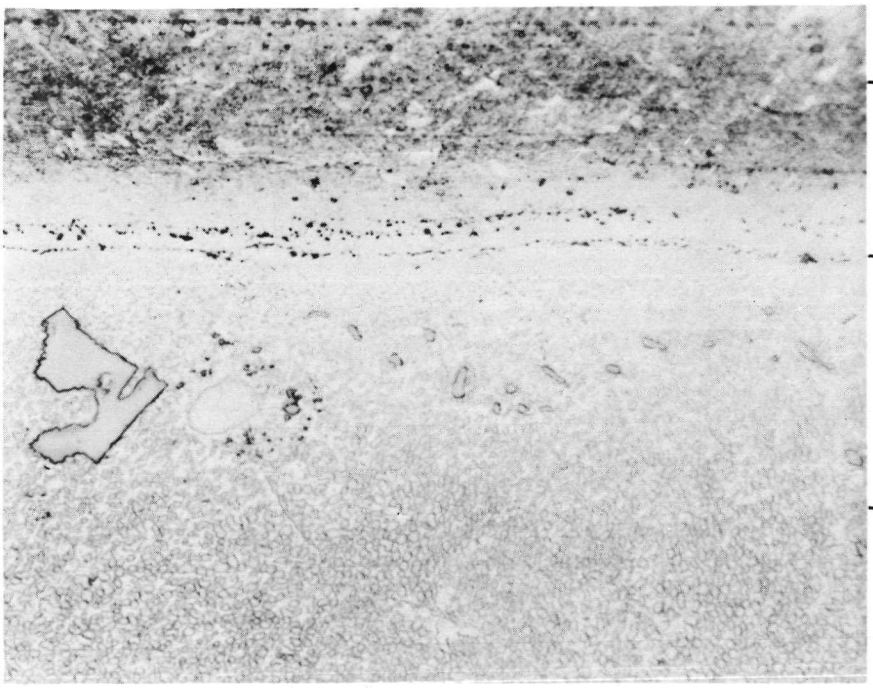

750X Marble's Etch 6C008

b. Higher Magnification View of Electroetched Surfaces

FIGURE 31. TD NiCr/B1900 DIFFUSION BONDS PRODUCED UNDER CONDITIONS OF 2200 F/10,000 PSI/1 HR

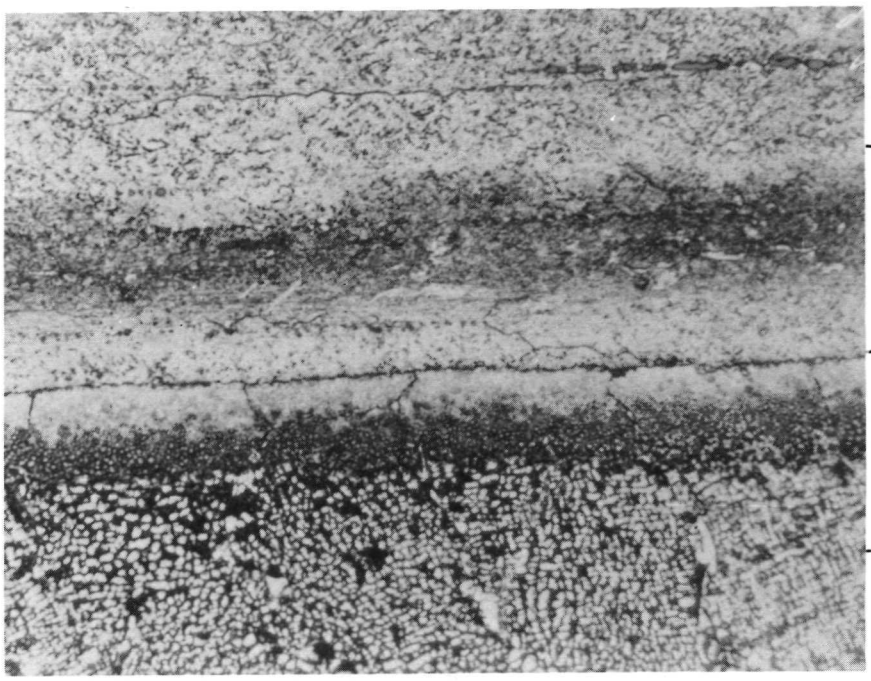

750X Marble's Etch 5C959

c. B1900 Surface Grit Blasted (100 μin. rms)

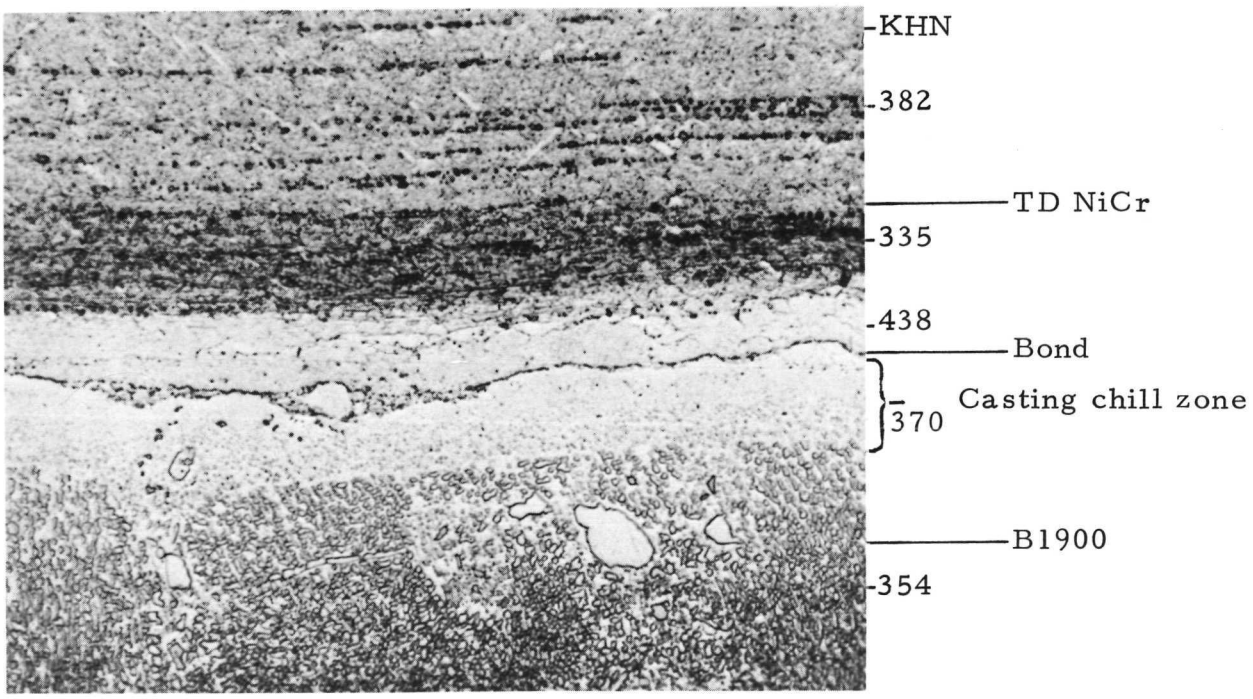

750X Marble's Etch 5C999

d. B1900 Surface Grit Blasted (150 μin. rms)

FIGURE 31. (CONTINUED)

TABLE 8. SUMMARY OF RESULTS FOR PLATEN-PRESS AND VACUUM-FURNACE BONDED TORSION SPECIMENS[a]

Specimen Number/ Type	Surface Preparation (Shell/Strut)	Experiment Identification	Bonding Conditions			Shear Strength, psi	Observations
			Temperature, F	Pressure, psi	Time, hr		
				Udimet 700/B1900			
U-10A/TT	E1/E1	PP1	2150	10,000	<0.1	51,300	Tabs were slightly deformed; failure occurred in U-700 and bond interface
U-13D/TR	EP/EP	PP4	2000	30,000	<0.1[b]	68,500	Ring slightly deformed; failure occurred in U-700 and bond interface
U-13B/TT	EP/EP	VAC1	2200	1,800	3	23,800	No deformation of tabs; only five tabs bonded
U-14A/TT	E2/GP	VAC2	1900	5,000	1	19,600	No deformation of tabs; pressure distribution questionable
				TD NiCr/B1900			
T-12C/TR	EP/EP	PP2	1800	10,000	<0.1	--	No bond; no deformation of ring
T-12D/TR	EP/EP	PP3	2000	15,000	<0.1	67,900	Excellent bond; no ring deformation; failure primarily in TD NiCr

(a) Explanation of symbols:
- TR - 0.7-in.-square torsion ring specimen
- TT - 0.7-in.-square torsion tab specimen
- E1 - chemical etch in HNO_3-HF-H_2O solution at 125 F
- EP - electroetch per Table 7
- E2 - chemical etch in equal volumes of HNO_3, HCl, and 42-deg Bé $FeCl_3$
- GP - mechanical abrasion with SiC paper
- PP - bonded in vacuum under platen press load; pressures are approximate
- VAC - bonded in vacuum of 10^{-5} torr under dead-weight load.

(b) Subsequent to bonding, specimen was given a 3-hr diffusion anneal at 2000 F in vacuum.

press runs were conducted in a retort dynamically evacuated in the range of 10^{-4} torr. The retort and specimen were heated to the desired temperature. After a 1-hr soak at temperature, the retort was rapidly removed from the furnace and placed between insulated platens of a small laboratory press. A predetermined load was then applied and maintained until the specimens cooled to 250 F. The time at temperature and pressure was less than 5 min. The dead-weight bonding experiments were conducted in a vacuum of 10^{-4} to 10^{-5} torr. Shear strengths of the order of 70 percent of parent-metal tensile yield strength were obtained from specimens processed at 2000 F. These results, in concert with the microstructural examinations made on gas-pressure bonded specimens produced at 2000 F/10,000 psi/3 hr, indicated that bonds meeting the program objectives could be achieved under those conditions.

Investigation of Support Tooling Materials

With the apparent need for temporary support tooling in the 0.086-in. (Zone M) channels of the finned shell, it was necessary to consider and select promising materials for the tooling. The usual method employed for tooling removal after bonding is selective acid leaching. Hence, the tooling material candidate must dissolve in an acid solution in which TD NiCr, Udimet 700, and B1900 are nonreactive. The usual practice with such high nickel- and chromium-bearing alloys is to employ tooling materials that can be dissolved in warm, 150 F, dilute, 35 v/o, nitric acid. Copper, iron, carbon steel, and molybdenum fall in this category. Copper could not be a serious candidate in the finned shell application because the bonding temperature required exceeds its melting point. Since there was no plan to support the 0.028-in.-wide channels (Zones L and N) of the finned shell, the molten copper would offer no support where needed as it would simply flow under pressure to fill the Zones L and N volumes. The remaining candidates were investigated.

In gas-pressure bonding Experiments 2, 3, and 4, which were summarized in Tables 5 and 6, SAE 1095 carbon steel (1.0 w/o carbon) tooling inserts were employed in the unsupported regions of the basic torsion specimen bonding coupon. The coupon and tooling inserts were illustrated previously in Figure 13. This steel was evaluated both bare and electroplated with a 0.0005-in.-thick flash of soft chromium. Neither condition yielded satisfactory results in the torsion coupon configuration. The lack of satisfactory service could have been caused by one or more of the contributing factors listed below:

(1) Bond rupture during the cooling stage as a result of differential thermal contraction between the steel tooling and the specimen alloys

(2) Inefficient pressure transfer of autoclave gas pressure through the bonding container to the bond interface

(3) Oxidation or other contamination of the bond surfaces from outgassing

(4) Contamination from an alumina slurry coating used as a diffusion barrier to prevent a bond between the bonding container and specimens.

In a systematic study, Factors (2) through (4) were eliminated. Since intact torsion samples still could not be produced in the presence of steel support tooling, it appeared that adverse thermal stresses were the cause of failure. No effort, however, was expended to obtain conclusive proof to this effect since, as will be pointed out in a later section of this report, it was demonstrated that support tooling in practice would not be required to bond the finned shell structure.

Microstructural Effects of Bare and Chromium-Plated Steel Tooling. Figures 32 through 34 illustrate the metallurgical effect of carbon steel support tooling on TD NiCr, Udimet 700, and B1900 using bonding temperatures of 2200 F and 2000 F. The photomicrographs shown are from various gas-pressure bonded torsion shear coupons. It was apparent that fairly extensive diffusion of iron, carbon, and, in the case of coated tooling, chromium into the specimen materials occurred at both process temperatures. The diffused elements caused striking changes in the microstructures of Udimet 700 and B1900. In the modified zones, secondary phases have precipitated in grain boundaries and about cells within grains. At low magnification, the structures have the appearance of having undergone grain refinement.

Udimet 700 appeared the most affected. The affected zone in this alloy was essentially the same depth with or without the presence of chromium. While no attempt was made to positively identify any of the precipitated phases, the elements involved and morphology suggested that they might be predominantly $M_{23}C_6$ carbide and sigma phase. The temperature history and elements present favor formation of these phases. B1900 appeared affected in a manner similar to Udimet 700. TD NiCr appeared to suffer only a surface reaction. Formation of excessive carbides and the presence of sigma phase degrade the mechanical properties of nickel-base superalloys such as B1900 and Udimet 700. It was concluded that bare or chromium-plated iron or steel tooling could lead to reduced elevated-temperature base-metal strength in diffusion bonded structures.

Figures 32 through 34 also illustrate the bond separation typically encountered in the torsion specimen geometry. This separation was attributed to the difference in expansivity between 1095 steel and either of the sheet alloys. Both TD NiCr and Udimet 700 have higher expansion and contraction coefficients than iron or steel. At the bonding temperature and pressure, the specimen collapses fully onto the tooling. During cooling, therefore, the tabs and rings of the torsion coupon were put in tension. The residual tensile stress was calculated to be of the order of 50,000 to 75,000 psi. The room-temperature bond separation predicted by expansivity is approximately 0.0001 in., which is very close to the dimension of the observed separation. Separation was forced, probably by the fact that the tooling area greatly overwhelmed the bond area.

Leaching Rate and Base-Metal Corrosion. In the course of preparing the initial torsion shear coupons, it was found that up to 100 hr of leaching could be required to completely dissolve the steel tooling. This time was later reduced to about 5 hr by machining a hole in the center of the specimen, adding a passivation inhibitor (2 to 3 g per liter of urea, NH_2CONH_2), and increasing the leaching bath temperature from 150 to 190 F. This procedure appeared to minimize, if not eliminate, the corrosion reaction discussed below.

Figures 35 and 36 illustrate the effect of long-term contact at 150 F with 35 v/o HNO_3 on B1900 and TD NiCr. Attack effects on Udimet 700 were shown earlier in Figure 34. In all cases extensive intergranular attack occurred. Samples of B1900, Udimet 700, and TD NiCr were tested in the leaching solution; the results of those tests are summarized in Figure 37. The alloys were exposed in both the as-received condition and after a heat treatment at 2000 F for 1 hr in fore-pump vacuum. Heating and cooling rates were controlled to simulate those of an autoclave cycle, 2.5 hr to temperature and a cooling period of 6 to 8 hr. Corrosion resistance, as shown in Figure 37, was depressed by the heat treatment.

While the corrosion rate of TD NiCr was satisfactory, that of Udimet 700 was marginal, and B1900 corrosion began to approach catastrophic proportions after 24 hr of exposure. TD NiCr tended to stabilize very quickly to a uniform loss rate of 0.05 to 0.1 mil per day. Udimet 700 similarly rapidly stabilized but at a higher final rate, 0.1 to 1.0 mil per day depending on heat-treatment conditions. B1900, on the other hand, did not stabilize until after approximately 100 hr of exposure. The stabilized rate was on the order of 2 to 4 mils per day, again depending on heat treatment. Thus, it could be expected that a specimen requiring even the 24-hr leaching period originally anticipated would suffer a 1-mil Udimet 700 and 2-mil B1900 loss and the probability of yet deeper penetration at grain-boundary penetration; TD NiCr should suffer negligible loss during that period.

It was of interest to determine the relative difference in dissolution rates of SAE 1095 and SAE 1018 steel in 35 v/o HNO_3 at ambient temperature. The former steel has 1 w/o carbon; the latter has 0.15 w/o carbon. There was a significant difference. SAE 1018 steel dissolved at a rate 2.5 times faster than SAE 1095 steel.

Evaluation of Alternative Tooling Materials. TD NiCr/B1900 Specimens T-23 and T-29 were gas-pressure bonded at 2000 F and 10,000 psi for 2 hr in order to evaluate SAE 1018 steel, Armco iron, and molybdenum as support tooling for Zone M of finned shells. SAE 1018 steel was examined bare, electroplated with nickel, and plated with electroless nickel (0.0005-in.-thick plate). Armco iron was similarly evaluated in bare and nickel-plated conditions. The molybdenum was used bare. The purpose of the investigation was to determine if any of these candidates could eliminate the metallurgical and leaching problems discussed previously.

100X As Polished 5C988

a. Typical Bond Line Separation

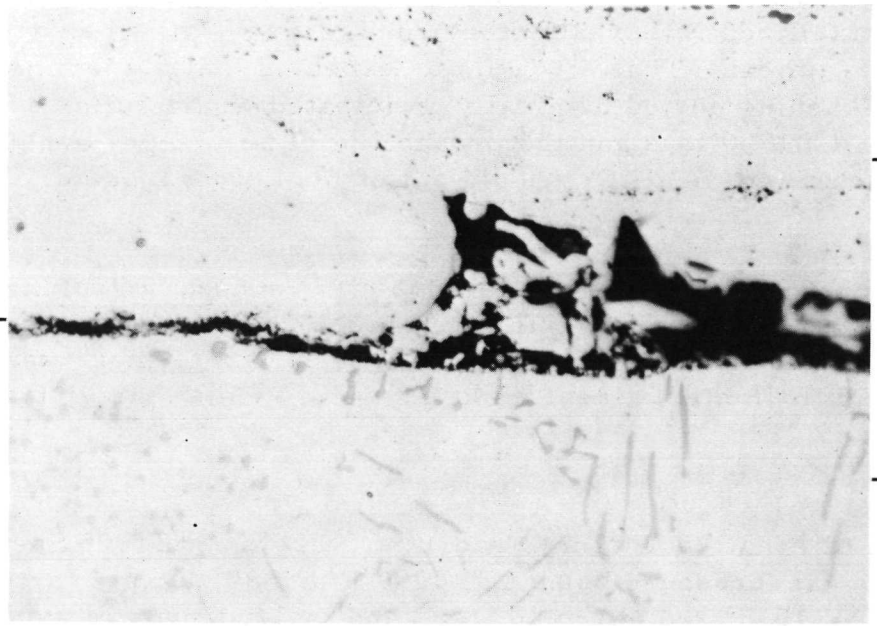

750X As Polished 5C985

b. Tooling Extrusion

FIGURE 32. EFFECT OF CHROMIUM-PLATED 1095 STEEL SUPPORT TOOLING UNDER BONDING CONDITIONS OF 2200 F/10,000 PSI/1 HR

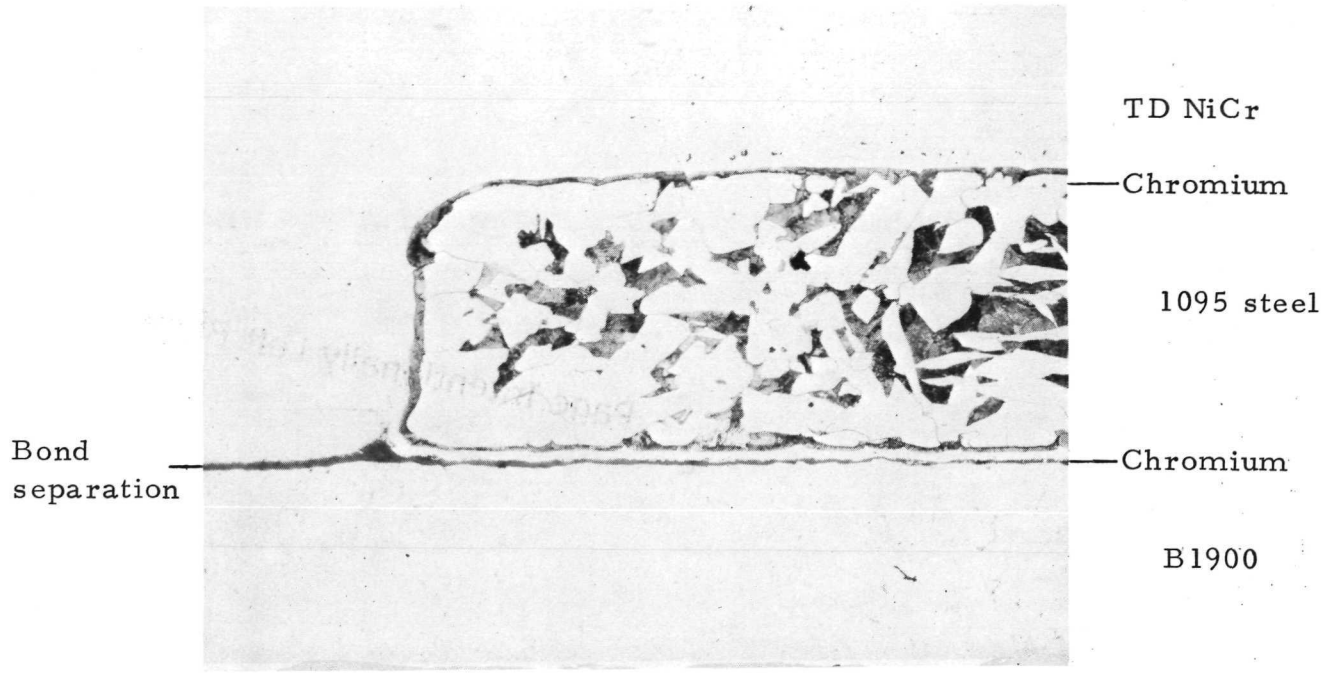

100X 2% Nital 5C976

c. Chromium-Steel Interaction

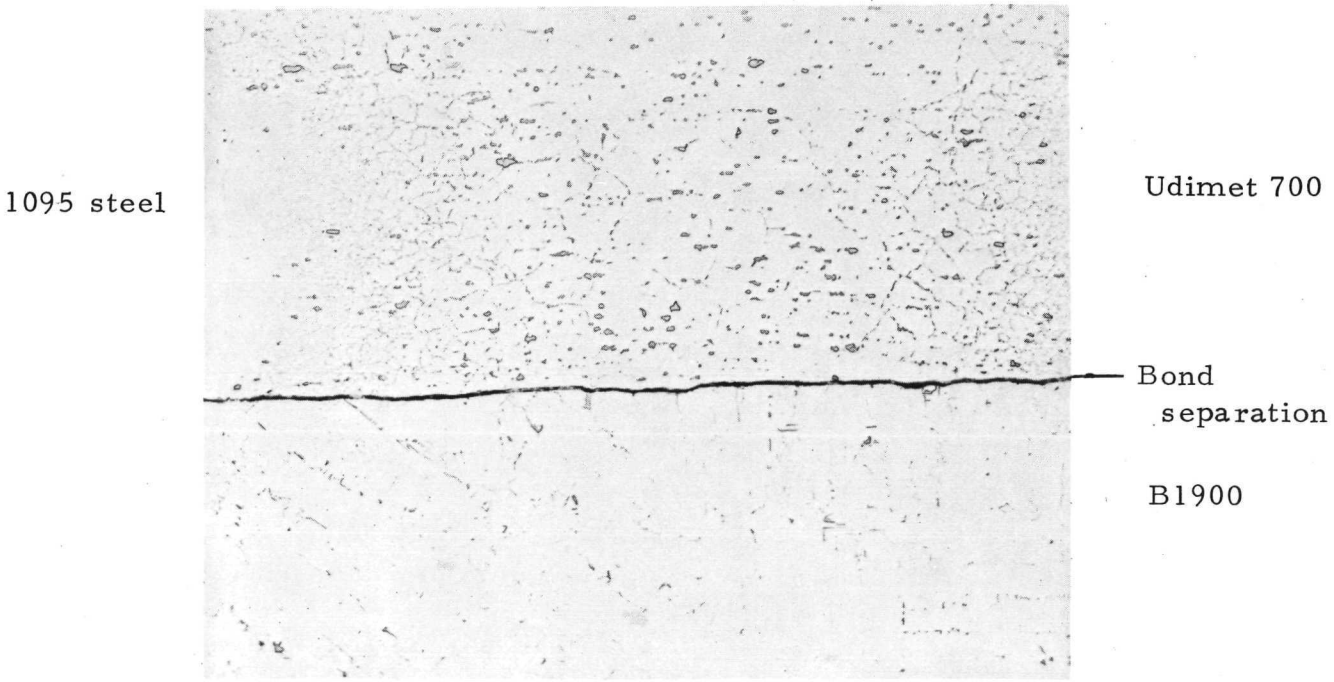

100X As Polished 5C994

d. Modification of Udimet 700 Microstructure

FIGURE 32. (CONTINUED)

Page Intentionally Left Blank

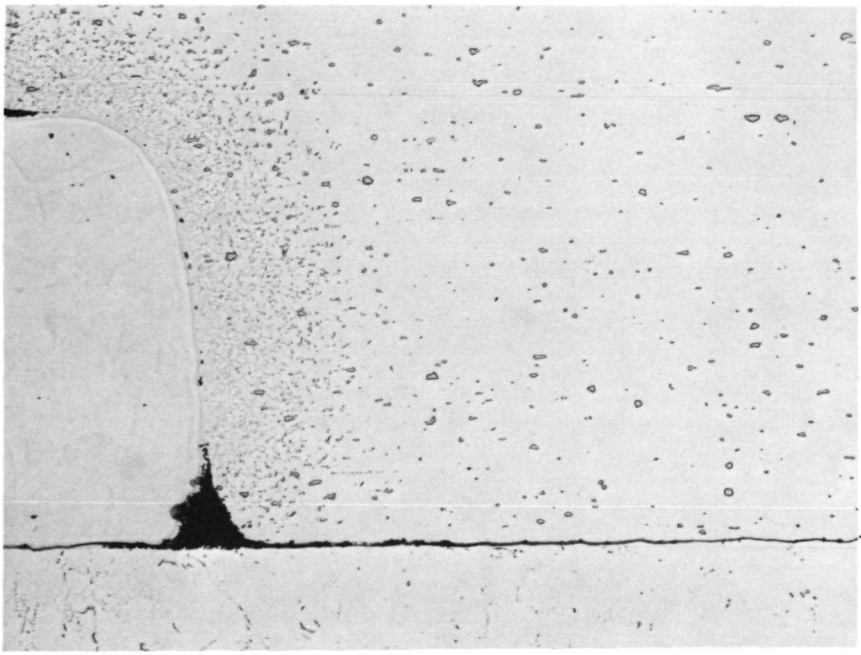

100X As Polished 8C420

a. Udimet 700 and B1900 Microstructure Modification

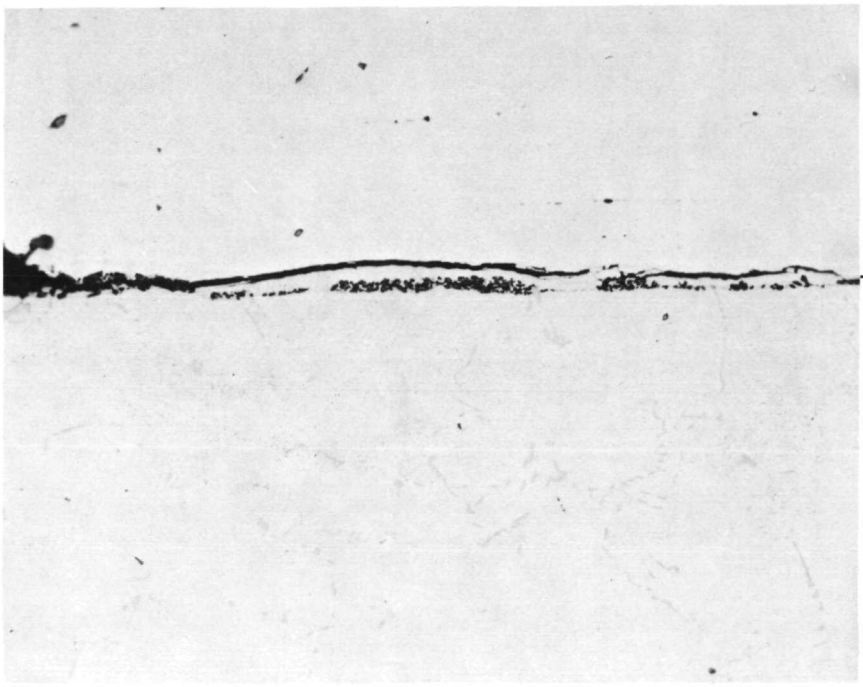

250X As Polished 8C423

b. Contraction Crack and Alumina Contamination at B1900/Tooling Boundary

FIGURE 33. EFFECT OF CHROMIUM-PLATED 1095 STEEL SUPPORT TOOLING UNDER BONDING CONDITIONS OF 2000 F/10,000 PSI/3 HR

100X As Polished 8C428

a. Steel-TD NiCr Reaction Layer

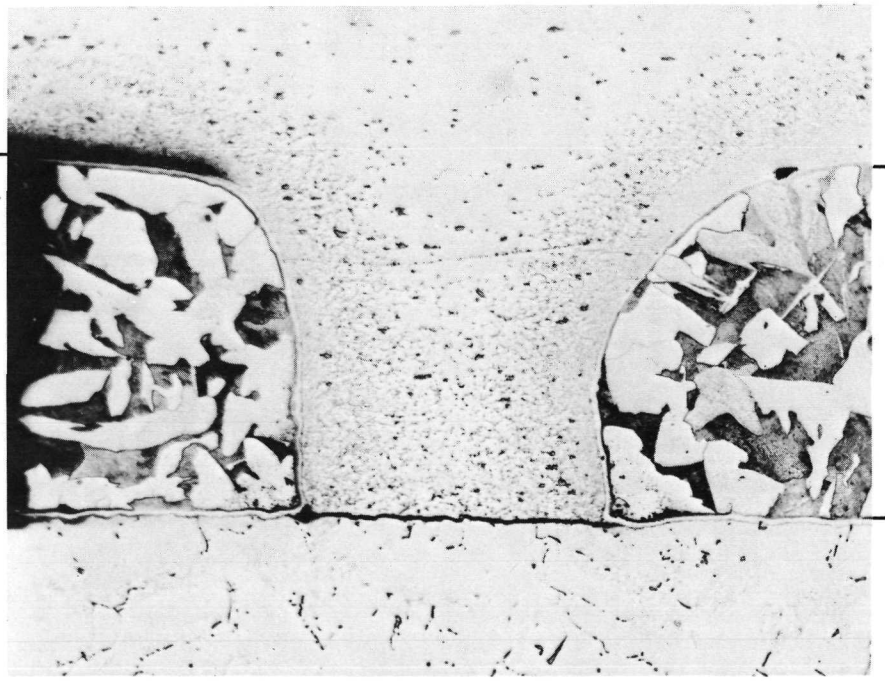

100X 2% Nital 8C411

b. Bond Separation and Diffusion Reaction in Udimet 700/B1900 Tab Specimen

FIGURE 34. EFFECT OF BARE 1095 STEEL SUPPORT TOOLING UNDER BONDING CONDITIONS OF 2000 F/10,000 PSI/1 HR

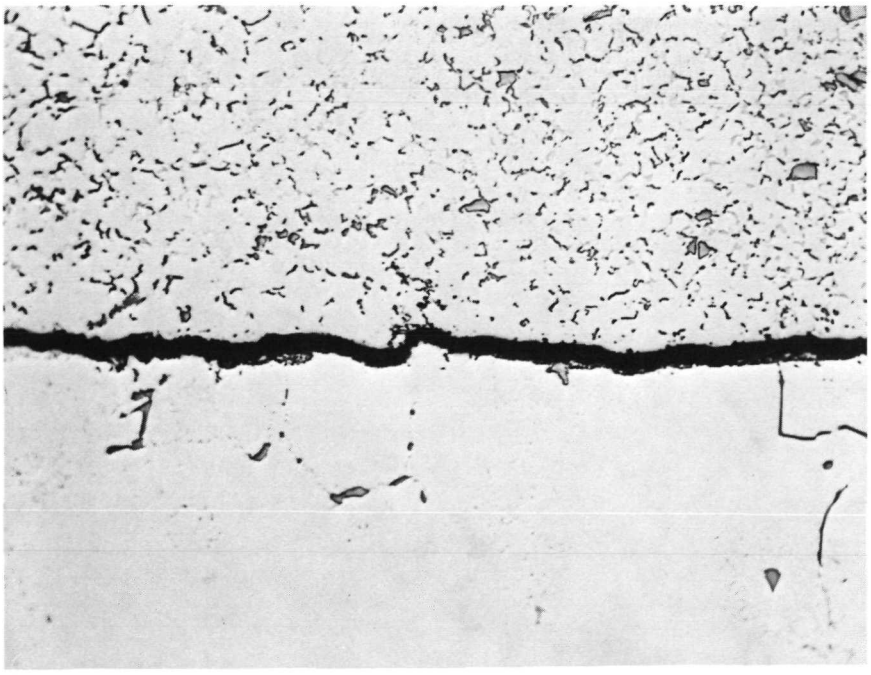

500X 2% Nital 8C415

c. Higher Magnification Field of Specimen in Figure 34b, Illustrating Extensive Precipitation

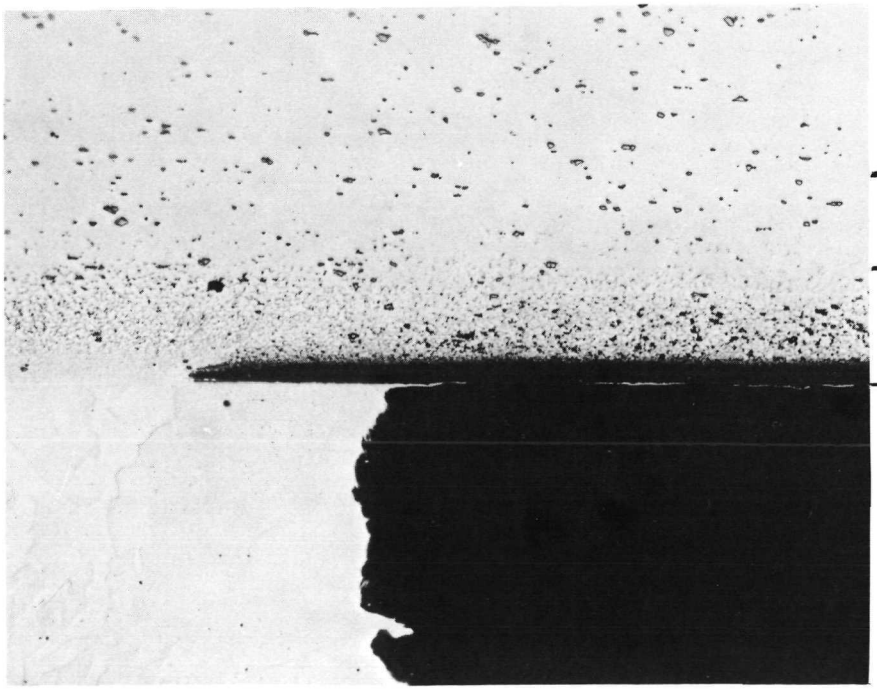

100X As Polished 8C412

d. Partially Dissolved Steel Tooling

FIGURE 34. (CONTINUED)

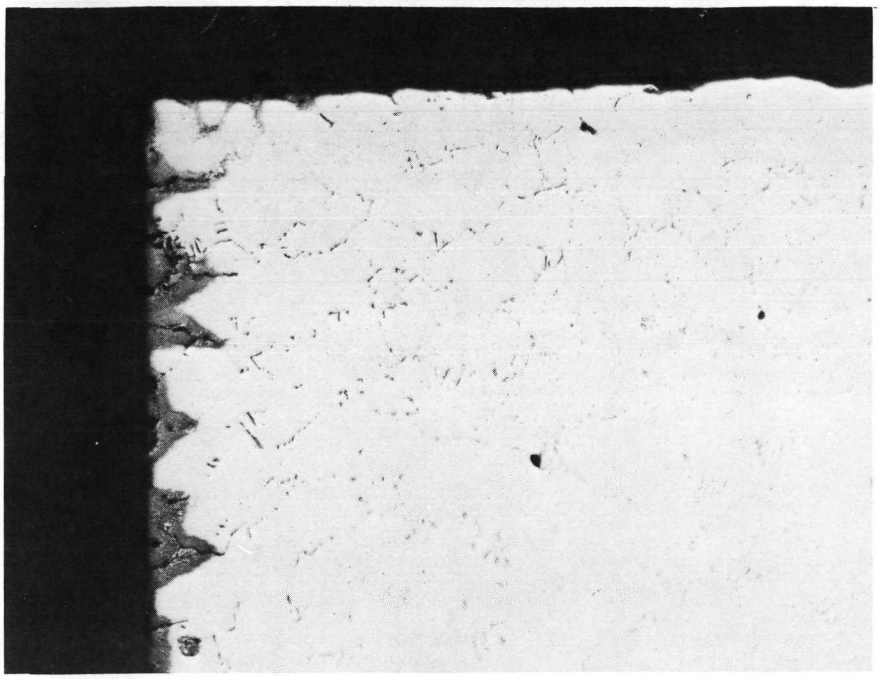

100X As Polished 8C413

a. Exterior Surface

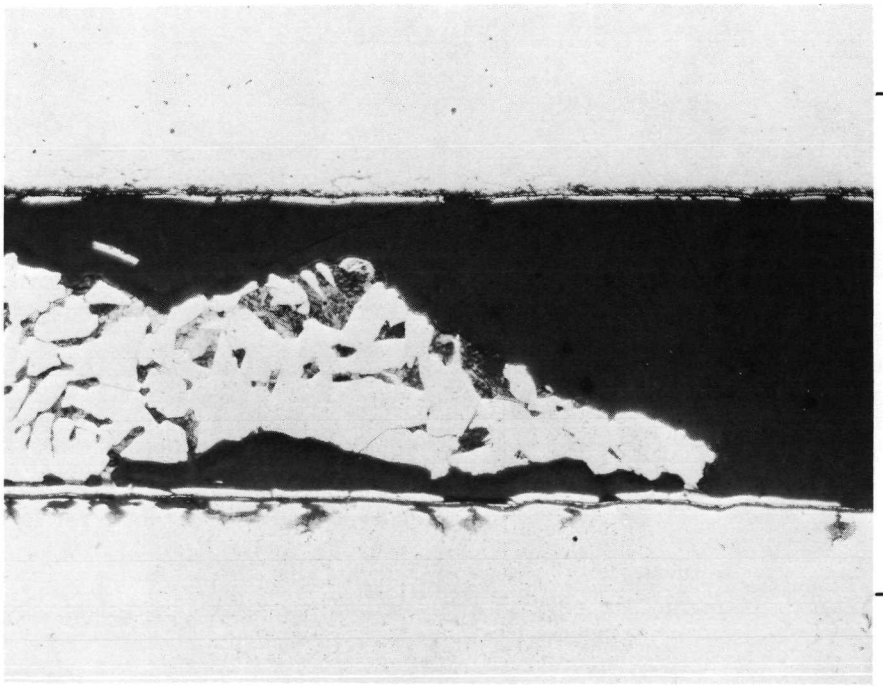

100X 2% Nital 5C978

b. Partially Dissolved Area

FIGURE 35. EFFECTS OF HOT NITRIC ACID ATTACK ON B1900

The specimen was exposed to 35 v/o HNO_3 at 150 F with 2 to 3 g per liter of urea depassivator.

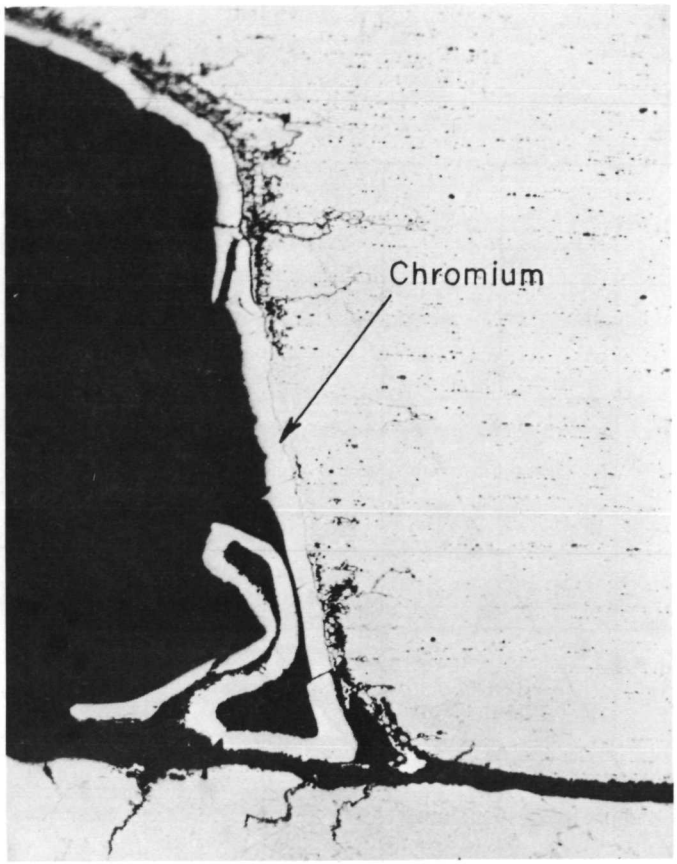

250X 2% Nital 5C970

a. Specimen T-8D

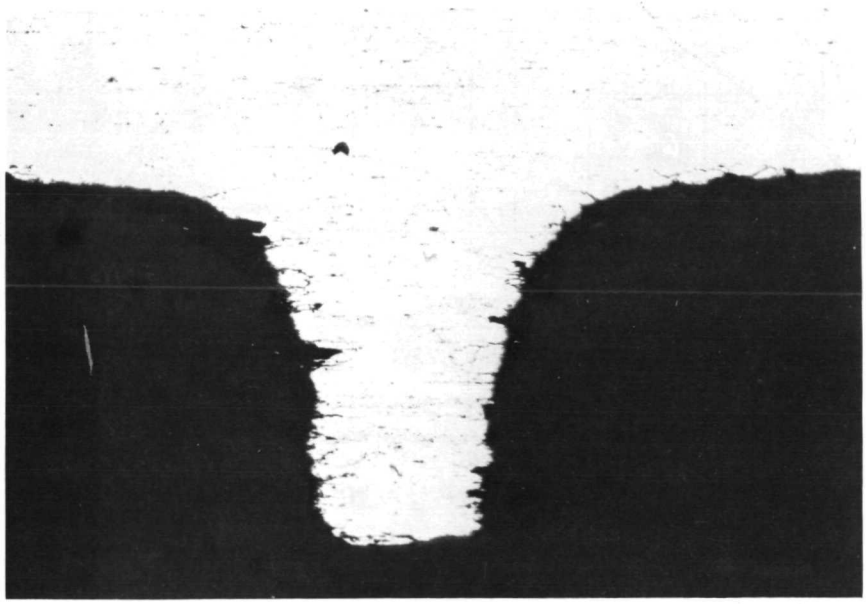

100X Marble's Etch 5C980

b. Specimen T-9B

FIGURE 36. EFFECTS OF HOT NITRIC ACID ATTACK ON TD NiCr
The specimens were exposed to 35 v/o HNO_3 at 150 F for 90 hr.

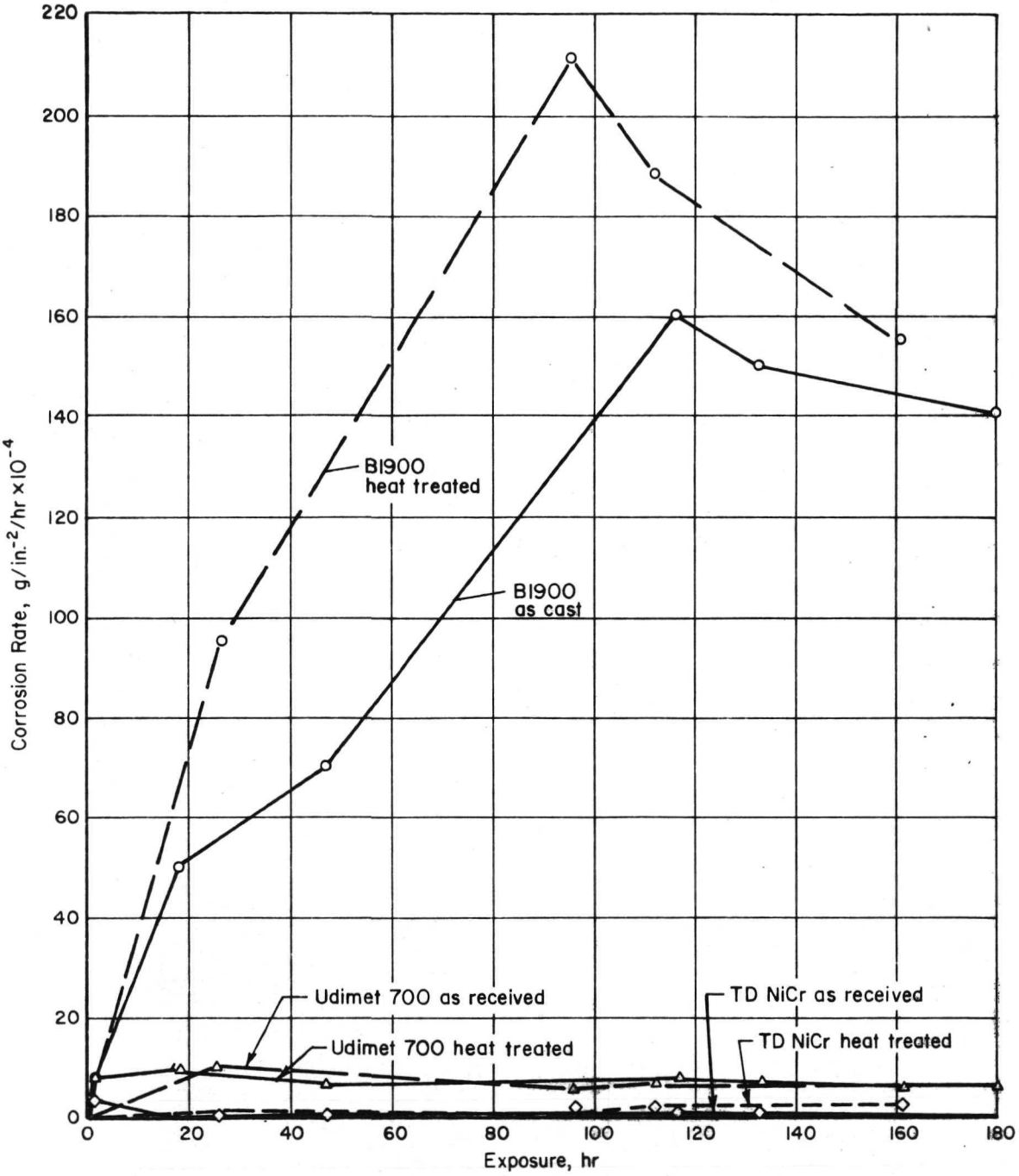

FIGURE 37. BASE-ALLOY CORROSION RATES IN 150 F INHIBITED NITRIC ACID

None of the candidate internal support tooling systems evaluated in Specimens T-23 and T-29 were wholly satisfactory. The candidates are listed below in order of decreasing observed dissolution rate:

(1) Molybdenum (uncoated)
(2) Nickel-plated Armco iron
(3) Nickel-plated SAE 1018 carbon steel
(4) Uncoated Armco iron
(5) Uncoated SAE 1018 carbon steel.

Molybdenum was promising with respect to compatibility and leachability. Leaching time for a 1-in. length was about 6 hr using 35 v/o HNO_3 at 150 F. It was necessary to add approximately 5 v/o of concentrated H_2SO_4 to sustain the leaching reaction. Unfortunately, the thermal expansion mismatch between molybdenum and nickel-base alloy is even higher than that of steel and iron, and the thermal stress problem discussed previously is further aggravated.

In Specimen T-23 (TD NiCr finned shell) three out of four fins located between a molybdenum and SAE 1018 carbon steel insert were ruptured. The specimen is shown in Figure 38. All other fins gave the appearance of being well

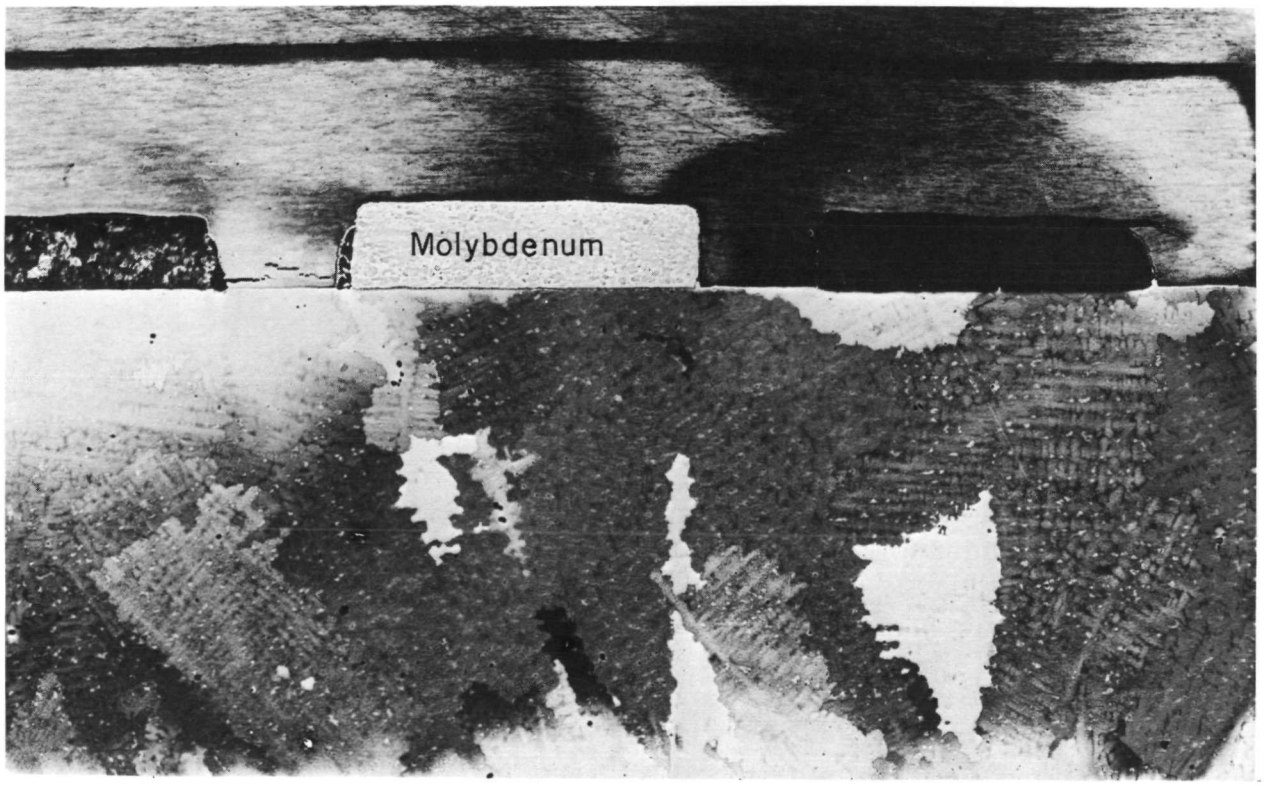

20X Marble's Etch 8C568

FIGURE 38. CRACKED TD NiCr ZONE M FIN IN SPECIMEN T-23 CAUSED BY MOLYBDENUM TOOLING

Specimen was gas-pressure bonded under conditions of 2000 F/10,000 psi/2 hr.

bonded. Significantly, the rupture occurred almost exclusively in the TD NiCr and not at the bond interface. In Specimen T-29, which consisted of TD NiCr ribs bonded to a TD NiCr sheet and B1900 plate, the TD NiCr self-bond was found to be ruptured in the three ribs adjacent to molybdenum-filled channels. Like Specimen T-23, ribs adjacent to steel or iron-filled channels in Specimen T-29 appeared satisfactorily bonded. Both conditions are illustrated in Figure 39. While nickel plating appeared beneficial with respect to the condition of the base-alloy surface after leaching, urea was still required to maintain the leaching reaction. Use of an inhibitor such as urea was considered undesirable as it tended to promote attack of the B1900 strut plate. A typical attacked area was shown previously in Figure 35. Leaching times of the four iron-base candidates were about the same from a practical viewpoint; approximately 25 to 30 hr were required for a 1-in. length.

Elimination of Channel Support Tooling

Specimens T-23, -25, -26, and -29 were gas-pressure bonded at 2000 F and 10,000 psi for 2 hr. The results obtained from these specimens are summarized in Table 9. The objectives of this experiment were:

(1) To investigate the practicability of bonding a finned shell to a strut plate without internal support tooling

(2) To evaluate several candidate support tooling systems with regard to compatibility and leachability

(3) To continue the evaluation of candidate shell and strut surface preparations.

Evaluation of Unsupported TD NiCr Finned Shell. Specimen T-23 was employed to establish the feasibility of bonding finned shells without internal support. During assembly, every fourth channel in Zone M was left unfilled, and all Zone L and N channels were unfilled. The remaining 12 Zone M channels were filled with loosely fitting molybdenum, bare SAE 1018 steel, and bare Armco iron strips. A clearance of at least 0.002 in. was left between the respective heights of the fin and strip so that there could be no interference to fin/strut contact during bonding. To prevent bowing of the channel span, a bridge in the form of a 0.062-in.-thick TD NiCr 2 by 2-in. plate was placed over the finned shell. Calculations had shown that an unbridged channel 0.084 in. wide by 0.035 in. thick would deform under the 10,000-psi overpressure employed in this experiment. The addition of a 0.060-in.-thick bridge, however, raises the resistance to collapse by a factor slightly greater than seven.

Visual, radiographic (Figure 40), and metallographic examination (Figures 41 and 42) of Specimen T-23, TD NiCr finned shell, indicated that bonding without internal channel support would be practical. Bowing of the unsupported spans both in the 0.084- and 0.028-in.-wide channel zones was found to be very slight, and

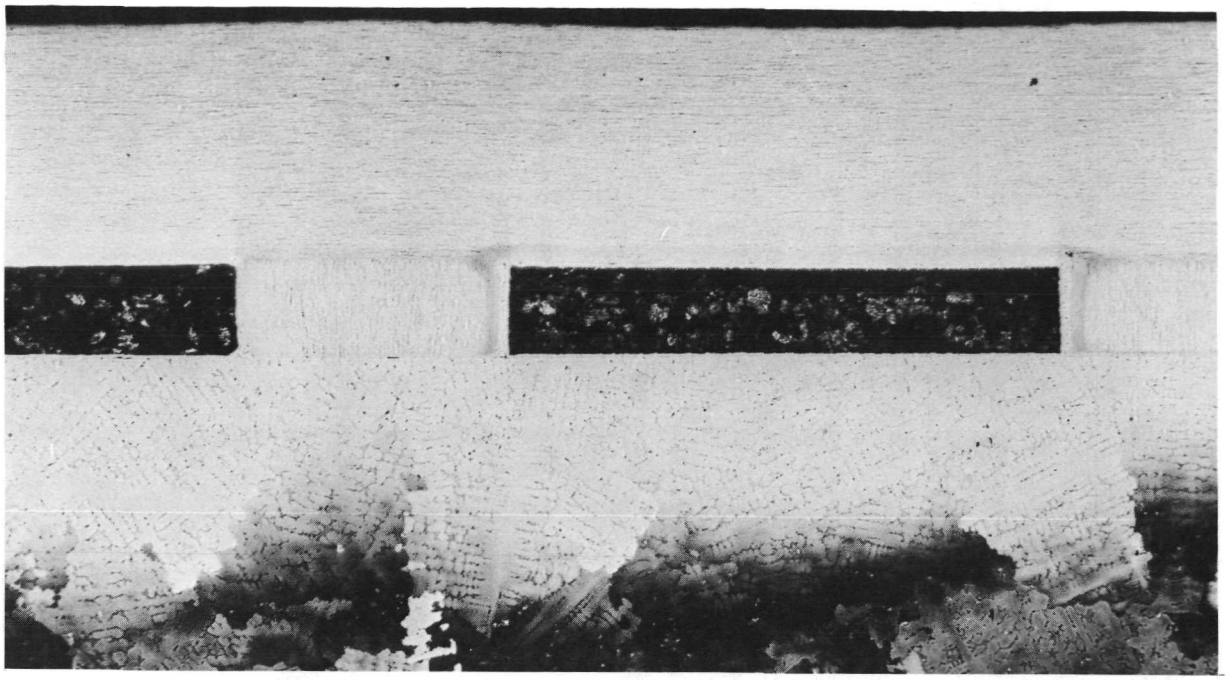

20X Marble's Etch 8C576

a. Ribs Surrounded by Iron and Steel Tooling

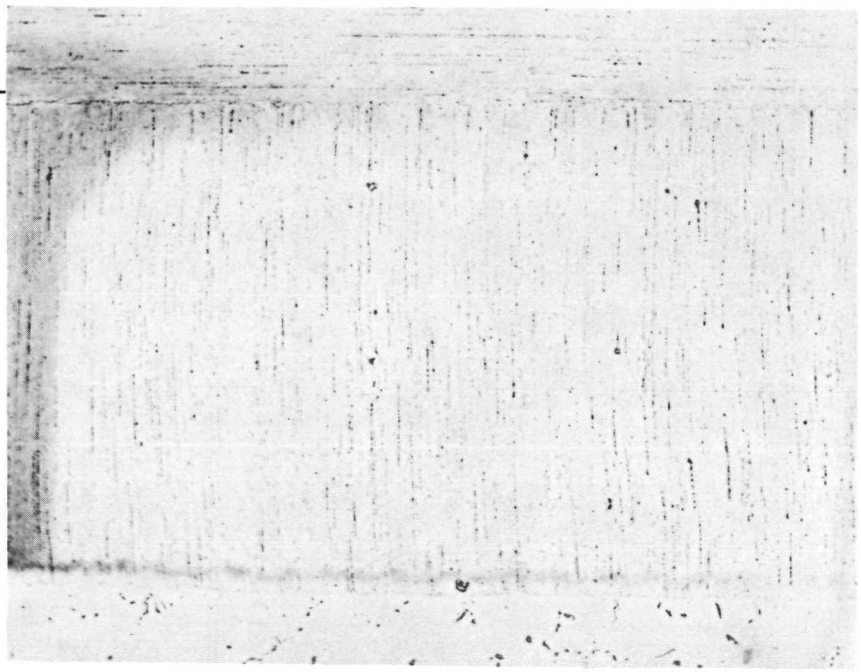

100X Marble's Etch 8C560

b. Rib Adjacent to Molybdenum Tooling

FIGURE 39. TD NiCr/B1900 CHANNEL SPECIMEN FABRICATED FROM INDIVIDUAL PLATES AND RIBS FOR TOOLING EVALUATION

Specimen T-29 was gas-pressure bonded under conditions of 2000 F/10,000 psi/2 hr.

TABLE 9. SUMMARY OF TD NiCr/B1900 SPECIMENS PREPARED IN GAS-PRESSURE BONDING EXPERIMENT 5[a]

Specimen Number/ Type	Surface Preparation (TD NiCr/B1900)	Objective	Shear Strength, psi	Observations
T-23/F	VE/VE	Evaluation of unsupported channel approach and evaluation of molybdenum, 1018 steel, and Armco iron channel tooling	--	Well bonded; fins deformed from excess compression; unsupported channels open; thermal expansion cracking from molybdenum tooling
T-25/C	EP/EP	Surface preparation evaluation	A - 52,000 B - 64,700	Fracture divided between TD NiCr and bond; clean microstructure
T-26/C	E1/EP	Surface preparation evaluation	A - >14,500 B - >48,000	Fracture divided between TD NiCr and bond; clean microstructure; buckling prevented full test
T-29/RP	VE, E1/EP[b]	Evaluation of molybdenum, 1018 steel, and Armco iron tooling materials; evaluation of TD NiCr self-bonding	--	Well bonded clean microstructure; TD NiCr self-bonds cracked from molybdenum tooling

(a) Explanation of symbols: F - finned shell
C - unmachined 2 by 2-in. coupon
RP - rib and plate specimen; 2-in. - square TD NiCr and B1900 plates with 0.060 by 0.025 by 2.000-in. TD NiCr ribs
VE - vacuum etch; 2200 F for 1 hr in vacuum of 10^{-5} torr
EP - electroetch per Table 7 except T-25 TD NiCr employed 80 v/o H_3PO_4-20 v/o H_2SO_4 solution (2 min at 250 amp/ft^2 and 120 F)
E1 - chemical etch in HNO_3-HF-H_2O at 125 F for 10 min.

(b) TD NiCr plate was vacuum etched; TD NiCr rubs were chemically etched.

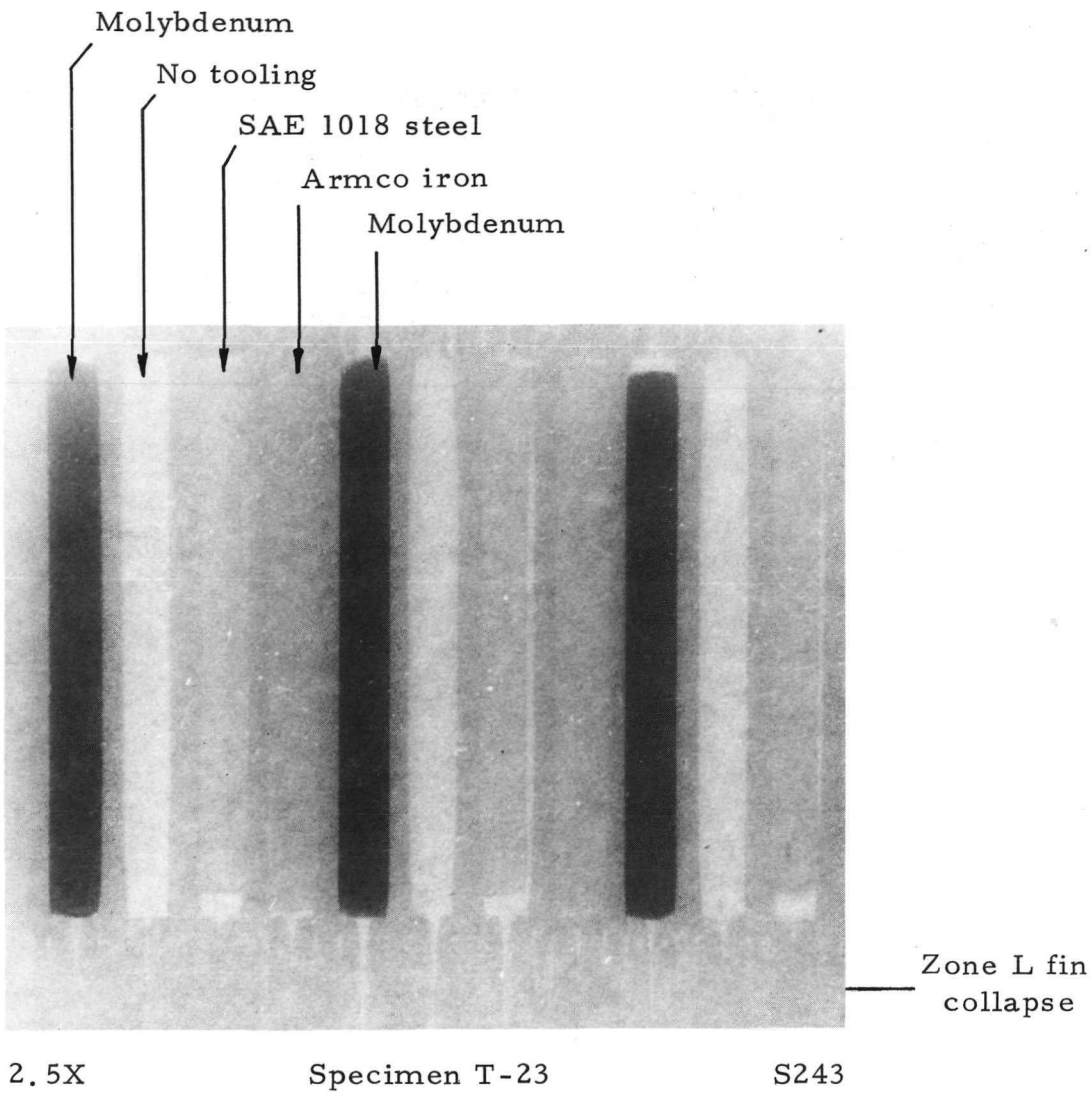

FIGURE 40. RADIOGRAPH OF FINNED SHELL CONTAINING UNSUPPORTED CHANNELS AND CANDIDATE CHANNEL SUPPORT MATERIALS

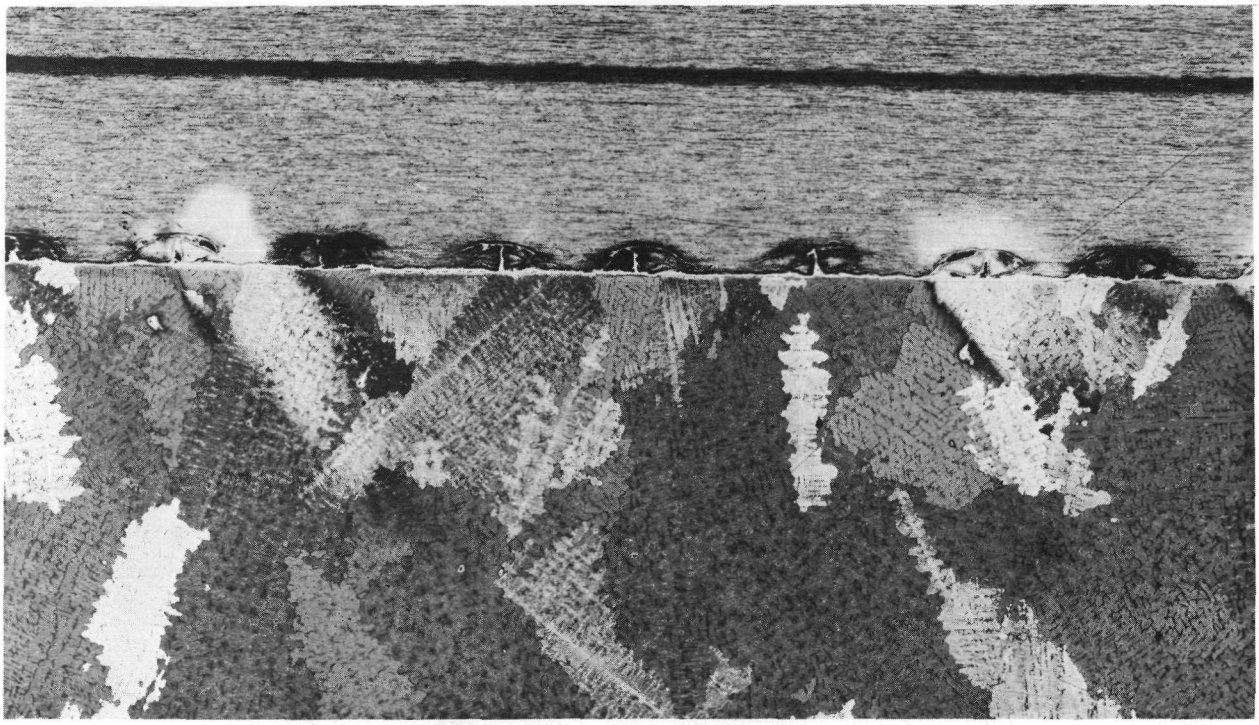

20X 8C574

a. Fin Deformation in Zone L Under 33,000-Psi Interface Pressure

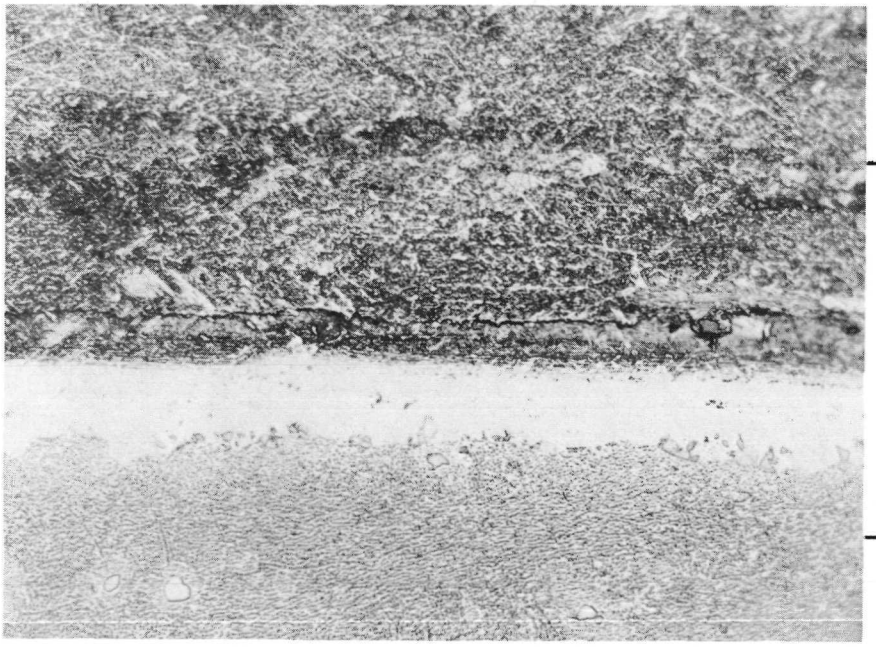

500X 8C567

b. Typical Bond Area

FIGURE 41. ZONE L OF SPECIMEN T-23 AFTER GAS-PRESSURE BONDING CYCLE AT 2000 F AND 10,000 PSI HELD FOR 2 HR

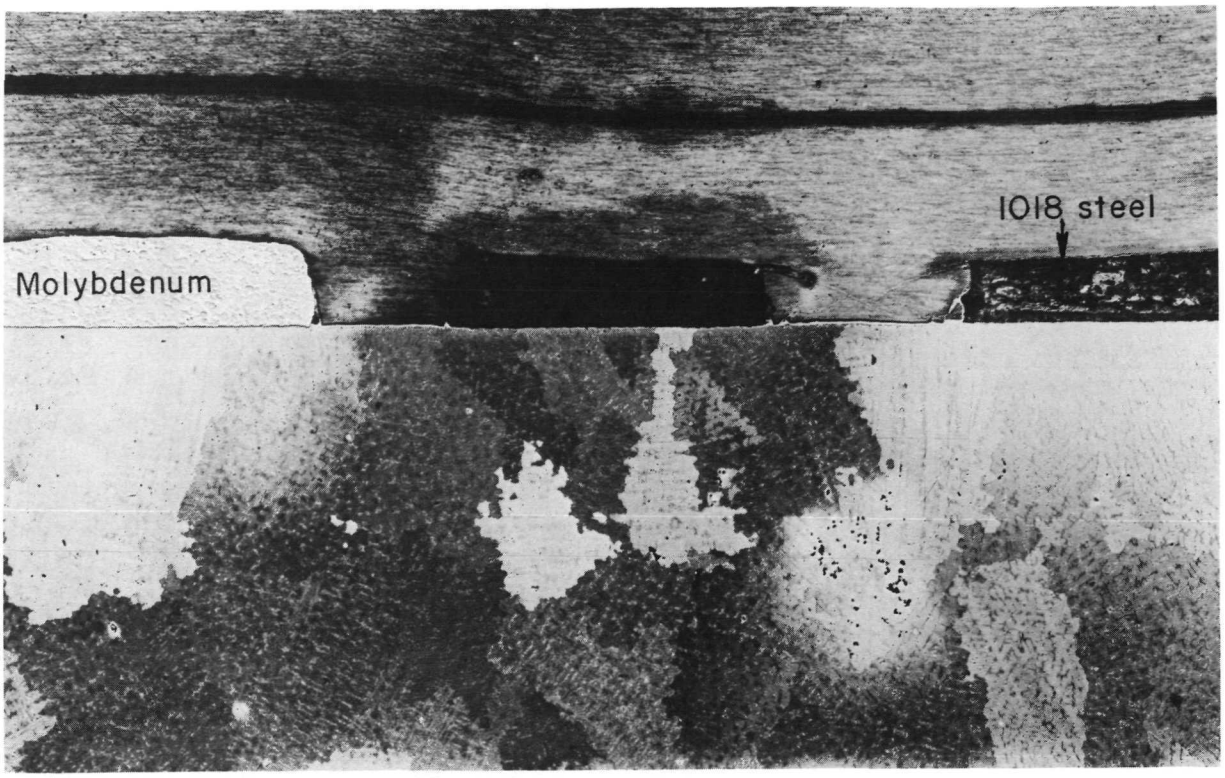

20X 8C572

a. Comparison of Molybdenum and Steel Filled Channels and Unsupported Channel

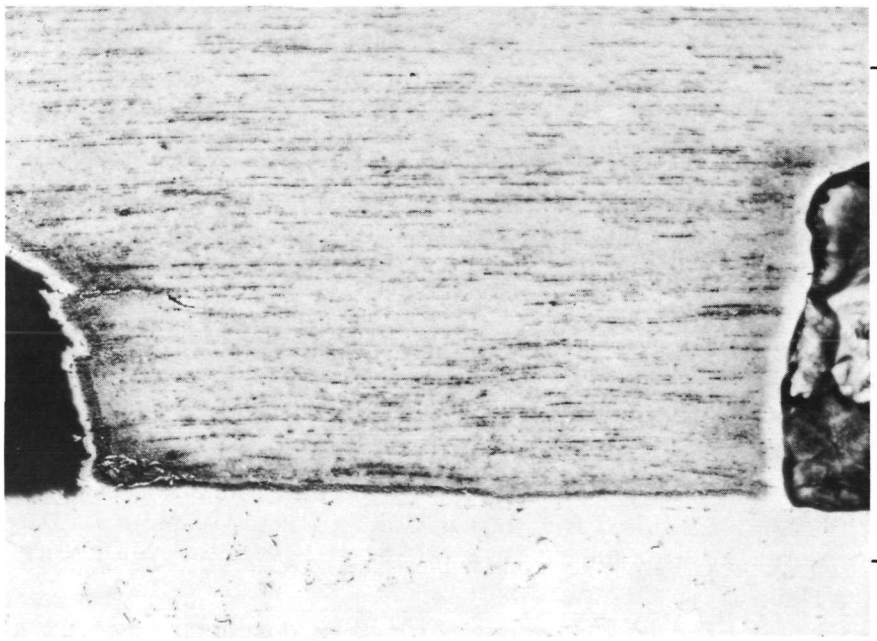

100X 8C562

b. TD NiCr Rib Adjacent to Unsupported Channel

FIGURE 42. ZONE M OF SPECIMEN T-23 AFTER GAS-PRESSURE BONDING CYCLE AT 2000 F AND 10,000 PSI HELD FOR 2 HR

the cross-sectional area of the channel would probably have changed by less than 10 percent as a result of bowing alone. However, the fins were unable to withstand the bearing pressure generated by the 10,000-psi autoclave pressure. This was anticipated and unavoidable. Assuming elastic behavior, bearing pressure at the fin/strut interface in this experiment was 33,000 psi. As a result, the 0.012-in.-thick fins (Zones L and N) deformed to half their original height, and the 0.036-in. fins (Zone M) were shortened by 20 to 25 percent.

Evaluation of Strength and Surface Preparation. Ring torsion shear specimens were prepared from flat-plate Specimens T-25 and T-26. Shear strengths in the range of 50,000 to 65,000 psi were obtained. On the basis of these tests and examination of bond microstructures, it was concluded that a chemical etch was an acceptable alternative shell-material surface treatment to electroetching. Electroetching of the shell-material surface tended to round the fins, which effectively reduced contact area and increased the probability of a notch at the fin/strut interface.

During the macroexamination of torsion specimen fracture surfaces (Specimens T-25 and T-26) at magnifications up to 60X, a black deposit in the base of some TD NiCr surface scratches was detected. It was concluded that the deposit was burnt EDM dielectric oil. The oil had evidently been pulled into small capillaries formed between normal grinding scratches in the TD NiCr surface and the surface of the B1900 strut plate. Samples from Specimens T-25 and T-26 were examined parallel and transverse to the final rolling direction of the TD NiCr sheet. This examination confirmed that capillaries approximately 0.001 to 0.002 in. wide by 0.0005 in. deep are formed at the TD NiCr/B1900 bond interface. Since the capillaries cannot be closed under pressure and temperature conditions compatible with stress limitations imposed by the finned shell geometry, it was decided that the TD NiCr should be smoothed with successively finer SiC grit paper through No. 600 to remove the objectionable surface. Figure 43 illustrates typical capillaries and bond appearances in Specimens T-25 and T-26. The capillaries viewed transversely exhibit a roughly regular pattern of rounded defects approximately 0.002 in. long by 0.0005 in. high. Viewed in a parallel section, the capillaries, when exposed, appear as an array of irregular defects approximately 0.010 to 0.015 in. wide by 0.0005 in. high. Figure 43 also illustrates that the bond microstructures resulting from electroetching and chemical etching surface treatments were equivalent. Bond quality appeared quite comparable to bonds prepared at 2200 F and 10,000 psi (see Figure 28).

This experiment concluded the preliminary investigation of process requirements. From the work conducted to this point it was concluded that:

(1) No totally satisfactory support tooling materials were established. All materials investigated required either excessive leaching time or, in the case of molybdenum, resulted in fin rupture because of thermal expansion mismatch; excessive leaching degraded the base materials.

(2) Bonding of the finned shell geometry without channel support tooling was feasible.

(3) Room-temperature shear strengths on the order of 70 percent of shell-material yield strength were feasible from a 2000 F process temperature and appropriate interface pressure.

(4) A variety of shell and strut component surface treatments were suitable for promoting good bonding results.

(5) Chemical etching of the shell material was to be preferred for good retention of fin detail.

(6) The original surface topography of TD NiCr is not altered during bonding; the surface must be polished to avoid voids at the bond interface.

Refinement of Bonding Process Parameters

TD NiCr/B1900 Finned Shell Bonding Process

Three gas-pressure bonding experiments were conducted to bracket process conditions yielding finned shell structures meeting the program objectives of bond continuity and dimensional control. On the basis of these experiments, gas-pressure bonding parameters of 2000 F/3500 psi/1 hr appeared near optimum. Further refinement is of course possible. Photomacrographs of Specimen T-31, produced under those conditions, is shown in Figure 44. All four specimens produced in this 2000 F/3500 psi/1 hr cycle exhibited literally no fin or channel dimension change during bonding. This is indicated in the radiograph shown in Figure 45. Furthermore, all four appeared to be well bonded.

Table 10 summarizes the results of the three refinement experiments and of Specimen T-40 which was processed with the cylindrical TD NiCr/B1900 specimens discussed later. It may be seen that a process pressure lower than 3500 psi tends to result in poor bond quality. Alternatively, raising the process pressure to 4000 psi resulted in unacceptably high fin deformation and, consequently, channel flow area reductions larger than the 15 percent allowed by the program goal. The fins in Specimens T-35 through T-39 were undersize, and the bearing stress on the fins was of the order of 16,000 psi in Zone M and 20,000 psi in Zone L. Only incremental gains in joint strength resulted from the increased pressure, however. The specimens in Experiments 9 and 12, represented by Specimens T-37 and T-40, respectively, in Figures 46 and 47, tend to bracket the maximum allowable fin stress for TD NiCr at 2000 F. Zone M of Specimen T-37 at 16,000 psi, and Zone L of Specimen T-40 at 17,500 psi, show no yielding of the TD NiCr. Conversely, Zone L of Specimen T-37 at 20,000 psi, has deformed. Therefore, the 2000 F bearing stress limit, σ_f, lies apparently between 17,500 and 20,000 psi.

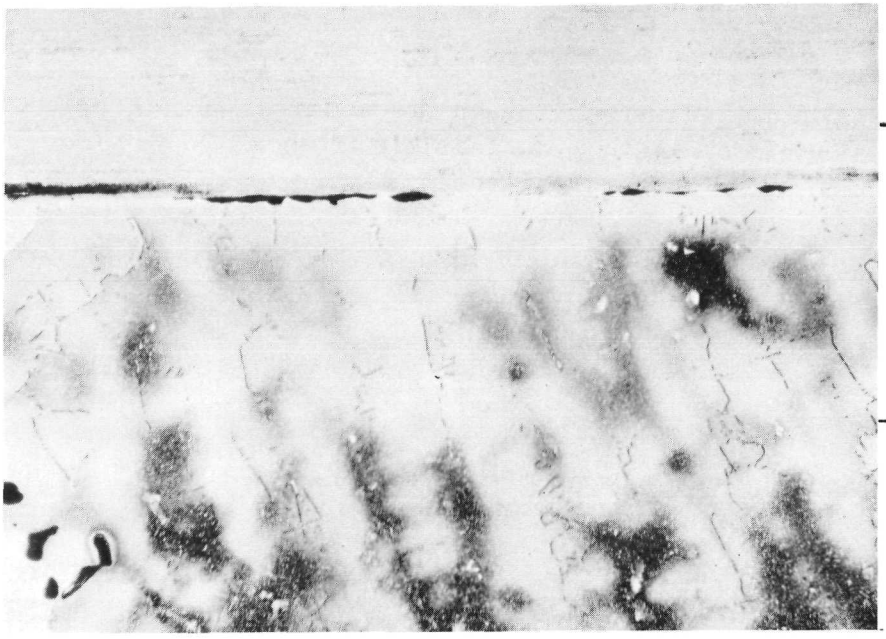

100X Marble's Etch 0D106

a. Parallel Section of Specimen T-25 (TD NiCr Surface Prepared by Electroetching)

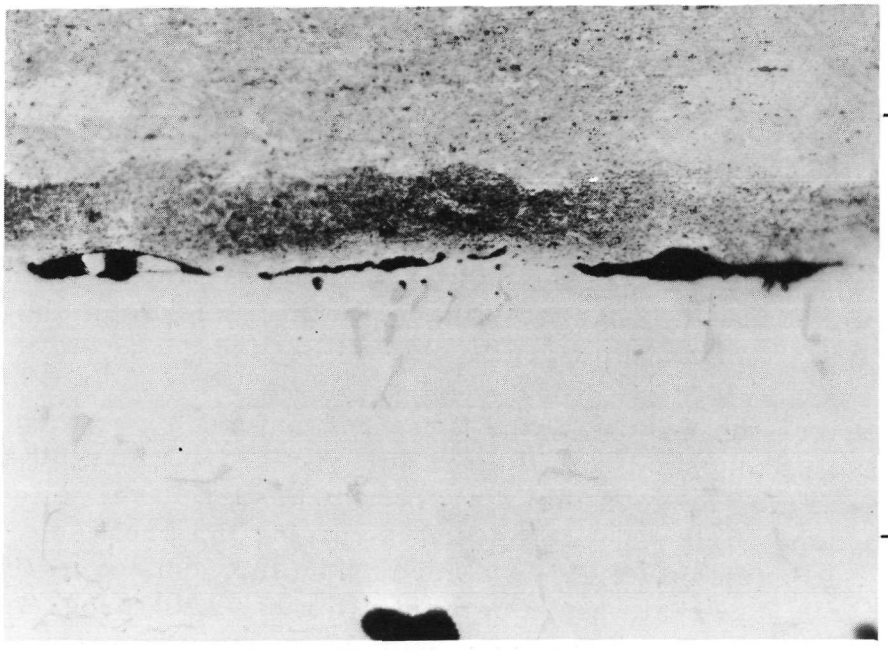

500X Marble's Etch 0D111

b. Transverse Section of Specimen T-25

FIGURE 43. MICROSTRUCTURE OF TORSION SHEAR SPECIMENS GAS-PRESSURE BONDED UNDER CONDITIONS OF 2000 F/10,000 PSI/2 HR

Sections were taken either parallel or transverse to the TD NiCr grinding direction.

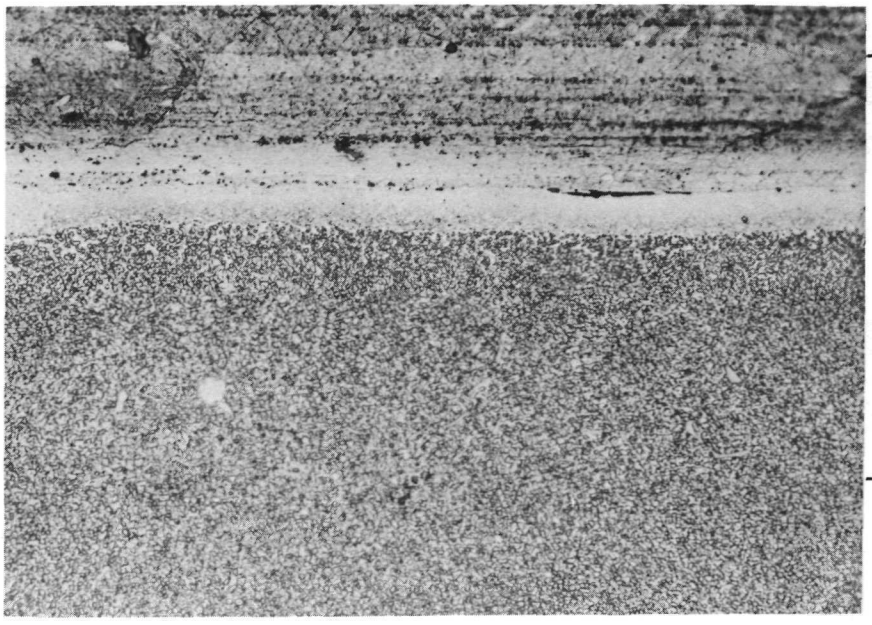

500X Marble's Etch 0D110

c. Parallel Section of Specimen T-26 (TD NiCr Surface Prepared by Chemical Etching)

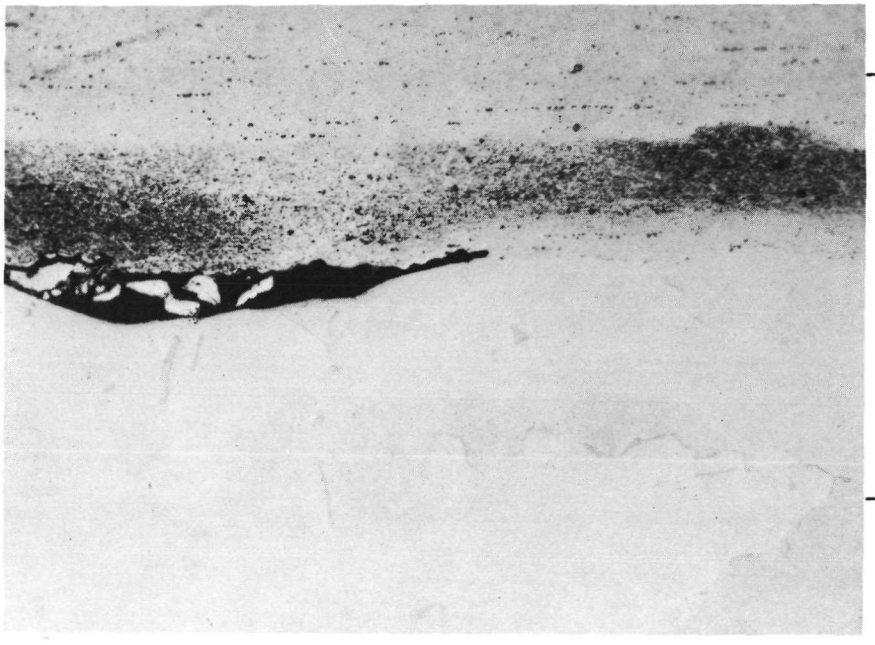

500X Marble's Etch 0D114

d. Transverse Section of Specimen T-26

FIGURE 43. (CONTINUED)

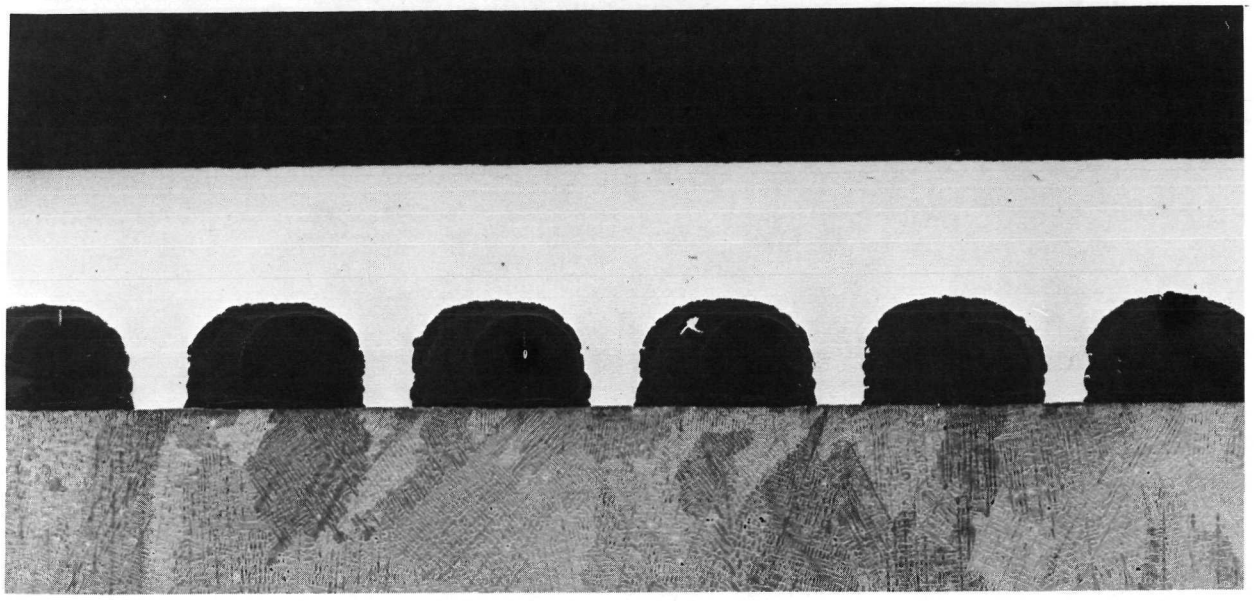

20X 50 Acetic:50 HNO_3:0.5 g $FeCl_3$ 0D364

a. 0.012-In. Zone of TD NiCr Finned Shell

The horizontal dimension is magnified 1.4 times actual.

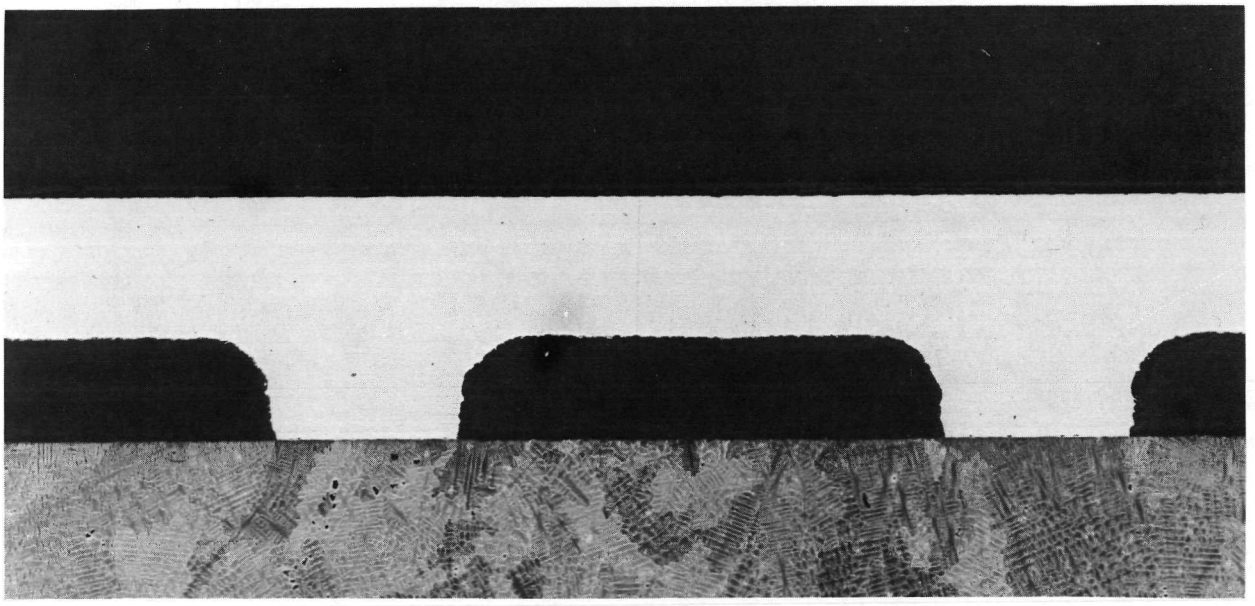

20X 50 Acetic:50 HNO_3:0.5 g $FeCl_3$ 0D362

b. 0.036-In. Zone of TD NiCr Finned Shell

The horizontal dimension is magnified 1.4 times actual.

FIGURE 44. FINNED SHELL SPECIMEN T-31 GAS-PRESSURE BONDED UNDER CONDITIONS OF 2000 F/3500 PSI/1 HR

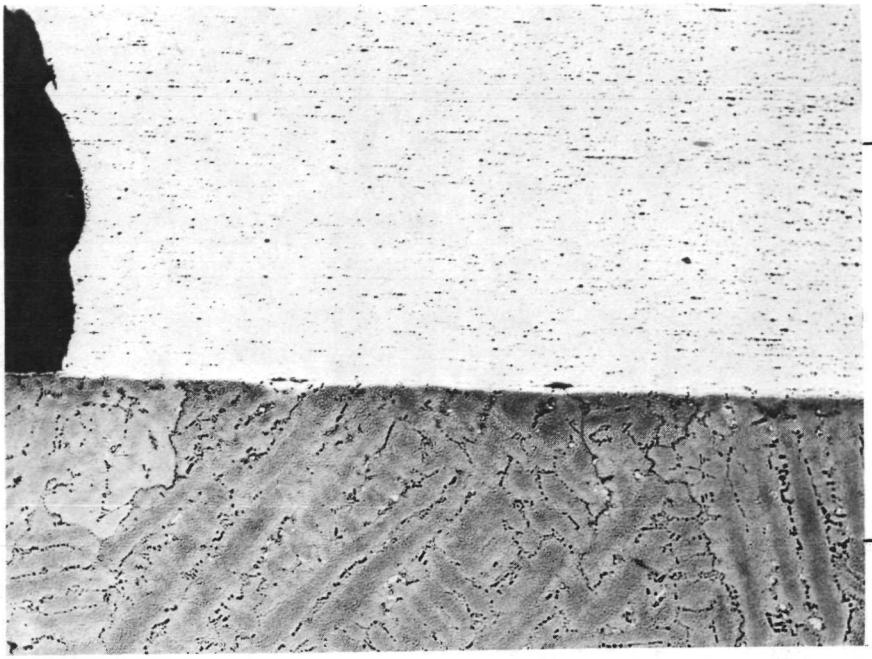

100X 50 Acetic:50 HNO_3:0.5 g $FeCl_3$ 0D360

c. Typical 0.036-In. Fin Zone Bond

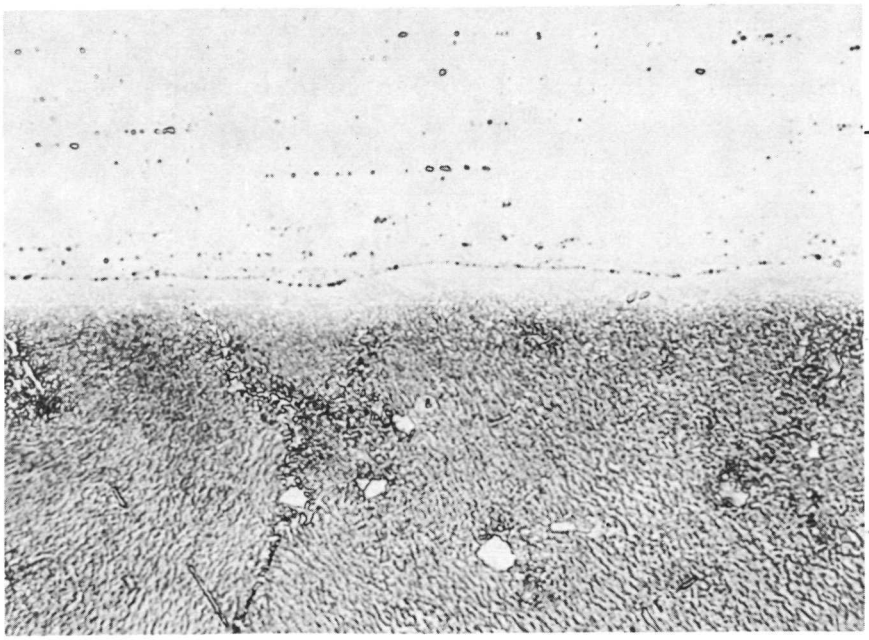

750X 50 Acetic:50 HNO_3:0.5 g $FeCl_3$ 0D361

d. Typical TD NiCr/B1900 Bond

FIGURE 44. (CONTINUED)

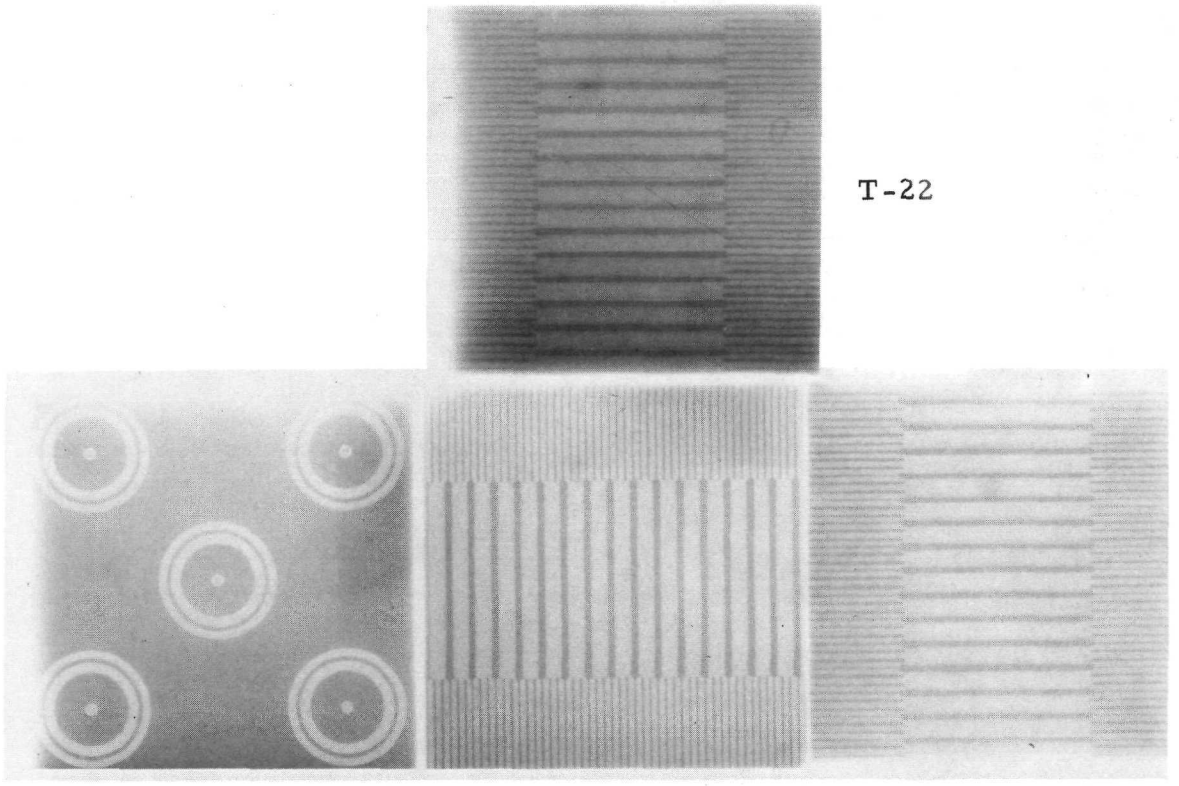

a. Radiograph Indicative of No Fin Deformation

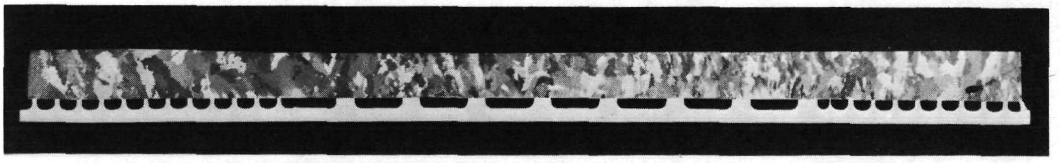

2X 50 Acetic:50 H:0.5 g $FeCl_3$ 0D363

b. Photomacrograph From 45-Deg Section of Specimen T-31

The horizontal dimension is magnified 1.4 times actual.

FIGURE 45. RADIOGRAPH OF TD NiCr/B1900 SPECIMENS PROCESSED AT 2000 F/3500 PSI/1 HR AND PHOTOMACROGRAPH OF SPECIMEN T-31

TABLE 10. SUMMARY OF RESULTS OBTAINED DURING TD NiCr/B1900 FINNED SHELL PROCESS REFINEMENT

Specimen	Experiment	Surface Preparation[a] (Shell/Strut)	Bonding Conditions[b]		Shell Deformation, percent			Bond Microstructure	Compression Shear Strength, ksi							
			Temperature, F	Pressure, psi	Channel	L Fin	M Fin		Room Temperature				1750 F			
									Longitudinal		Transverse		Longitudinal		Transverse	
									L	M	L	M	L	M	L	M
T-22	6	E1/EP	2000	3500	0	0	0	Good	NDT specimen; no mechanical property evaluation							
T-30	6	E1/EP	2000	3500	0	0	0	--	NDT specimen; no mechanical property evaluation							
T-31	6	E1/EP	2000	3500	0	0	0	Good	59.0	55.0	40.0	--	--	--	--	--
T-32	6	E2/EP	2000	3500	0	0	0	Good	55.5	37.8	18.7	30.0	4.4	5.8	1.6	5.3
T-34	7	E1/EP	1900	2500	0	0	0	Poor	Very weak bond; no evaluation							
T-35	9	E1/EP	2000	4000	0	0	0	Fair	56.7	13.5	48.2	--	Not evaluated			
T-36	9	E2/240	2000	4000	0	15-40	0	Good	--	19.3	--	--	Not evaluated			
T-37	9	E2/EP	2000	4000	0	15-20	0	Good	65.4	54.9	62.5	47.1	--	8.9	--	--
T-38	9	600/240	2000	4000	0	10	0	--	Specimen failed prior to testing							
T-39	9	E2/240	2000	4000	0	15-20	0	--	NDT specimen; no mechanical property evaluation							
T-40	12	E2/EP	2000	3500	0	0	0	Excellent	--	45.9	40.6	44.0	13.2	3.5	5.2	2.5

(a) Symbols:
- E1 - chemical etch in 23 v/o HNO_3:4 v/o HF:73 v/o H_2O at 125 F for 10 min
- E2 - chemical etch in equal volumes of HNO_3, HCl, and 42-deg Bé $FeCl_3$ for 5 min at less than 100 F
- EP - anodic etch per Table 7
- 600 - fin surface carefully polished successively with 180-, 240-, 400-, and 600-grit SiC paper using hard backing to prevent rounding of fin edges.
- 240 - strut plate surface polished with 240-grit SiC paper using soft backing.
- L - Zones L and N geometry
- M - Zone M geometry.

(b) Autoclave pressure is listed; pressure at bond interface is 3.33 to 4.0 times indicated pressure. Dwell time for all gas-pressure bonding cycles was 1 hr.

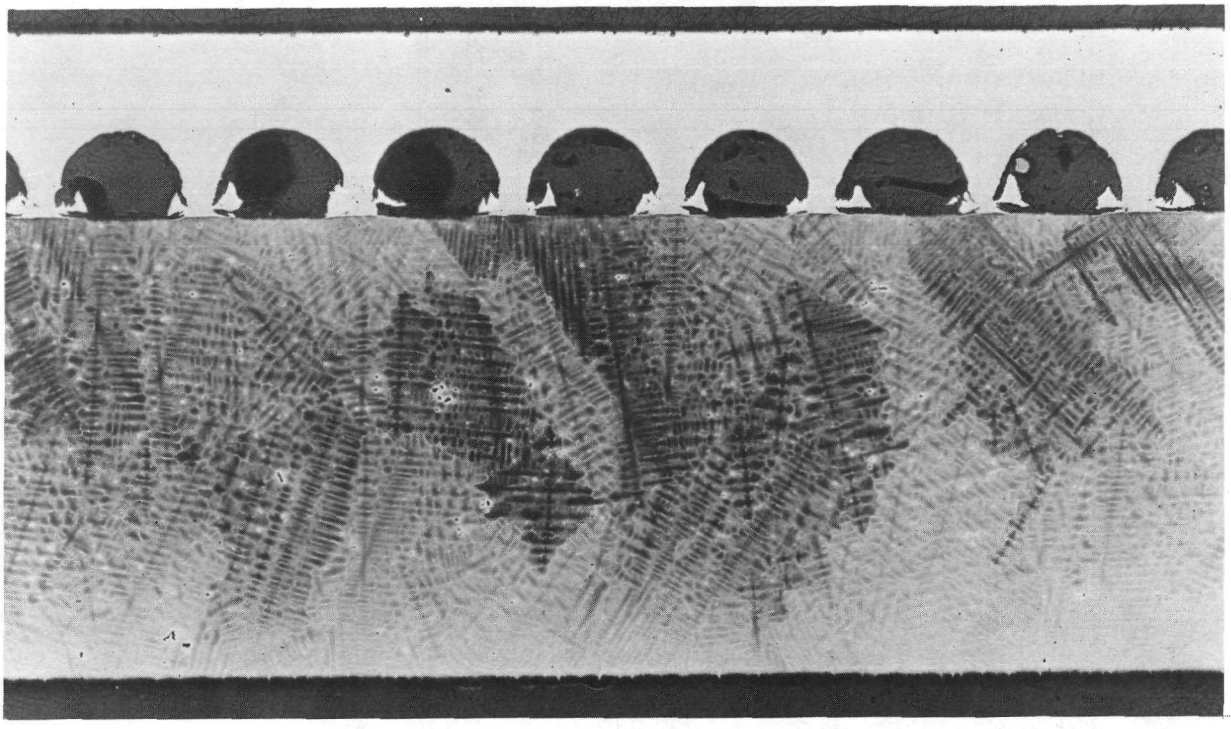

20X 30 Acetic:30 HNO_3:1 g $FeCl_3$ 0D844

a. Zone L; 20,000-Psi Bearing Stress

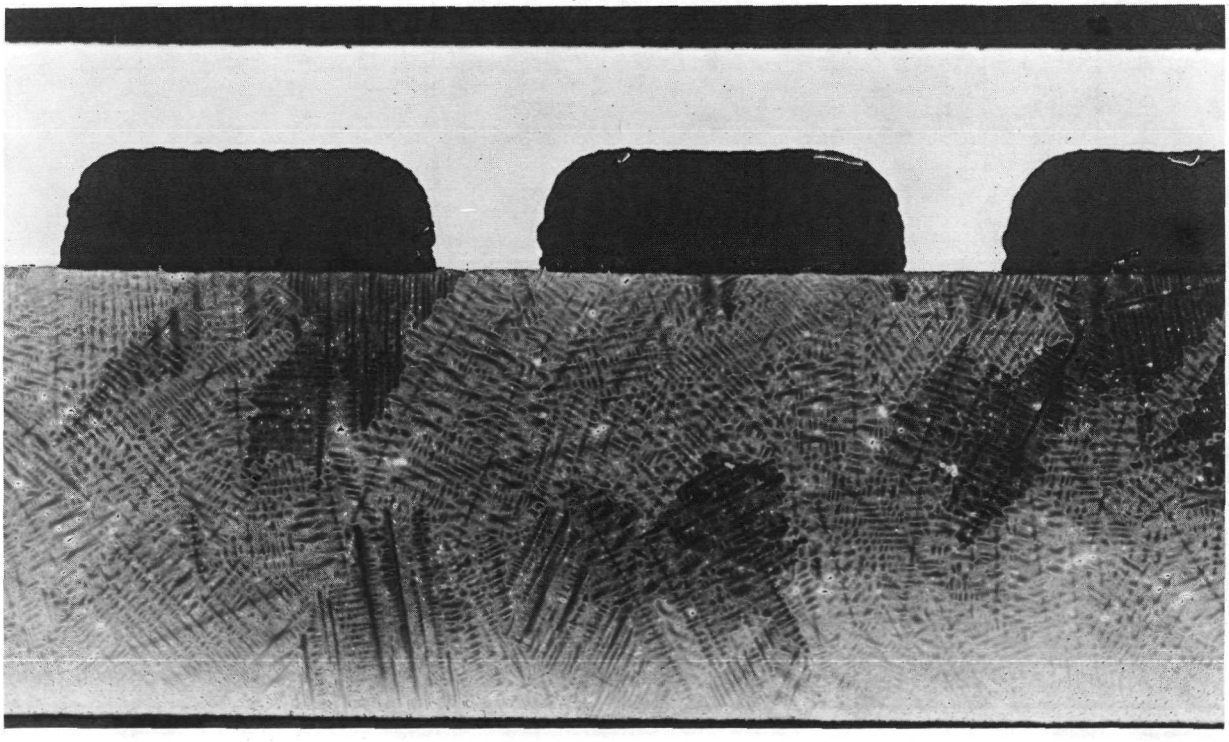

20X 30 Acetic:30 HNO_3:1 g $FeCl_3$ 0D840

b. Zone M; 16,000-Psi Bearing Stress

FIGURE 46. FINNED SHELL SPECIMEN T-37 GAS-PRESSURE BONDED UNDER CONDITIONS OF 2000 F/4000 PSI/1 HR

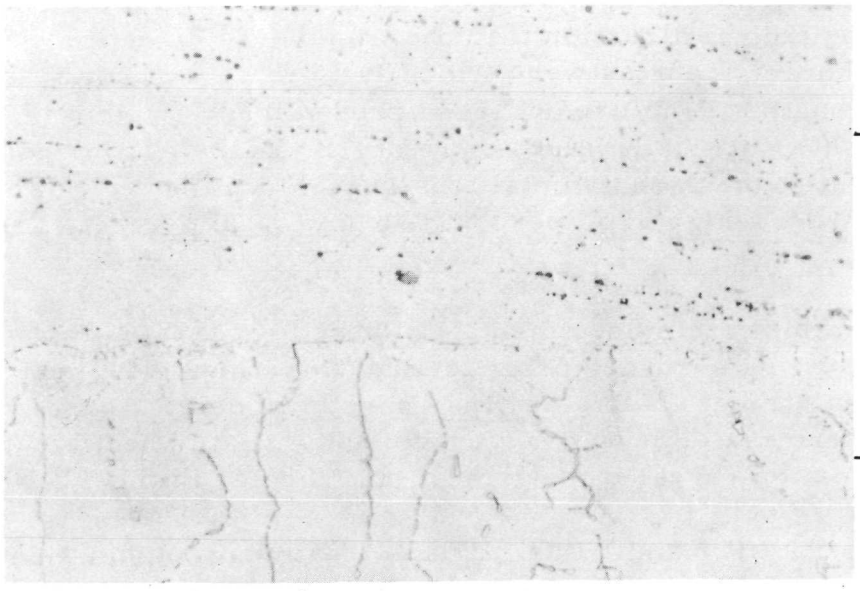

750X 20 Glycerin:20 HCl:6 HNO_3 9D094

a. Typical Bond Microstructure

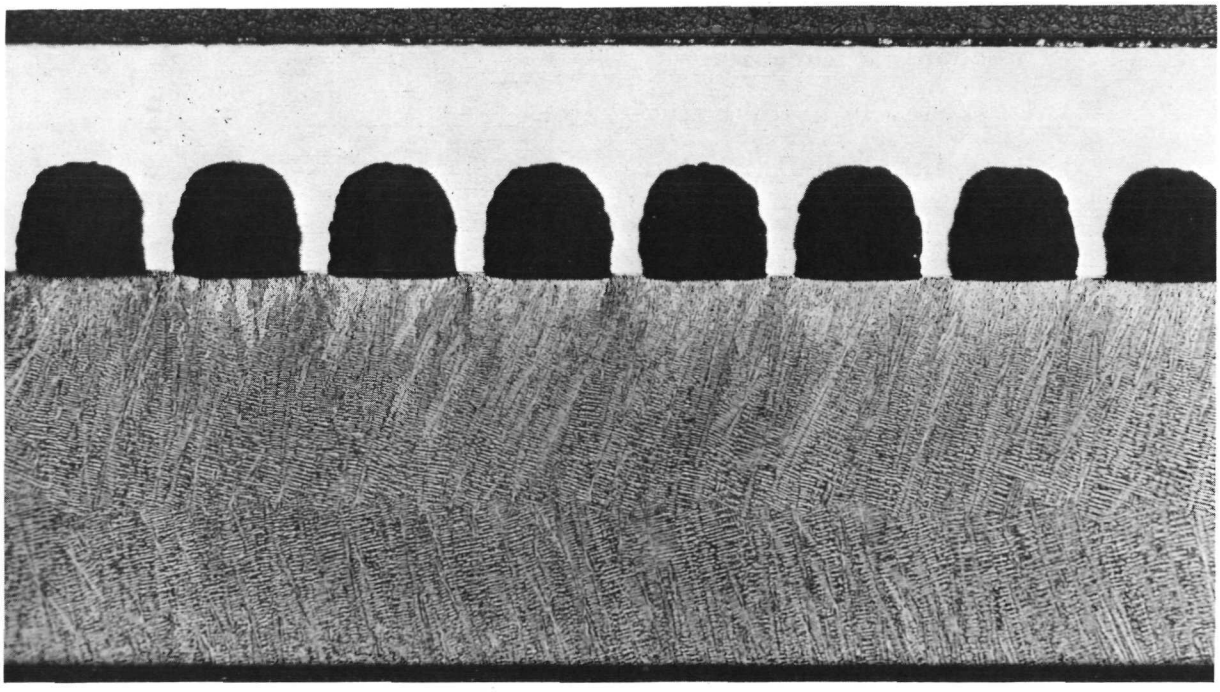

20X 20 Glycerin:20 HCl:6 HNO_3 9D103

b. Zone L; 17,500-Psi Bearing Stress

FIGURE 47. FINNED SHELL SPECIMEN T-40 GAS-PRESSURE BONDED UNDER CONDITIONS OF 2000 F/3500 PSI/1 HR

As expected, joint strength determined from the same fin geometry was higher in the longitudinal direction than the transverse direction. At room temperature, bond shear strengths were typically 50 to 70 percent of the TD NiCr tensile yield strength. Fracture occurred predominantly within the TD NiCr fins. At 1750 F, the shear strength values were of the order of 5,000 psi or approximately 30 percent of the parent-metal tensile yield strength. However, the 1750 F range extended from a high of 80 percent to a low of 10 percent of the TD NiCr yield strength.

Several samples from Specimen T-32 were heat treated through the B1900 solutionizing and aging sequence prior to 1750 F testing. The heat treatment did not increase bond strength but rather may have been deleterious. However, insufficient data were available to draw conclusions. After heat treatment, metallographic examination revealed that cracks had formed in the TD NiCr.

Of several TD NiCr and B1900 surface treatment combinations evaluated, chemically etched TD NiCr with anodically etched B1900 appeared to yield the best shear strength results. A summary of the refined cleaning, assembly, canning, and bonding procedures established for TD NiCr finned shells on the basis of the preceding study is presented below:

B1900 Strut Surface Preparation

(1) Remove 0.001 to 0.003 in. from surface by mechanical abrasion

(2) Degrease in methyl ethyl ketone

(3) Rinse in alcohol (methyl or ethyl)

(4) Scrub in detergent solution (Shipley Scrub Cleaner II)

(5) Rinse in hot water

(6) Soak in alkaline cleaner at 140 to 160 F for 2 to 3 min

Na_2CO_3	20 g/l
Na_2PO_4	20 g/l
NaOH	15 g/l
SNAP	0.5 g/l (wetting agent)

(7) Rinse in water

(8) Anodic etch at 2 amp per $in.^2$ for 3 min in HNO_3-methanol solution (1 part HNO_3 to 2 parts methanol by volume)

(9) Ultrasonic clean in hot (180 F minimum) Alconox detergent solution

(10) Rinse in hot water

(11) Rinse in hot distilled water (180 F minimum)

(12) Rinse and store in ethyl alcohol (200 proof).

TD NiCr Finned Shell Surface Preparation

(1) Perform Steps (1) through (7) of B1900 procedure

(2) Etch in room-temperature solution of equal parts by volume 42-deg Baumé $FeCl_3$, HCl, and HNO_3 for 5 min

(3) Perform Steps (9) through (12) of B1900 procedure.

Canning and Bonding Procedure

(1) All can components are to be clean (degreased and pickled) stainless steel or an aluminum or titanium killed steel such as Tinamel

(2) All container welds made after specimen assembly must be by electron beam; beam chamber must be pumped for at least 1 hr prior to welding

(3) Container welds made prior to specimen assembly may be TIG type; welded subassembly must be degreased and pickled after welding

(4) Assemble the specimens and can components in a clean area using rubber gloves

(5) After canning, inspect the assembly for leakage by pressurizing externally with helium at 300 psi; methanol is employed as the bubble-detection medium

(6) A bonding cycle of 2000 F and 3500 psi held for 1 hr is employed

(7) Reinspect the specimens for leakage after the bonding cycle

(8) Remove the bonding container by machining off the welds and strip off remaining metal.

Udimet 700/B1900 Finned Shell Bonding Process

In a fashion similar to the TD NiCr refinement, several experiments were conducted to bracket a temperature and pressure which would produce high bond strength with no structural deformation. Seemingly, this was satisfactorily accomplished under conditions of 1900 F/1100 psi/1 hr. The bonding temperature, 1900 F, was held constant throughout the series of experiments. The temperature was chosen primarily because it is below the solutionizing temperature of Udimet 700. Consequently, the influence of temperature variation on strength was considered to be less critical at 1900 F than at the 2000 F temperature chosen for

TD NiCr. The tensile yield strength of Udimet 700 at 1900 F is approximately 15,000 psi; hence, the maximum gas pressure permissible for the model finned shell was 3800 psi. At those conditions the Zone M channel would theoretically collapse. As may be seen from the results presented in Table 11, gas pressures of the order of 50 percent of the theoretical limit still apparently caused unacceptable deformation. It was later postulated on the basis of cylindrical specimen results that the specimens experienced a temperature higher than that measured by the bonding autoclave thermocouples. In any event, additional process refinement placed the results of this experimental series in question, and the deformation response observed in this series would appear more consistent with a 2000 F bonding temperature. Examination of several of the specimens prepared in Experiments 7, 8, and 10 indicated, on the basis of deformed fin width, that an equilibrium between fin bearing stress, σ_f, and yield strength occurred at 5100 ± 300 psi. Again, this strength level is more consistent with higher temperatures. Figure 48 presents radiographs of specimens processed at 2500 and 2000 psi.

A torsion shear specimen (U-21) of the type described earlier in Figure 18 was prepared in the 1900 F/2500 psi/1 hr cycle. Room-temperature tests performed on this specimen yielded circumferential shear strength values ranging between 74,000 and 80,000 psi, about 70 percent of parent-metal tensile yield. Interface pressure on this specimen was approximately 5000 psi.

Specimens U-33 and U-34 were bonded with an interface pressure of 4500 to 5500 psi as a result of undersize fins. These specimens exhibited excellent strength at room temperature in the as-bonded condition. Specimen U-33 yielded a longitudinal average of 113.2 ksi and a transverse average of 95.9 ksi. Specimen U-34 exhibited longitudinal and transverse strengths of 90.5 and 80.0 ksi, respectively. It was discovered, however, that the 1750 F strength of this joint system could be enhanced by the Udimet 700 solutionizing and aging heat treatment. The heat-treated specimens are illustrated in Figures 49 and 50. Figure 49 presents a general view of the fin geometry of Specimen U-34. Figure 50 compares the microstructures of Specimens U-33 and U-34. The shear test samples shown exhibited 1750 F longitudinal strengths of, respectively, 54.7 ksi, essentially full Udimet 700 yield strength, and 27.3 ksi. Overall, Specimen U-33 yielded a longitudinal strength average of 53.0 ksi and a 40.0-ksi transverse average. Specimen U-34 exhibited a significantly lower strength, averaging 18 ksi in either test direction.

There appears to be microstructural justification for the difference in strength. In Specimen U-34 there is a rather continuous film of what is assumed to be $M_{23}C_6$ carbides which have precipitated at the bond interface. The carbides at the interface of Specimen U-33, however, are present as discrete particles. Metallographic examination of fractured test samples from Specimen U-33, as shown in Figure 51, and electron microscopy of the fracture surfaces reveal that failure at 1750 F appears to propagate along grain boundaries, although some transgranular failure was observed in the Udimet 700. This observation is consistent with the conclusion that grain-boundary precipitates control elevated-temperature strength and that excessive quantities can reduce strength markedly.

TABLE 11. SUMMARY OF RESULTS OBTAINED DURING UDIMET 700/B1900 FINNED SHELL PROCESS REFINEMENT

Specimen	Experiment	Surface Preparation(a) (Shell/Strut)	Bonding Conditions(b) Temperature, F	Bonding Conditions(b) Pressure, psi	Shell Deformation, percent Channel	Shell Deformation, percent L Fin	Shell Deformation, percent M Fin	Bond Microstructure	Compression Shear Strength, ksi Room Temperature Longitudinal L	Room Temperature Longitudinal M	Room Temperature Transverse L	Room Temperature Transverse M	1750 F Longitudinal L	1750 F Longitudinal M	1750 F Transverse L	1750 F Transverse M
U-22	7	E1/EP	1900	2500	25	80	75	Excl.	Excessive deformation; not evaluated							
U-23	7	E1/240	1900	2500	10	10	30	Excl.	38.0	45.0	18.4	44.9	Not evaluated			
U-25	8	E1/EP	1900	2000	5	10	10	--	NDT specimen; no destructive evaluation							
U-26	8	E1/EP	1900	2000	5	10	10	--	Bond separation; surfaces oxidized							
U-27	10	E1/EP	1900	1800	<5	35-40	40	--	Apparent surface oxidation; no bond							
U-28	10	E1/EP	1900	1800	<5	60	40	--	No bond; intentional argon atmosphere in bonding container							
U-29	10	E1/EP	1900	1800	<5	50-60	65	Poor	Apparent surface oxidation; weak bond							
U-30	10	E2/240	1900	1800	<5	50-70	50	Good	60.6	37.6	45.2	39.2	9.7	--	--	--
U-33	11	E2/240	1900	1100	0	20	20	Excl.	114.6	111.7	104.2	87.6	52.9	35.1	37.4	43.0
U-34	11	E2/240	1900	1100	0	20	20	Very good	90.4	90.5	82.6	77.3	27.2	13.0	10.0	26.5

(a) Symbols:
- E1 - chemical etch in 23 v/o HNO_3:4 v/o HF:73 v/o H_2O at 125 F for 10 min
- E2 - chemical etch in equal volumes of HNO_3, HCl, and 42-deg Bé $FeCl_3$ for 5 min at less than 100 F
- EP - anodic etch per Table 7
- 600 - fin surface carefully polished successively with 180-, 240-, 400-, and 600-grit SiC paper using hard backing to prevent rounding of fin edges
- 240 - strut surface polished with 240-grit SiC paper using soft backing.
- L - Zones L and N geometry
- M - Zone M geometry.

(b) In light of subsequent results, it was suspected that the specimens in this series experienced a temperature higher than indicated. Autoclave pressure is listed; pressure at the bond interface is 3.33 to 4.0 times the indicated pressure. Dwell time for all gas-pressure bonding cycles was 1 hr.

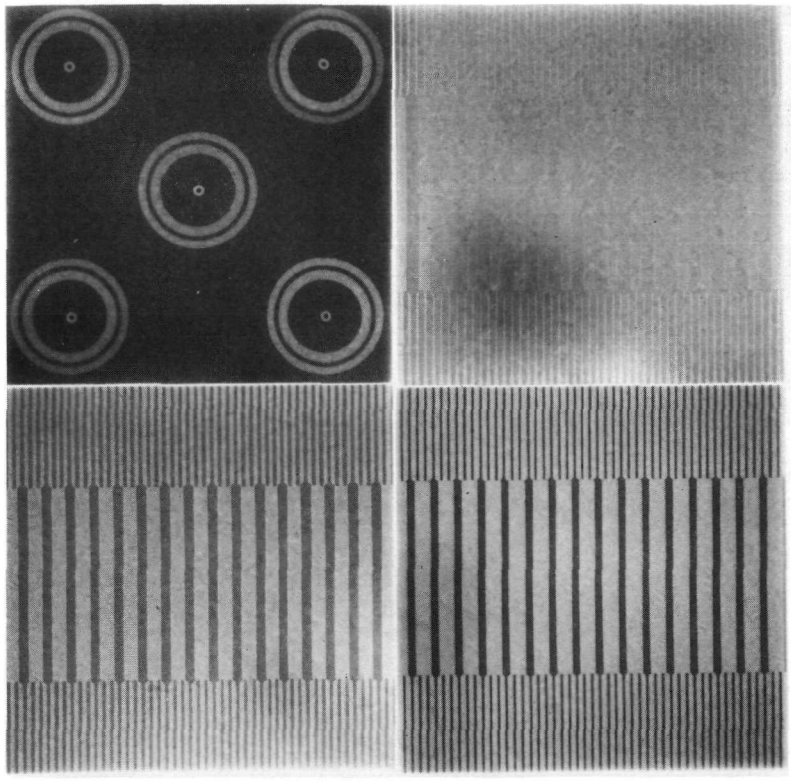

U-21

U-22

U-23

T-34 (TD NiCr specimen for comparison)

1X

S311

a. Bonded at 2500 Psi

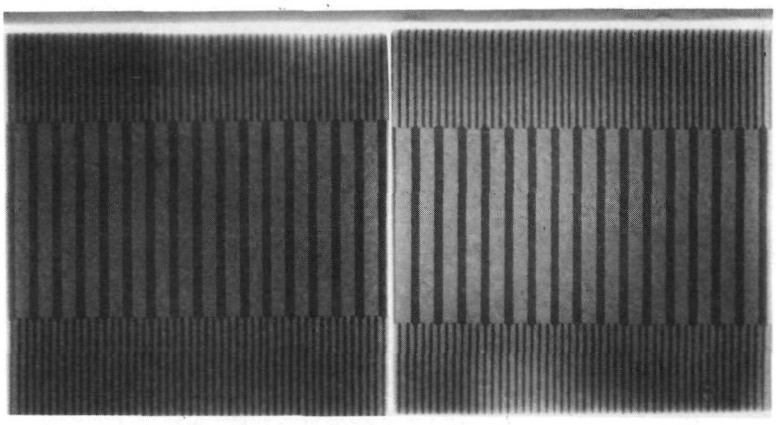

U-25

U-26

1X

S319

b. Bonded at 2000 Psi

FIGURE 48. RADIOGRAPHS OF UDIMET 700/B1900 FINNED SHELLS AND TORSION SHEAR SPECIMEN

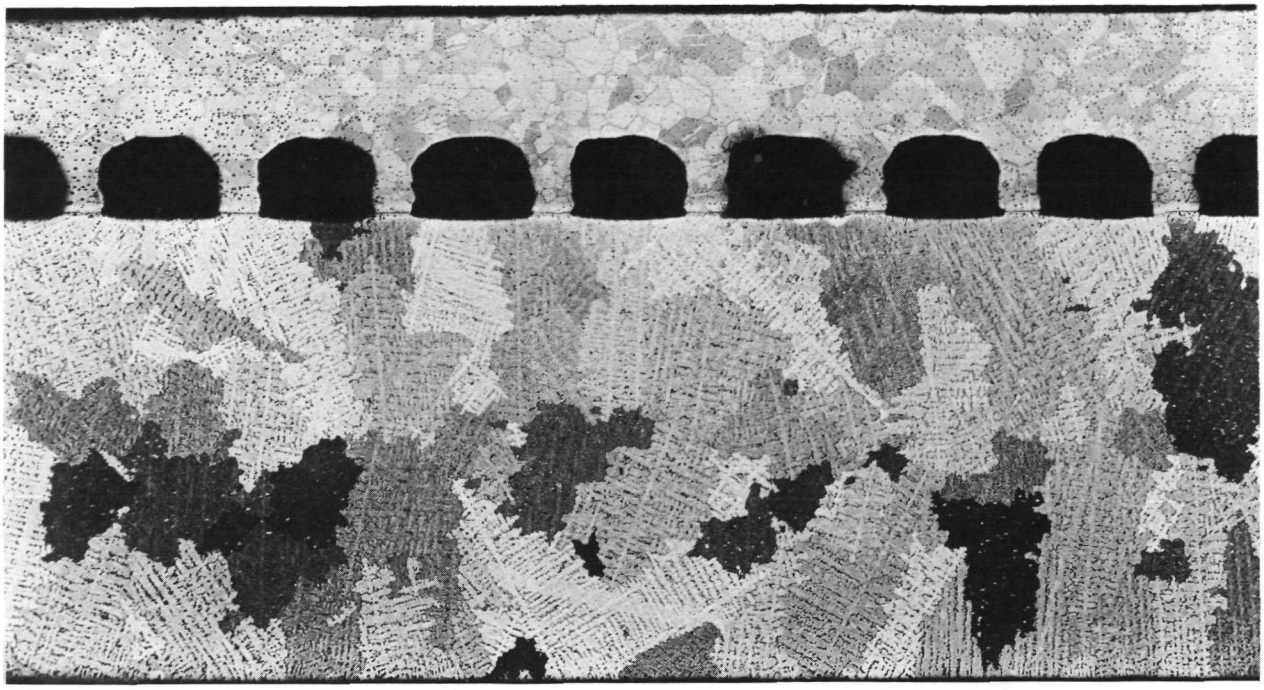

20X 20 Glycerin:20 HCl:10 HNO_3 2D947

a. Zone L; 5500-Psi Bearing Stress

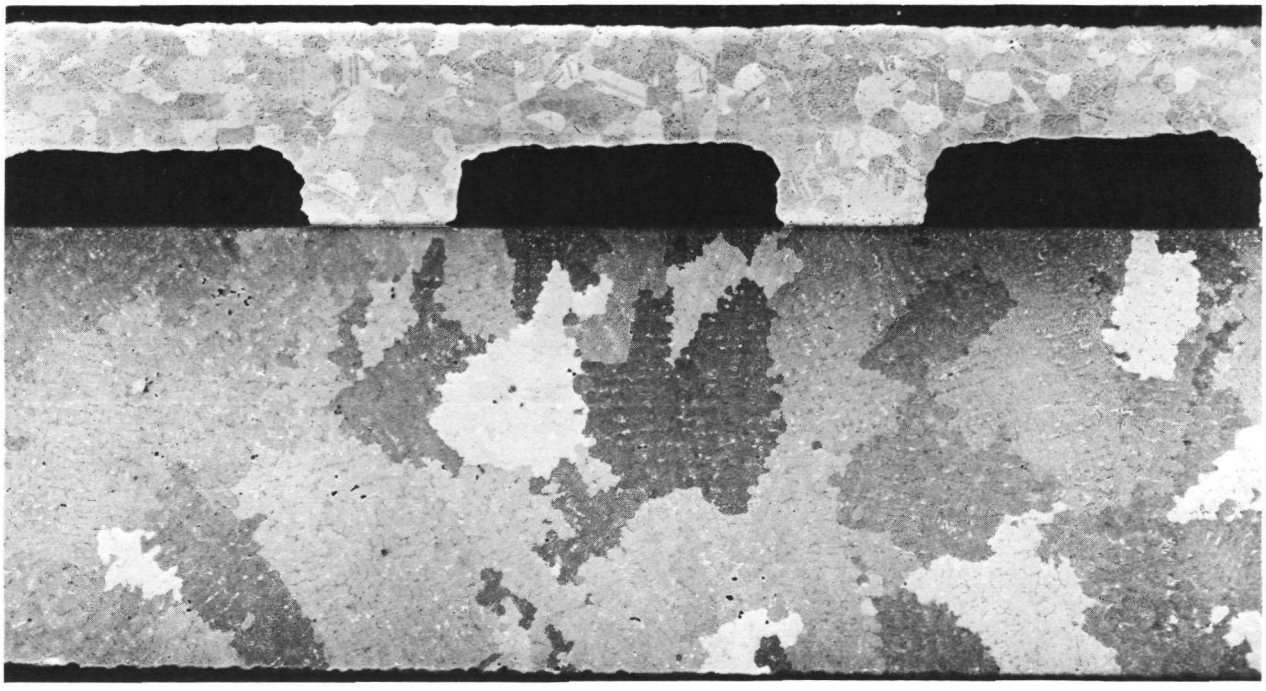

20X 20 Glycerin:20 HCl:10 HNO_3 2D946

b. Zone M; 4500-Psi Bearing Stress

FIGURE 49. SAMPLES FROM FINNED SHELL SPECIMEN U-34 BONDED AT 1900 F/1100 PSI/1 HR AND SUBSEQUENTLY HEAT TREATED

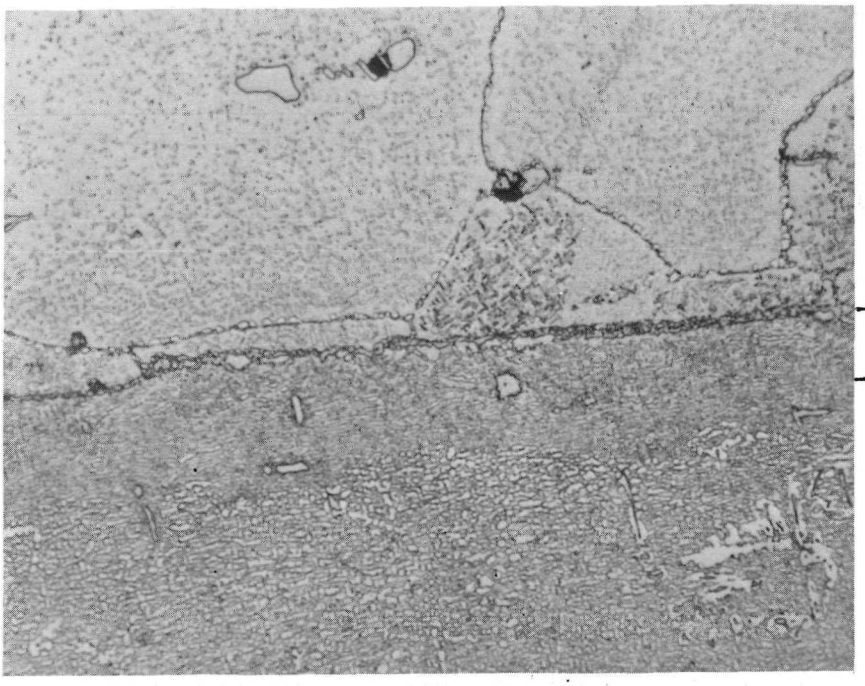

750X 20 Glycerin:20 HCl:10 HNO_3 2D944

a. Specimen U-34C; 27.3-Ksi Shear Strength at 1750 F (Note Precipitate at Bond and Grain Boundaries)

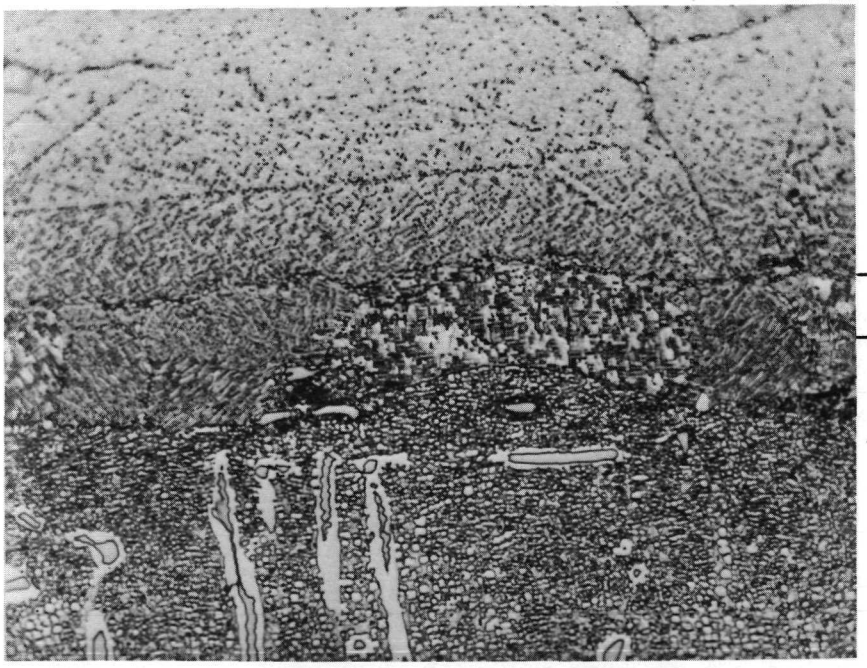

750X 20 Glycerin:20 HCl:10 HNO_3 2D634

b. Specimen U-33C; 54.7-Ksi Shear Strength at 1750 F

FIGURE 50. COMPARISON OF THE MICROSTRUCTURES OF SPECIMENS U-33 AND U-34 AFTER HEAT TREATMENT

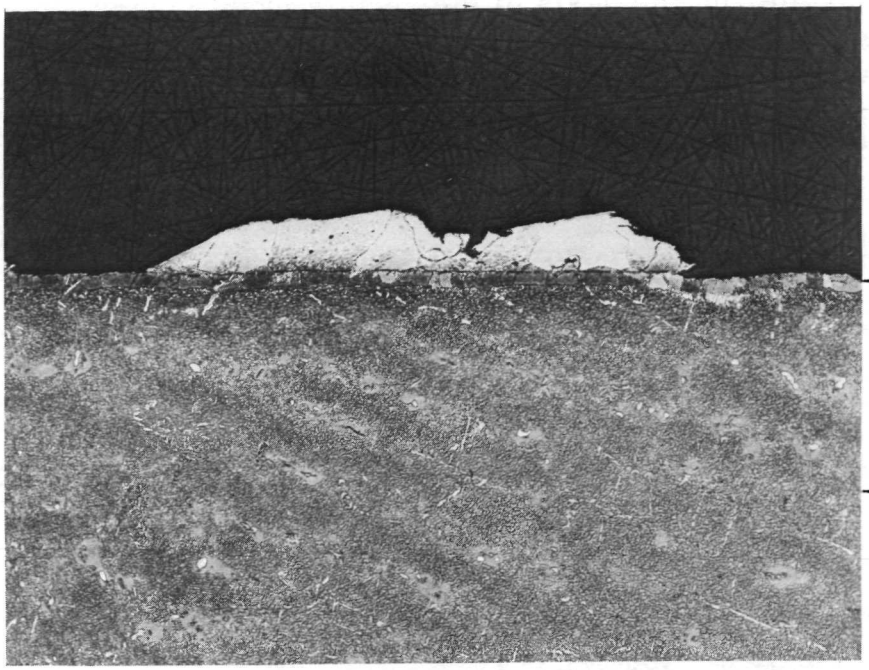

100X 20 Glycerin:20 HCl:20 HNO_3 4D994

a. Section of Udimet 700 Fin Adhering to Strut After 1750 F Shear Test

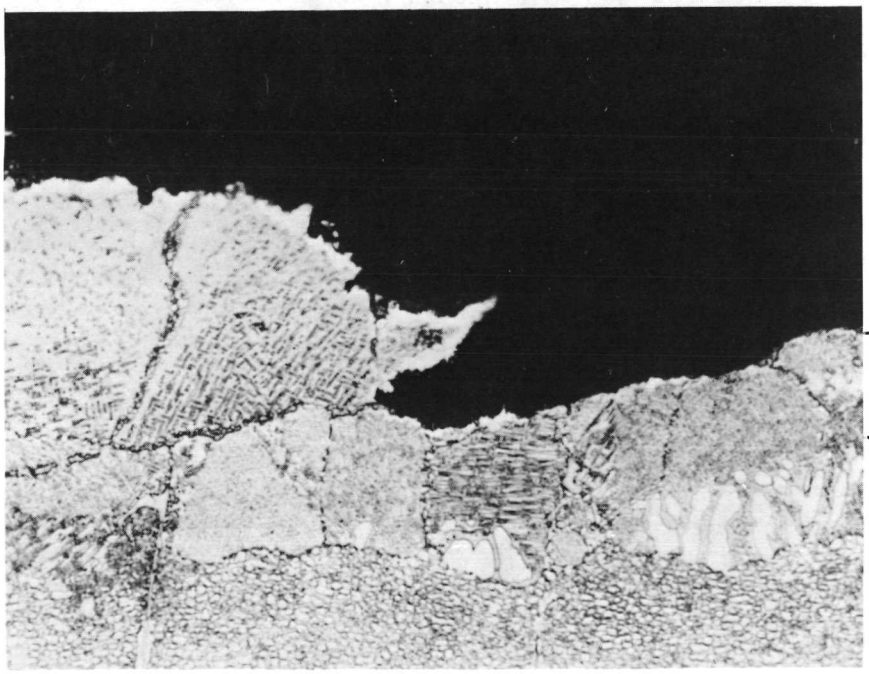

750X 20 Glycerin:20 HCl:20 HNO_3 4D996

b. Area Above at Higher Magnification

FIGURE 51. PHOTOMICROGRAPHS OF SPECIMEN U-33C AFTER 1750 F SHEAR TEST

It was not possible, on the basis of the results of this study, to unequivocally recommend a refined processing procedure for Udimet 700 finned shells. There were many metallurgical questions yet unanswered. However, the tentative process recommendation was as follows:

B1900 Strut Surface Preparation

(1) Remove 0.001 to 0.003 in. from surface by mechanical abrasion

(2) Degrease in methyl ethyl ketone

(3) Rinse with alcohol (methyl or ethyl)

(4) Scrub in detergent solution (Shipley Scrub Cleaner II)

(5) Rinse in hot water

(6) Soak in alkaline cleaner at 140 to 160 F for 2 to 3 min

Na_2CO_3	20 g/l
Na_2PO_4	20 g/l
NaOH	15 g/l
SNAP	0.5 g/l (wetting agent)

(7) Rinse in water

(8) Abrade with 240-grit SiC paper

(9) Ultrasonic clean in hot (180 F minimum) Alconox detergent solution

(10) Rinse in water

(11) Rinse in hot distilled water (180 F minimum)

(12) Rinse and store in ethyl alcohol (200 proof).

Udimet 700 Finned Shell Surface Preparation

(1) Perform Steps (1) through (7) of B1900 procedure

(2) Etch in room-temperature solution of equal parts by volume 42-deg Baumé ferric chloride, HCl, and HNO_3 for 5 min

(3) Perform Steps (9) through (12) of B1900 procedure.

Canning and Bonding Procedure

(1) All can components are to be clean (degreased and pickled) stainless steel or a killed steel such as Tinamel

(2) All container welds made after specimen assembly must be by electron beam; beam chamber must be pumped for at least 1 hr prior to welding

(3) Container welds made before specimen assembly may be TIG type; welded subassembly must be degreased and pickled after welding

(4) Assemble the specimen and can components in a clean area using rubber gloves

(5) After canning, inspect assembly for leakage by pressurizing externally with helium at 300 psi; methanol is employed as the bubble detection medium

(6) A bonding cycle of 1900 F and 1100 psi held for 1 hr is to be employed

(7) Reinspect the specimens for leakage after the bonding cycle

(8) Remove the bonding container by machining off the welds and stripping the metal

(9) Subject the specimens to the following heat-treatment sequence in air:

2135 ± 15 F/4 hr/air cool
1975 ± 25 F/4 hr/air cool
1550 ± 25 F/24 hr/air cool
1400 ± 25 F/16 hr/air cool.

Modification of Udimet 700/B1900 Bonding Process

Bonding Pressure Reevaluation. An apparent inability to fabricate cylindrical Udimet finned shells, employing the process tentatively established in process development, required that a deeper investigation be conducted on the mechanical and metallurgical response of the Udimet 700/B1900 system. The medium chosen for obtaining the needed information was a simple unmachined 2-in. square. A 0.030-in.-wide by 0.025-in.-deep slot was placed in the Udimet 700 coupon to indicate the presence or absence of bulk material flow under applied pressure. All experiments in the series were performed at 1900 F with a 1-hr dwell; pressure was varied from 3,700 to 10,000 psi. Various sheets of Udimet 700 were evaluated, and further refinement of Udimet 700 surface preparation was investigated. Table 12 summarizes the results obtained. Bond quality was found to be quite poor at pressures below 10,000 psi.

The specimens prepared in Experiment 17 at 10,000 psi were metallographically examined both parallel and transverse to the Udimet 700 rolling direction; no perceptible difference in bond quality was observed. The only voids detected in the sections examined were contained in the Udimet 700 component and were caused by the original surface condition of the sheet. (During preparation of the developmental sheet, the vendor grit blasted the surface to remove oxide scale from an annealing treatment; subsequently the sheet was roller leveled. In the

TABLE 12. RESPONSE OF UNMACHINED UDIMET 700/B1900 COUPONS TO VARIOUS PRESSURES AT 1900 F FOR 1 HR

Specimen	Udimet Sheet Identification[a]	Udimet 700 Surface Preparation	Experiment Identification	Bonding Pressure, psi	Metallographic Observations	
					Slot Deformation	Bond Quality
U-42	2	Outgassed[b]	15	3,700	None	>50 percent unbond in all specimens; no observable difference in bond quality as a function of surface preparation
U-43	2	Outgassed	15	3,700	None	
U-44	2	Etched[c]	15	3,700	None	
U-45	2	Etched	15	3,700	None	
U-46	2	Etched and outgassed[d]	15	3,700	None	
U-47	2	Etched and outgassed	15	3,700	None	
U-48	7	Etched and outgassed	15	3,700	None	
U-49	7	Etched and outgassed	15	3,700	None	
U-50	10	Etched and outgassed	15	3,700	None	
U-51	10	Etched and outgassed	15	3,700	None	
U-52	2	Outgassed	16	6,000	None	40 percent unbond in both specimens
U-53	2	Outgassed	16	6,000	None	
U-54	2	Outgassed	17	10,000	None	100 percent bond contact; normal precipitation at bond interface
U-55	2	Outgassed	17	10,000	None	

(a) Sheets 2 and 10 were heat treated by vendor at 2000 F and quenched; Sheet 7 was annealed at 2135 F and quenched subsequent to the previous treatment.
(b) Vacuum outgassing at 2150 F for 1 hr was substituted for etching step in previously used cleaning procedure. B1900 prepared in normal manner in all samples.
(c) Normal $FeCl_3$-HCl-HNO_3 etch and standard cleaning procedure.
(d) Normal cleaning procedure plus vacuum outgassing at 2150 F.

course of leveling, the pits developed during blasting were partially closed and formed voids. In the same operation, remnants of the oxide scale were trapped beneath the surface.)

Samples 1-in. square from Specimens U-54 and U-55 were subjected to the following heat-treatment sequence:

1975 F/4 hr/air cool

1550 F/24 hr/air cool

1400 F/16 hr/air cool.

Other similar samples of the two specimens were subjected to a heat treatment consisting of the latter two steps only. Samples from the two heat-treatment variations were examined metallographically and compared to the as-bonded condition. The modifications in microstructure and bond appearance from the as-bonded condition were subtle. In general, both heat treatments appeared to promote a very slight increase in grain-boundary precipitate and, consequently, increased precipitation at the bond interface since the latter may be considered a grain boundary for metallurgical purposes. There also appeared to be some initiation of grain growth across the original bond interface after heat treatment. However, again this indication was not marked. No difference of significance could be noted between the microstructures resulting from the two variations in heat treatment.

Comparison of Direct and Nickel-Aided Udimet 700/B1900 Bonds. Several additional specimens were prepared to further evaluate the effect of 1900 F/10,000 psi bond interface conditions and the effect of a nickel foil inserted at the interface. In these specimens, the Udimet 700 was etched after degreasing in an effort to remove oxide inclusions noted earlier. After etching, the Udimet 700 was vacuum outgassed at 2150 F. The specimens contained in the experiment are identified in Table 13.

Only the flat specimens, U-56 and U-60, of those listed in Table 13 will be discussed at this point. The remainder are covered in a subsequent section of this report dealing with Udimet 700/B1900 cylindrical specimens. After bonding, both coupon specimens were sectioned into halves. One half of each was then solutionized and aged according to the standard sequence for Udimet 700. Both indicator slots in Specimen U-56 were found to be dimensionally unchanged. Consequently, it was concluded that conditions of 1900 F and 10,000 psi do not cause bulk flow in Udimet 700.

Figures 52 through 54 compare the bond microstructures of Specimen U-56 (direct Udimet 700/B1900 bond) and Specimen U-60 (0.0007-in. nickel foil diffusion aid) in the as bonded, and Udimet 700 heat treated conditions, and after 500 hr at 1750 F. In the as-bonded condition, Specimen U-56 appeared well bonded and exhibited microyielding of the Udimet 700 component as expected. Precipitate can be noted at the interface and the base-alloy grain boundaries.

TABLE 13. SPECIMENS PREPARED FOR EVALUATION OF 1900 F/10,000-PSI BOND INTERFACE CONDITIONS

Specimen	Udimet 700 Component	Indicator Slot Number and Position	B1900 Component
U-56	2 by 2 in.	Two 0.060 in. wide by 0.025 in. deep; each 0.5 in. from edge	2 by 2-in. plate
U-57	One-piece 2.5-in.-ID rolled cylinder	Four equally spaced axial and one circumferential 0.030 in. wide by 0.025 in. deep	2.5-in.-OD by 2-in.-long cylinder
U-58	Four 90-deg, 2.5-in.-ID cylindrical segments	Three axial and one circumferential in each segment. A and B segments have 0.030-in.-wide slots and C and D segments 0.060-in.-wide slots	Ditto
U-59	One-piece 2.5-in.-ID rolled cylinder	Nineteen 0.060-in.-wide by 0.005-in.-deep circumferential grooves	"
U-60[a]	2 by 2-in. sheet	No slots	2 by 2-in. plate

(a) 0.0007-in.-thick nickel foil inserted between Udimet 700 and B1900 components.

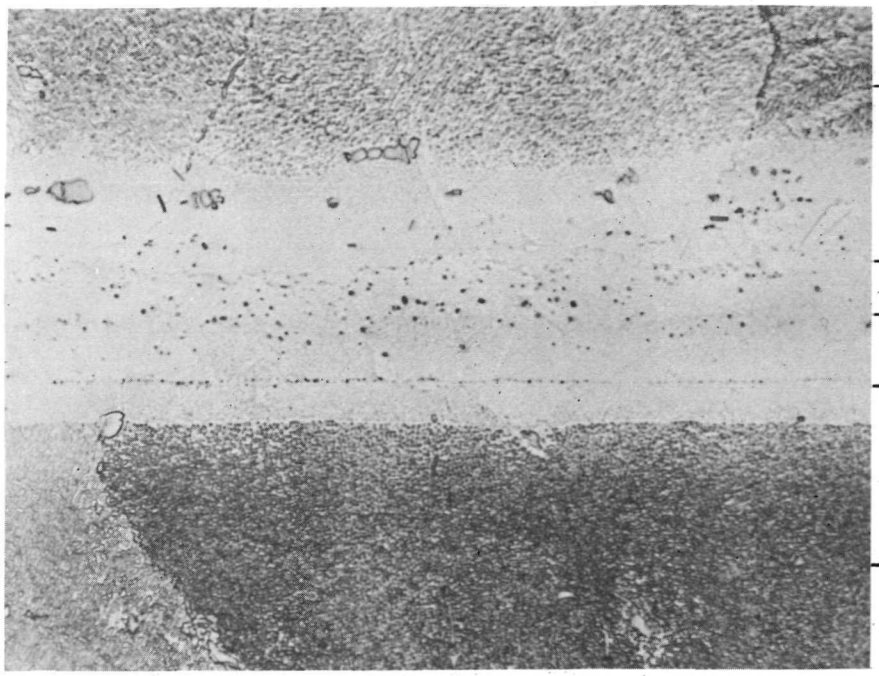

750X Marble's Etch 4E215

a. Specimen U-60

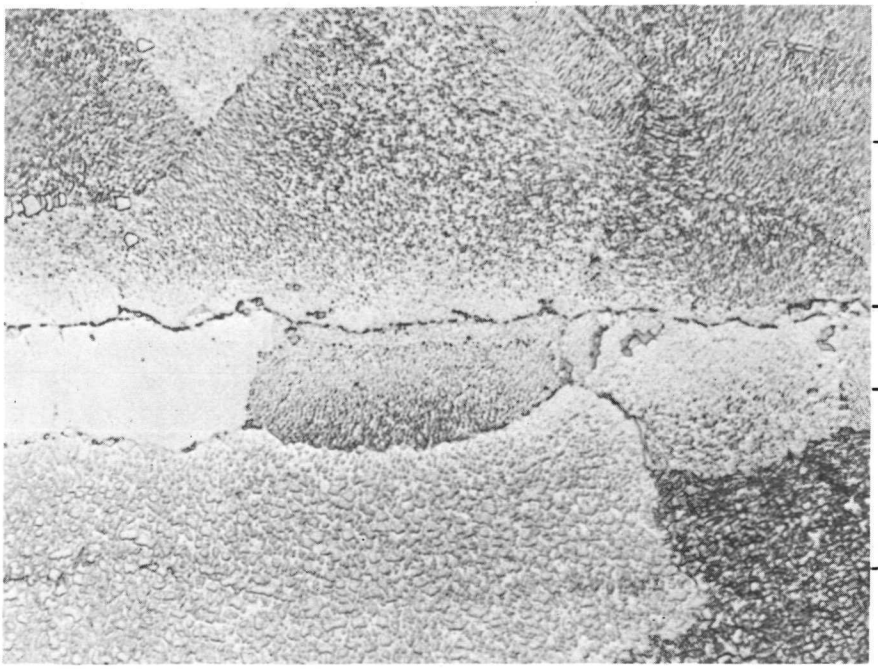

750X Marble's Etch 4E209

b. Specimen U-56

FIGURE 52. COMPARISON OF AS-BONDED MICROSTRUCTURE OF UDIMET 700/B1900 JOINT WITH AND WITHOUT NICKEL FOIL DIFFUSION AID

Both specimens were gas-pressure bonded at conditions of 1900 F/10,000 psi/1 hr.

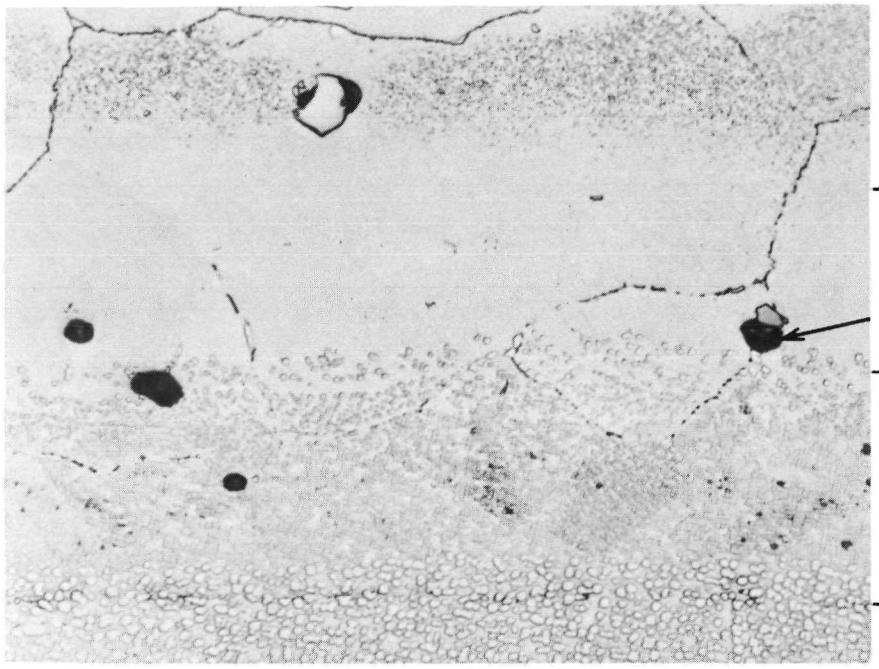

750X 20 Glycerin:20 HCl:6 HNO_3 7E024

a. Specimen U-60

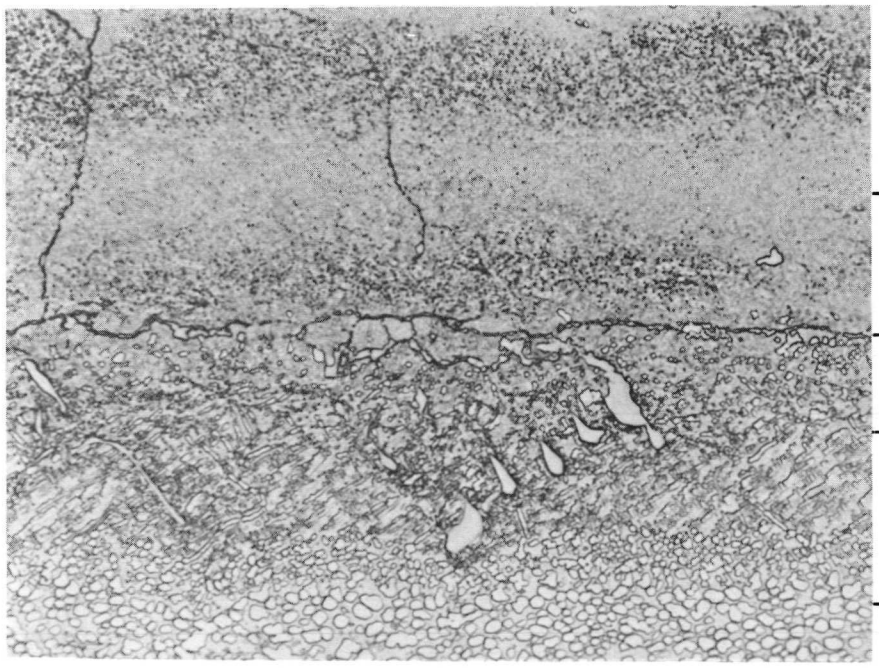

750X 20 Glycerin:20 HCl:6 HNO_3 7E020

b. Specimen U-56

FIGURE 53. COMPARISON OF UDIMET 700/B1900 BOND MICROSTRUCTURES WITH AND WITHOUT NICKEL FOIL DIFFUSION AID AFTER SOLUTIONIZING AND AGING HEAT TREATMENTS

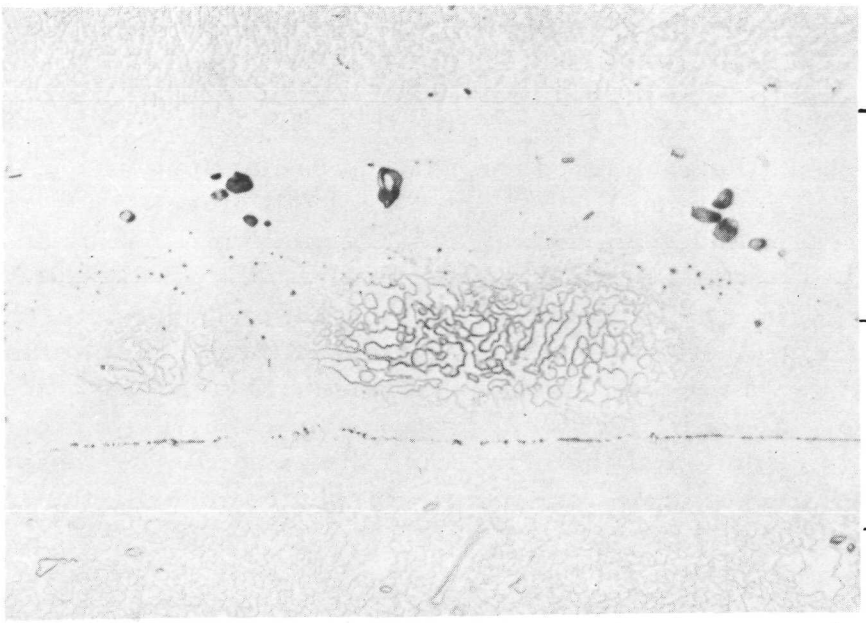

750X 20 Glycerin:20 HCl:6 HNO_3 7E147

a. Specimen U-60

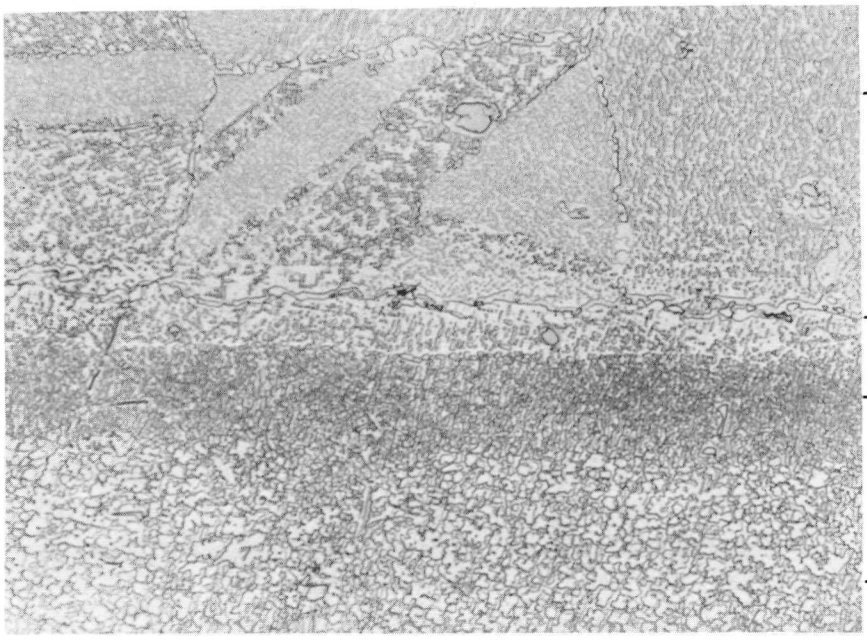

750X 20 Glycerin:20 HCl:6 HNO_3 7E146

b. Specimen U-56

FIGURE 54. COMPARISON OF UDIMET 700/B1900 BOND MICROSTRUCTURES WITH AND WITHOUT NICKEL FOIL DIFFUSION AID AFTER 1750 F THERMAL CYCLES

Both specimens were water quenched from 1750 F 37 times and were at temperature for 500 hr.

The precipitate appeared semicontinuous and about 0.5 μ thick. Occasional voids 2 to 5 mils wide by 0.5 mil high were found on the Udimet side of the bond. These stem from the surface condition of the Udimet 700.

As would be expected, the as-bonded microstructure of Specimen U-60 is quite different from that of Specimen U-56. The nickel foil closed the interface microvoids normally present and seemed to prevent formation of the usual bond-line precipitate. A line of particles or extremely small voids can be noted at what appears to be the original nickel/Udimet 700 and nickel/B1900 interfaces. These bordered on the limit of resolution, a few tenths of a micron in diameter; their cause or significance was therefore not determined. Numerous 2 to 3-μ-diameter microvoids were noted in the nickel proper; these may be Kirkendall porosity induced by rapid diffusion of the nickel into the base alloys. It appears that the nickel alloyed to a depth of 0.3 and 1 mil, respectively, with the B1900 and Udimet 700.

The solutionized and aged appearance of Specimen U-56 is normal. Specimen U-60 was altered significantly by the additional diffusion time. Nickel was no longer an identifiable constituent. The microstructure suggests that nickel continued its diffusion into the B1900 and Udimet 700 while aluminum and titanium diffused to the original nickel-rich zone with resultant gamma-prime formation. It was also noted that some of the fine porosity noted in the as-bonded condition has coalesced into a few small nearly round pores during heat treatment.

The condition illustrated in Figure 54 is after 37 water quenches from 1750 F and an accumulation of 500 hr at temperature. The portion of Specimen U-56 without nickel interleaf, presented base-alloy microstructures normal for the thermal history involved. Some general coarsening as compared to the as-bonded condition of the gamma-prime precipitate was noted in both the B1900 and Udimet 700. Udimet 700 grain-boundary precipitates coarsened during thermal cycling and appeared surrounded by a second-phase material. The Udimet 700-B1900 bond interface appeared quite similar to the Udimet 700 grain boundaries. As a result of thermal cycling shocks, the bond in Specimen U-56 separated to a depth of 0.125 in. at one edge. It appeared that the separation progressed by a ratcheting mechanism in which oxide penetration served as a lever to continued propagation of the crack tip. The crack tip preceded the oxide-penetration limit. Oxidation attack of the parent alloys consisted of penetration along grain boundaries to a depth of 5 to 10 mils, an alloy depleted zone of about 3 mils, and an actual oxide film thickness of approximately 0.5 mil. The bond interface did not appear to be attacked preferentially.

The microstructure of Specimen U-60 after thermal cycling was quite similar to that of the direct-bonded specimen except for the expected lack of precipitate at the bond interface. No bond separation was noted in the section examined, and no preferential oxidation attack was found at the bond interface. Considerable interdiffusion had occurred between the nickel foil and parent alloys, and there appeared to be some grain growth across the original interfaces. The original nickel foil zone was multiphased after thermal cycling.

Microhardness traverses were made on the as-bonded, heat treated, and thermally cycled portions of Specimen U-60 to determine the degree of homogenization of the nickel interleaf with the base alloys. The hardness data are shown in Figure 55. These data may be compared to the results of TD NiCr/B1900 hardness traverses shown in Figures 31c and 31d.

As expected, hardness decreased at the nickel position in the as-bonded condition. The Knoop hardness number (KHN) determined at the nickel position is typical for annealed nickel. The base alloys appear, from the hardness values determined, to be in a fully annealed state after bonding. A rough conversion from KHN to C-scale Rockwell hardness number yields R_C values in the range of 5 to 10. Subjecting the specimen to the Udimet 700 heat-treatment sequence brought about an expected hardness increase. The hardness values of the base alloys are typical for the fully aged condition and equivalent to an R_C value in the range of 40 to 45. Curiously, the nickel-rich zone of the Udimet 700 component of Specimen U-60 was apparently hardened more than the base alloy. When converted to R_C values, however, the KHN values determined in this harder zone relate to an R_C of about 50 which is not inconsistent for fully aged Udimet 700. The thermally cycled portion of Specimen U-60 was not aged before being put through the thermal-cycle series. Note in this case, although the base alloys have hardened to a level similar to the fully aged case, that the nickel-rich zones of both alloys have apparently not fully hardened. Again, however, a conversion to R_C hardness indicates values, except for the low point (R_C of 28), that are fairly consistent with the alloy condition.

The implication of this simple experiment was that the solutionizing and aging sequence is beneficial, and perhaps necessary, to the development of an optimized bond-region microstructure with a nickel diffusion aid. On the basis of this one experiment, it was tentatively concluded that up to 0.0007 in. of pure nickel can be applied to a Udimet 700/B1900 bond interface without apparent deleterious effect. Proof of this conclusion required mechanical property data, which were obtained later in a reproducibility study.

Preliminary Evaluation of Nickel Diffusion Aid on Finned Shells. Two finned shell specimens, U-61 and U-62, were bonded under conditions of 1900 F and 3200 psi held for 1 hr. The B1900 components of these specimens had been plated with 0.0002 in. of borane-reduced electroless nickel. Before assembly, the nickel plate was dissolved off half the surface of both B1900 plates. This was accomplished by masking the half to be preserved and briefly dipping the plate in nitric acid. Subsequently, the masking compound was removed with methyl ethyl ketone (MEK). The Udimet 700 and B1900 surfaces were cleaned using previously developed techniques, and the nickel surface was cleaned using an aqua regia (3:1 HCl/HNO_3) etch.

After bonding, the specimens were separated from their bonding container and cut into three strips. One strip from each was examined metallographically. Another strip was solutionized and aged, and the third strip was subjected to shock thermal cycles from 1750 F to room temperature in which the specimens

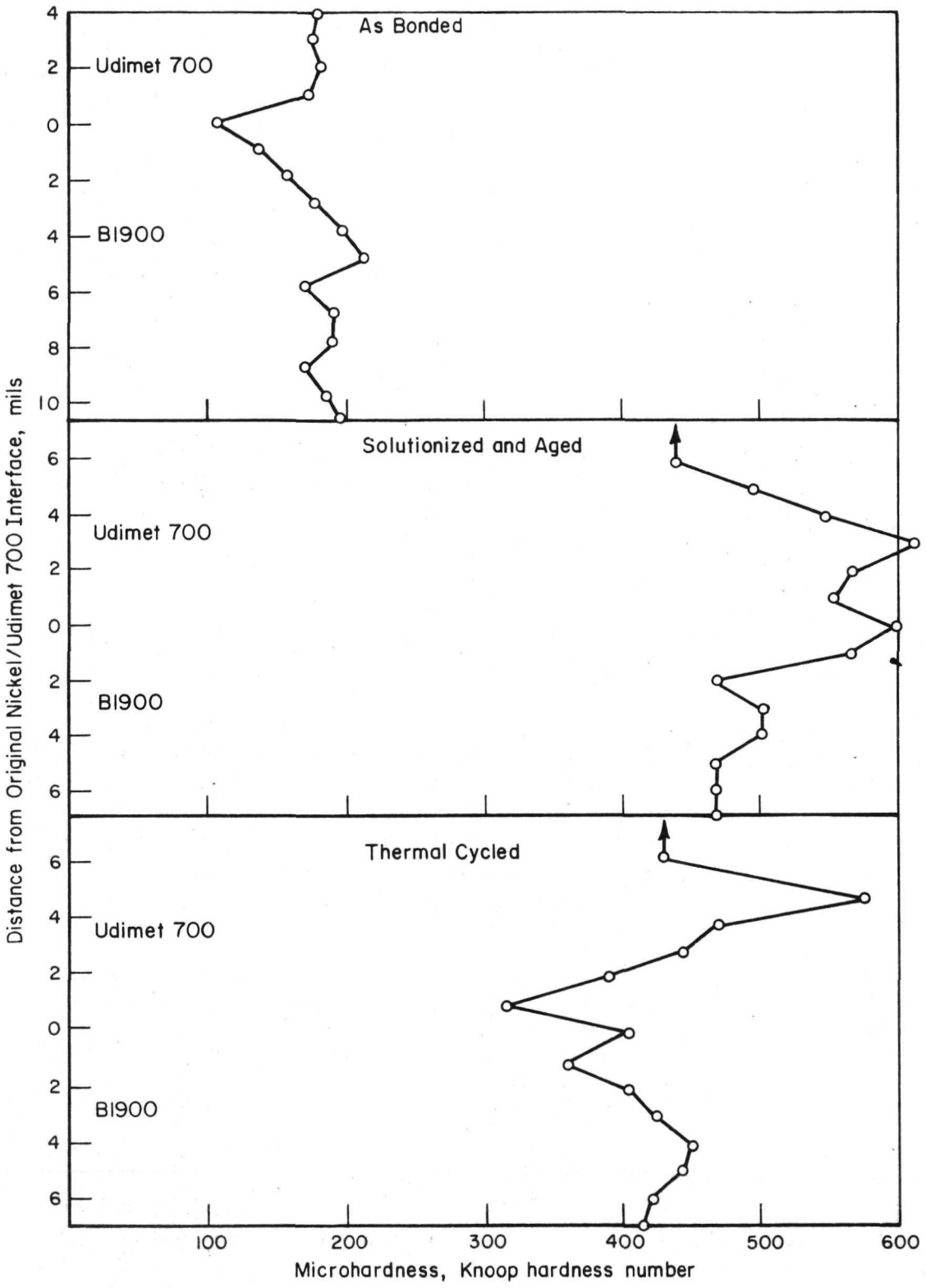

FIGURE 55. BOND REGION MICROHARDNESS OF SPECIMEN U-60 AS A FUNCTION OF THERMAL HISTORY

were pulled from the furnace hot and cooled as rapidly as possible with a compressed air blast.

Examination of the specimens in the as-bonded condition revealed that there was no fin distortion, and the nickel flash had diffused completely into the Udimet 700 and B1900 base metal as desired. However, the cleaning treatment used to prepare the B1900 surface for plating had severely attacked the former, as shown in Figure 56. The attack appeared essentially interdendritic, and consequently the B1900 surface was very porous. These pores, due to the strength of the B1900, could not close during bonding. Hence, the actual bonded area was considerably less than 25 percent of the anticipated contact area. Where physical contact had been achieved, the bonds appeared to be of high quality, but the overall strength of the specimens was necessarily poor.

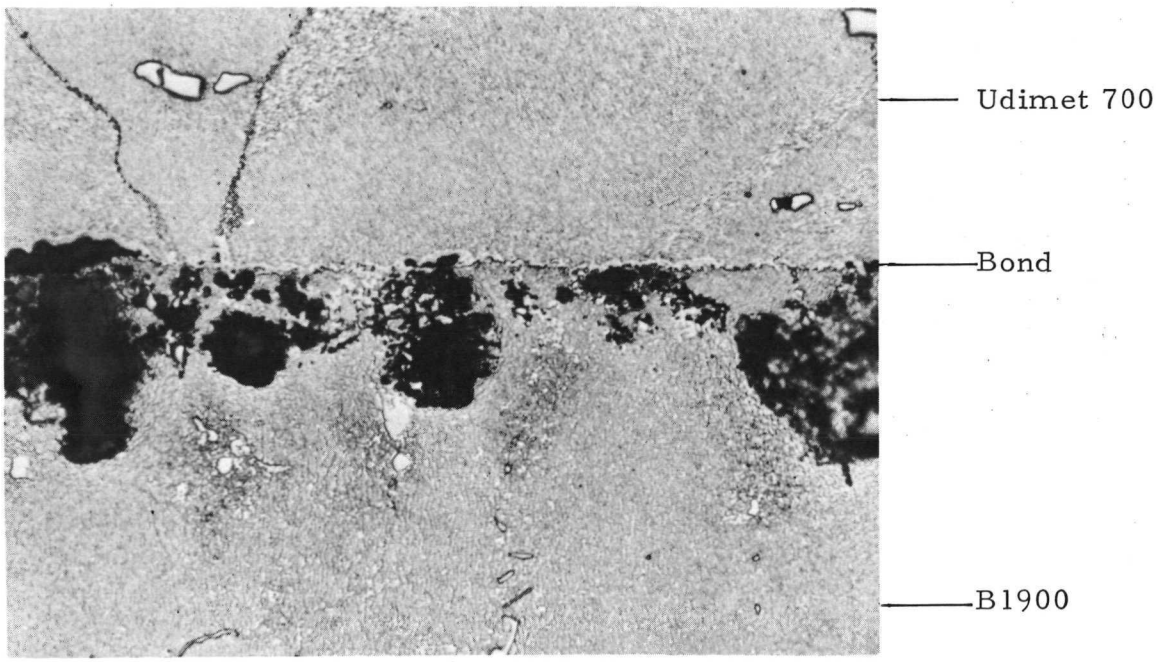

750X 25 HNO_3:25 HCl:50 H_2O 4E730

FIGURE 56. UDIMET 700/B1900 FINNED SHELL SPECIMEN WITH BOND UNDERCUT BY B1900 NICKEL PLATING SURFACE PREPARATION

Not unexpectedly, many fins in both specimens failed during heat treatment. Failure was caused by a combination of thermal stress and, more importantly, the rapid buildup of oxide facilitated by the porous B1900. As in the case of the thermal-cycle samples, separation was first noted in the area that did not have the nickel diffusion aid. Specimen U-62 was the first to exhibit failure in the thermal-cycle tests. The "non-nickel" portion of Specimen U-62 separated after four quenches to room temperature and a cumulative period of 3.5 hr at 1750 F. After one further cycle, the separation progressed into the "nickel" portion of the specimen. Testing of this specimen was consequently terminated after five

quenches and a cumulative period of 5 hr at temperature. The specimen was later separated by hand pressure.

The first indications of separation in Specimen U-61 were noted after the seventh quench and about 22 hr at temperature. As in the previous cases, the separation initiated in the "non-nickel" portion of the specimen. The separation progressed, and after the 20th cycle to room temperature and 100 hr at temperature the specimen finally became fully separated. Both specimens were examined after failure, and it was found that failure was caused by the rapid surface oxidation of the B1900 permitted by porosity. It appeared that the bond was literally undercut by B1900 oxidation.

Process Reproducibility. Six flat Udimet 700 finned shell specimens, U-63 through U-68, of the design shown in Figure 57 were prepared and gas-pressure bonded employing the process procedure refinements determined from the immediately preceding studies. The surface treatment and diffusion bonding procedures are presented in Table 14. Both the Udimet 700 and B1900 components were vacuum outgassed prior to bonding. All B1900 plates were coated in vacuum with 0.0002 to 0.0005 in. of pure nickel by electron-beam evaporation. No surface etching was needed for this coating technique. Gas-pressure bonding pressure was adjusted to effect a 10,000-psi bearing stress at the finned shell/strut interface. The six specimens were divided between three autoclave cycles to establish a measure of process reproducibility. The finned shells in each cycle had been prepared from two different sheets of Udimet 700 Heat No. 6541, as tabulated below:

Finned Shell Specimen	Udimet 700 Sheet Identification	Experiment Identification	Autoclave Pressure, psi
U-63	11	20	3,500
U-64	10	20	3,500
U-65	11	21	3,500
U-66	10	21	3,500
U-67	11	22	3,200
U-68	10	22	3,200

Subsequent to bonding, the specimens were solutionized and aged through the full Udimet 700 heat-treatment schedule per the initial Udimet 700 finned shell bonding process recommendation. A fin cross section and Udimet 700/B1900 bond microstructure subsequent to heat treatment typical of the six specimens is presented in Figure 58. The bonds appeared to be of high quality with a favorable microstructure at the interface. No fin deformation occurred in any of the six specimens. After aging, the specimens were cut, and half of each finned shell was thermally cycled between 1750 F and room temperature. Specimens U-63 and U-64 were thermally cycled 11 times. The time-at-temperature intervals ranged between 4 and 66 hr; total time at temperature was 212 hr. Specimens U-65 through U-68 were cycled 10 times. Time-at-temperature intervals on these four specimens varied between 6 and 72 hr. Total time at temperature was 209 hr. During thermal cycling, one corner each of Specimens U-63, U-65, and U-67

Super alloy finned shell

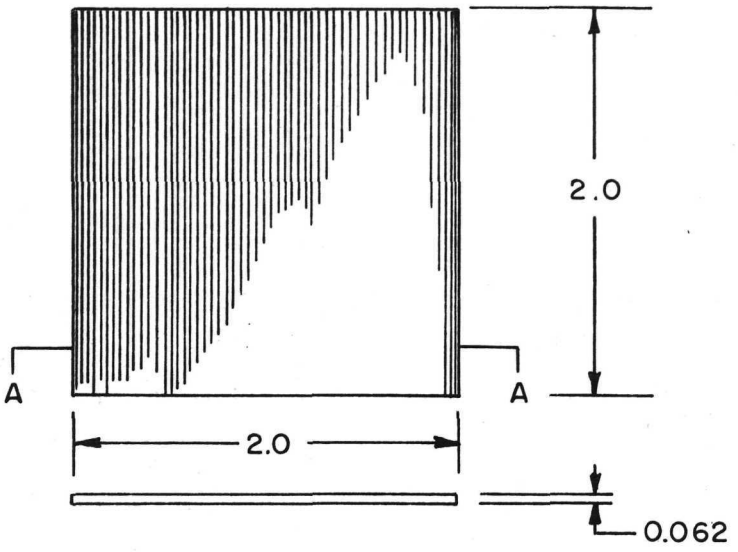

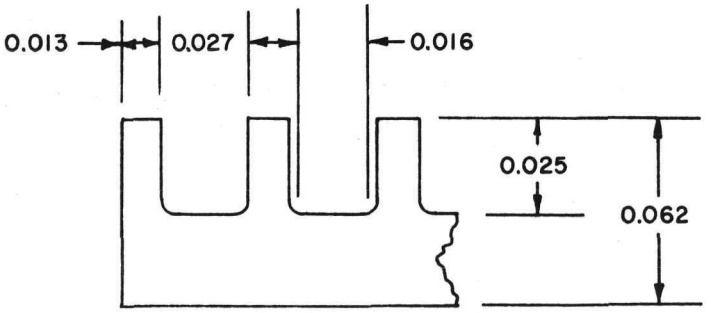

Section A-A (Approx. 15 X)
Typical from edge

All measurements are in inches

Note: Shell composed of 50 fins @ 0.013 thick plus 49 channels @ 0.027 wide

FIGURE 57. UDIMET 700 FINNED SHELL DESIGN FOR REPRODUCIBILITY STUDY

TABLE 14. PROCESSING PROCEDURES FOR UDIMET 700 FINNED SHELLS

B1900 Strut Surface Preparation

(1) Remove 0.001 to 0.002 in. from surface with belt abrader; use 240-grit SiC

(2) Degrease in methyl ethyl ketone

(3) Rinse with alcohol (methyl or ethyl)

(4) Ultrasonic clean in 130 F Alconox detergent solution

(5) Rinse in hot water

(6) Rinse in distilled water

(7) Rinse in ethyl alcohol (200 proof)

(8) Outgas in vacuum of 10^{-5} to 10^{-6} torr at 2150 F with 2 to 5-min initial excursion to 2175 F; total time at or above 2150 F is 1 hr. Store in argon.

(9) Electron-beam evaporate 0.0002 to 0.0005-in. nickel coating on surface to be bonded

(10) Use in as-plated condition; surfaces may not be touched.

Udimet 700 Finned Shell Surface Preparation

(1) Degrease in methyl ethyl ketone

(2) Rinse in alcohol

(3) Etch in room-temperature solution of equal parts by volume 42-deg Baumé ferric chloride, HCl, and NHO_3 for 30 sec

(4) Rinse in water

(5) Perform Steps (4) through (8) of B1900 procedure.

Canning and Bonding Procedure

(1) All can components are to be clean (degreased and pickled) stainless steel

(2) Container welds made before specimen assembly may be TIG type; welded subassembly must be degreased and pickled after welding

(3) All container welds made after specimen assembly must be by electron beam; beam chamber must be pumped for at least 1 hr prior to welding

(4) Fin and channel dimensions must be verified for application of correct gas pressure to effect 10,000-psi interface pressure; 3,500-psi gas pressure for 0.014-in. fins

(5) Assembly of the specimen and can components must be accomplished in a clean area using rubber gloves; assembly should take place within 24 hr of nickel coating operation

TABLE 14. (Continued)

(6) After canning, inspect the assembly for leakage by pressurizing externally with helium at 300 psi. Methanol is employed as the bubble detection medium

(7) A bonding cycle of 1900 F and 3200 to 3800 psi [function of Step (4)] held for 1 hr is to be employed

(8) Reinspect the specimens for leakage after the bonding cycle

(9) Remove the bonding container by machining off the welds and strip off remaining metal

(10) Subject the specimens to the following heat-treatment sequence in air:

2135 ± 15 F/4 hr/air cool
1975 ± 25 F/4 hr/air cool
1550 ± 25 F/24 hr/air cool
1400 ± 25 F/16 hr/air cool

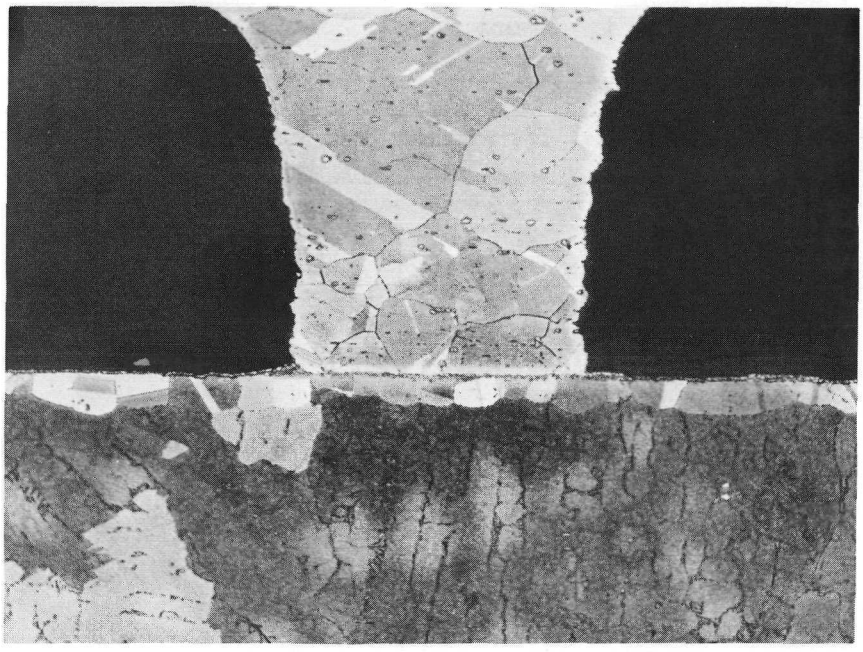

100X Marble's Etch 4E759

a. Typical Fin Cross Section

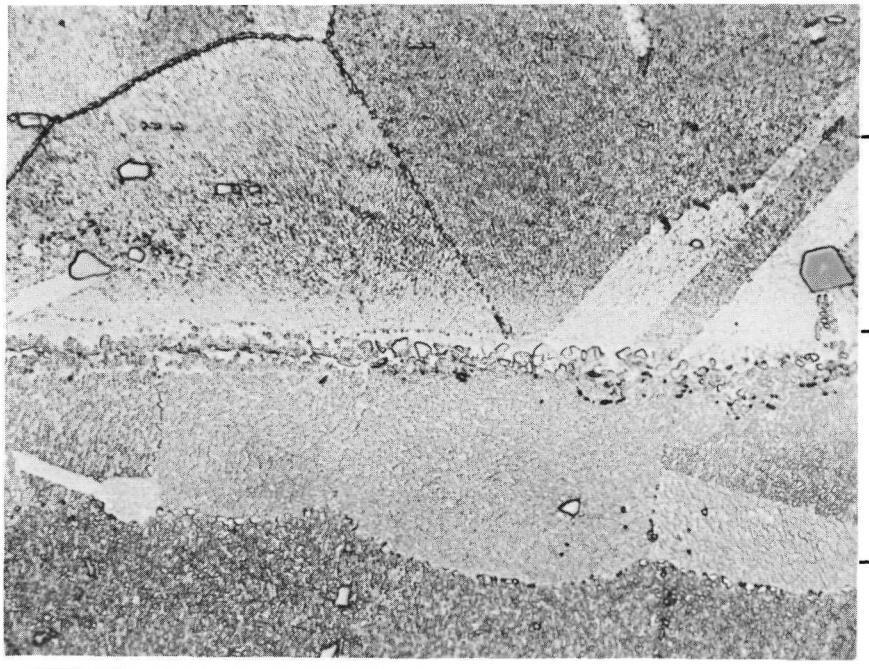

750X Marble's Etch 4E761

b. Typical Udimet 700/B1900 Bond

FIGURE 58. SPECIMEN U-64 AFTER GAS-PRESSURE BONDING AT CONDITIONS OF 1900 F/3500 PSI/1 HR

Specimen was solutionized and aged after bonding.

was observed to separate slightly. Figure 59 shows specimens before and after thermal cycling.

Subsequent to an inspection by neutron radiography, the specimen halves were cut and machined into the parallel and transverse compressive shear specimens of the design shown in Figures 60 and 61. Twelve specimens, taken from the four corners, the center, and two other locations, were evaluated from each finned shell specimen. All tests were conducted at 1750 F in air.

Test direction – parallel or transverse to the fin direction – fracture load, and fracture strength are presented in Figure 62 for all specimens. The results of the shear testing program are summarized in the bar graph of Figure 63. Samples labeled A, B, F, E, J, and M in Figures 62 and 63 were tested in the aged condition. Those labeled A, B, and F were tested parallel to the fin direction; samples labeled E, J, and M were tested transverse to the fin direction. Samples C, D, G, H, K, and P were thermally cycled prior to testing. Sample designations C, D, or G indicate that the shear load was applied parallel to the fin direction. Conversely, a H, K, or P designation indicates that the sample was tested transverse to the fin direction. Sample U-63P was inadvertently machined to the parallel test configuration.

Samples U-64M, U-65K, and U-66K fractured before a measurable load could be applied. Samples U-66J, U-68C, U-68G, and U-68M did not fracture in the 0.040-in. displacement permitted by the fixture before reestablishing the 0.080-in. displacement maximum. Hence, the bond area of these samples could not be measured after the test. It is estimated that the strength of those four specimens exceeded 40,000 psi.

An examination of the fractured surfaces revealed that the fractures in Specimens U-63 and U-64 were primarily at the bond interfaces, while in most of the specimens from U-65 through U-68, the fractures occurred in the parent metal. Generally, the specimens having the lowest fracture strengths had high percentages of the fractured surface through the bond interface, but there were exceptions to this.

Fracture-stress levels for Specimens U-63 and U-64 were lowest in the series of tests and were nearly all below 15,000 psi. In the U-65 through U-68 series, the parallel shear-test specimens almost always achieved a fracture strength of 30,000 psi or greater. Transverse shear strengths were generally lower and less reproducible than parallel strength values. Thermal cycling appeared to have a more adverse effect on transverse strength than on specimens tested parallel to the fins. There was no conclusive trend on the effect of thermal cycles in the latter case.

The U-63 and U-64 series of specimens showed practically no ductility, as indicated by the load-time curves recorded for each test. Fracture usually occurred within a shear deformation of about 0.020 in. Considerable ductility was observed in many of the U-65 to U-68 series specimens. Fracture in this series was usually preceded by signs of plastic deformation and occurred after about 0.040 to 0.055-in. displacement. Typical fractures are illustrated in Figure 64.

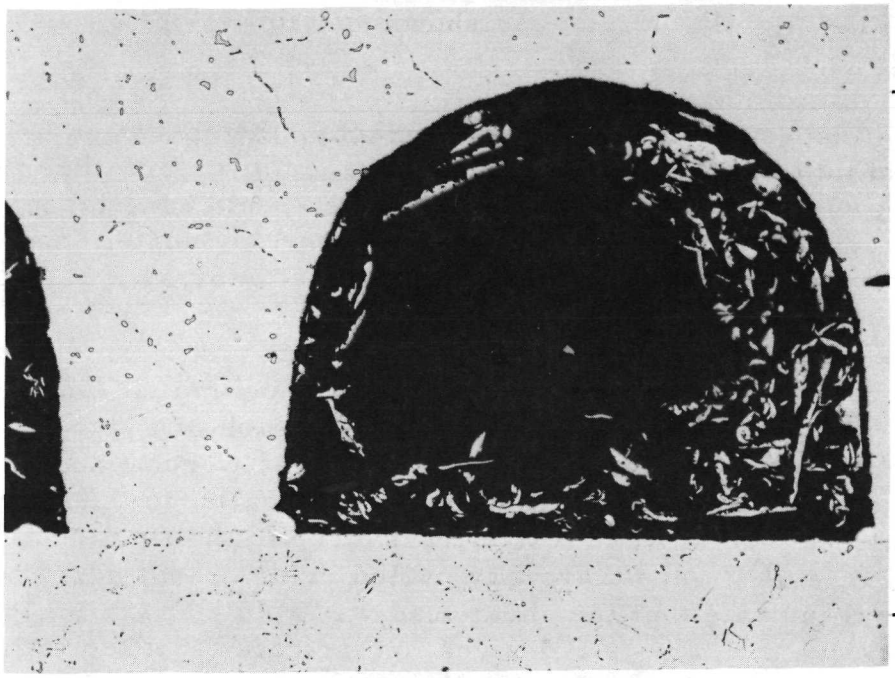

100X As Polished 8E828

a. Aged

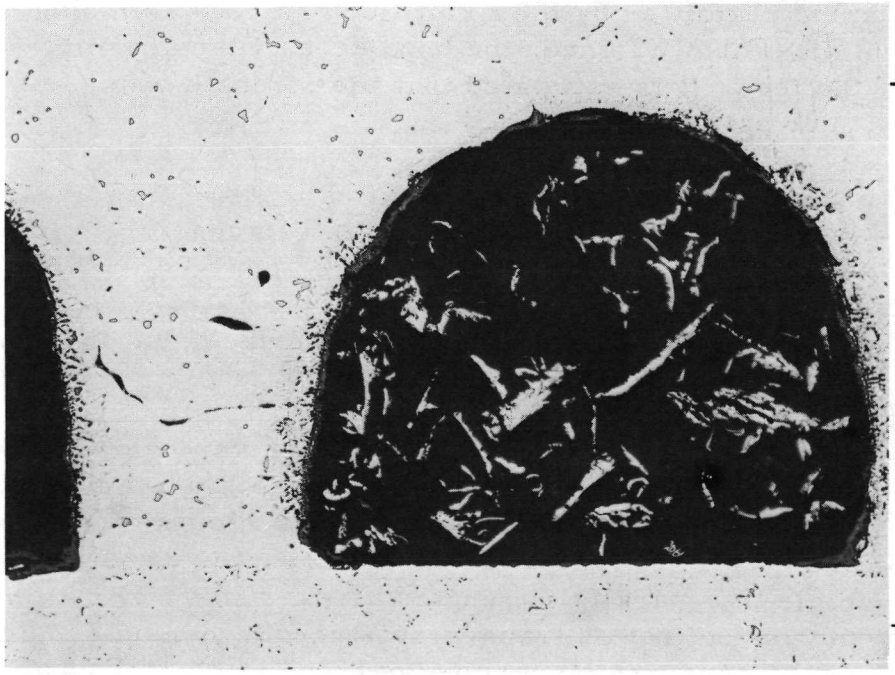

100X As Polished 8E831

b. Thermal Cycled; Note Grain-Boundary Separation

FIGURE 59. UNTESTED SAMPLES OF SPECIMEN U-67 BEFORE AND AFTER 1750 F THERMAL CYCLES

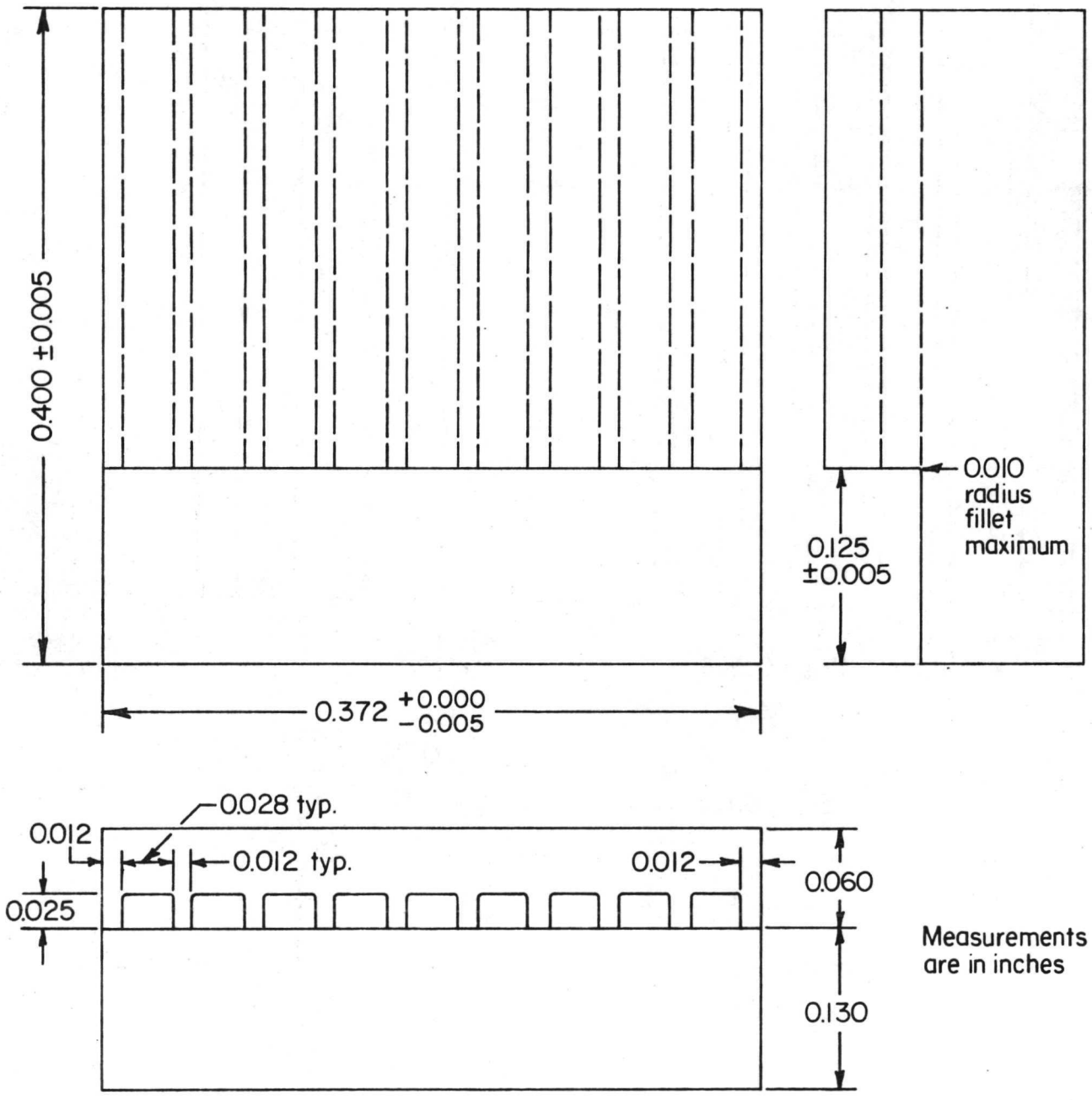

FIGURE 60. PARALLEL SHEAR TEST SPECIMEN

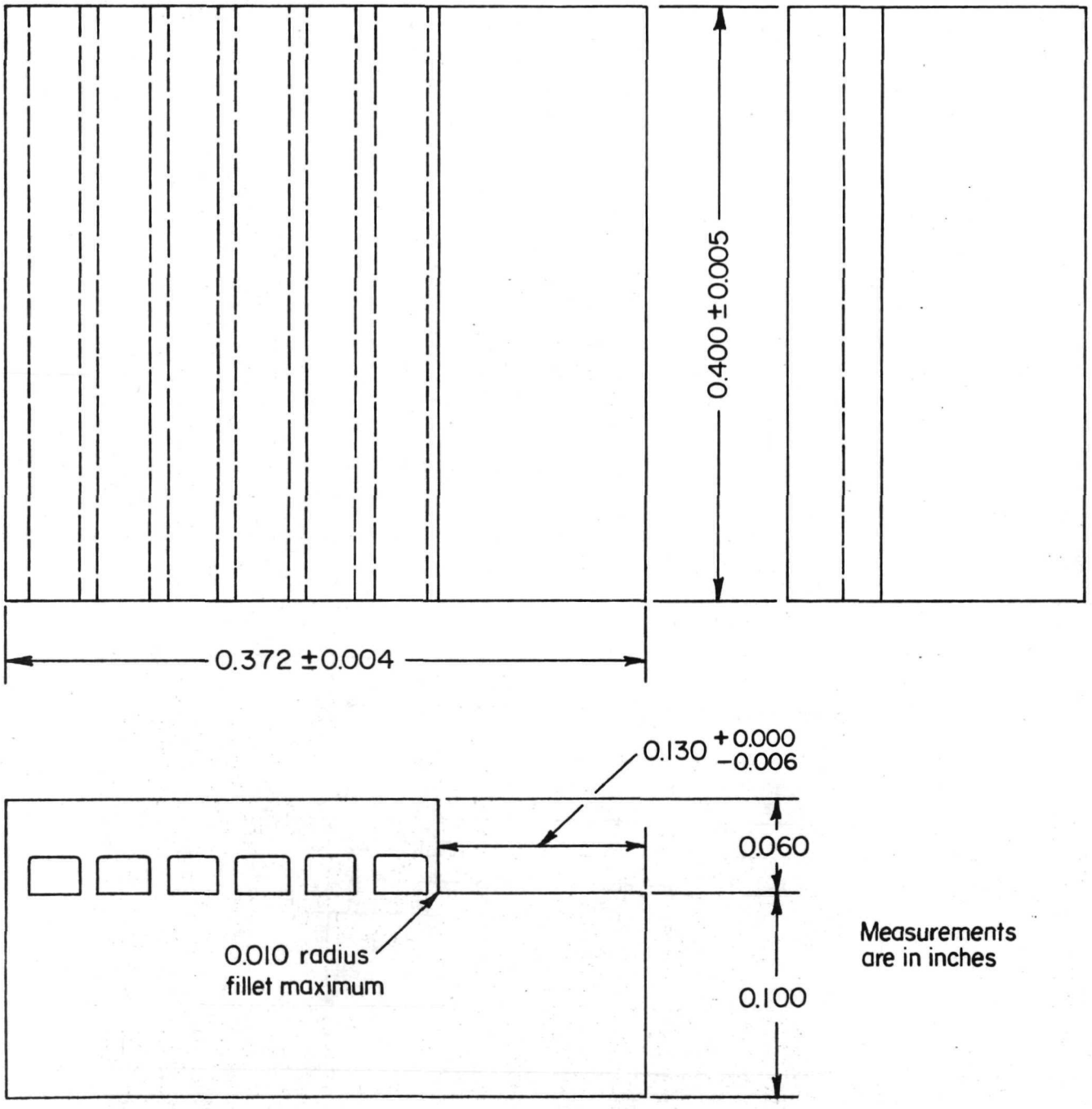

FIGURE 61. TRANSVERSE SHEAR TEST SPECIMEN

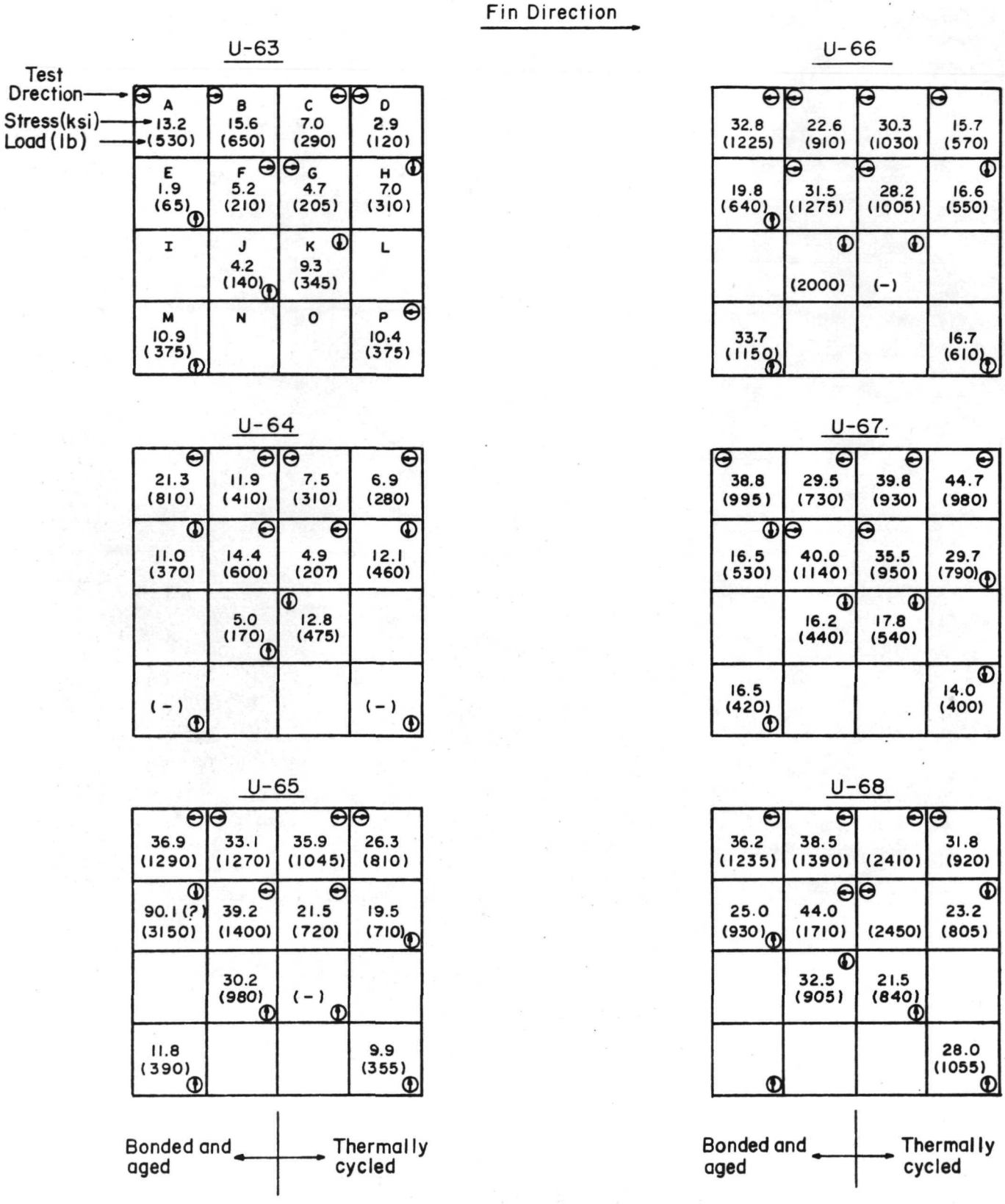

FIGURE 62. TABULATION OF SHEAR TEST RESULTS ON SPECIMENS U-63 THROUGH U-68

Page Intentionally Left Blank

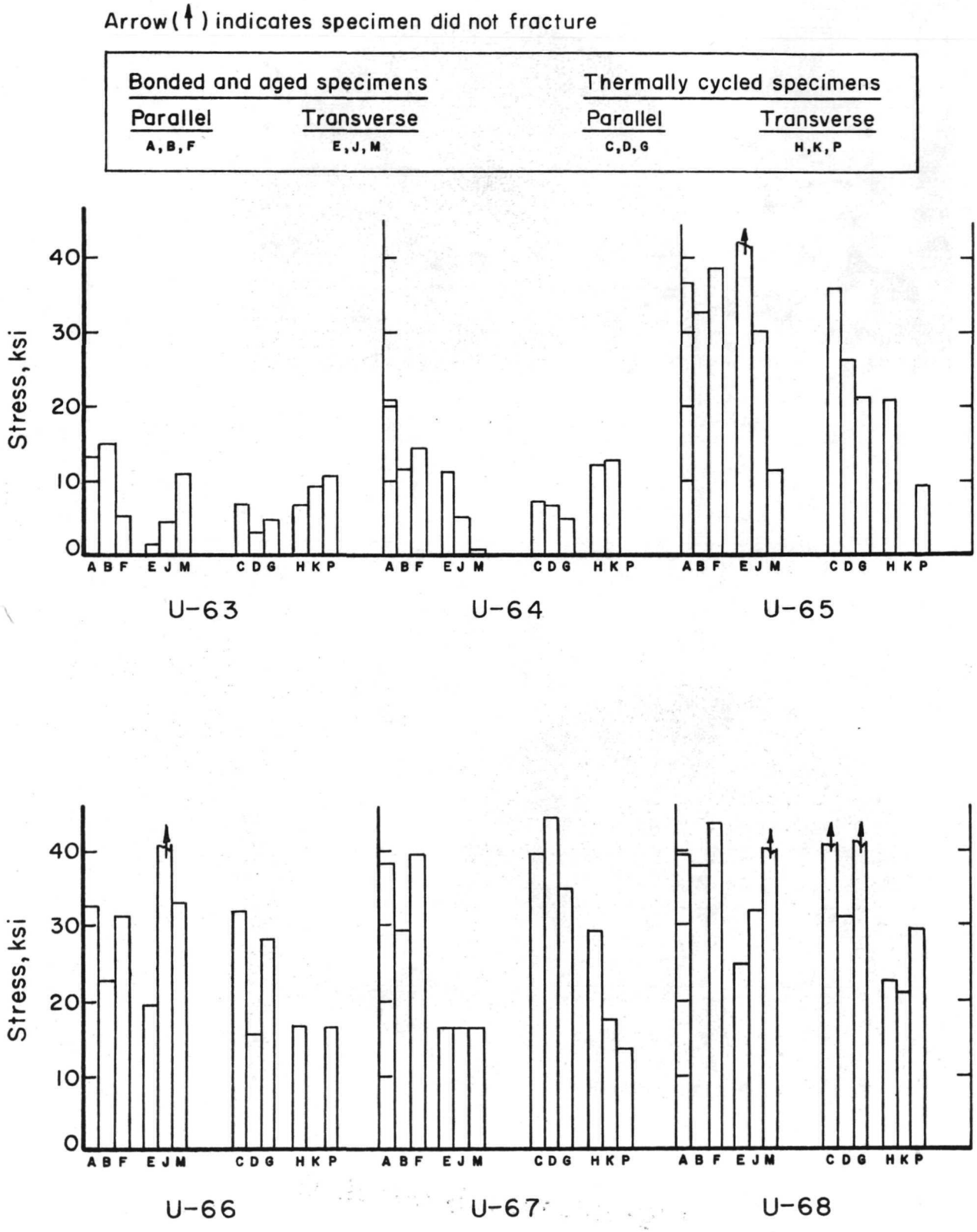

FIGURE 63. SUMMARY OF FLAT UDIMET 700 FINNED SHELL 1750 F SHEAR TESTING RESULTS

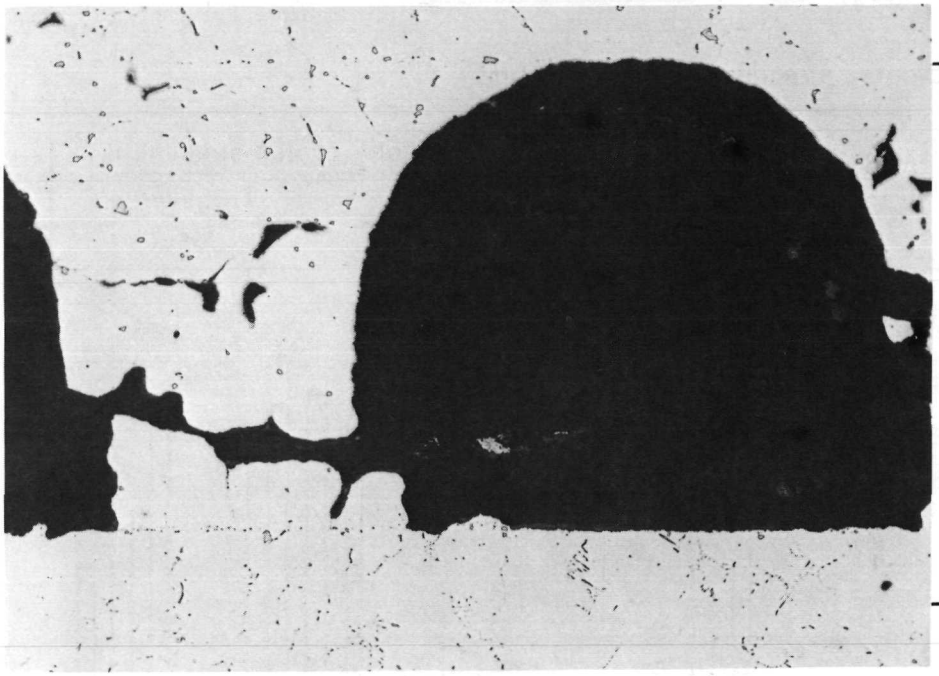

100X As Polished 8E830

a. Sample U-66J; Aged; Transverse Test

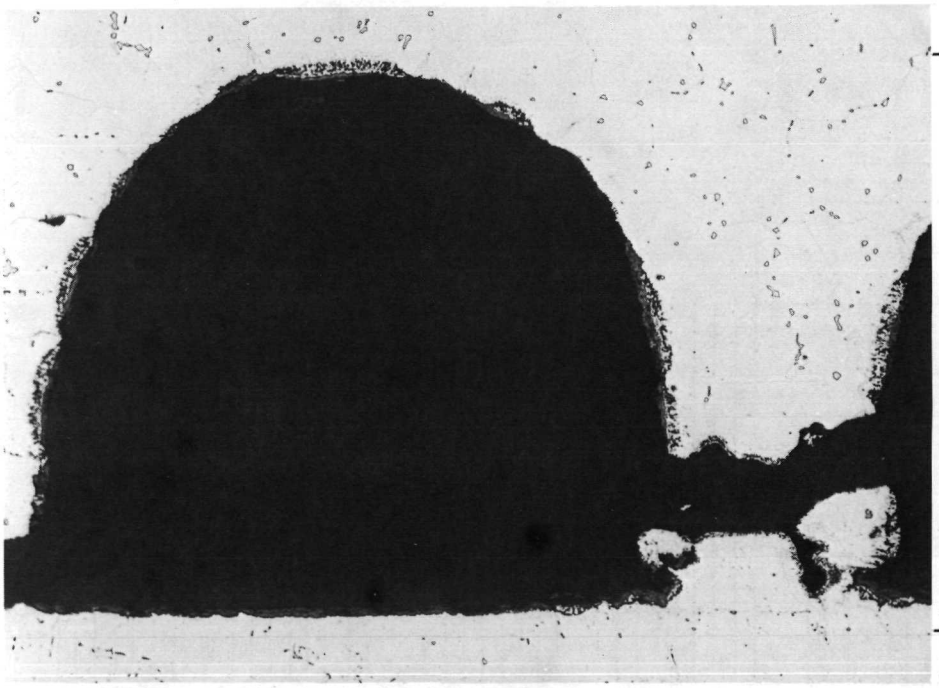

100X As Polished 8E827

b. Sample U-67C; Thermal Cycled; Parallel Test

FIGURE 64. TYPICAL FRACTURES FROM 1750 F SHEAR TEST

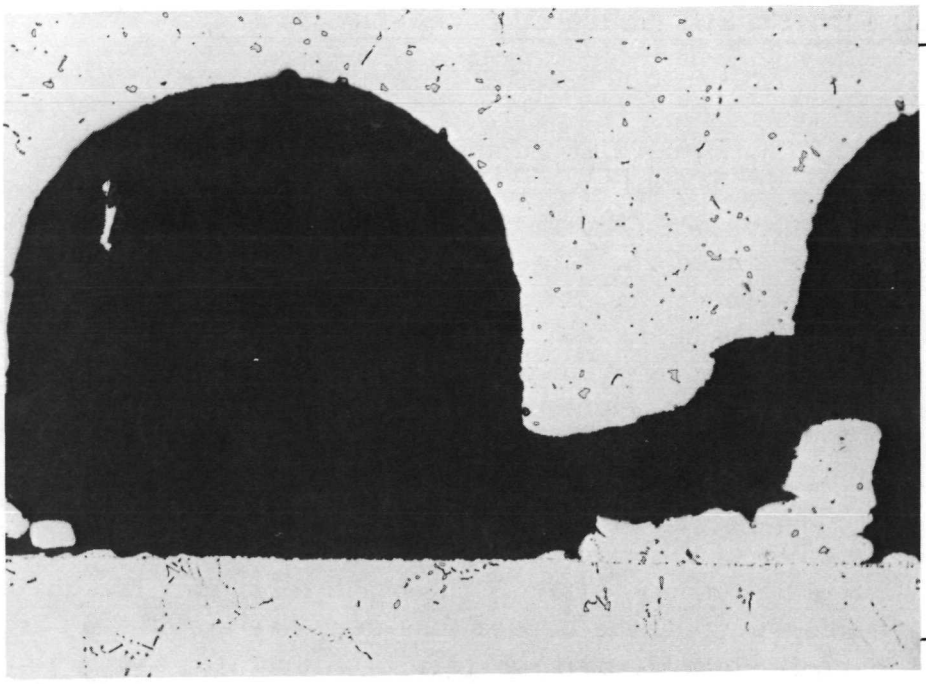

100X As Polished 8E832

c. Sample U-68B; Aged; Parallel Test

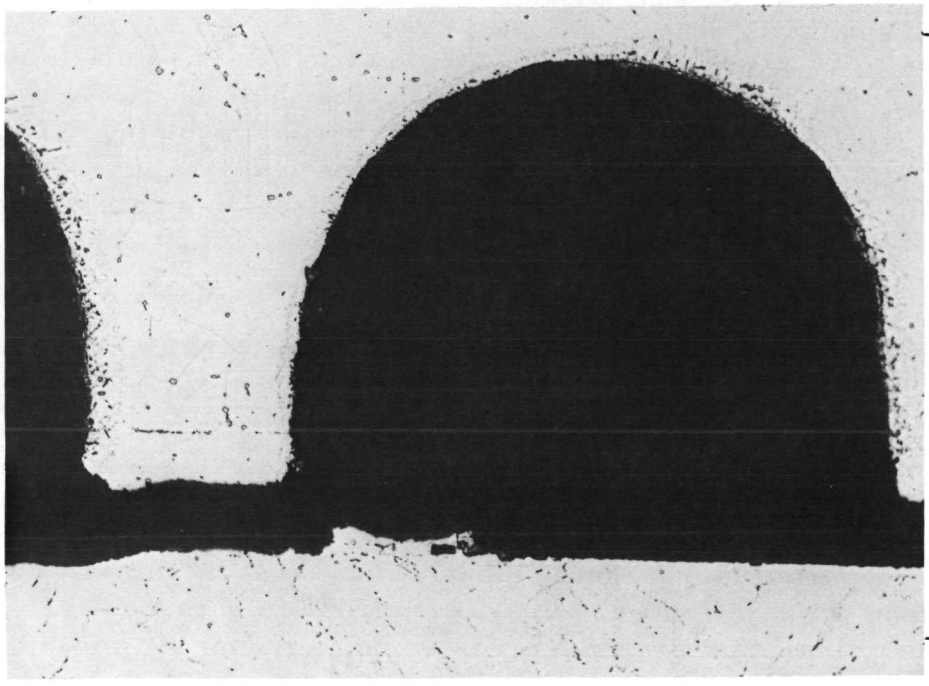

100X As Polished 8E829

d. Sample U-67D; Thermal Cycled; Parallel Test

FIGURE 64. (CONTINUED)

SIMULATED FINNED SHELL-STRUT AIRFOIL STUDIES

Finned Shell Specimen Design and Fabrication

Figure 65 illustrates the finned shell design recommended and approved for use in burst tests. Zone M fins were not employed in the design as failure would initiate in that zone during a burst test due to the longer unrestrained span. Failure, once initiated, would proceed rapidly to completion, as the unit stress on each fin is increased by failure of its neighbors. It was of primary interest to determine the strength of Zone L fin-to-strut joints. The test grid consisted, therefore, of thirty-seven 0.012-in. -wide by 1.452-in. -long fins separated by 0.028-in. -wide channels. The grid is bordered by four peripheral fins of the same width and channel spacing as the grid itself. Figure 66 illustrates the grid and border fins at a typical corner. During the burst test, only the channels between the grid fins are pressurized; the border fins serve as a seal. Four such samples were joined to each B1900 cylinder. Figure 67 illustrates the method of specimen assembly for bonding the four shells to the B1900 cylinder. Two finned shells are bonded with fins attached circumferentially and the two remaining shells bonded with the fins of the test grid oriented longitudinally on each cylinder. The cylindrical radius, specimen thickness, and chord length were chosen to simulate a typical turbine blade airfoil geometry.

The finned shells were prepared by EDM; the electrode used to machine the shells was shown previously in Figure 13. In general, the shell geometry selected was found to be a difficult one for electrical-discharge machining. The primary difficulty arises from the closed nature of the channel design. This impeded flow of EDM dielectric oil and required that the machining rate be maintained at a low level to avoid erratic cutting. The procedures established previously were used in regard to blank preparation and fixturing.

The machined blanks were subsequently ground to size, 1.80 in. square, and rolled to an inside radius of 2.5 in. Half the shells were rolled with the test-grid fins in a circumferential orientation and the other half in an axial orientation. The TD NiCr and Udimet 700 shells and B1900 cylinders were prepared for diffusion bonding by the recommended procedure described previously. Each shell was examined at 60X magnification and dimensionally inspected subsequent to completion of the surface preparation procedure. It was found that the fin and channel dimensions after surface preparation were 0.010 and 0.030 in., respectively. The etching step of the preparation procedure was found to reduce fin width by about 0.001 in. This exception to the nominal design dimensions of 0.012-in. fin and 0.028-in. channel width was expected and unavoidable. Precision milling saws 0.016 in. wide were desired in the EDM electrode preparation step to generate a final fin width of slightly greater than 0.012 in. However, 0.0135 to 0.014-in. -wide saws were the nearest available size in stock in the quantity required.

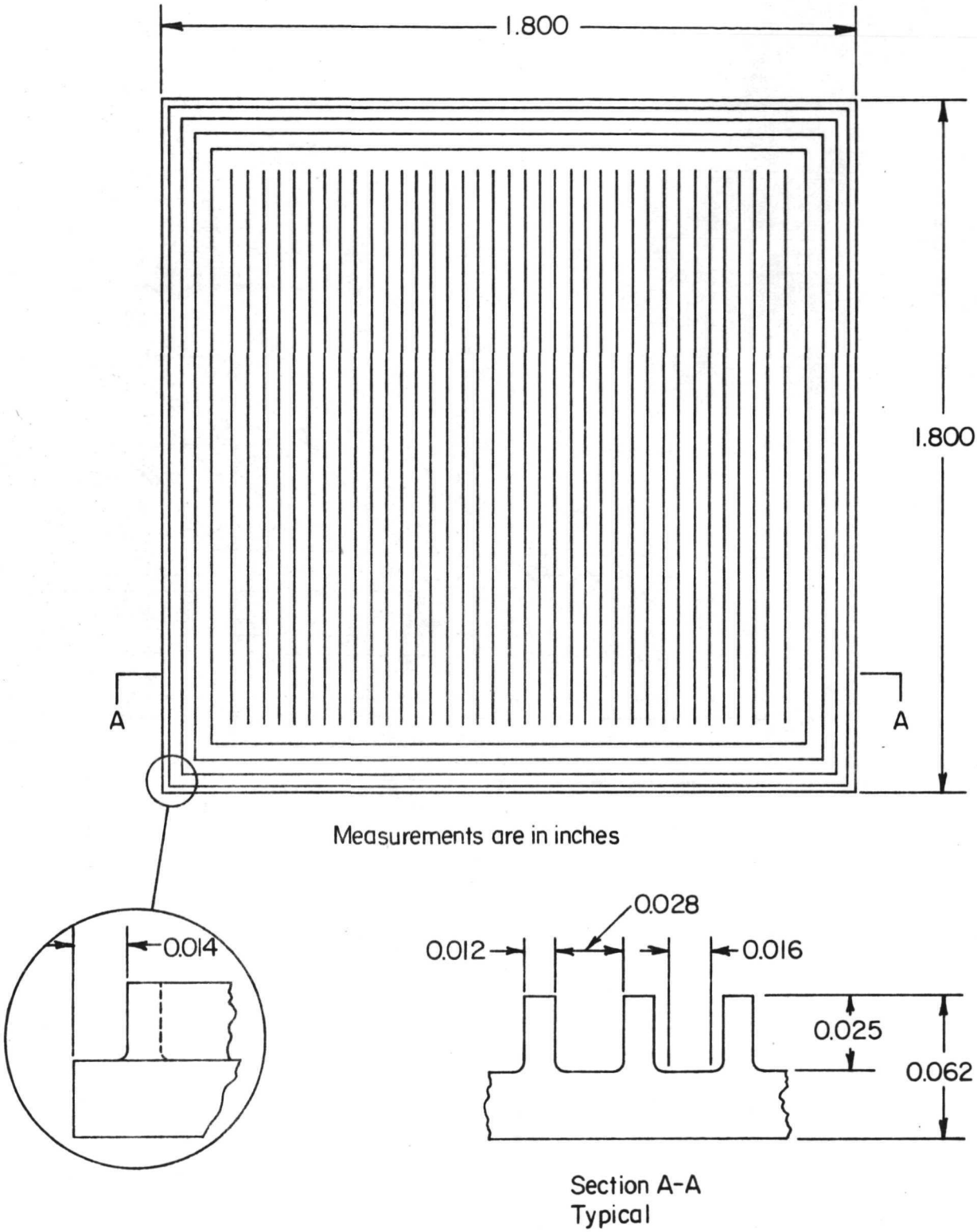

FIGURE 65. SKETCH ILLUSTRATING FINNED SHELL FOR BURST TEST USE

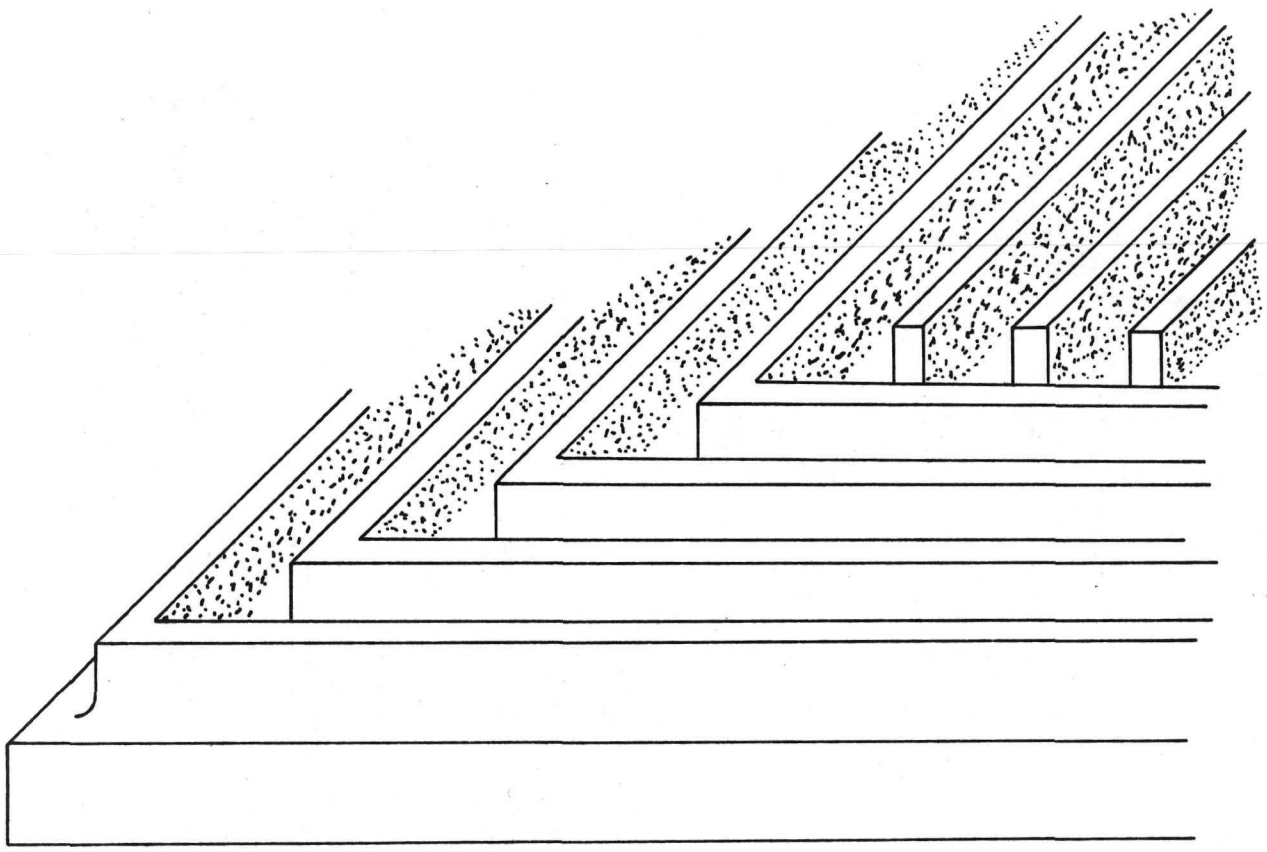

FIGURE 66. CORNER DETAIL OF FINNED SHELL DESIGN

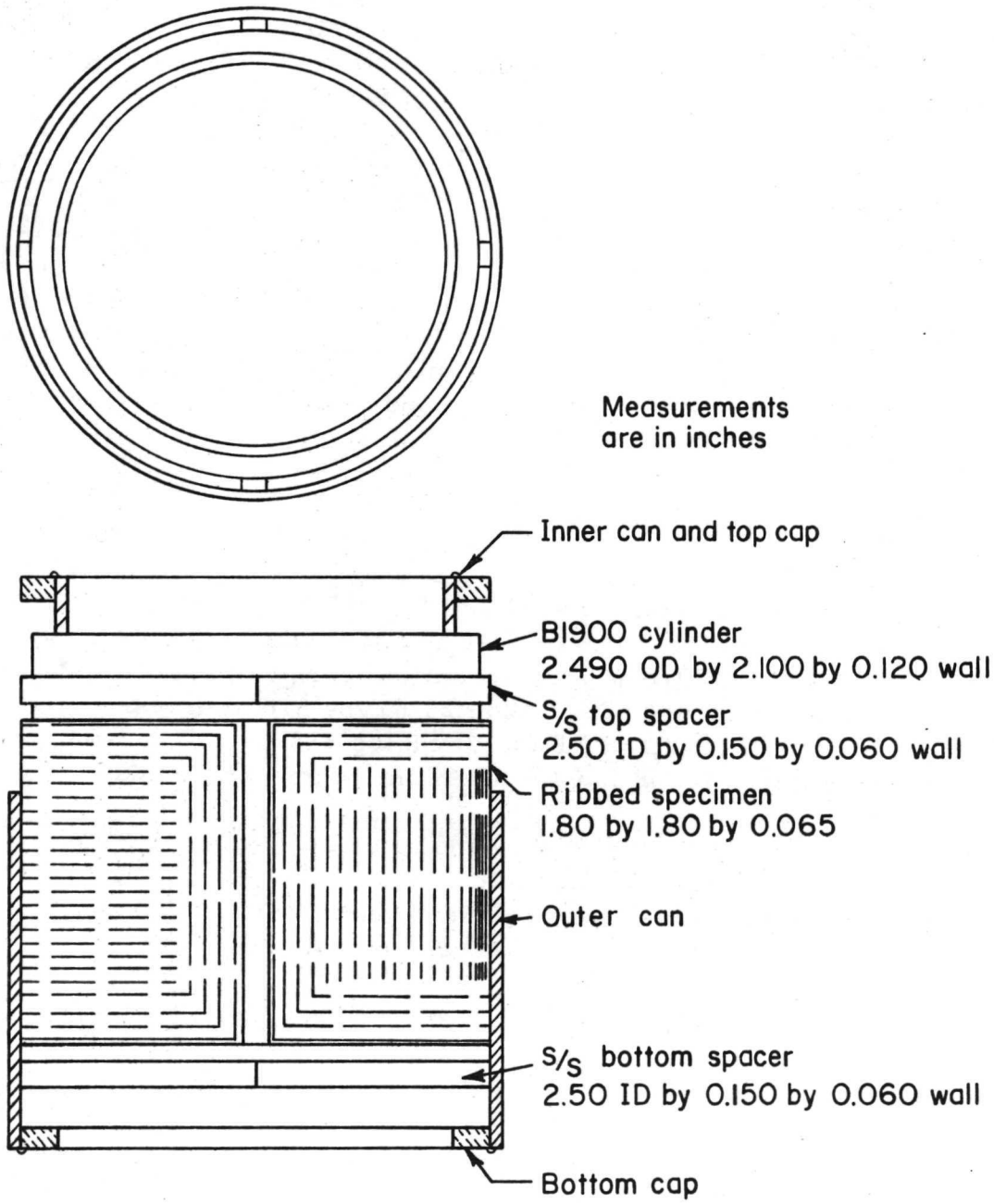

FIGURE 67. CYLINDRICAL SPECIMEN ASSEMBLY

TD NiCr/B1900 Cylindrical Specimen Burst Tests

Four TD NiCr shells were assembled about each of six B1900 cylinders. Two each of the axial and circumferential orientation shells were used with each cylinder. The TDNiCr/B1900 specimens were designated T-41 through T-46. After assembly, the specimens were evacuated and sealed by an electron-beam welder. The six cylinders plus a seventh, Specimen T-47, in which braze sealing was investigated as an alternative to canning in stainless steel, were subjected to a 2000 F/3500 psi/1 hr gas-pressure bonding cycle. Following the cycle, Specimens T-41 through T-46 were decanned, and all were sectioned to yield the four sample segments. Each segment was radiographed, and the radiographic negatives mated to index marks on the respective segment. From the negative it was possible to locate the proper position for a pressure access port through the B1900. Several segments were again radiographed after the port was pierced, and it was found that the port was centered over the chosen finned shell channel as desired. No material had been removed from the fins adjacent to the channel. Lastly, a flat axial slot 3/4 in. wide was ground into the concave surface of the segment to facilitate tube attachment.

Burst Test Preparation

Attachment of the pressurizing tube to the cylindrical test specimen presented a challenging problem. The tube attachment and its joint are subject to hydraulic pressures up to 50,000 psi at room temperature and gas pressures potentially in the range of 26,000 psi at 1750 F. Type 316 stainless steel tubing 5/8 in. in OD by 3/16 in. in ID and René 41 tubing 5/8 in. in OD by 1/8 in. in ID were selected, respectively, to handle the room-temperature and 1750 F pressures.

Fusion welding and brazing were found to be unsatisfactory for attaching the tubes to B1900. Friction welding was successfully applied. Test B1900/stainless steel tube friction welds were evaluated with a successful oil pressurization of 100,000 psi at room temperature. No leakage or rupture occurred. Figure 68 shows a B1900 segment with a friction-welded stainless steel tube attachment. Composite tubes were needed for 1750 F tests. In this case, a 3.5-in. length of aged René 41 tube was friction welded to the B1900. Subsequently, a 6-in. length of Type 316 stainless tube was friction welded to the René 41. This system was qualified in a duplicate specimen test at 1775 F under 31,000-psi helium pressure. No leakage or rupture occurred at either joint of either specimen.

The access port through the B1900 component of the burst specimens was 0.010 in. in diameter. Using appropriate indexing and radiographic techniques, it was possible to locate an access port of that size completely within a channel. This precaution was taken to avoid knowingly weakening any fin. The port was later enlarged to 1/16 in. after completion of the initial six-specimen series at room temperature and 1750 F demonstrated that the access port diameter had a negligible effect on failure mode or values. Further friction welding experiments

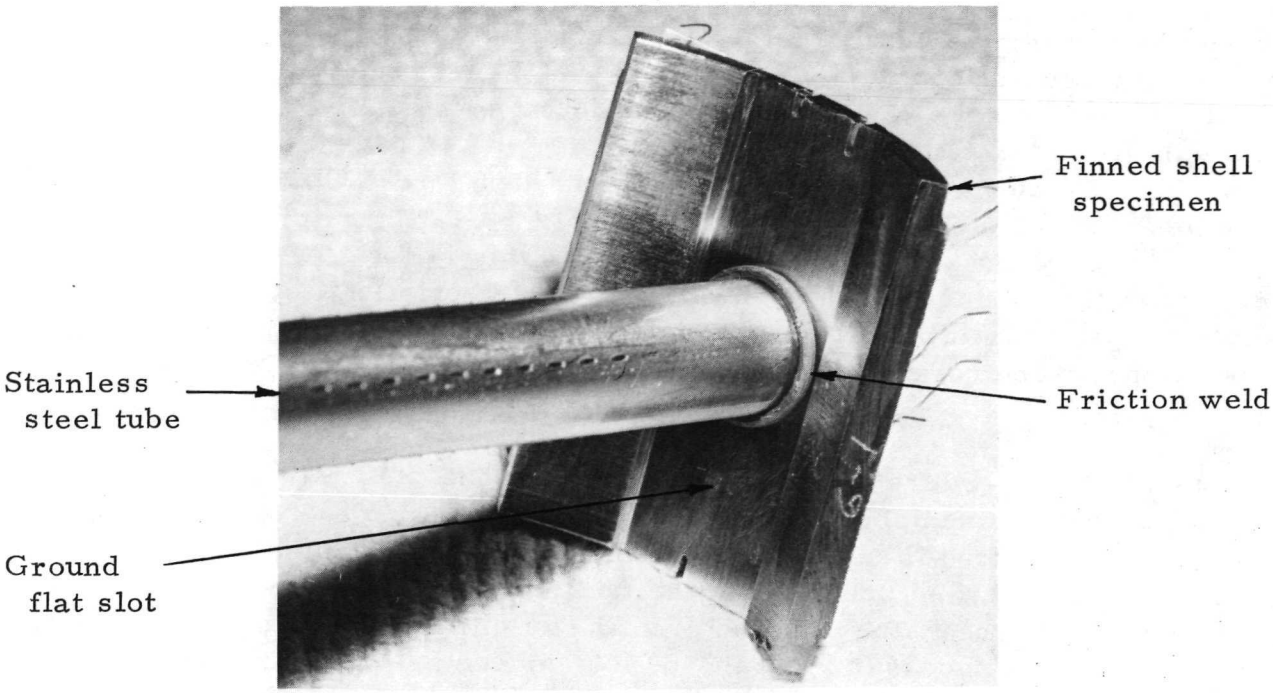

~1X 44896

a. Typical Weld

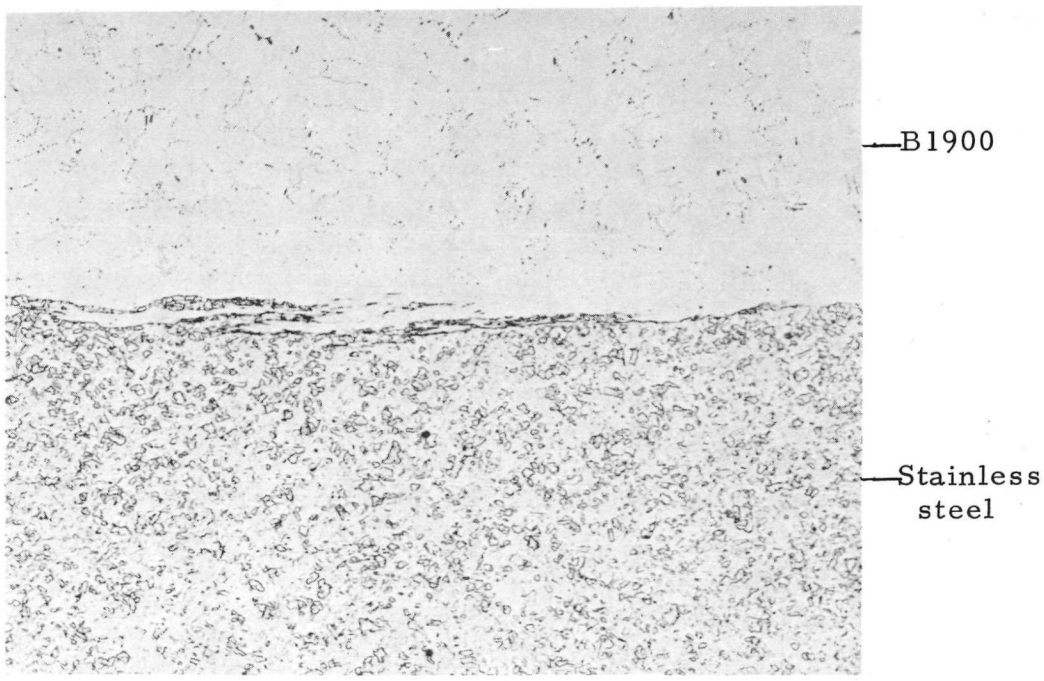

100X 5D335

b. Weld Interface

FIGURE 68. FRICTION-WELDED STAINLESS STEEL PRESSURIZATION TUBE ATTACHMENT

were performed to determine whether leaktight joints could be made with limited internal flash required to prevent plugging of the access port in the B1900. Several stainless steel and Rene 41 tube samples were counterbored to increase the tube ID from 3/16 and 1/8 in., respectively, to 1/4 in. The René 41 was counterbored 0.020 in. and the stainless steel, 0.060 in. In the case of stainless steel tubes, reducing axial upset during joining to 0.025 in. limited the internal flash to a collar approximately 1/16 in. thick. This left a 1/16-in.-diameter passage through the flash collar. Similar results were obtained with René 41 tubes when axial upset was limited to 0.008 in. The samples appeared to be gastight. However, they were not evaluated at high pressure; the test was limited to air at approximately 80 psi.

The above procedure was employed to attach stainless steel tubes and René 41 tubes to the specimen segments evaluated in the as-bonded condition. Some difficulty was experienced in reproducibly effecting gastight joints. With the axial upset limitation specified previously, the friction welding process was found to be rather sensitive to the flatness of the ground slot and alignment of the segment. Specifically, it was necessary that the B1900 surface be coplanar with the end of the tube within 0.001 in. A slight angle between tube face and slot surface almost invariably resulted in a leak approximately 180 deg away from the point at which the tube initially contacted the B1900 surface. Since the B1900 castings are irregular, the alignment procedure became quite involved. In the case of two room-temperature and two 1750 F segments of the as-bonded evaluation, the required alignment could not be achieved and leaks resulted. The stainless steel/B1900 joints were repaired successfully by applying a silver-base braze. However, attempts to repair gas leakage at the René 41/B1900 joints by vacuum furnace brazing caused the B1900 to crack. The "repaired" sepcimens could not be pressurized, as gas leaked through the cracks in the B1900. Consequently, René 41/B1900 friction welds for the second series of 1750 F tests – thermally cycled condition – employed the more conservative welding parameters used for the original weld qualification samples. The increased-diameter access port used in the second series permitted reboring by EDM, which removed any interfering internal flash produced from friction welding.

After tube welding, specimens destined for 1750 F evaluation had five Chromel/Alumel thermocouples attached directly to the TD NiCr finned shell. The thermocouples and a pressure transducer installed approximately 1 ft upstream from the specimen connection were attached to a strip chart recorder. In one room-temperature test, strain gages were attached to the TD NiCr shell. The specimen is shown in Figure 69. This practice was discontinued, as the shell deflection was essentially nil during pressurization.

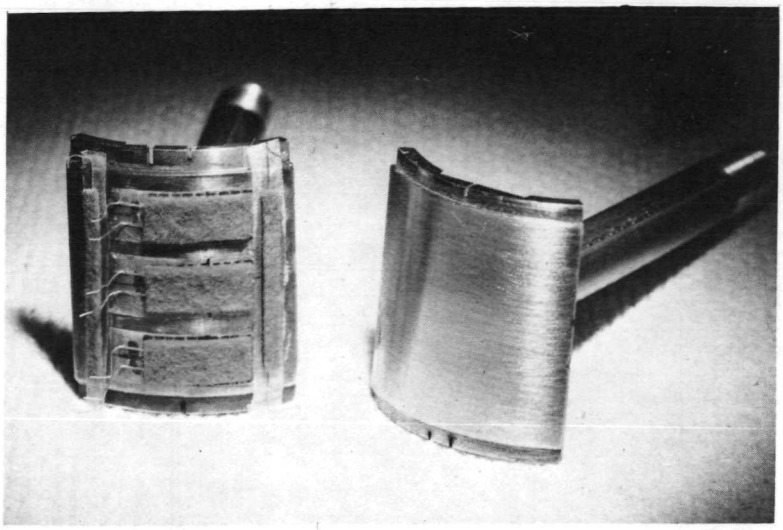

~1/2X 44897

FIGURE 69. TD NiCr/B1900 CYLINDRICAL FINNED SHELL SEGMENTS PREPARED FOR BURST TEST EVALUATION

The specimen on the left has been instrumented with three circumferential and two axial direction strain gages to measure deflection during pressurization.

Burst Test Evaluation

Tables 15 through 18 summarize the mechanical property and metallographic examination results obtained from the burst test program. All tests were terminated prematurely by leakage at either the margin fins, tube weld, or shell face. This made it very difficult to analyze the data. In general, axial specimens tended to exhibit higher strength levels than circumferential specimens. At both room temperature and 1750 F, prior thermal cycling degraded strength. At room temperature the as-bonded strength was of the order of 50,000 to 100,000 psi; after thermal cycling, strength at room temperature was typically 40,000 to 85,000 psi with extensive failure occurring in the TD NiCr fins. Similarly, the 1750 F strength prior to thermal cycling appeared to be 10,000 to 15,000 psi. After thermal cycling, strength dropped to the 1000 to 4000-psi range, and again a significant degree of TD NiCr fin failure was observed. These results tend to indicate a possible thermal fatigue problem in TD NiCr. The inferred cause of this indicated thermal fatigue is a thermal expansion mismatch between TD NiCr and B1900. However, the thermal expansion data available in the literature would suggest that the combination is quite compatible. It was noted that the strength values obtained from uncycled specimens were reasonably consistent with compression shear test strength values obtained earlier on flat finned shells.

TABLE 15. RESULTS OF ROOM-TEMPERATURE INTERNAL BURST TESTS PERFORMED ON TD NiCr/B1900 FINNED SHELL SEGMENTS PREPARED BY GAS-PRESSURE BONDING[a]

Specimen	Fin Direction	Failure Location	Fluid Pressure, psi	Tensile Stress[b], psi	Average Fin Width, mils	Metallographic Examination[c]		
						Degree of Fin Deformation	Percent Fins With TD NiCr Failure	Percent Fins With Bond Failure
T-41-2	Axial	Margin seal	17,250	54,000	9.7	Moderate	0[d]	0
T-43-2	Axial	Margin seal	13,500	51,000	8.4	None	0	50
T-45-2	Axial	Margin seal	35,000	92,000	11.0	Heavy	0[d]	0
T-42-1	Circumferential	Tube weld	30,000	94,000	9.7	Moderate to heavy	0	0
T-44-1	Circumferential	Margin seal	47,000	147,000	9.7	Moderate	67	0
T-46-1	Circumferential	Margin seal	1,000	4,200	7.8	None	0	77
T-47-1	Circumferential	Shell face	15,000	(e)	9.5	None	--	--

(a) Bonding conditions of 2000 F and 3500 psi were held for 1 hr.

(b) Calculated by dividing fluid pressure at failure by the average fin-to-channel width ratio as determined by direct measurement of the metallographic section.

(c) The percentages were determined by dividing the number of fins fitting each category by 37, the total number of test grid fins.

(d) In a second section taken close to the margin seal leak, failure was found to be exclusively in the TD NiCr fins.

(e) Excess braze metal apparently prevented contact between fin and strut during the bonding cycle, consequently it was doubtful that fin/strut bonds were created or subsequently stressed in the sense reported for the other six specimens.

TABLE 16. RESULTS OF 1750 F INTERNAL BURST TESTS PERFORMED ON TD NiCr/B1900 FINNED SHELL SEGMENTS PREPARED BY GAS-PRESSURE BONDING[a]

Specimen	Fin Direction	Failure Location	Fluid Pressure, psi	Tensile Stress[b], psi	Average Fin Width, mils	Metallographic Examination[c]		
						Degree of Fin Deformation	Percent Fins With TD NiCr Failure	Percent Fins With Bond Failure
T-41-4	Axial	Hole melted in shell by electrical short	5,000	16,600	9.3	Light	0	75
T-43-4	Axial	Margin seal	2,500	9,400	8.4	Light	0	81
T-45-4	Axial	Margin seal	3,500	12,100	9.0	Moderate	0	0
T-42-3	Circumferential	Attempts to repair tube leakage unsuccessful, could not be pressurized						
T-44-3	Circumferential	Hole melted in shell by electrical short	1,200	4,300	8.7	Light	0	30
T-46-4	Axial	Attempt to repair tube leakage unsuccessful, could not be pressurized						

(a) Bonding conditions of 2000 F and 3500 psi held for 1 hr were used.
(b) Calculated by dividing fluid pressure at failure by the average fin-to-channel width ratio as determined by direct measurement of the metallographic section.
(c) The percentages were determined by dividing the number of fins fitting each category by 37, the total number of test grid fins.

TABLE 17. RESULTS OF ROOM-TEMPERATURE INTERNAL BURST TESTS PERFORMED ON THERMAL-CYCLED TD NiCr/B1900 FINNED SHELL SEGMENTS PREPARED BY GAS-PRESSURE BONDING[a]

Specimen	Fin Direction	Failure Location	Fluid Pressure, psi	Tensile Stress[b], psi	Average Fin Width, mils	Metallographic Examination[c]		
						Degree of Fin Deformation	Percent Fins With TD NiCr Failure	Percent Fins With Bond Failure
T-42-4	Axial	Margin seal	95,000[d]	336,800	8.8	Heavy	40	0
T-44-2	Axial	Margin seal	21,000	84,000	8.0	Moderate	56	14
T-46-2	Axial	Margin seal	12,000	46,500	8.2	Moderate	0	54
T-41-1	Circumferential	Margin seal	11,500	50,200	7.5	Moderate	22	7
T-43-1	Circumferential	Margin seal	9,500	40,500	7.6	Moderate	0	48
T-45-1	Circumferential	Margin seal	1,000[d]	3,500	9.0	Light	44	32

(a) Bonding conditions of 2000 F and 3500 psi held for 1 hr were used; all specimens thermally cycled between 1750 F and room temperature 10 times with cumulative 200 hr at 1750 F.

(b) Calculated by dividing fluid pressure at failure by the average fin-to-channel width ratio as determined by direct measurement of the metallographic section.

(c) The percentages were determined by dividing the number of fins fitting each category by 37, the total number of test grid fins.

(d) Second pressurization after redrilling access hole to ensure free flow of pressurizing fluid. Specimens would not hold 80-psi air pressure but held oil pressure shown above. Results are not considered valid.

TABLE 18. RESULTS OF 1750 F INTERNAL BURST TESTS PERFORMED ON THERMAL-CYCLED TD NiCr/B1900 FINNED SHELL SEGMENTS PREPARED BY GAS-PRESSURE BONDING[a]

Specimen	Fin Direction	Failure Location	Fluid Pressure, psi	Tensile Stress[b], psi	Average Fin Width, mils	Metallographic Examination[c]		
						Degree of Fin Deformation	Percent Fins With TD NiCr Failure	Percent Fins With Bond Failure
T-42-4	Axial	Margin seal	1,050	3,570	9.1	Moderate	49	0
T-44-4	Axial	Margin seal	900	2,680	10.1	Moderate	84	0
T-46-3	Circumferential	Margin seal	375	1,170	9.7	None	0	100
T-41-3	Circumferential	Margin seal	900	3,100	9.0	Moderate	100	0
T-43-3	Circumferential	Margin seal	750	2,660	8.8	Moderate	100	0
T-45-3	Circumferential	Margin seal	300	910	9.9	Very light	5	95

(a) Bonding conditions of 2000 F and 3500 psi held for 1 hr were used; all specimens thermally cycled between 1750 F and room temperature 10 times with cumulative 200 hr at 1750 F.

(b) Calculated by dividing fluid pressure at failure by the average fin-to-channel width ratio as determined by direct measurement of the metallographic section.

(c) The percentages were determined by dividing the number of fins fitting each category by 37, the total number of test grid fins.

Except for the general trends discussed above, the data presented in Tables 15 through 18 are inconclusive. The failure characterization had to be conducted by metallographic examination. In no case did the TD NiCr shell separate from its B1900 substrate. Further, separation could not be forced without totally distorting and destroying the sample, as many of the fin/strut bonds were yet firmly intact. To the unaided eye, the specimens underwent no visible change as a result of the burst test. Leakage location had to be determined by gas bubble check. It was detrimental to posttest examination of fracture that the shell was firmly intact, since the specimen could not be examined as a whole. It was assumed that the metallographic sections examined were representative of the entire specimen with respect to degree and location of failure, but that is not necessarily a valid assumption.

It was noted that bond failure was generally associated with those specimens in which negligible fin deformation was observed. Conversely, those specimens in which noticeable fin deformation was observed generally failed within the TD NiCr fins leaving intact bonds. Figures 70 and 71 illustrate an example of each failure type. There are inconsistencies between average fin width and the degree of deformation. On the basis of the temperature distribution data collected in a subsequent Udimet 700/B1900 cylindrical specimen experiment, it was considered possible that actual segment temperature could have ranged 50 F above or below the nominal bonding temperature. This may be the source of the inconsistencies. It is also possible that the metallographic sections examined simply were not truly representative of the overall cylindrical segment. Subsequent cylindrical experiments in the Udimet 700/B1900 system also indicated that a portion of the applied pressure could be consumed in bringing the shell segments into contact with the cylinder; this could also account for variations in deformation.

Udimet 700/B1900 Cylindrical Specimen Tests

Direct-Bonded Finned Shells

A series of six Udimet 700 cylindrical specimens of the design described previously in the discussion of TD NiCr burst specimens were prepared, assembled, and gas-pressure bonded per the initial, tentative Udimet 700 process recommendation established at the conclusion of process development. The gas-pressure bonding conditions were 1900 F/1100 psi/1 hr. After the bonding cycle, the cylinders were processed through the 2135 F step of the Udimet 700 heat-treatment schedule. The stainless steel bonding container was then removed with the intention that the remaining three steps in the Udimet 700 heat treatment would be completed with cylindrical segments.

Upon removal of the containers, however, it was found that the Udimet 700 shells had not bonded to the B1900 cylinder. It appeared that the experiment had failed as a result of volatile contaminants evolved from the Udimet 700 components. Every member of each specimen that was in contact with or within line of sight of

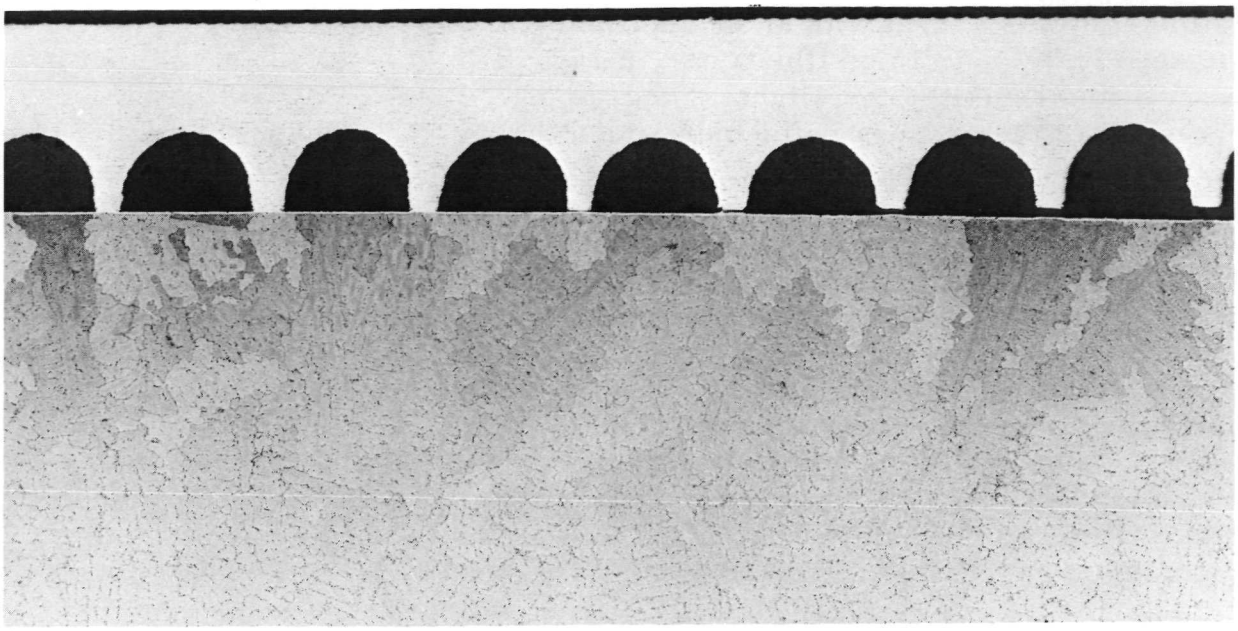

20X 20 Glycerin:20 HCl:6 HNO_3 9D035

FIGURE 70. POSTTEST SECTION OF BURST SPECIMEN T-43-1 WHICH EXHIBITED BOND FAILURE

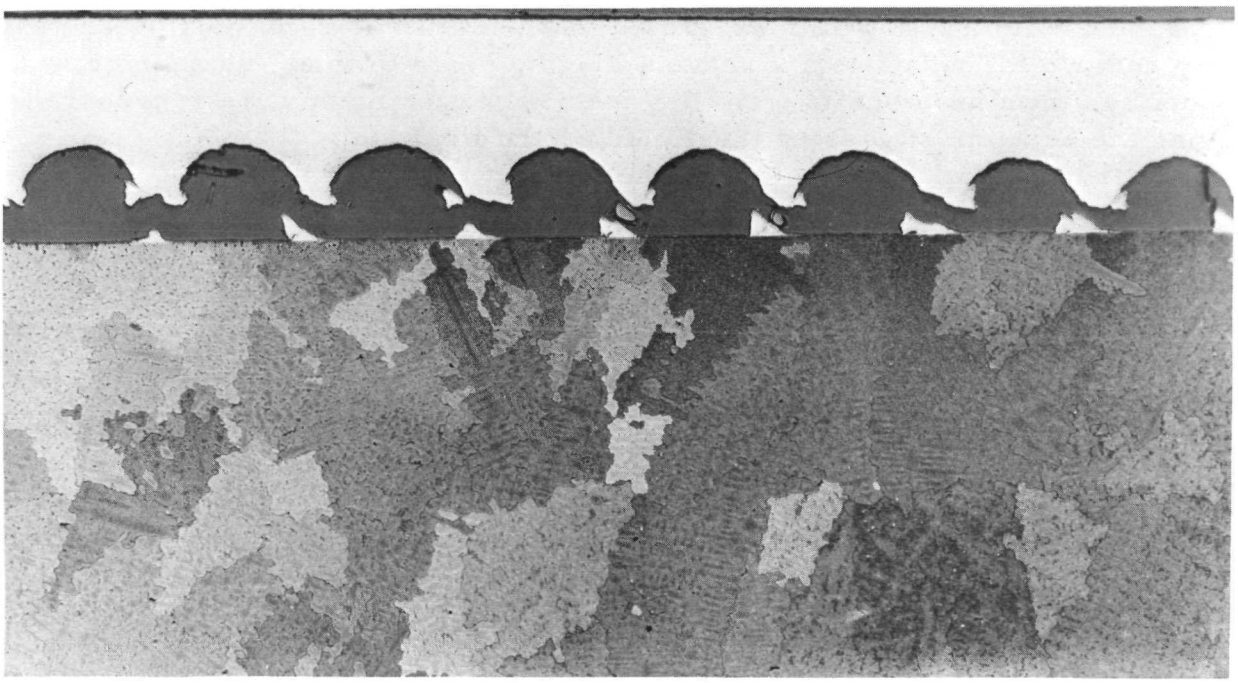

20X Marble's Etch 8D527

FIGURE 71. POSTTEST SECTION OF BURST SPECIMEN T-44-1 WHICH EXHIBITED TD NiCr FIN FAILURE

the Udimet 700 was coated with an unidentified film, presumably an oxide, which may be seen on the specimen illustrated in Figure 72. It was observed that none of the shell fins exhibited the slightest degree of compressive flow. On the basis of the results of the process refinement study (Table 11) a modest degree of fin upset was expected under the 5000-psi bearing pressure exerted by the gas pressure used. Similar anomalies had been observed among the TD NiCr cylindrical burst specimens as well, and it is suspected that a portion of the applied pressure was consumed in bringing the shells into conformity with the B1900 cylinder. Hence, the effective bearing pressure could be significantly less than anticipated.

Outgassing, thermogravimetric analysis, mass spectrometer, and X-ray diffraction experiments were conducted to better understand the behavior of Udimet 700 under conditions similar to those during bonding. These experiments confirmed that Udimet 700 does yield volatile products when heated in vacuum. Using a heating rate similar to that of the gas-pressure bonding cycle, Udimet 700 was found to outgas at the rate of 0.75×10^{-9} g per sec per cm^2. The outgassing products during heatup were H_2O and CO in the ratio of 2:1. At the bonding temperature only chromium is released. The vaporization rate was 0.25×10^{-8} g per sec per cm^2, a value quite consistent with the theoretical prediction. The quantity of water and carbon monoxide released during heating are sufficient to theoretically form an oxycarbide compound layer 1 mμ thick at all interfaces contacting a Udimet 700 shell, assuming a 5-A cubic lattice. This was consistent with the observed appearance of the films on the failed specimens. X-ray diffraction, however, was unable to identify the actual compound.

By trial, it was established that a 10^{-5} to 10^{-6}-torr vacuum outgassing treatment at 2150 F with a 2 to 5-min excursion to 2175 F would reproducibly and effectively remove the volatiles and leave a bright, clean Udimet 700 surface. Consequently, the finned shells from the previous experiment were reprepared employing the vacuum outgassing treatment as the final step of surface preparation. The B1900 and all components of the bonding container were also outgassed under the same conditions. Because the fins of the shells had been thinned during repreparation of the surface, it was necessary to reduce autoclave pressure to 800 psi to retain the same contact pressure as the immediately previous experiment. After processing at the conditions of 1900 F/800 psi/1 hr, the cylindrical samples were decanned and aged.

Many of the shells broke away from the B1900 during various stages of the solutionizing and aging schedule. A specimen in which all four shells separated during cooling from 2135 F in air is shown in Figure 73. It may be seen that, if anything, the degree of contact achieved during this experiment was less than that achieved at 1100 psi. Again, no compressive flow was observed. It was concluded that gas pressures of the order of 800 to 1100 psi were insufficient to bring the Udimet 700 shell into full conformity with the B1900 cylinder. At this point, the bonding pressure reevaluation study presented earlier was undertaken.

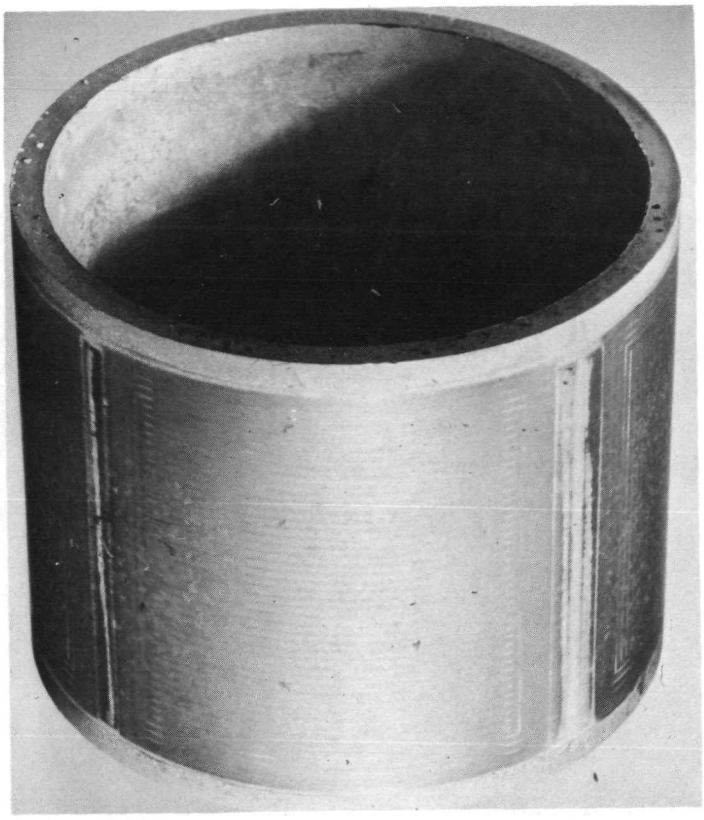

~1X 44986

a. B1900 Surface

Note coating except where in contact with bonding container and in areas of limited Udimet 700 fin bonding.

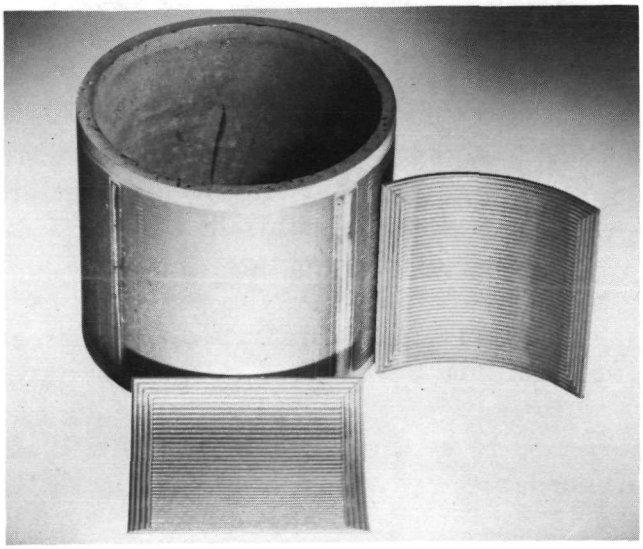

44987

b. Cylinder and Finned Shells

FIGURE 72. UDIMET 700/B1900 CYLINDRICAL SPECIMENS PROCESSED AT 1900 F/1100 PSI/1 HR

Finned shells separated from B1900 upon removal of bonding container.

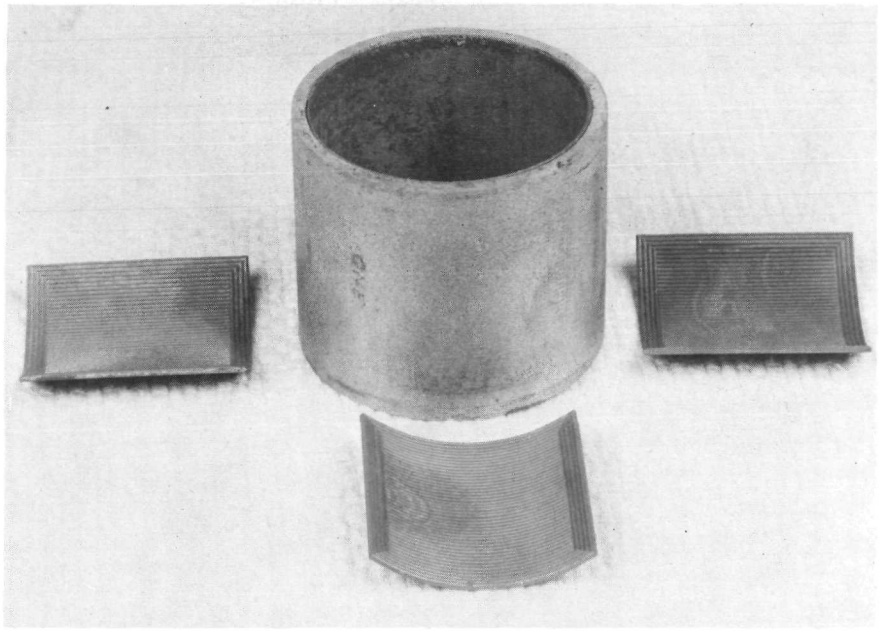

45351

FIGURE 73. UDIMET 700/B1900 CYLINDRICAL SPECIMENS PROCESSED AT 1900 F/800 PSI/1 HR

Finned shells separated during Udimet 700 aging.

Unmachined Cylindrical Specimens

Three Udimet 700/B1900 cylindrical specimens, U-57, U-58, and U-59, were prepared from rolled Udimet 700 sheet in a gas-pressure bonding cycle employing conditions of 1900 F/10,000 psi/1 hr. These specimens were previously described in Table 13. The various indicator slots listed in the specimen description of Table 13 were employed to establish whether Udimet 700 would resist plastic flow under the influence of the bonding pressure and temperature needed to effect satisfactory joint efficiency. The previous cylindrical finned shell samples just discussed had shown that interface pressures of the order of 3,000 to 3,500 psi were insufficient; subsequent coupon investigations had established that an interface pressure of 10,000 psi produced satisfactory joints. This experiment was undertaken to evaluate the effect of a 10,000-psi interface pressure on a cylindrical geometry.

Indicator slots were placed in the Udimet 700 sheet by grinding prior to rolling the sheet into the cylindrical configuration. Because of the difference in thickness, the area above the axial slots did not roll into the desired radius. Specimen U-58, with three axial slots per 90-deg segment, could be more properly described as a nine-sided polygon than a cylinder. Consequently, both Specimens U-57 and U-58 presented some difficulty during assembly. Being polygonal, neither would slip inside a properly sized bonding container. These specimens

were forced into a near cylindrical shape and pressed into the container. However, both retained a degree of their as-rolled configuration as the walls of the OD stainless steel container stretched to accommodate the points of the polygon.

Cylindrical Specimens U-58 and U-59 were each instrumented with a Chromel/Alumel thermocouple by welding the thermocouple bead directly to the OD surface of the stainless steel bonding container. During the gas-pressure bonding cycle, the temperature registered by these two thermocouples was used as the control point. Both thermocouples indicated virtually the same temperature. However, the thermocouples that would have normally been used for control purposes indicated temperatures as much as 90 F higher than that of the specimen thermocouples. In view of this temperature profile and the arrangement of the specimens in the autoclave furnace, it is quite likely that the portions of Specimens U-57, U-58, and U-59 nearest the furnace wall were at a temperature higher than 1900 F.

Upon sectioning after completion of the bonding cycle, all slots in Specimens U-58 and U-59 were found to be unchanged. Specimen U-57 was found to have two axial slots undeformed and two completely collapsed. It was concluded that this surface of Specimen U-57 was adjacent to the furnace hot wall and may have been heated to approximately 2000 F.

Specimen U-57 was sectioned transverse to the cylindrical axis and examined. Analysis of this section was clouded by the possibility that the section line coincided with the edge of the circumferential indicator slot. Metallurgically, fields surrounding either the undeformed and collapsed axial slots of this specimen were quite similar. No bond line precipitate was found and the bond would have been undistinguishable except for the presence of voids on the Udimet 700 side of the bond. It is uncertain whether the voids were remnants of the circumferential slot or caused by dissolution of subsurface oxide particles during surface preparation.

Specimen U-58 was examined parallel and transverse to the cylindrical axis. The bond appearance in both directions was comparable and similar to that noted in Specimen U-57. A small amount of discrete particle precipitate was noted at the bond line; however, the greater share appeared as a homogeneous transition from B1900 to Udimet 700, and it is believed that bond quality was generally good. The axial sections revealed that bond quality dropped off at the edge of the segment, probably as a result of initially poor fitup. Similarly, the transverse sections showed that the segments were not in contact with the B1900 for a distance of about 1/16 in. on either side of the axial indicator slots. The results of this specimen point up the need for good initial fitup on cylindrical shells and the desirability of high gas pressure where feasible.

Specimens U-57 through U-59 were solutionized and aged using the standard sequence for Udimet 700. A portion of Specimen U-59 separated at the bond after the initial step of the heat treatment. The separation did not propagate during subsequent steps, nor was its initiation unexpected. It was strongly

suspected that this specimen did not experience full pressure during the bonding cycle due to partial leakage of the bonding container.

Metallographic examination revealed that all specimens had responded to the heat treatment in a generally favorable manner. There was some coarsening of the gamma prime in the B1900, but the bond interface consisted of a continuum of gamma prime with dicrete particles of apparent carbide precipitate. The particulate precipitate varied considerably in density, but did not, in the sections examined, appear concentrated to the point of forming a film. It was concluded that the microstructure observed would offer good high-temperature mechanical properties.

Cylindrical Specimens With Nickel Diffusion Aid

Four cylindrical Udimet 700 finned shells of the design shown earlier in Figure 64 were roll formed to fit the 2.5-in. OD of a B1900 cylinder. Additionally, two flat specimens of the type described previously were prepared for bonding as control specimens. Fin direction and Udimet 700 sheet identification are tabulated below:

Finned Shell Specimen Identification	Udimet 700 Sheet Identification	Fin Direction
U-71	10	Axial
U-72	11	Axial
U-73	10	Circumferential
U-74	10	Circumferential
U-69	9	Flat specimen
U-70	9	Flat specimen

All six specimens were prepared and processed according to the procedures specified previously in Table 14. The gas-pressure bonding cycle conditions, selected on the basis of fin dimensions, were 1900 F/3500 psi/1 hr.

Postbonding inspection revealed that the 0.030-in.-thick stainless steel bonding container had deformed into the space between shells on the cylinder. Cracks had formed in the stainless steel at those locations which had caused pressure loss on the specimen during the cycle. Consequently, while the fin surfaces had made nearly 100 percent contact with the B1900, there was no bond formed. The two flat specimens were well bonded and were successfully solutionized and aged.

Later, the four cylindrical shells and B1900 were reprepared and assembled in a stainless steel bonding container which was subsequently overcanned with 1010 aluminum-killed carbon steel. The specimen was again gas-pressure bonded at 1900 F/3500 psi/1 hr. After bonding, the container was removed and the cylinder cut into four segments. The segments were then solutionized and aged

per Table 14. After aging, the specimens were cut in half, and one half was examined metallographically. Figures 74 through 76 illustrate the results of that examination.

Bond quality was found to be excellent in the center region of all four samples. However, at the periphery where thermal stress is maximized many fins had fractured. Since the specimens were not examined in the as-bonded condition, it was not possible to determine whether fracture occurred during the cooling stage of the bonding cycle or as a result of the several thermal cycles incurred during heat treatment. The relatively unoxidized appearance of the fractures suggests failure as a result of heat-treatment stresses. The intact bonds, as illustrated in Figure 75, appeared to be of excellent quality. A blocky phase identifies the original position of the nickel film. There is no "bond line"; the joint consists of a transition from the Udimet 700 microstructure to the psuedo-B1900 structure occupying the nickel position and from that structure to the normal B1900 microstructure.

As illustrated in Figure 76, fracture occurred through the interface structure. The geometry of the joint dictated the failure location. During either the initial bonding cycle or repreparation, the bonding surfaces of all fins were severely rounded. The shells, once rolled to the desired curvature, cannot be conveniently surface ground. In the preparation of flat shells, care is taken to grind the top of the fins to establish flatness. The joint shown earlier in Figure 58 is a good example of the desired joint geometry. A rounded fin gives rise to a twofold weakening of the structure. First, the notch formed is a severe stress riser. Secondly, the bonded area is reduced by 25 to 50 percent, and load-bearing capability is a direct function of bond area. Hence, there was a strong possibility that the fins at the specimen edges would not have ruptured had the fin surface been of the correct profile. Because of the unfavorable joint geometry, it was decided not to evaluate the specimens in elevated-temperature shear.

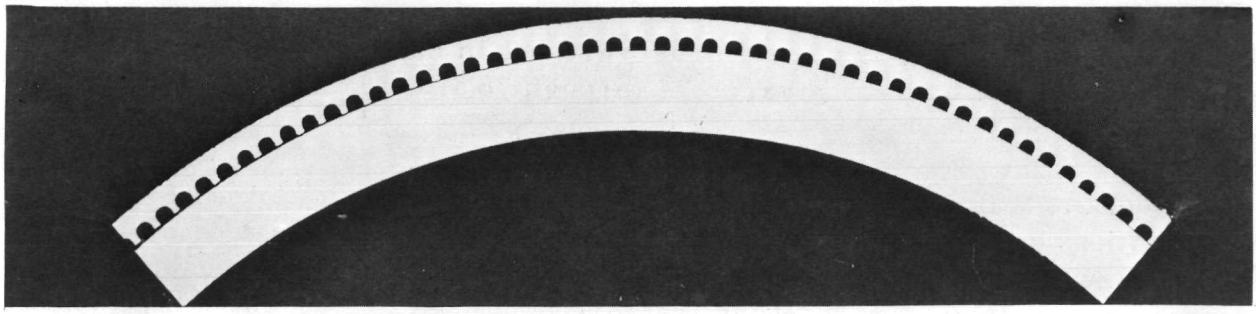

3X As Polished 0F706

a. Specimen U-71

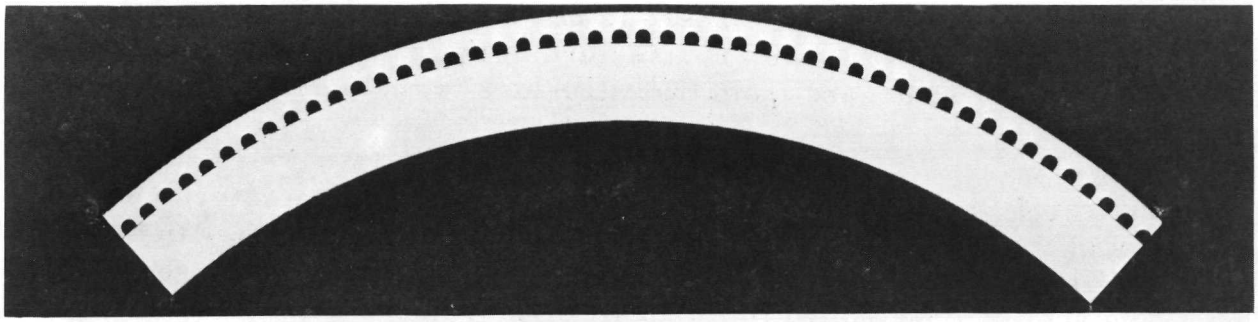

3X As Polished 0F707

b. Specimen U-72

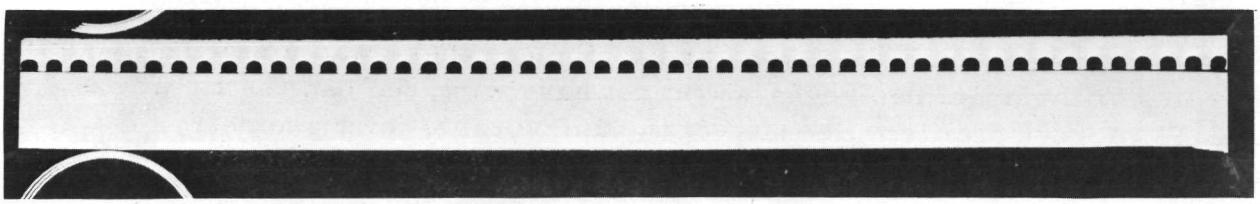

3X As Polished 0F708

c. Specimen U-73

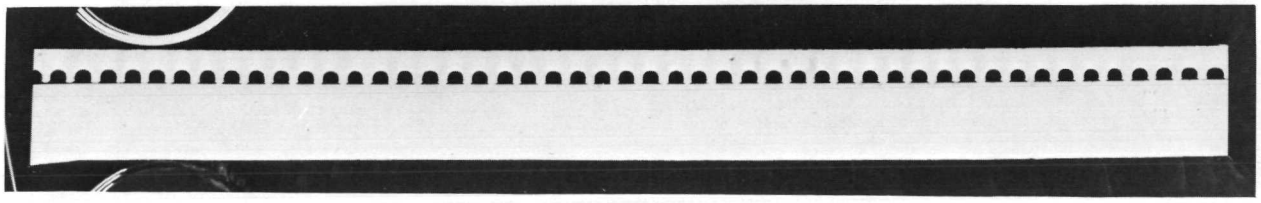

3X As Polished 0F709

d. Specimen U-74

FIGURE 74. PHOTOMACROGRAPHS OF AGED UDIMET 700 CURVED FINNED SHELLS

Specimens were gas-pressure bonded at conditions of 1900 F/3500 psi/1 hr.

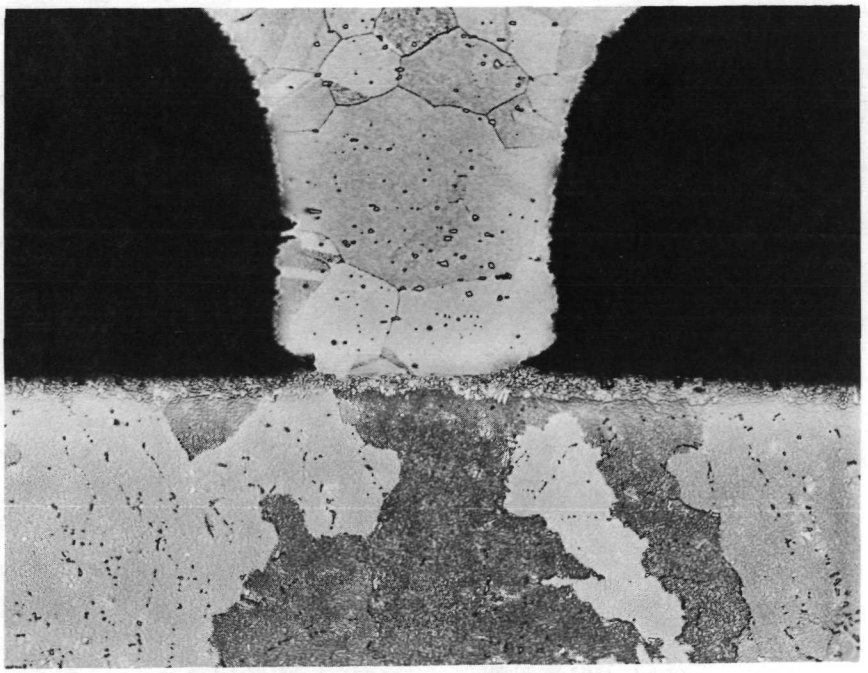

B1900

100X 20 Glycerin: 10 HCl: 10 HNO_3 0F686

a. Typical Fin; Note Notches Formed by Rounded Fin Surface

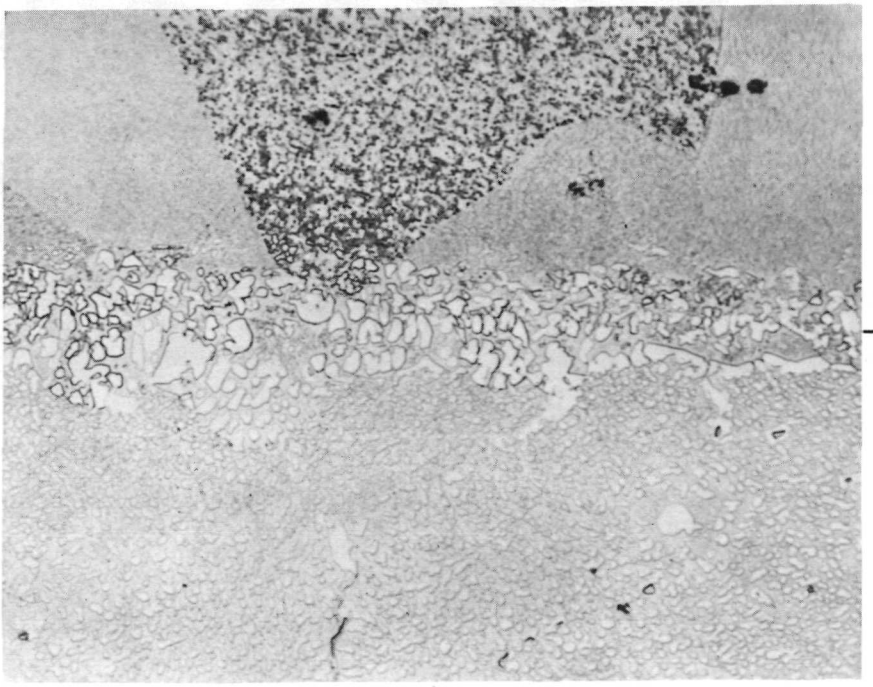

Udimet 700

"Nickel" zone

B1900

750X 20 Glycerin: 10 HCl: 10 HNO_3 0F688

b. Typical Bond

FIGURE 75. MICROSTRUCTURE OF NICKEL AIDED BOND IN CURVED UDIMET 700 FINNED SHELLS

Specimen is shown in aged condition; bonding conditions were 1900 F/3500 psi/1 hr.

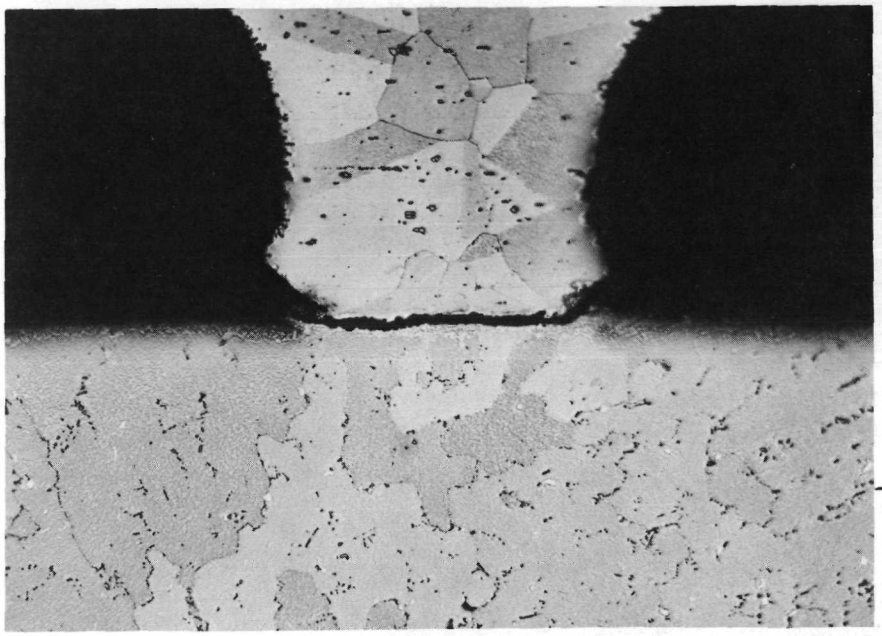

100X 20 Glycerin: 10 HCl: 10 HNO_3 0F704

a. Typical Fin Cross Section

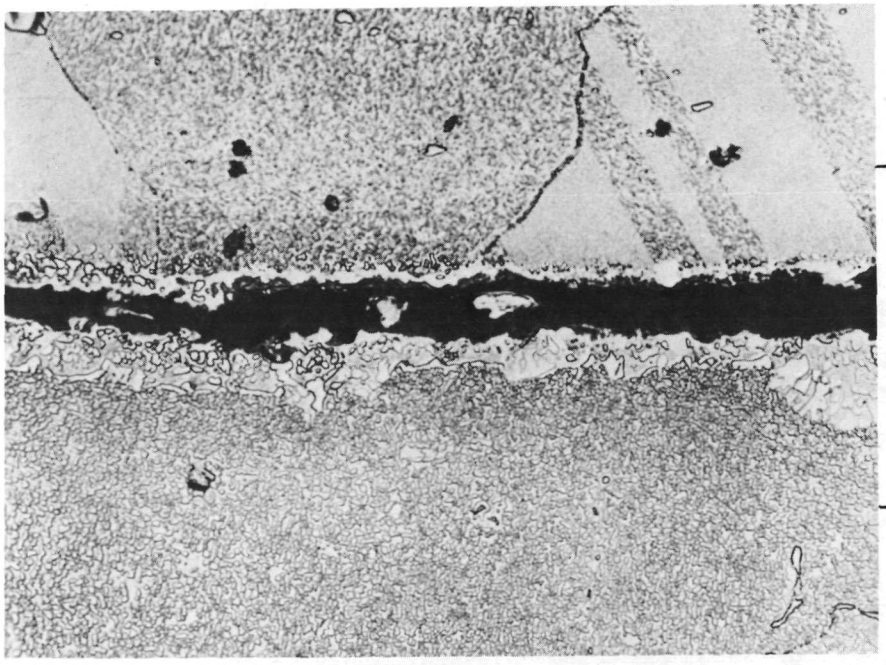

500X 20 Glycerin: 10 HCl: 10 HNO_3 0F700

b. Typical Fracture

FIGURE 76. TYPICAL BOND FRACTURE OBSERVED AFTER AGING OF CURVED UDIMET 700 FINNED SHELLS

Fracture occurred only at edges of specimens.

NONDESTRUCTIVE INSPECTION STUDIES

Fabrication of Specimens With Intentional Defects

A standard test specimen with intentional defects was prepared for each of the two complex joint systems under study. These finned shell specimens were produced during the process refinement study discussed previously. The Udimet 700/B1900 sample, Specimen U-25, was produced under conditions of 1900 F/2000 psi/1 hour. The TD NiCr/B1900 sample, Specimen T-30, was prepared employing a 2000 F/3500 psi/1 hour bonding cycle. Both specimens were of the three-zone finned shell configuration shown previously in Figure 10.

Two types of bond interface defects were initially contemplated, air gap and oxide inclusion. However, after it was observed that an air gap was very difficult to detect, plans to fabricate oxide-inclusion specimens were suspended because oxide inclusions are more difficult to resolve than the air-gap type. Gaps were produced at the fin/strut bond by milling shallow slots by EDM in the shell fins transverse to the fin direction. Figure 77 describes the size and position of the slots in the finned shell as viewed from the B1900 surface of a bonded sample. All slots were 0.005 in. deep. Widths of 0.005, 0.010, 0.020, 0.040, and 0.080 in. were desired. However, the actual slots were 0.007, 0.008, 0.024, 0.035, and 0.086 in. wide. The milling operation produced individual defects of the length and depth established by the milling cut. Defect width was established by the width of the particular fin. Hence, the smallest defects were found in the Zone L or N (0.012 in.) fin areas of the shell; the largest were located in the Zone M fin (0.036 in.) area. During bonding, the transverse slots did not collapse. Consequently, gaps ranging from 0.005 by 0.005 by 0.012 in. to 0.005 by 0.080 by 0.036 in. remained at the shell/strut joint at the slot positions.

The two standard defect samples were subsequently inspected by X-radiography, neutron radiography, liquid crystals, and ultrasonic inspection techniques. The results of those inspections are presented and discussed below.

Ultrasonic Inspection

Two basic inspection arrangements were evaluated, back reflection and through transmission. The better results were obtained with through transmission. The problem with back reflection stemmed from the small specimen thickness, approximately 3/16 in. It was very difficult to precisely and reproducibly separate by an electronic gating circuit the interface reflection signal, from the front and back signals. The latter fall on either side of the interface signal. Only the interface reflection signal is wanted for bond-quality display.

In the first of two sessions with a commercial inspection vendor, it was determined that when electronic gating was behaving properly, a clear display of Zone M

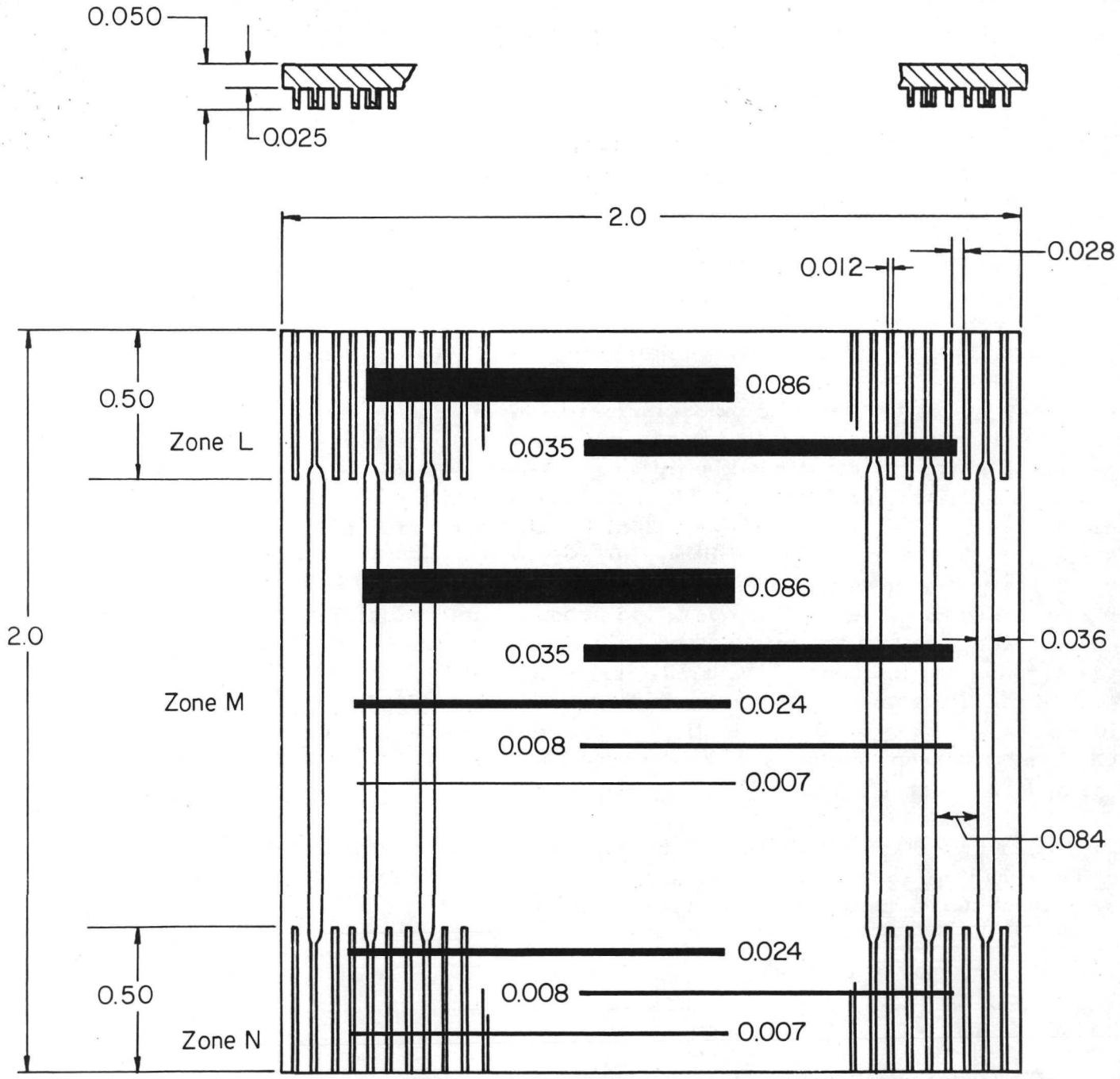

FIGURE 77. DEFECT WIDTHS AND POSITION IN STANDARD NONDESTRUCTIVE INSPECTION SPECIMENS

fins and channels and a fair display of the Zone L and N fins and channels could be attained. It was possible to detect in Zone M the two largest defect sizes, 0.080 by 0.036 in. and 0.035 by 0.036 in. None of the defects present in Zones L or N were detected.

In the second session, the ultrasonic recordings were considerably less sharp. Further, no unbonds were detected in the samples. This was discouraging since completely unbonded Specimen U-26 was in the group. It was apparent that the gating circuit was not performing properly. Both inspection sessions employed the same equipment set-up with a 25 MHz, spherically focused transducer.

It appeared that commercial ultrasonic inspection methods were not yet equal to the problems presented by a bonded finned shell/strut turbine blade configuration, since it was not possible to detect most of the intentional defects and to distinguish at times between bonded and unbonded specimens. However, some positive results were obtained, and it is believed that the method has good potential, if given an adequate development effort.

Through transmission ultrasonic methods were investigated with Battelle's equipment. Two basic arrangements were employed. In the first, the test specimen was suspended a few inches above and parallel with the bottom of the water tank employed as the coupling medium. The reflection off the tank bottom was gated manually by amplifying horizontal sweep of the cathode ray tube until only that signal was displayed. Acquisition of the signal thus indicated that the ultrasonic pulse had successfully transversed twice through the sample and, consequently, the joint under inspection. A joint not in intimate contact did not efficiently transmit the pulse, and the test signal was reduced to zero. Beam width of the transducer was quite large, 1 cm diameter, in comparison to the defect sizes under study. The beam aperture was reduced to 3 mm, 1 mm, and 0.5 mm by means of rubber collars placed over the transducer. These widths permitted inspection of one fin at a time. Restricting the beam in this manner, however, reduced the energy of the beam. The largest aperture was satisfactory for inspecting Zone M of the test coupon. Defects as small as 0.020 in. long were detected. However, the attenuation of the smaller two apertures needed for Zone L or N was too great. The test signal could not be discerned from normal noise background.

This situation was corrected by the second technique. In this case, a receiving transducer was positioned under the sample in such a manner that it tracked with the sending transducer. Consequently, the signal had only to traverse the sample once, and sensitivity was vastly improved. The 1 mm and 0.5 mm apertures, which were positioned between the transmission transducer and test sample, performed satisfactorily in this setup. Defects as small as 0.010 by 0.040 in. were detected and verified by metallographic examination.

Inspection of Specimen T-30 and Specimen U-25 proved to be a tedious exercise owing to the manual scanning and recording procedure employed. The results of the scans were not in great measure different from the back reflection work. The two larger defects in Zone M were detected and good definition of Zone M fins was obtained. The Zone L and N fins tended to disperse the beam and "smear" the

display. Since the objective of the inspection effort was to determine which candidate method, if any, had potential rather than develop methods advancing the state of the art, no effort was expended in attempting to refine either the through transmission or back reflection methods. Both appeared to have promise. Given an adequate development effort either method could be expected to yield useful inspection data. The back reflection method was believed to be the more amenable to the turbine blade configuration. The construction and operation of a receiving transducer from the inside of a hollow turbine blade would require a significant engineering effort.

Neutron Radiography

Several specimens, including the two with intentional defects were inspected by neutron radiography. Figure 78 illustrates schematically the reactor core and peripheral arrangements for neutron radiographic inspection. The specimens were placed with the Udimet 700 or TD NiCr finned shell next to the photographic film (aerial photography film Type SO-243) and away from the neutron beam. The neutron beam passed through the specimen and film before striking a gadolinim foil which was attached to the back side of the film. The foil emits back soft electrons which expose the film.

To enhance the contrast between fin and channel and, more importantly, between bond and unbond in the fin, methods for filling the channels and unbonds with a liquid were investigated. Liquids with concentrations of atoms with high neutron capture or scattering cross sections were desired. Boron, carbon, and hydrogen are such elements. Capture or scattering of the neutron source beam in the channel and defect areas effects a relative underexposure of the film in that particular area. Three liquid solutions were evaluated.

Initially, an attempt was made to fill the cavities of several fin specimens with a supersaturated solution of boric acid. About 10 g H_3BO_4 was dissolved in 100 cc of boiling H_2O. The specimens were submerged in the solution, and the solution was cooled in a vacuum desiccator to room temperature. Upon cooling, H_3BO_4 crystals precipitated from the solution. Excess boric acid crystals were wiped off the surfaces. The resulting neutron radiographs distinguished clearly between the boric acid crystals and the fins, but air bubbles in the channels could not be completely extracted. In a second variation, distilled water containing 1 part in 1000 of detergent to increase surface wetting was used to fill the finned shell channels. The specimens were placed in vacuum desiccator and left overnight to remove air bubbles. Parawax and polyethylene tape were employed to contain the filler solution within the shell. The resulting radiographs were clear, no air bubbles were evident in the channels, but the channels were not as well distinguished from the fins as when the boric acid solution was used. A third variation, which proved to be satisfactory, was quite similar to that above except that the filler solution in this case was room-temperature saturated boric acid. One end of the finned shell was sealed with Parawax and polyethylene tape, the channels were injected with the boric acid solution, and the excess solution wiped carefully from the surface of the

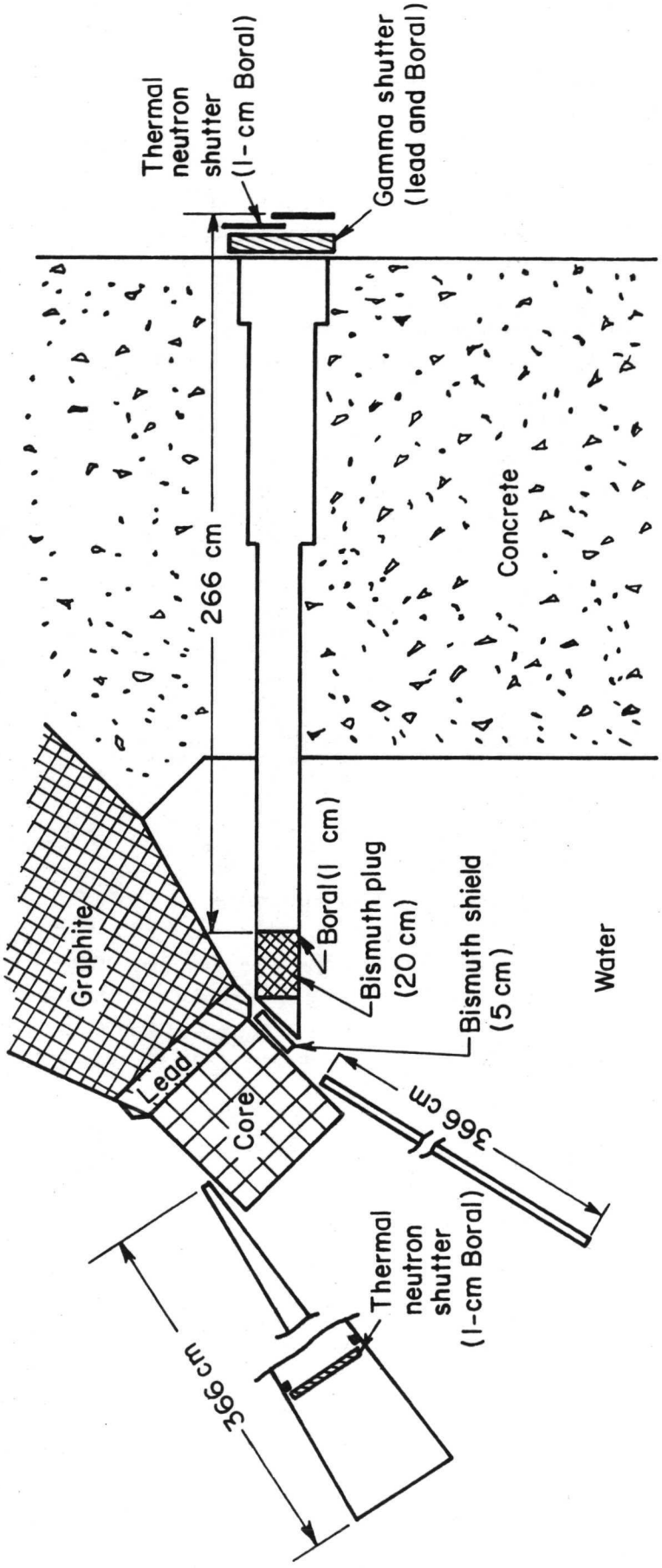

FIGURE 78. PLAN VIEW SHOWING GENERAL ARRANGEMENT OF REACTOR CORE AND NEUTRON RADIOGRAPHY TUNNELS

specimen. The specimens remained in a vacuum overnight to remove air bubbles; subsequently, the open end was sealed with Parawax and polyethylene tape, and the specimen exposed to the neutron beam. Good definition between channels and fins was achieved with this technique. Defects at the edges of Specimen U-71 through Specimen U-74 (cylindrical Udimet 700/B1900 with rounded fins) were noted and later verified by metallography. However, the only defects observed in Specimens U-25 and T-30 containing intentional defects were those already detected by ultrasonic inspection and X-radiography.

Neutron radiography appeared to yield the best results of any method investigated. The concept of introducing a contrast enhancer, in this case a boric acid solution, was demonstrated to be feasible. The contrast enhancer aided in discriminating between bond and nonbond where a physical gap existed. Still unanswered, however, is the question of how this technique might respond to defects presenting no opening but still of marginal quality. This case is typified by those instances observed during bonding process development in which the bond was degraded by carbide precipitation. It was concluded that neutron radiography could be readily applied to the turbine blade geometry to inspect for defects of a mechanical nature in the bond. Metallurgical defects resulting in a weak but fully coherent bond probably could not be resolved without a considerable development effort and perhaps not at all.

Other Inspection Techniques

X-Radiography

Radiographs of intentionally defected Specimen T-30 and Specimen U-25 were presented earlier in Figures 45 and 48, respectively. The 0.025-in.-wide defects can be observed in both the 0.036- and 0.012-in.-wide fin zone of both specimens. Apparently, the remaining defects were too shallow to display a detectable contrast. It is also possible, since neither specimen was destructively evaluated, that the thickness of the defects was decreased by deformation of the finned shell during bonding.

A liquid intrusion technique was employed with the objective of enhancing the contrast between bonded and unbonded areas. A saturated solution of lead nitrate, plus a wetting agent, was injected in the channels of the bonded specimens. It was expected that the solution would be pulled into the defect gaps by capillary action. This technique, which works well with low atomic-weight metals such as aluminum, did not show promise in this case. The radiation level required to satisfactorily penetrate B1900 completely overwhelmed the lead salt concentration. No contrast enhancement was achieved.

X-radiography yielded results consistent with neutron radiography. Both techniques are useful methods for examining mechanical features of the bonded finned shell/strut structure such as fin deformation, channel blockage, and physical

separation of the joint. X-radiography can only be useful in the last category, however, when the separation is caused by a gap in one of the joint components. That is, there must be a distinguishable difference in material thickness at the defect location. Since neutron radiography responded to liquid intrusion, it was considered to be the superior technique.

Liquid Crystals

The use of liquid crystals as a means of detecting flaws was investigated. As liquid crystals are heated over a narrow-response temperature range (of the order of a few degrees), they change in sequence from colorless to red, orange, yellow, green, blue, and finally colorless again. Therefore, within the response-temperature range, the color of the liquid crystal is a good measure of relative temperature. This property can be used as a means of detecting flaws by coating one surface with the crystals and then heating the specimen from the opposite side. It is generally desirable to paint the detection surface black before applying the liquid crystals to enhance color detection. Defects may be detected as either low or high-temperature areas resulting from abnormal thermal conduction through the defective area.

In practice, several major difficulties were encountered. One of these was that, from any given point, heat flow is radial under transient conditions. Since heat flow is not collimated, the defect display becomes very badly "smeared". Secondly, since this was a dynamic test and the response range is narrow, the color spectrum was traversed in approximately one second. The liquid crystals are sensitive to other uncontrolled temperature effects such as normal air-convection currents; this also caused difficulties. Only the Zone M fins could be detected by this technique; occasionally the 0.080-in.-wide defect in this zone could also be detected. No response was obtained in either Zone L or N. The difficulties associated with this technique appeared to be of sufficient magnitude to preclude immediate or reasonably short-term application to blade assemblies.

Gaseous Radioisotope

The feasibility of applying radioactive tracer techniques was considered. No experimental work was performed, however. Krypton^{85} gas appeared to have several points in its favor. Krypton^{85} may be handled with little concern of radiological hazard and is readily available commercially. The inspection procedure is basically similar to that employed in liquid intrusion radiography. However, the gas should make the procedure simpler and more effective with respect to resolving power. Furthermore, the gas concentrations in the specimen are the energy source for exposing film for record. No source of X-rays or neutrons is needed. Therefore, multiple line-of-sight exposures should not be needed, since the film is wrapped in contact with the blade outside surface.

Despite its attractive features, this technique was not, at the time of the investigation, sufficiently developed to warrant an experimental trial. Subsequently,

the method has been commercialized and employed with success on diffusion bonded compressor and turbine blades. The commercial technique involves, as postulated during the investigation, surrounding the blade cavities and surface with a moderate over-pressure of Kr^{85}. The pressure is released and subsequently the test piece wrapped with film for the autoradiograph. The radiograph is interpreted by the degree of exposure of the film. Dark areas are indicative of a residual Kr^{85} concentration and hence a defect.

Nondestructive Inspection Conclusions

None of the candidate techniques experimentally evaluated demonstrated outstanding results, and it would appear that none are capable of immediate implementation. Each would require some level of development beyond the limit consistent with the present effort to insure reliable and readily interpretable results. Radiographic methods yield the best definition of shell internal geometry, but more work is needed to establish confidence in its ability to identify defects. Ultrasonic methods were limited by the resolving power of the transducers and recording equipment. Fin definition was poor, especially in 0.012-in. fins. It did appear that relatively small defects in moderate width fins could be detected in simple specimen geometries such as a small flat coupon. Ultrasonic detection of similar sized, approximately 0.040 by 0.040 in., defects in a complex turbine blade would be much more difficult and would require development of both the fixturing for traversing the probe and a reliable interpretation procedure.

While improvements in the state of the art of NDI may have been made which alter the situation, it must be generally concluded from the specific work conducted in this investigation that available NDI methods are not equal to the task of assuring the bond quality of complex air-cooled turbine blades. The results generally support a recommendation for further development of ultrasonic and neutron radiography techniques.

SUMMARY AND DISCUSSION OF RESULTS

This investigation established a diffusion-bonding process for joining TD NiCr and Udimet 700 finned shells to B1900 struts. The process utilizes isostatic gas pressure at elevated temperature to uniformly bring each of the cooling fins into intimate contact with the strut to permit thermal diffusion across the fin/strut interface. In the specific technique developed, no support was found to be needed in the channel areas between fins. A process gas pressure of 3500 psi was chosen. This pressure yielded adequate pressure at the joint without developing stresses which would cause macrodeformation of the structure. Relatively low gas pressures were required because the joint contact area was one-third of the area exposed to the gas. The developed process was demonstrated on both flat and curved geometries with the latter simulating a typical turbine blade airfoil camber. Joint strength equivalent to the shell material at typical blade operating temperatures was frequently achieved. This was evidenced by the fact that most test samples failed by rupture of the cooling fins with the bond remaining intact. Udimet 700/B1900 average short-time shear strength at 1750 F was 27,000 psi with the force applied transverse to the fin direction and 35,000 psi with the load applied parallel with the fins. TD NiCr/B1900 samples exhibited strengths of the order of 10,000 at 1750 F prior to thermal cycling. The strength of this joint never exceeded 5000 psi after thermal cycling, however. This poor thermal-fatigue response would appear to severely limit the usefulness of TD NiCr in blade and vane applications. Both joint systems appeared to be subject to variations in strength level at 1750 F. It would be desirable to perform additional development work on the Udimet 700/B1900 system to determine if the observed scatter in strength data is process or test-method oriented and to reduce the variation to less than 10 percent.

The investigation concluded with the fabrication of cylindrical specimens simulating blades with chordwise (circumferential) and spanwise (axial) cooling fins. Pressure transfer from the gas medium to the joint in the cylindrical geometry was observed to be influenced by the initial fit-up between the shell and strut. Pressure could be partially consumed in deforming the shell since the shell alloys have significant strength at the bonding temperature. Fit-up appeared to be of little concern in the flat geometry despite the fact that flat shells were frequently deformed 0.010 to 0.020 in. over short-span distances during the bonding process to bring them into contact with the uneven as-cast strut. It is to be expected that a curved geometry, such as an airfoil, would offer more resistance to flow than the flat geometry. More experience is needed with curved geometries so that the effect of curvature can be determined more precisely.

The data from this work would establish a firm foundation for fabricating a composite blade. Blade fabrication and evaluation should be pursued to establish final feasibility as there are processing areas not covered in detail by the present work that would be necessary ingredients in blade fabrication. In the current case, it was not necessary to be concerned with structural support matters beyond the finned shell. As noted, procedures for efficiently handling that problem were successfully established. However, in preparing a blade, the hollow strut casting

might require structural support as well. The difficulty of achieving support would vary considerably with the internal complexity of the strut. For example, a heavy section strut having a small air supply manifold might be self-supporting. In this case the blade would be canned on the outside surface and treated as if the strut were solid. More typically, however, the hollow strut would have a large hollow core with relatively thin airfoil surfaces and internal stiffener webs. Assuming that the webs are not sufficiently close spaced to enable the strut to withstand the gas overpressure during the bonding process, the air-supply core would have to be given auxiliary support. Specifically, auxiliary support members would have to be introduced to shorten the span between members to a distance compatible with the strength of the strut material, bonding temperature, and bonding pressure. For B1900 in a 0.060-in.-thick surface thickness under the bonding conditions established in the program, the acceptable span between core webs would be in the range of 0.250 to 0.300 in. Thus, a typical first-stage blade would require five to six support members running the span length of the blade airfoil. The support members could be either temporary, permanent, or a mixture of the two. Permanent span supports could either be an integral part of the strut casting or separate spars diffusion bonded to the strut during the shell-bonding cycle. Temporary spars would be prepared from molybdenum sheet or other suitable material and removed by leaching. Mechanical removal schemes may also be feasible. Given a blade designed from the start with gas-pressure bonding fixed as the fabrication process, it should not be difficult to handle internal support of the strut. A wide latitude of shell, fin, and strut designs are fabricable by the process. The key to success is coordination between the designer and fabricator.

After dealing with the strut support area, the next step in preparing a blade for bonding is the canning operation necessary to seal the joints from the pressure source. In the current effort, conforming metal containers were employed exclusively. That does not have to be the case, however. Recent work at Battelle suggests that it is much more cost effective in diffusion bonding titanium-alloy compressor blades, for example, to use a pressure-transmitting medium between the container and blade. In the example quoted, glass costing a few cents per pound was used as the transmission medium. The container was an inexpensive carbon steel cylinder. The resulting bonds were of excellent quality. The same technique has been used for stainless steel at 2000 F. Hence, the groundwork for applying the technique to superalloy blades appears well in hand. The latest application of pressure transmitters was for cladding the complete airfoil of a Udimet 700 blade with NiCrAlSi alloy foil as an experimental thermal fatigue suppressing composite. While there are no doubt specific problems to be identified and overcome, neither the internal support nor canning operations would appear to necessarily limit the technical feasibility of gas-pressure bonding complex air-cooled turbine blades in a reasonably economical fashion. Given the current high cost of cast blades, it is quite possible to achieve cost savings as well as design enhancement through use of the methods investigated.

Diffusion bonding must be compared technically and economically with casting, brazing, and alternative joining methods. Based on the results of this investigation, plus other experience, it is believed that gas-pressure bonding offers the following advantages:

- Diffusion bonded joints may be accomplished at a lower process temperature with correspondingly greatly reduced opportunity for excessive grain growth and other adverse metallurgical changes in the base material.

- No foreign elemets are introduced into the base metal which could degrade the strength and metallurgical stability of the base metal.

- The joint produced by diffusion bonding has the same operational limit as the base metal. Consequently, the operational limit can often be increased over that of brazed components.

- Components fabricated by diffusion bonding may be attached to each other and other structural members in the system by electron-beam welding or other welding methods without danger of joint interface remelt or metallurgical degradation.

- The joint interface (due to the absence of foreign elements) is not subject to selective corrosion or oxidation.

- No voids, such as those possible from the shrinkage and non-flow of braze metal, are left at the joint interface to reduce strength and initiate crack formation providing that the joint has been adequately prepared.

- Mechanical properties of the diffusion bonded joint can be equivalent to those of the base metal.

- A multiplicity of joints lying in any of several planes may be produced simultaneously with each experiencing the same process conditions and consequently possessing the same quality.

- The process produces relatively small dimensional changes in comparison to many other joining processes.

- The microstructure at the bond between relatively similar alloys is homogeneous with no sharp changes at the joint.

- Metals can be solid state bonded successfully to ceramic members without cracking of the ceramic.

- A cladding of the thermal fatigue and/or oxidation resistant materials such as FeCrAlY can be applied to the blade during the joining operation; the cladding material can also serve as the gas-pressure-bonding can.

- Components with very complex external surface geometries can be successfully joined.

- Large extended surfaces can be bonded without the need for large tonnage presses and expensive, if not impractical, high-temperature dies.

- The gas-pressure-bonding process is an established batch production technology for turbine components.

On the negative side, the gas-pressure-bonding process tends to be more costly than simple brazing or welding in that the equipment investment is higher and unit operations probably, in the short run, more expensive. Over long production runs, however, gas-pressure bonding has been shown to be quite cost competitive with other high-quality joining processes. A low deformation diffusion bond, such as produced by gas-pressure bonding, leaves a sharp corner at such joint configurations such as a Tee joint. Hence, the diffusion bonded joint can be more strain sensitive than a similar joint with a generous fillet. The joint surface condition in low deformation bonding processes is also more critical than in brazing or fusion welding. Since fit-up requirements are about the same, gas-pressure bonding may have an advantage in that the isostatic pressure application can overcome some degree of initially poor fit between components. Overall, gas-pressure bonding should find broad application in the joining of simple to complex turbine blade configurations as well as other high-temperature components. Its greatest application will probably center on those components where the demand for highest quality compensates extra cost.

CONCLUSIONS

It was demonstrated that cooling shells with 0.012- and 0.036-in. fins and 0.028- and 0.084-in. channels, respectively, can be bonded in both TD NiCr/B1900 and Udimet 700/B1900 systems.

While metallurgical bonds of excellent appearance were achieved in curved form for Udimet 700/B1900, a portion of the bonds did not survive thermal cycling, probably because of severe stress risers caused by fin round off. Consequently, this system was not fully demonstrated in cylindrical form; however, the system showed excellent promise.

Room-temperature and 1750 F joint efficiencies approximating 100 percent appear possible in both bond systems before thermal cycling. Average values are lower due to scatter.

TD NiCr/B1900 joints are seriously degraded by multiple thermal cycles from 1750 F. It is probable that a thermal expansion mismatch exists between these materials although this is not supported by the literature. Udimet 700/B1900 joints with transverse fins are less susceptible to thermal fatigue. Udimet 700/B1900 joints with longitudinal fins appear to be very resistant to thermal fatigue.

Nickel is a beneficial diffusion activator in the Udimet 700/B1900 bond system. With a nickel diffusion aid, bond reproducibility is considerably more consistent among process cycles than that exhibited by Udimet 700/B1900 direct bonds. Nickel appears to prevent carbide formation at the bond interface; the nickel is assimilated with the superalloys and becomes a complex phase at the original interface.

Vacuum outgassing at 2150 F is beneficial, if not mandatory, for achieving reproducible bonding results with Udimet 700.

Within the constraints imposed by self support of the finned shell during bonding, joint interface conditions of 1900 F/10,000 psi/1 hr were concluded to yield the best strength in the Udimet 700/B1900 system. Similarly, conditions of 2000 F/10,000 psi/1 hr were concluded to be near optimum for the TD NiCr/B1900 system.

Aging after bonding appears necessary to achieve optimal properties in the Udimet 700/B1900 system. Aging the B1900 in the TD NiCr/B1900 system appears to degrade strength in a fashion similar to thermal cycling.

Steel, iron, or molybdenum support tooling, when the supported area exceeds the bond area, is likely to rupture the bond in either system due to thermal stress during cooling. Molybdenum is especially susceptible because of its low thermal expansion.

Acid leaching of iron and steel support tooling from small cross-section areas is harmful to B1900 as a result of the extensive contact time, which causes intergranular attack.

Fit-up between the shell and strut in curved configurations can affect the degree and quality of bonding obtained. The maximum gap is not known. Gaps up to 0.010 in. can be accommodated in flat geometries without apparent difficulty when employing a gas overpressure of 3500 psi.

Further investigation into the response and reproducibility of curved finned shell geometries is required. Subsequently, a demonstration program on prototype blade hardware should be undertaken.

DISTRIBUTION LIST

	Copies
NASA-Lewis Research Center 21000 Brookpark Road Cleveland, Ohio 44135 Attn:	
Report Control Office, MS: 5-5	1
Technology Utilization Office, MS: 3-19	1
Library, MS: 60-3	2
Fluid System Components Division, MS: 5-3	1
W. L. Stewart, MS: 501-5	1
L. W. Schopen, MS: 500-206	1
J. B. Esgar, MS: 60-4	1
A. Kaufman, MS: 77-2	15
R. H. Kemp, MS: 49-1	1
F. S. Stepka, MS: 60-6	1
R. O. Hickel, MS: 60-6	1
Dr. D. Spera, MS: 49-1	1
Dr. J. Livingood, MS: 60-6	1
NASA Scientific and Technical Information Facility P. O. Box 33 College Park, Maryland 20740 Attn: NASA Representative RQT-2448	6
NASA Headquarters 600 Independence Avenue, S.W. Washington, D. C. 20546 Attn: N. F. Rekos, Code RAP	1
Department of the Army U. S. Army Aviation Material Laboratory Fort Eustis, Virginia 23604	1
Headquarters Wright-Patterson AFB, Ohio 45433 Attn: J. L. Wilkins, SESOS	2
AFAPL (APTC) Wright-Patterson AFB, Ohio 45433 Attn: Mr. J. Richens	1
Air Force Office of Scientific Research Propulsion Research Division USAF Washington, D. C. 20025	1

DISTRIBUTION LIST
(Continued)

	Copies
Defense Documentation Center (DDC) Cameron Station 5010 Duke Street Alexandria, Virginia 23314	1
Department of the Navy Bureau of Naval Weapons Washington, D. C. 20025 Attn: Robert Brown, RAPP14	1
Department of the Navy Bureau of Ships Washington, D. C. 20360 Attn: G. L. Graves	1
NASA Langley Research Center Langley Station Technical Library Hampton, Virginia 23365 Attn: Mark R. Nichols John V. Becker	1 1
United Aircraft Corporation Pratt & Whitney Aircraft Division Florida Research & Development Center Post Office Box 2691 West Palm Beach, Florida 33402 Attn: R. A. Schmidtke	1
United Aircraft Corporation Pratt & Whitney Aircraft Division 400 Main Street East Hartford, Connecticut 06108 Attn: G. Andreini Library	2 1
United Aircraft Research Laboratories 400 Main Street East Hartford, Connecticut 06108 Attn: Library	1
Northern Research & Engineering Corporation 219 Vassar Street Cambridge, Massachusetts 02139 Attn: K. Ginwala	1

DISTRIBUTION LIST
(Continued)

	Copies
General Electric Company - Flight Propulsion Division 930-1000 Western Avenue West Lynn, Massachusetts 01905 Attn: Dr. C. W. Smith - Library Bldg. 2-40M	1
Curtiss-Wright Corporation Wright Aeronautical Division Wood-Ridge, New Jersey 07075 Attn: S. Lombardo G. Provenzale	1 1
Air Research Manufacturing Company The Garrett Corporation, Arizona Division 402 South 36th Street Phoenix, Arizona 85934 Attn: Robert O. Bullock	1
Air Research Manufacturing Company The Garrett Corporation 9851 Sepulveda Boulevard Los Angeles, California 90009	1
AVCO Corporation Lycoming Division 550 South Main Street Stratford, Connecticut 06497 Attn: C. W. Bolton Charles Huintzle	1 1
Continental Aviation & Engineering Corporation 12700 Kercheval Avenue Detroit, Michigan 48215 Attn: Eli H. Benstein Howard C. Welch	1 1
International Harvester Company, Solar 2200 Pacific Highway San Diego, California 92112 Attn: P. A. Pitt Mrs. L. Walper	1 1
Goodyear Atomic Corporation Box 268 Piketon, Ohio 45661 Attn: Department No. 433 For: C. O. Longebrake	1

DISTRIBUTION LIST
(Continued)

	Copies
George Derderian AIR 53622 B Department of Navy Bureau of Navy Washington, D. C. 20360	1
The Boeing Company Commercial Airplane Division P. O. Box 3707 Seattle, Washington 98124 Attn: J. G. Schott MS 80-66	1
The Boeing Company Missile and Information Systems Division 224 North Wilkinson Street Dayton, Ohio 45402 Attn: Warren K. Thorson	1
Wall Colmonoy Corporation 19345 John R. Street Detroit, Michigan (3) Attn: R. L. Peaslee	1
Aerojet-General Corporation P. O. Box 1947 Sacramento, California 95809 Attn: M. L. Nylin Library	1 1
The Bendix Corporation Research Laboratories Division 20900 - 10½ Mile Road Southfield, Michigan 48076 Attn: A. R. Spencer	1
Battelle Memorial Institute 505 King Avenue Columbus, Ohio 43201 Attn: Defense Metals Information Center	1
Bendix Filter Division 434 West 12 Mile Road Madison Heights, Michigan 48071 Attn: A. G. McLemore F. W. Cole	1 1

DISTRIBUTION LIST
(Continued)

	Copies
Air Force Materials Laboratory Wright-Patterson AFB, Ohio 45433	
Attn: MAAM, Mr. Hughes	1
MAMP, Mr. Hendricks	1
Douglas Aircraft Company 3855 Lakewood Boulevard Long Beach, California 90801	
Attn: Technical Information Center, CL-250	
For: J. E. Merriman	1
General Motors Corporation Allison Division P. O. Box 24013 Indianapolis, Indiana 46206	
Attn: J. N. Barney	1
G. E. Holbrook	1
Library	1
H. E. Helms	1
Engineering Library TRW Inc. 23555 Euclid Avenue Cleveland, Ohio 44117	
Attn: Elizabeth Barrett, Librarian	1
J. Edward Taylor, Director Product Development Jet & Ordnance Division	1
Westinghouse Electric Corporation Small Steam and Gas Turbine Engineering B-4 Lester Branch P. O. Box 9175 Philadelphia, Pennsylvania 19113	
Attn: S. M. DeCorso	1

Page Intentionally Left Blank